FINAL REPORT

Fundamental Study of the Delivery of Nanoiron to DNAPL Source Zones in Naturally Heterogeneous Field Systems

SERDP Project ER-1485

September 2012

Gregory Lowry
Tanapon Phenrat
Fritjof Fagerlund
Carnegie Mellon University

Tissa Illangasekare
Colorado School of Mines

Paul Tratnyek
Richard L. Johnson
Oregon Health & Science University

SERDP
DOD ▪ EPA ▪ DOE

Report Documentation Page

Form Approved
OMB No. 0704-0188

1. REPORT DATE	2. REPORT TYPE	3. DATES COVERED
SEP 2012		**00-00-2012 to 00-00-2012**

4. TITLE AND SUBTITLE	5a. CONTRACT NUMBER
Fundamental Study of the Delivery of Nanoiron to DNAPL Source Zones in Naturally Heterogeneous Field Systems	5b. GRANT NUMBER
	5c. PROGRAM ELEMENT NUMBER
6. AUTHOR(S)	5d. PROJECT NUMBER
	5e. TASK NUMBER
	5f. WORK UNIT NUMBER
7. PERFORMING ORGANIZATION NAME(S) AND ADDRESS(ES) **Carnegie Mellon University,5000 Forbes Ave,Pittsburgh,PA,15213**	8. PERFORMING ORGANIZATION REPORT NUMBER
9. SPONSORING/MONITORING AGENCY NAME(S) AND ADDRESS(ES)	10. SPONSOR/MONITOR'S ACRONYM(S)
	11. SPONSOR/MONITOR'S REPORT NUMBER(S)

12. DISTRIBUTION/AVAILABILITY STATEMENT
Approved for public release; distribution unlimited

13. SUPPLEMENTARY NOTES

14. ABSTRACT

Chlorinated solvent DNAPLs can be consistent long-term sources of groundwater contamination. Remediation is costly and poses significant technical challenges. Nanoiron (NZVI) is a proposed in situ remediation agent for DNAPL source zones, but the effectiveness of NZVI treatment relies on the ability to emplace and retain the NZVI near or within the DNAPL source area. The dominant physical and chemical processes controlling the reactivity and migration and distribution of NZVI in the subsurface are poorly understood, however, making it difficult to ensure that NZVI will be delivered where it is needed and whether or not it can be an effective treatment alternative for DNAPL source zones. Objectives The overall study objective was to evaluate if and where NZVI may provide a rapid costeffective method to diminish the mass and ?strength? of DNAPL sources. Specific research objectives were to 1) obtain a fundamental understanding of the physical and geochemical processes governing the migration and distribution of polymer modified NZVI in DNAPL contaminated zones of a naturally heterogeneous subsurface where the free phase is entrapped in a complex architecture and 2) understand in situ treatment efficiency of DNAPL and dissolved chlorinated organics by polymer modified NZVI. Technical Approach Controlled investigations in small 1-dimensional and 2-dimensional laboratory test systems, large intermediate scale 2-dimensional test tanks and a field scale 3-dimensional tank and mathematical models were used to determine the primary physical and chemical principles controlling colloid transport (e.g. particle-particle interactions, fluid velocity, grain/pore size). Particle and environmental factors affecting NZVI reactivity and the ability to provide DNAPL targeting were also evaluated experimentally. The effect of porous media heterogeneity on nanoiron transport and the ability of emplaced NZVI to decrease the source mass and mass emission were evaluated in 2-dimensional small and intermediate scale tanks. Several combinations of nanoiron types and polymeric surface modifiers were used to identify optimal nanoiron surface properties. Finally, the transport the 2 types of NZVI was evaluated in the in a field-scale 3-dimensional tank study to determine transport distances in realistic heterogeneous porous media. Results The mobility of NZVI in porous media depends on the surface modifier properties seepage velocity, ionic strength and composition, pH, heterogeneity in the hydraulic conductivity field, and the presence of silica fines and clay fines. A small amount (e.g., 2 wt%) of fine particles and clay particles added to the sand matrix was found to limit NZVI transport. The presence of excess free polymer in the injection solution partially alleviates this problem. Transport was limited by aggregation of NZVI, and by deposition and pore plugging near

15. SUBJECT TERMS

16. SECURITY CLASSIFICATION OF:			17. LIMITATION OF ABSTRACT	18. NUMBER OF PAGES	19a. NAME OF RESPONSIBLE PERSON
a. REPORT	b. ABSTRACT	c. THIS PAGE			
unclassified	**unclassified**	**unclassified**	**Same as Report (SAR)**	**144**	

2. Front Matter

Table of Contents

List of Figures

List of Tables

3. Abstract

Chlorinated solvent DNAPLs can be consistent long-term sources of groundwater contamination. Remediation is costly and poses significant technical challenges. Nanoiron (NZVI) is a proposed in situ remediation agent for DNAPL source zones, but the effectiveness of NZVI treatment relies on the ability to emplace and retain the NZVI near or within the DNAPL source area. The dominant physical and chemical processes controlling the reactivity and migration and distribution of NZVI in the subsurface are poorly understood, however, making it difficult to ensure that NZVI will be delivered where it is needed and whether or not it can be an effective treatment alternative for DNAPL source zones.

Objectives:

The overall study objective was to evaluate if and where NZVI may provide a rapid cost-effective method to diminish the mass and "strength" of DNAPL sources. Specific research objectives were to 1) obtain a fundamental understanding of the physical and geochemical processes governing the migration and distribution of polymer modified NZVI in DNAPL contaminated zones of a naturally heterogeneous subsurface where the free phase is entrapped in a complex architecture and 2) understand in situ treatment efficiency of DNAPL and dissolved chlorinated organics by polymer modified NZVI.

Technical Approach:

Controlled investigations in small 1-dimensional and 2-dimensional laboratory test systems, large intermediate scale 2-dimensional test tanks and a field scale 3-dimensional tank, and mathematical models were used to determine the primary physical and chemical principles controlling colloid transport (e.g. particle-particle interactions, fluid velocity, grain/pore size). Particle and environmental factors affecting NZVI reactivity and the ability to provide DNAPL targeting were also evaluated experimentally. The effect of porous media heterogeneity on nanoiron transport and the ability of emplaced NZVI to decrease the source mass and mass emission were evaluated in 2-dimensional small and intermediate scale tanks. Several combinations of nanoiron types and polymeric surface modifiers were used to identify optimal nanoiron surface properties. Finally, the transport the 2 types of NZVI was evaluated in the in a field-scale 3-dimensional tank study to determine transport distances in realistic heterogeneous porous media.

Results:

The mobility of NZVI in porous media depends on the surface modifier properties, seepage velocity, ionic strength and composition, pH, heterogeneity in the hydraulic conductivity field, and the presence of silica fines and clay fines. A small amount (e.g., 2 wt%) of fine particles and clay particles added to the sand matrix was found to limit NZVI transport. The presence of excess free polymer in the injection solution partially alleviates this problem.

Transport was limited by aggregation of NZVI, and by deposition and pore plugging near the injection well. Magnetic attraction between NZVI particles caused rapid aggregation, but could be slowed through surface modification with polymers. NZVI suspensions of 6 g/L could move through model porous media, however the mobility decreases as NZVI polydispersity and concentration increases, primarily due to enhanced aggregation and straining. NZVI transport decreased with decreasing seepage velocity, however the extent depends on the type of polymer modifier. Mobility decreases with increasing ionic strength. In heterogeneous porous media, NZVI transports preferentially through high conductivity regions where fluid velocities are

greatest. NZVI deposits in regions of low flow and stagnation points. Injecting too much NZVI leads to pore plugging and diversion of dissolved contaminants around the reactive zone. A model coupling both the fundamental particle properties and flow fields can successfully model the transport and deposition of polymer modified NZVI at 6g/L in 2-D heterogeneous porous media. Injection methods that enhance fluid shear and disaggregate surface modified particles may improve mobility in situ.

The mobility significantly decreased as the solution pH was lowered from 8 to 6 due to enhanced aggregation and deposition. The presence of excess free polymer (~0.1wt %) in the injection solution increases mobility compared to cases where excess free polymer is not present. To maximize mobility, injection schemes should use low concentrations of excess free polymer (~0.1 wt%) in solution. Importantly, the presence of more than a few wt% of silica fines or clay (kaolinite) fines decreased mobility. Clay (kaolinite) had a greater effect than silica at the same wt%. NZVI transport in a field scale tank was less than what is predicted according to bench scale column experiments using model porous media. The low mobility was a result of the fines particles in the sand matrix, consistent with laboratory findings. The decreased transport was also a result of near-well plugging for one type of NZVI.

Polymer modified NZVI can be targeted to the NAPL-water interface in situ. Targeting is a result of the affinity of the polymer coated NZVI for the NAPL-water interface. The targetability increases as NAPL saturation decreases because of greater NAPL-water interface at low NAPL saturation. However, NZVI placed at the NAPL water interface is rapidly oxidized and does not enhance NAPL dissolution.

Surface modification required for mobility decreases the reactivity of RNIP by a factor of 5 to 24 depending on the type of surface modifier used. However, the rate of H_2 evolution is unchanged by the surface coatings. The reactivity is sufficient, however, for NZVI emplaced just down gradient of the source to decrease mass flux measured down gradient by up to 85%. . Emplaced NZVI acts primarily as a reactive barrier treating dissolved phase contaminants dissolved from the entrapped NAPL.

Benefits:

These results indicate that emplaced NZVI can decrease the flux of contaminants emanating from entrapped DNAPL, however they also suggest that NZVI available commercially today still needs to be optimized to work as an effective reactive barrier. This will require mobility of a greater fraction of the injected iron than found in this study. This will likely require innovative injection/emplacement methods. The lessons learned in this study can be used to determine the most promising innovative solutions to attempt in field trials (e.g. inclusions of free polymer in the injection solution), and be used by project managers to determine site conditions that are favorable or unfavorable for NZVI application. These results also provide guidance on the properties of NZVI with the greatest potential for success, i.e. those having sufficient reactivity to attenuate the concentrations of dissolved contaminants emanating from the source zone, but also having greater selectivity for the dissolved contaminants such that the NZVI reactive lifetime can be extended.

4. Objectives

Nanoscale zero-valent iron (NZVI) is proposed as an in situ chemical reduction agent for treating dense non-aqueous phase (DNAPL) source zones. NZVI have particle diameters ranging from 10nm-500nm. NZVI oxidation by chlorinated solvents such as trichloroethylene (TCE) causes the solvent to rapidly degrade to non-toxic products. To be effective, NZVI must be emplaced into the source zone in a manner that promotes contact between the NZVI and the target contaminants. An understanding of the dominant physical and chemical processes controlling the migration and distribution of nanoiron is needed to design effective NZVI injection strategies. Understanding the effects of NZVI treatment on DNAPL mass and mass emission from the source is needed to predict the effectiveness of NZVI for source zone treatment at a site. This project

- provides a fundamental understanding of physical and hydrogeochemical factors controlling NZVI migration and distribution in heterogeneous porous media,
- identified delivery methods and NZVI surface modifications that increase the probability of NZVI locating and remaining at the water-entrapped DNAPL interface or in the vicinity of the entrapped DNAPL,
- quantified the effect of NZVI surface modifications on NZVI reactivity, and
- determined the effect of NZVI treatment on mass emission from the source

Overall, the study evaluated if and where NZVI may provide a rapid cost-effective method to diminish the mass and strength of a DNAPL source. Specific hypotheses that guided the work were that 1) surface coatings on NZVI can be used to provide stable suspensions of NZVI that can be distributed into the source area and can target the DNPAL-water interface, 2) an injection method and rate, and NZVI surface properties, can be optimized for delivery based on site-specific physical characteristics and hydrogeochemistry, and 3) emplacement of NZVI into the DNAPL source zone, or as a reactive barrier down gradient of the source, will mitigate contaminant mass flux from the source zone, and 4) the effectiveness of NZVI for DNAPL source reduction can be assessed based on site specific parameters.

Organization of this report

A substantial body of research was produced during this project through a combination of experimental and modeling efforts. This report includes background information to place the work into the context of what was known at the initiation of the project (section 5), materials and methods (section 6), and results and discussion (section 7) according to the ten tasks. However, we present the results and discussion based on a logical flow of the topics rather than based on task order. A mapping of the SERPD project tasks with the sections of this report can be found in Appendix A.

5. Background

Chlorinated solvent DNAPL source zones are a consistent long-term source of groundwater contamination. Remediation is costly and poses significant technical challenges. Lifecycle treatment costs are estimated to exceed $2 billion for ~3000 contaminated DoD sites (Stroo et al. 2003). Even though the benefits of mass removal from a source zone in meeting regulatory goals are controversial, reducing entrapped DNAPL mass will lower the longevity of the source and reduce mass flux. This can mitigate future human and ecological exposure risk and the duration and cost of treatment (US EPA, 2003). Aggressive treatment technologies (e.g. surfactant and alcohol flooding, bio-augmentation, and chemical oxidation) remove DNAPL mass with the expectation of reducing the loading of the soluble constituents into the flowing groundwater. *In situ* treatment methods can accelerate the rate at which contaminated sites are restored back to an acceptable condition and lower the treatment costs, but all *in situ* treatment methods are limited by the ability to get the treating agent to the desired location, usually due to flow bypassing and inaccessibility. Recently, reactive nanoscale iron particles delivered *in situ* has been proposed and evaluated in the field with the goal of overcoming these limitations (Lowry 2007; Tratnyek and Johnson 2006; Zhang 2003). In principle, their small size (10-100 nm) provides an opportunity to deliver these remedial agents to subsurface contaminants *in situ*, and provides access to contamination trapped in the smallest pores in an aquifer matrix.

The Fe^0 in the NZVI is oxidized by the chlorinated solvent, which is subsequently reduced. For chlorinated hydrocarbons, the reduction typically results in the replacement of a chlorine atom with a hydrogen atom (Liu et al. 2005a; Liu and Lowry 2006; Nurmi et al. 2005).
The reduction of the contaminant is surface-mediated, and the NZVI is the reductant. The attractiveness of NZVI is that the particles have a high surface-to-volume ratio and therefore have high reactivity with the target contaminants. The following generalizations can be made about the reactivity and lifetime of all nanoparticulate remedial agents that are themselves the reactive material, i.e. not true catalysts according to the formal definition of a catalyst.

- Any process that affects the surface properties of the particles (e.g. formation of a Fe-oxide on the surface) can affect their *reactivity*.
- Any oxidant (e.g. O_2 or NO_3^-) competing with the target contaminant will utilize electrons and may lower the rate and efficiency of the NZVI treatment for the target contaminants.
- Reactive nanoparticles that serve as a reactant will have a finite lifetime, the length of which depends on the concentration of the target contaminant, the presence of competing oxidants, and the selectivity of the particles for the desired reaction.

Potential advantages of NZVI include the ability to provide significant DNAPL mass reduction without generating secondary waste streams, the potential for controlling the delivery distance (e.g. selective placement of subsurface treatment zones), and the potential to provide residual treatment capacity to mitigate mass flux from diffusion-controlled low permeability zones. NZVI also has the potential for lower initial capital and lifecycle costs compared to other source zone treatments if existing wells can be used for delivering the NZVI to the source. Realizing these benefits, however, requires a fundamental understanding of the factors affecting the migration and distribution of NZVI in the naturally heterogeneous subsurface.

More than 30 field demonstrations injecting NZVI have been conducted in the US and internationally, with varying degrees of success. The dominant factor limiting the success of NZVI treatment of DNAPL source zones is the low mobility of NZVI in the subsurface. Schrick et al (2004) was the first to report the low mobility of NZVI in water saturated porous media, and that enhanced mobility required the use of hydrophilic supports (Schrick et al. 2004). Quinn et al. (2005) describes the emplacement and performance of an emulsified zero valent iron (EZVI) at NASA's Launch Complex 34(Quinn et al. 2005). NZVI was injected into the subsurface at a TCE-contaminated aquifer, using a surfactant/vegetable oil emulsion to make the NZVI mobile. The technique demonstrated that TCE DNAPL was degraded using the EZVI, but also that EZVI could not be delivered significant distances or uniformly in the subsurface. Studies of NZVI, bare or surface modified, under typical groundwater conditions are needed to understand the effects of surface modifiers and geochemical effects on NZVI mobility in order to determine the expected mobility.

Relatively inexpensive direct push wells (GeoProbe™) have been successfully used to deliver NZVI to treat contaminated groundwater plumes containing chlorinated solvents (Varadhi et al. 2005) and a similar approach can be used in a DNAPL source area (Figure 5.1). Ideally, NZVI might locate itself at the water-entrapped DNAPL interface (Figure 5.1, inset) and degrade the DNAPL without causing unfavorable changes in the DNAPL architecture. For example, the high rate of injection of an NZVI slurry could disperse the entrapped NAPL, leading to greater surface area for DNAPL dissolution and a subsequent increase in mass emission from the source. Pore plugging due to emplaced NZVI may lead to unfavorable changes in flow through the entrapped DNAPL, also increasing the mass emission from that source. At the very least, the NZVI should remain in the general vicinity of the source area until the iron is completely reacted.

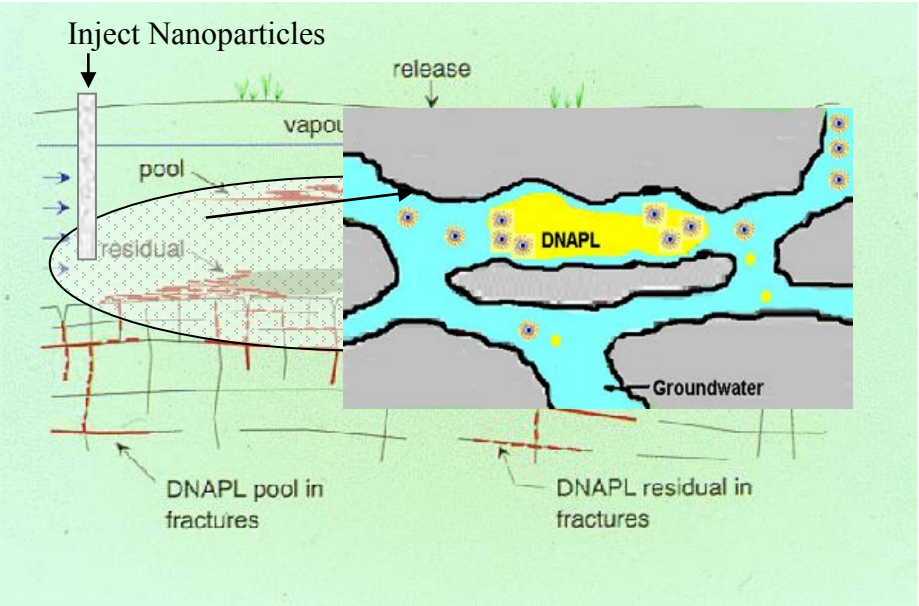

Figure 5.1. Conceptual model of nanoiron transport and targeting (inset).

The effectiveness of this approach is limited because the particles may not transport a significant distance from the injection well (Quinn et al. 2005; Saleh et al. 2007; Schrick et al. 2004), may not locate themselves at or near the DNAPL-water interface, or may continue to

transport down gradient away from the source zone. There are a number of reasons for this including heterogeneity, improper injection rate, NZVI aggregation and physical straining, sorption to aquifer media, and a lack of affinity for the DNAPL. It is also possible that aggregated NZVI or evolved H_2 gas trapped in pores will divert groundwater flow and NZVI around the DNAPL source. Poor understanding of the fundamental processes affecting the mobility of NZVI during injection and migration makes it difficult to optimize the rate and method of injection (e.g. direct push, hydraulic fracture), or to optimize the nanoiron properties for specific site geology and hydrogeochemistry. A brief description of the major processes expected to control the migration of nanoiron are described.

Delivering NZVI an appreciable distance in the subsurface requires that the NZVI be transported through water saturated porous media without aggregating and being filtered out by the media grains or organic carbon. DNAPL targeting requires that the NZVI properties change when they are in the vicinity of the DNAPL and remain there. The NZVI properties and flow conditions required to achieve these criteria must be determined. Recent advances in particle filtration (Tufenkji and Elimelech 2004) can be used to develop hypotheses about the impact of specific NZVI properties and physical and hydrogeochemical conditions affecting NZVI transport and fate in water saturated porous media. Experiments must be conducted to test these hypotheses, however, because filtration models employ simplifying assumptions that may not be applicable in naturally heterogeneous porous media or under injection conditions where particle concentrations are high (1-10 g/L) and where the fluid velocity is high and no longer laminar.

One potentially important process limiting NZVI transport is the aggregation and filtration of the particles. All nanoparticles (colloids) will tend to aggregate into larger particles which are easily filtered out by adsorption to the porous media grains. Surface coatings can be used to decrease aggregation and attachment of to aquifer media grains. Several chemical factors will control the aggregation and attachment potential of surface-modified NZVI particles including pH, ionic strength, and surface charge, and the presence of excess free polymer in solution. Physical factors also control the filtration efficiency including porewater velocity, aquifer grain/pore size, and physical and chemical heterogeneity (e.g. grain type).

5.1 Potential NZVI surface coatings.

Typical NP surface coatings include polymers, polyelectrolytes (charged polymers), and surfactants (Table 5.1.1). Both natural and synthetic varieties of each are available. In general, high molecular weight polymers (synthetic or natural) provide steric repulsions that may limit NP-bacteria interactions. Polyelectrolytes are large polymers containing charged functional groups (anionic or cationic) and provide electrosteric repulsions. Surfactants can provide electrostatic repulsive or attractive forces (depending on their charge), but are less effective than polymers or polyelectrolytes because their small size is unsuitable for steric repulsions. Polymers typically adsorb strongly (effectively irreversible) to NPs while surfactants adsorption is more easily reversible(Evans and Wennerstrom 1999; Fleer et al. 1993).

Poly(methacrylic acid)-b-poly(methylmethacrylate)-b-poly(styrene sulfonate) triblock copolymers (PMAA-PMMA-PSS), PSS homopolymer polyelectrolyte, sodium dodecylbenzene sulfonate (SDBS), polyethylene glycol (PEG), carboxymethyl cellulose (CMC), and guargum have been shown to adsorb to and stabilize dispersions of nanoiron and Fe-oxide NPs and/or to improve particle mobility in the environment due to steric, electrosteric, or electrostatic repulsions between the particles and between the particles and soil grains (He et al. 2009; He et al. 2007; Saleh et al. 2005a). Poly(aspartate), an anionic polypeptide, adsorbs to iron oxide

surfaces via acid-base interactions through the carboxyl groups (Chibowski and Wisniewska 2002; Nakamae et al. 1989). Alkyl polyglucosides are an emerging class of surfactant synthesized from renewable raw materials and are nontoxic, biocompatible, and biodegradable. They adsorb to metal oxide surfaces(Matsson et al. 2004). The latter, poly(aspartate) and alkyl polyglucosides are desirable due to their low cost and "green" nature and widely used as detergents in manufacturing.

5.2 Interaction potential affected by polymer surface modification

For bare nanoparticles, aggregation and deposition in aqueous environment are generally modeled using Derjaguin-Landau-Verwey-Overbeek (DVLO) theory (Elimelech et al. 1995). According to classical DLVO theory, the van der Waals forces (V_{vdW}) are the primary attractive force, while repulsive forces are derived from the electrostatic double layer (V_{ES}). Polymeric surface modification can enhance dispersion stability of NZVI by providing additional electrosteric repulsions (a combination of osmotic and elastic repulsions) against van der Waals attraction which can prevent agglomeration(Phenrat et al. 2008). In addition to electrosteric repulsion, the adsorbed macromolecule layer also serves as a lubricant. The macromolecule yields a higher local viscosity compared to the bulk, resulting in the reduction of the frictional force between a particle and a collector (Cayer-Barrioz et al. 2009). It should be noted that electrosteric repulsions may result in reversible deposition in a secondary minimum (Franchi and O'Melia 2003; Phenrat et al. 2009a) which makes the attachment efficiency sensitive to fluid velocity (e.g. sliding and rolling as a result of the reduced frictional force) and solution chemistry (Cayer-Barrioz et al. 2009; Franchi and O'Melia 2003; Phenrat et al. 2009a; Phenrat et al. 2008). Models are available to calculate the magnitude of all of the forces acting on a polymer or polyelectrolyte coated NZVI particle (Israelachvili 1992), (Brant et al. 2007; de Vicente et al. 2000) (Fritz et al. 2002) (Cayer-Barrioz et al. 2009).

Table 5.1.1. Potential coatings from each class to be evaluated.

Coating	Charge	Stabilization type	Relevance
Polymers			
Polyethylene Glycol (PEG)	Nonionic	Steric	Common non-toxic polymer used to stabilize NP dispersions. Adsorbed PVA reduces bacterial adsorption to surfaces(Koziarz and Yamazaki 1999). Cellulose is used to prepare stabilized nanoiron dispersions(He and Zhao 2005). Inexpensive and biodegradable.
Polyvinyl Alcohol (PVA)	Nonionic	Steric	
guargum	Nonionic	Steric	
Polyelectrolytes			Used to prepare stabile nanoiron dispersions that partition to the TCE/water interface (Saleh et al. 2005a; Saleh et al. 2005b). PSS homopolymer is a common inexpensive alternative used to stabilize NP dispersions. Polylysine is a biodegradable polypeptide and bactericidal(Roddick-Lanzilotta and McQuillan 1999). Poly(aspartic acid) should be biodegradable and less bactericidal.
Triblock Copolymers ($PMAA_x$-$PMMA_y$-PSS_z)	Anionic	Electrosteric	
Polystyrene Sulfonate	Anioinc	Electrosteric	
Polylysine	Cationic	Electrosteric	
Poly(aspartic acid)	Anionic	Electrostatic	
Carboxymethyl cellulose	Anionic	Electrosteric	
Surfactants			SDBS is a common anionic surfactant shown to enhance nanoiron mobility(Saleh et al. 2007) but resists biodegradation. Alkyl polyglucosides are biodegradable(Matsson et al. 2004)
SDBS	Anionic	Electrostatic	
Alkyl polyglucosides	Nonionic	Steric/ Hydration	

5.3 Effect of pH, ionic strength, and surface charge.

In the absence of steric or electrostatic stabilization, NZVI will aggregate into larger particles that are essentially immobile in water saturated porous media under typical groundwater conditions (Schrick et al. 2004). Surface modifications using an organic layer (polyelectrolyte or surfactant) significantly deceases aggregation and improves the colloid stability (Saleh et al. 2005a), decreases NZVI affinity for the media grains, and enhances particle migration (Schrick et al. 2004). The improved colloidal stability and mobility is provided by electrostatic and steric repulsions from the coatings which inhibits aggregation and attachment to aquifer media as described in the previous section. Solution pH, ionic strength, and the surface charge on NZVI will affect the magnitude of the electrosteric repulsions and hence the stability of nanoiron suspensions. As the pH moves away from the point of zero charge, pH_{pzc}, the nanoiron surface charge becomes greater and the ability to maintain a stable suspension increases due to electrostatic stabilization. At $pH<pH_{pzc}$ NZVI maintains a net positive charge, and for $pH>pH_{pzc}$ NZVI maintains a negative charge. Most aquifer minerals and soil organic carbon are negatively charged, so NZVI with a negative surface charge should resist sticking to those surfaces. The pH_{pzc} of unmodified NZVI ranges from ~5.6 to ~8, indicating that without NZVI surface modification the site-specific soil pH, which ranges from 6 to 8, could have a significant impact on the nanoiron surface charge (i.e. change from a net negative to a net positive charge) and its mobility. The pH of groundwater could also affect that interaction between the NZVI and the charged polymer coating, especially since the pHpzc for NZVI is near neutral. This will affect the conformation of the coating on the surface and the stability against aggregation.

For purely electrostatically stabilized particles, the ionic strength will affect the ability of NZVI to maintain a stable suspension. As the ionic strength increases, the electric double layer compresses and the effective net charge on the particles decreases leading to aggregation or attachment to aquifer media. A higher ionic strength, or the presence of divalent cations (e.g. Ca^{2+} and Mg^{2+}) will lead to increased particle aggregation and decrease the mobility of nanoiron. Modifying the NZVI surfaces with high molecular weight polyelectrolytes increases their surface charge and also physically separates particles (steric stabilization). This provides electrosteric stabilization that will decrease the aggregation and attachment potential of NZVI and increase their transport distance. Further, electrosteric repulsions should not be affected as significantly by changes in ionic strength or composition.

5.4 Porewater velocity and aquifer grain/pore size.

Injecting NZVI into a well will result in radial flow away from the well. The flow velocity will be highest at the well and decrease with radial distance from the well, eventually decreasing to the natural groundwater velocity dictated by the natural gradient and aquifer permeability. NZVI will therefore be subjected to a wide range of flow velocities during injection and migration that may affect the filtration efficiency (Lecoanet and Wiesner 2004). Based on filtration theory it is expected that higher injection rates will increase the radius of influence by decreasing the efficiency of all three attachment mechanisms (diffusion, interception, and sedimentation) and the time for particle attachment to collector grains. Correlating the filtration efficiency with the pore fluid velocity and site geochemistry will help to predict the radius of influence for a given nanoparticle size and surface charge density. This understanding is needed to plan an injection scheme for a given site to achieve a specific region of treatment.

Contaminated sites cover a range of aquifer material with different grain/pore sizes and permeability. It is important to correlate grain/pore size and degree of sorting with the expected

radius of influence for a given injection velocity to determine the types of soils that are amenable to NZVI injection. It is anticipated that the filtration efficiency increases as the particle size of the aquifer media decreases relative to the size of the NZVI, and as the degree of sorting and permeability decreases leading to a decrease in the radius of influence of the injection wells.

5.5 Physical heterogeneity

Subsurface heterogeneity can impact the ability to deliver NZVI, but not necessarily in a negative way. The distribution of DNAPL after a spill is controlled by many factors that include the spill configuration (time, rate and volume of spill) and the underlying soil and moisture conditions. After entering the saturated zone, the DNAPL migrates by the action of gravity and capillarity. The fluid properties in combination with characteristics of the soil both at the pore and macro-scale will determine how the DNAPL ultimately gets distributed (Illangasekare 1998; Illangasekare et al. 1995). In general, DNAPLs migrate through fingering and pools at capillary barriers (coarse-fine interfaces). The final entrapment architecture will contain both residual zones and pools. The pools that contribute to the longevity of mass flux generation are formed in the coarse sand formations. These coarse sand layers also preferentially carry the aqueous phase and may be used to effectively deliver the nanoiron to the locations where the DNAPL is entrapped.

Chemical heterogeneity also exits. For example, some aquifers may contain fines of clay minerals whereas others contain fines of quartz or sandstone. These fines have different surface chemistry and will interact with surface-modified NZVI differently. It is important to understand how the collector grain surface chemistry affects the mobility of surface-modified NZVI in order to assess the potential for success at a given site.

5.6 DNAPL targeting

There are two mechanisms by which NZVI may target DNAPL. First, the hydrophobic nature of the polymer-coated surface may provide a thermodynamic affinity for the DNAPL-water interface. Polystyrene sulfonate-coated silica nanoparticles (~20 nm), and triblock co-polymer modified NZVI have been shown to target the TCE-water interface ex situ with sufficient energy input (Saleh et al. 2005a; Saleh et al. 2005b), presumably due to the hydrophobic nature of the polystyrene polymer grafted to the particles. PSS homopolymer and diblock copolymer modified NZVI were unable to emulsify any NAPL phase. Particle surface coatings with the most apolar characteristics should provide the best NAPL interfacial targeting. A second potential targeting scheme is to use a polymer or surfactant that enables transport, but is released in the presence of TCE leaving behind bare NZVI that is immobile. The targeting aspect is the highest risk component of the proposed research, but some form of DNAPL targeting should be possible. For example, making use of multi-level samples to deliver NZVI into high hydraulic conductivity zones that are the conduit for most of the TCE mass emission form the source may allow for selective placement into critical areas of the source zone. Information gathered on the fundamental parameters controlling the movement of NZVI in heterogeneous porous media can be used to evaluate alternative methods to deliver NZVI to the source area and ensure that the NZVI remains there, e.g. using injection rates that provide a known radius of influence, or coatings than can are tuned to the site specific geochemistry to provide a specific radius of influence.

5.7 Impact of NZVI emplacement technique and location on flux reduction.

The goal of NZVI treatment is to decrease the DNAPL mass and to decrease the mass flux from the source area. The NZVI emplacement method will affect the ability to meet this goal. NZVI can be injected directly into the source area (A), up gradient of the source area (B), or down gradient of the source area (C) (Figure 5.5). Precisely locating the source area is difficult and NZVI injection directly into this area may result in unwanted DNAPL migration so injection at point A is probably not practical. Injecting NZVI down gradient of the source (C) is a reasonable approach as DNAPL targeting and the ability to concentrate NZVI at the down gradient edge of the source could provide residual treatment, while simultaneously providing plume treatment if a fraction of the nanoiron were to also transport down gradient. Injecting up gradient of the source (B) is also reasonable. The intent is to allow NZVI to transport down gradient through high permeability zones which will deliver the nanoiron to the DNAPL. This approach may load iron at the up gradient edge of the source and be less effective than injecting at point (C). Injection at both locations B and C may ultimately provide the best mass flux reduction. The benefit of multiple injection locations will have to be weighed against the increased cost. Ideally, injecting over the entire depth of the source would provide the best results. There have been no reports of the effect of NZVI placement on mass emission from an entrapped DNAPL source.

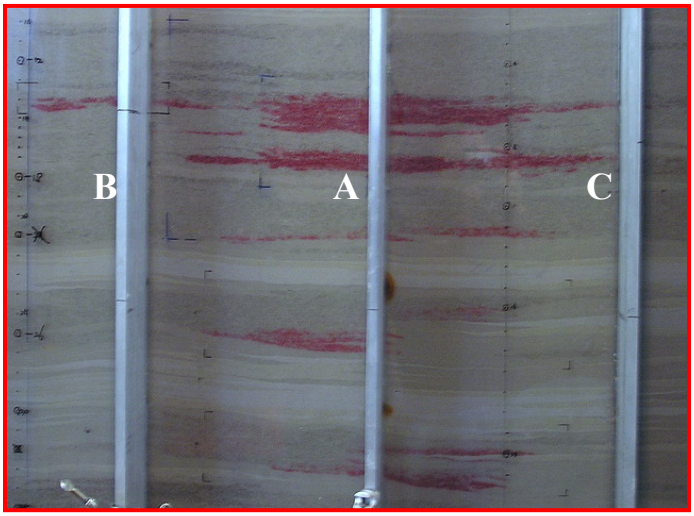

Figure 5.5 Potential nanoiron injection points around a DNAPL (red) source zone.

6. Materials and Methods

6.1 Materials.

Common materials used in all experiments include the following chemicals and media.

Uncoated NZVI. The NZVI used in this study, Reactive Nanoscale Iron Particles (RNIP), is supplied by Toda Kogyo, Inc. (Onoda, Japan). The properties of these materials have been reported previously(Liu et al. 2005b; Nurmi et al. 2005). Briefly, uncoated RNIP, is comprised of ~20 to 70 nm Fe^0/Fe_3O_4 core-shell iron nanoparticles. They are received as a 250 g/L slurry (pH=10.6 to 11) in a 1-L container. Although the particles are shipped in an inert headspace and stored in an Ar-filled glovebox to avoid exposure to O_2, the particles are slowly oxidized by water to form H_2 and OH^- and the Fe^0 content of the particles decreases over the life of the particles. The Fe^0 content of the fresh particles we receive is approximately 50 wt %, with a Fe^0 ½ life time of roughly 3 months when stored in water (Liu and Lowry 2006). It is important to note that NZVI is oxidized by water to form H_2 and OH^-. This consumes Fe(0) in the particles, thereby decreasing their ability to degrade contaminants. The rate of oxidation of the Fe(0) depends on particle size and pH of water. Very small particles are more reactive and oxidize rapidly (hour to days), larger particles can last for many months (Liu and Lowry, 2006). Storing NZVI in high pH water can slow its oxidaiton, allowing for longer storage times in water, but the reaction will ultimately consume all of the Fe(0). Storing NZVI in non-aqueous based fluids (e.g. alcohol or glycols) can extend their shelf life, essentially indefinitely if one excludes air. Drying NZVI and storing it anaerobically can also maintain the Fe(0) content, but this leads to irreversible aggregation that hampers delivery in situ. Synthesizing NZVI prior to injection, or storing it in non-aqueous fluids is the best option at present. The Fe(0) content of the RNIP is measured prior to use in any experiment. A summary of important RNIP properties is provided in Table 6.1.

Two additional types of NZVI products evaluated in a treatability study for a TCE contaminated area using NZVI: Reactivity and Reactive Life Time (Section 7.7.1). These were RNIP-R (Toda America, Onada, Japan) and Z-Loy (On Materials). Z-Loy™ is a nanocomposite between a zerovalent metal exterior and a less-dense ceramic core while RNIP-R is bare RNIP modified by a proprietary catalyst to increase reactivity and dechlorination rate.

Table 6.1. RNIP properties (Liu et al. 2005a; Liu et al. 2005b; Phenrat et al. 2007)

Primary particle size	20-70nm [a]
N_2 BET surface srea	15-23 m^2/g [a]
Density	6.15 g/cm^3 [a]
Shell (Fe_3O_4) thickness	5-10 nm [a]
Shell composition[a]	Fe: 26%
	O: 52-54%
Crystallinity	crystalline [a]
Fe^0 content	27-70%[a]
Zeta potential (pH=7.4, 1 mM $NaHCO_3$)	-31.7±0.8[b]
Saturation magentization	570 kA/m[b]

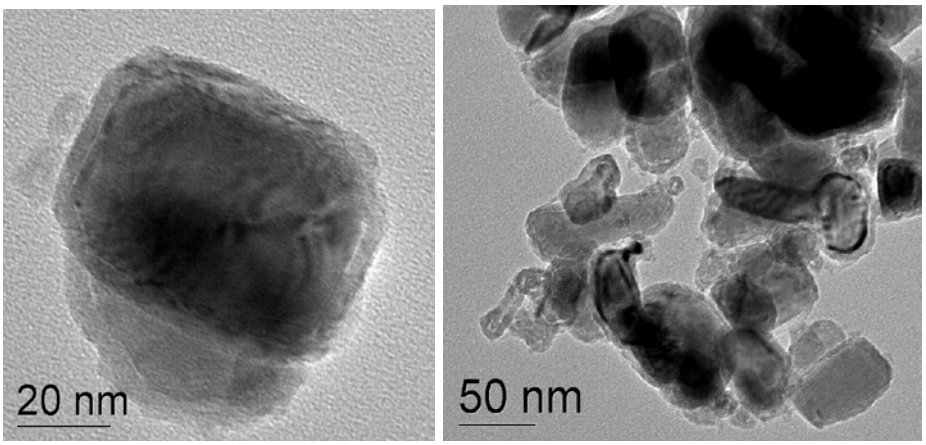

Figure 6.1. TEM image of fresh RNIP particles. Primary particles are 20-70 nm and are present as aggregates on the TEM grid.

Polymer modified NZVI. Several types of polymer modified NZVI were used in this study. Two were supplied by Toda Kogyo Corp., MRNIP and MRNIP2, and others were synthesized by modifying uncoated RNIP with various polymer modifiers. MRNIP is a sodium polyaspartate (MW of 2,000–3,000 g/mol) stabilized RNIP supplied by Toda Kogyo Corp . MRNIP2 is Fe^0 nanoparticles modified by the weak polyelectrolyte olefin-maleic acid co-polymer (MW=16,000 g/mol) also supplied by Toda Kogyo, Japan. The stock MRNIP and MRNIP2 was 160 g/L and stored under inert atmosphere (N_2) in a glovebox. 15 mL of MRNIP and MRNIP2 stock was sonicated using ultrasonication (Fisher Scientific Model 550F Sonic Dismembrator at power level =3) for 15 minutes prior to dilution to the desired concentration. MRNIP2 has polymer adsorbed onto its surface to provide electrosteric repulsions against agglomeration and deposition. In addition, the MRNIP2 dispersion contains unadsorbed (free) polymer (~3 wt%).

To test the effects of various coatings on NZVI mobility, various polymeric coatings were used to modify uncoated RNIP using methods described in Phenrat et al., 2008 (Phenrat et al. 2008). These coatings included a 75,600 g/mol tri-block co-polymer $p(MAA)_{48}$-$p(MMA)_{17}$-$p(SS)_{650}$ synthesized using atom transfer radical polymerization (ATRP) (Saleh et al. 2005a), polyaspartate (PAP, 2000 to 3000 MW and 10,000 MW) (See 6.4.1), poly(styrene sulfonate) (PSS) (MW= 70k and 1M), and carboxymethyl cellulose (CMC) (MW=90k and 700k). PSS and CMC were from Aldrich. PAP at molecular weight of 2-3 kg/mol and 10 kg/mol was from Lanxess and NanoChem Solutions Inc., respectively. PAP consists of aspartic acid as a monomer unit with two different hydrolyzed bonds (α and β) and amide bonds. Aspartic acid is one of the 20 natural proteinogenic amino acids which are the building blocks of proteins. The properties and structure of these modifiers are summarized in Table 6.2.

Quality of commercial NZVI. The reactivity of NZVI will affect its ability to degrade contaminants in situ, especially since emplaced NZVI ultimately serves as a reactive barrier where dissolved phase contaminants flow through the reactive media. The various NZVI types evaluated here had different reactivity and different reactive lifetimes. The variability is a result of differences in particle size, aggregation state, modifier type, extent and type of oxide layer on the particles, and impurities in the iron (e.g. carbon). The reactivity may also vary from batch to batch, depending on how well controlled the synthesis process is. The site conditions and

composition of the site groundwater may also affect reactivity (e.g. presence of NOM or nitrate) (Liu et al., 2007). It is not possible to *a priori* determine the reactivity of a particular NZVI based solely on characterization of the iron (e.g. Fe(0) content, polymer content) and groundwater. As such, the reactivity of particular NZVI must be evaluated in the groundwater matrix at the site of intended use.

Chemicals. All water was deionized by reverse osmosis and further purified by a MilliPore MilliQ Plus system of ion exchange and carbon cartridges, and filtered with 0.45 μm nominal pore size polycarbonate filters. All chemicals were reagent grade and 99+% pure and used without further purification, unless noted. Sodium chloride, calcium chloride (anhydrous), sodium bicarbonate were supplied by Fisher Scientific. PCE, TCE, cis-1,2-dichloroethylene(c-DCE) (98%), trans-1,2-dichloroethylene(t-DCE) (98%), and 1,1-dichloroethylene(1,1-DCE) (99%) were from Aldrich. Olefin standards (1000 ppm of ethylene, propene, butene, pentene, hexene), paraffin standards (1020 ppm of methane, ethane, propane, butane, pentane, hexane), acetylene (1000 ppm and 1 %), ethylene (1 %), ethane (1 %), vinyl chloride (VC) (10 ppm) and hydrogen (1.08 %) were from Alltech. The balance of each gas standard was N_2 and all reported concentrations are ±2% of the reported concentration. Ultra high purity argon, hydrogen (5.18 %), and N_2 were from Butler Gas products (Pittsburgh, PA).

Sand. Model silica sand of approximately 300 μm average diameter (d_{50}) was used as porous matrix purchased from Agsco Corp. The grain shape of the sand used is spherical and the sand had specific gravity of 2.65 g/cc and pH of 6.8-7.2. In 2-D flow cells, six types of sorted sand (#8, #16, #30,#50, #70, and #125) obtained from crushed sandstone (GRANUSIL silica sand by UNIMIN Corporation) were used to create both heterogeneous and homogeneous media (Barth et al. 2001). These test sands have been extensively used in Dr. Illangasekare's lab over the last 16 years and all relevant properties have been well characterized (e.g. grain size distribution, porosity, hydraulic conductivity, dispersivity, retention functions and relative permeability). The hydraulic conductivity of these sands varies from 1036.8 m/d for #8 to 3.6 m/d for #125. Following the testing approaches we have developed, simple structured heterogeneities were created in the 2-D cells. These include layers of different soils (stratifications) and soil lenses (e.g. a silty sand lens in a homogenous coarse formation). The structured packing configurations in the 2-D cells allowed us to capture the processes of NZVI transport in simple 2-D flow fields.

6.2 General approach and methods

The project used a mix of experimental measurements and modeling to achieve the stated goals. The general technical approach for the research is provided in Figure 6.2. The general approach was to use column reactors and batch reactors to determine the fundamental hydrogeochemical processes affecting NZVI transport in porous media, its reactivity, and its ability to target entrapped DNAPL. Results from these studies were used to develop hypotheses regarding NZVI behaviors in more complex 2-dimensional flow cells, and to parameterize numerical models used to model their behavior. The predictions of those models were then tested using 2-dimensional flow cells, and modified as needed for the higher dimensionality of flow. Finally, the results from both the columns and 2-dimensional flow cells were used to design intermediate scale 2-dimensional flow experiments to determine the effect of NZVI emplacement on mass emission

from the entrapped NAPL, and to design large scale experiments to test the ability of NZVI to be injected under realistic conditions.

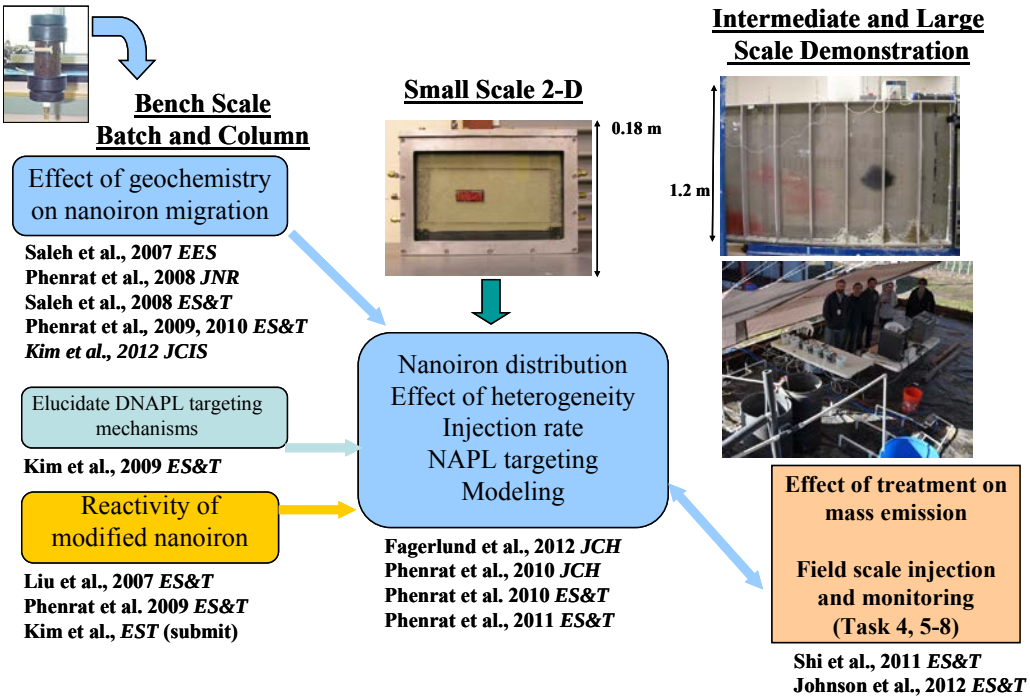

Figure 6.2. General technical approach for the project and resulting publications.

6.2.1 Surface modification and characterization

Bare Particle Characterization. The magnetic properties, electrophoretic mobility, particle size, hydrodynamic radius, and Fe^0 content were determined at 25 °C (298 K) as described in Phenrat et al., 2007 (Phenrat et al. 2007). The saturation magnetization and coercivity were analyzed by Superconducting Quantum Interference Device (SQUID)*(Clarke and Braginski 2004)*. The saturation magnetization is the maximum induced magnetic moment for a material when all magnetic domains in a particle are aligned parallel. A magnetic field of the opposite direction is then applied to reduce the remanent magnetization to zero. This demagnetizing field is the coercivity. The electrophoretic mobility of bare RNIP was measured for dilute dispersions (~30 mg/L) in 1 mM $NaHCO_3$ with a Malvern Zetasizer (Southborough, MA). Measured electrophoretic mobilities were converted to apparent ζ-potentials using the Helmholtz-Smoluchowski relationship. The Fe^0 content of RNIP was determined (separately from total iron) by acid digestion in a closed container with headspace as described in Liu et al., 2005 (Liu et al. 2005b). H_2 produced from the oxidation of Fe^0 in RNIP by H^+ is used to quantify the Fe^0 content of the particles.

Surface modification.
To obtain polymer modified RNIP, bare RNIP (at a desired concentration) was mixed with polyelectrolyte (at a desired concentration) in 1mM $NaHCO_3$. 48 hrs was typically allowed for physisorption to reach equilibrium as described in Phenrat et al., 2008 (Phenrat et al. 2008). After equilibration, the dispersions were centrifuged at 27,500 rpm for 80 min, washed to

remove free polymer from solution, and re-suspended in a desired electrolyte concentration. This process was repeated three times followed by ultrasonication for 10 minutes to remove all excess free polymer in the solution. The mass of polymer adsorbed on NZVI was determined by an adsorption isotherm for the polymer on 3g/L NZVI suspensions as described in Kim et al., 2009 (Kim et al. 2009). The adsorbed polyelectrolyte layer properties, including extended layer thickness, was determined to be important for understanding aggregation potential and transport. These properties were determined using electrophoretic mobility (EPM) measurements and Ohshima's soft particle theory as described in Phenrat et al., 2008 (Ohshima 1995). Use of the Ohshima method requires data for the EPM for both the bare particles and for the polyelectrolyte-coated particles as a function of the bulk solution ionic strength. The EPM was measured in 20 mg/L solutions of the washed, polyelectrolyte-coated RNIP for NaCl concentrations ranging from 1 to 61 mM (pH 8.5±0.1) after 3 hours of equilibration at the salt concentration used. It is assumed that the conformation of the adsorption layer is independent of the ionic strength over this range.

6.2.2 Aggregation

Aggregation of dilute suspensions. DLS (Malvern Zetasizer, Southborough, MA) was used to monitor the time-dependent hydrodynamic diameter of aggregates during the early stage of aggregation where the nanoparticles are too small to be investigated by the optical microscope. Dilute samples were used in order to avoid multiple scattering which can make data interpretation difficult. The CONTIN algorithm was used to convert intensity autocorrelation functions to intensity-weighted particle hydrodynamic diameter distributions, assuming the Stokes-Einstein relationship for spherical particles.

Table 6.2. Property and structure of surface modifiers

Acronym	Chemical name /category	M_w[a] (kg/mole)	D_P[b]	K_p	Structure
PSS70K	Poly(styrene sulfonate) /anionic polyelectrolyte	70	340	11.5±2.4	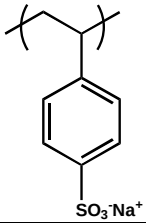
PSS1M		1,000	4,850	18.2±1.7	
CMC90K	Carboxymethly cellulose /anionic polysaccharide	90	342	11.9±2.4	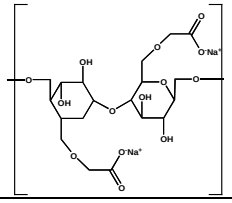
CMC700K		700	2,661	15.2±0.4	
PAP2.5K	Polyaspartate /anionic biopolymer	2-3	16	7.3±2.1	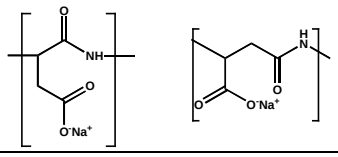
PAP10K		10	64	7.9±1.5	

[a] Molecular weight of the polyelectrolytes (g/mol), M_w, as specified by the manufacturers. [b] Average degree of polymerization, D_p, is estimated by dividing M_w of a polymer by the molecular weight of a monomer unit.
[c] Reported error is one standard deviation from the mean of K_p (dimensionless) measured at polyelectrolyte concentrations of 5 and 10 mg/L

In-situ optical microscopy. The aggregation and gelation of RNIP dispersions were observed in situ using optical microscopy (Nikon Eclipse TE300, Hauppauge, NY). A 4.5-mL capped UV-vis cuvette containing 4-mL of a RNIP dispersion at concentrations ranging from 60 to 425 mg/L was placed horizontally into the microscope. Images of RNIP aggregates in the dispersion were recorded 15/sec for 35 minutes at 400X magnification. All measurements were conducted at 25°C.

Sedimentation. NZVI sedimentation was determined for concentrations ranging from 2 mg/L (Φ=3.2 X 10^{-7}) to 1320 mg/L (Φ=2.1 X 10^{-4}) by monitoring the optical absorbance at 508 nm as a function of time by UV-vis spectrophotometry (Varian, Palo Alto, CA). All measurements were made at 25°C. Standard curves (Absorbance vs. concentration) were conducted for all polymer modified NZVI used in this study.

6.2.3 NZVI mobility in water-saturated sand columns (1-D)

Column experiments. The mobility of surface modified NZVI as a function of modifier type, particle concentration, pH, porewater velocity, grain size distribution, ionic strength, and ionic composition were determined from breakthrough curves collected in water saturated sand columns. The experimental apparatus consists of a stainless steel column with 1.1 cm ID and column lengths ranging from 10 cm to 61.3 cm length having an empty bed volume ranging from 9.4 mL to 57.4 mL as described in Phenrat et al., 2009 (Phenrat et al. 2009a). Columns were packed wet in all cases to avoid issues with entrapped air.

The column experiments were generally conducted as follows: The packed column was flushed with desired electrolyte concentration for more than 10 pore volumes (PV) to remove any background turbidity and to attain uniform collector surface charge. A suspension of polymer coated RNIP (NZVI) at a specified ionic strength was then homogenized using Sonic Dismembrator for 30 min before pumping into the column. The particle sample was kept under constant sonication during the injection process. After 1PV of particle injection, a background electrolyte of matching ionic strength is pumped through the column for more than 4 PVs to flush out any mobile particles. Effluent samples were collected using a fraction collector at 100 s intervals and then analyzed using either UV-vis spectrophotometer at 508 nm wavelength to determine the particle concentration or acid digestion of NZVI followed by atomic absorption to quantify total iron.

The column data was interpreted using deep a bed filtration mode, unless specified. According to deep bed filtration models, the extent of migration of colloids in saturated porous media can be estimated from the collision efficiency (α) which represents the probability that a particle successfully attaches to the surface of a collector (e.g. sand grain) once they come into contact. α is defined as the ratio between the actual dimensionless deposition rate of particles (η) and the dimensionless deposition rate under barrierless interaction (η_0) where all collisions result in attachment *(Elimelech et al. 1995)*.

$$\alpha = \frac{\eta}{\eta_0} \tag{6.6}$$

From column experiment, α is obtained from particle breakthrough at steady-state, C, in a packed column (a clean bed media of length L packed with a collector with an average radius a_c, porosity ε, and initial particle concentration C_0 (eqn.6.7).

$$\alpha_{\exp} = -\ln\left(\frac{C}{C_0}\right)\frac{4a_c}{3(1-\varepsilon)\eta_0 L} \tag{6.7}$$

η_0 was calculated using eqn 6.8 (Tufenkji and Elimelech 2004).

$$\eta_0 = 2.4A_S^{1/3}N_R^{-0.081}N_{Pe}^{-0.715}N_{vdW}^{0.052} + 0.55A_S N_R^{1.675}N_A^{0.125} + 0.22N_R^{-0.24}N_G^{1.11}N_{vdW}^{0.053} \tag{6.8}$$

Where A_s is a porosity-dependent parameter, N_R is respect ratio, N_{Pe} is Peclet number, N_{vdW} is van der Waals number, N_A is attraction number, and NG is the gravity number as defined in Tufenkji and Elimelech, 2004 (Tufenkji and Elimelech 2004).

6.2.4 Transport and emplacement of polymer modified NZVI in a 2-D flow through cell

A bench-scale 2-D flow cell (30 cm x 18 cm x 2.5 cm) was used in this study to model transport and deposition in porous media. Three different sands (Unimin, New Canaan CT) were used including fine (#140), medium (#50), and course (#16) sand with d_{50} of 99, 330, and 880 μm, respectively. The cell was packed wet as described in Phenrat et al. 2010 and Phenrat et al., 2011 (Phenrat et al. 2010a; Phenrat et al. 2011) to achieve the layered packing. The layers of fine, medium, and course sand had an average porosity of 0.3, 0.3, and 0.4, respectively. The total pore volume of the flow cell was ~660 mL. A brass tube was used as an NZVI injection well. A hole (0.1 cm in diameter) was made in the side of the tube for injecting NZVI in the fine sand layer above the course sand layer and below the medium sand layer. NZVI dispersion was injected through the brass tube using a peristaltic pump. A solution of 1mM $NaHCO_3$ was supplied at 0.3 ml/min through three side ports on the left cell to simulate the flow of background groundwater in the subsurface (30 cm/day).

One pore volume (~ 660 mL) of polymer modified RNIP in 1mM $NaHCO_3$ was injected through the brass tube using a peristaltic pump at the flow rate of 20 ml/min followed by flushing with seven PVs of 1mM $NaHCO_3$. A time series of photos was taken to illustrate the transport of NZVI. NZVI particles eluted through the cell were collected over time to develop a breakthrough curve. The concentration of eluted NZVI was quantified using atomic adsorption spectrometer after acid digestion as previous described (Phenrat et al. 2009a). The spatial distribution of deposited MRNIP2 after seven-PV of flushing was measured by removing the back cover of the cell and coring samples (25 to 30 points throughout the 2-D sand packing) followed by magnetic separation to recover deposited particles, acid digestion, and measurement of total Fe using flame atomic absorption spectrometry. The NZVI deposition maps were created from 25 to 30 data points using SigmaPlot 11 (Systat Software, Inc., San Jose, CA).

6.2.5 COMSOL simulation of water flow in the 2-D flow cell

Water flow through the 2D flow cell was simulated to determine the velocity distribution in the layers in the cell. The two-dimensional groundwater flow equation (Bear 2007) based on Darcy's Law was solved for the flow cell using COMSOL Multiphysics Software (COMSOL, Inc., Burlington, MA). Constant flow boundary conditions were set at the inlet and outlet ports represented by lines in the 2D model. The remaining boundaries including top, bottom and front and back were given no flow boundary conditions. The single-sided injection hole at the bottom of the brass tube was represented in 2D Cartesian coordinates as a rectangular closed domain with a size equal to the diameter of the hole. Constant flow of 20 mL/min was given to the right hand side boundary of the rectangular domain to represent injection from the single-sided brass tube. Complete details of the modeling procedure can be found in Phenrat et al., 2010 (Phenrat et al. 2010d).

6.2.6 Ex situ targeting potential

We adapted and modified the Pickering emulsion protocol (Saleh et al. 2005a) as a rapid screening test for *ex situ* NAPL targeting potential of polymer modified NZVI. Dodecane ($CH_3(CH_2)_{10}CH_3$) (>99%) (reagent plus grade, Sigma-Aldrich) was used as a model NAPL compound in this study. Dodecane was stained with Sudan IV (0.01% by wt.). The Pickering emulsion was prepared by mixing 5 mL of stained dodecane with 5 mL of polymer modified NZVI. Then, the mixture was vigorously shaken to mix the two phases. This mixing step is different from the original, more aggressive sonication protocol used by Saleh and coworkers, (Saleh et al. 2005a) since such intensive energy input is not available in subsurface NZVI application in a flow-through condition. The vigorous mixing protocol is viewed as a more relevant *ex situ* screen of NZVI affinity for the NAPL/water interface. To evaluate the effect of NZVI particle concentration on *ex situ* NAPL targeting, three different polymer modified NZVI concentrations (0.5 g/L, 3 g/L, and 15 g/L) were tested. Emulsion droplets were observed using optical microscopy (Nikon Eclipse TE300, Hauppauge, NY).

6.2.7 In situ targeting (1-D columns)

A column experiment was conducted to determine if an amphiphilic triblock copolymer modified NZVI could partition to a NAPL-water interface under in situ conditions. Two types of triblock copolymer were evaluated. One had a high hydrophobe to hydrophile ratio, and a second had a low hydrophobe to hydrophile ratio. Four column experiments were conducted similarly to the mobility studies as described above, with the following modification. To provide the maximum opportunity for targeting, the flow was stopped overnight to allow diffusion of the particles from the porewater to the collector surfaces. Flow was resumed to collect the effluent and was analyzed for particles using atomic absorption spectrometry as described above. One set of experiments used clean sand, and a second set used dodecane coated sand. A third set of experiments used entrapped TCE DNAPL (29% residual saturation). A difference in particle holdup between the two conditions indicates an affinity for the dodecane (NAPL)-water interface.

6.2.8 Destabilization targeting

Destabilization targeting requires that the surface modifier be released upon contact with TCE (or PCE). To assess the potential for destabilization targeting, the desorption of

polyelectrolytes adsorbed to RNIP were measured including polyaspartate (2.5k and 10k molecular weight), PSS homopolymer (70k and 1M molecular weight) and CMC (90k and 700k molecular weight) as described in Kim et al., 2009 (Kim et al. 2009). Adsorption of polyelectrolyte was determined from isotherms determined in 24 mL polycarbonate centrifuge tubes using 3g/L RNIP and 1g/L of polyelectrolyte in 1mM sodium bicarbonate. The mixtures of RNIP and polyelectrolytes were equilibrated for 5 days at 25°C using an end-over-end rotator at 30 rpm, then centrifuged and the supernatant analyzed as described in Kim et al., 2009 (Kim et al. 2009) to determine the adsorbed mass of polymer.

The polymer modified particles are washed 4 times to remove any excess polymer from solution and then allowed to equilibrate in polymer free solution for up to eight months. Desorption of polyelectrolytes was monitored by centrifuging the particles after equilibrating in polymer free 1 mM sodium bicarbonate solution after 2 weeks, 4 weeks, and 8 weeks, and measuring the concentration of free polymer in solution at each time step to determine the release of polymer. In addition, the electrophoretic mobility of RNIP particles removed from the tube at each time step are measured and compared with the electrophoretic mobility of RNIP with adsorbed polymer. Desorption of polymer should decrease the magnitude of electrophoretic mobility of particles such that they trend toward that of bare RNIP.

6.2.9 In situ NAPL targeting in two-dimensional (2-D) flow cell

A bench-scale quasi-2-D flow cell (30 cm x 18 cm x 2.5 cm) was used to simulate in situ delivery of polymer modified NZVI to NAPL source zones in a model porous media. The cell was packed wet to create a main homogeneous porous media domain with three NAPL source zones. Unimin sand #50 (Unimin, New Canaan CT) with median grain size (d_{50}) of 330 μm and porosity of 0.3 was used to pack the main homogeneous porous media domain while Unimin sand #16 with d_{50} of 880 μm and porosity of 0.35 was used to create three rectangular blocks (2 cm x 2.5 cm x 4 cm) for NAPL entrapment. The capillary barrier between Unimin sand #50 and Unimin sand #16 is required to entrap NAPL in the source zones. The top and the bottom of the 2-D cell was packed with Unimin sand #140 (d_{50} of 99 μm) to help seal the cell. The 2-D aquifer tank consists of back ports with septa at the locations corresponding to the center of each block of Unimin sand #16 for NAPL source zone creation. NAPL source zones of varying NAPL saturation were created by injection and withdrawal of dodecane from the course grained zone as described ion Phenrat et al., 2011 (Phenrat et al. 2011).

6.2.10 Batch study for evaluating effect of polymer coatings on NZVI reactivity with TCE

Batch experiments were conducted in 60mL serum bottles capped by Teflon Mininert™ valves. Each contained 32 mL of deoxygenated water with bare RNIP or polymer modified RNIP (at a particle concentration evaluated), and 30 mL of headspace. The bare and surface modified RNIP suspensions were prepared in the same manner as that for the bench-scale transport experiment except that the suspensions were deoxygenated by purging with argon and thus the reactor headspace is argon. A 175 μL aliquot of saturated TCE solution (1100 mg/L) was added to provide an initial TCE concentration of 6 mg/L in solution. The reactors were rotated on an end-over-end rotator at 30 rpm at 22±2°C. TCE degradation and the formation of products were monitored by periodically removing and analyzing a 100 μL headspace sample by GC/FID as previously described (Liu et al. 2005b). Replicate reactors were analyzed for each particle. TCE transformation rates were evaluated using a kinetic modeling software package,

Scientist, v.2.01 (Micromath, St. Louis, MO). The loss of TCE and formation of products were fit concurrently using reaction pathways previously proposed for RNIP (Liu et al. 2005b).

6.2.11 Batch treatability ttudy for a TCE contaminated area using NZVI

The TCE dechlorination rates afforded by various types of NZVI for the treatability study (section 7.7.1) were determined similarly as above, except that instead of using water alone in a reactor, aquifer material contained 40% solids by mass and 60% groundwater from the site was used. Details of these analyses are described in Phenrat et al., 2010b (Phenrat et al. 2010c).

6.2.12 Column experiments to evaluate effect on flow velocity on PCE dechlorination using polymer modified NZVI

The influence of seepage velocity on the in situ PCE dechlorination rate (k_{obs}) was determined in flow through column reactors. Four velocities were used (7 cm/day, 14 cm/day, 53 cm/day and 113 cm/day) in an up flow configuration. A glass column (9 cm × 2.68 cm ID) with glass frits at the both ends was packed with a homogeneous mixture of sand (300 μm) and enough MRNIP2 to provide 10 g/L of MRNIP2 in the pore water. The porosity of the sand column without nZVI was 0.43 as determined from a tracer test using D_2O.

The sand and MRNIP2 slurry were mixed in an anaerobic chamber with a spatula to provide as homogenous of a mixture as possible. The column was packed with the mixture in an anaerobic chamber to minimize oxidation of NZVI by air. A check valve with a constant cracking pressure of 10 psi was connected to the end of the column. The pressure corresponds to the pressure of water at a depth of 7 m. Connecting this check valve avoids degassing of N_2 in the column feed water and is representative of the pressure of an aquifer where NZVI will be emplaced. The sodium bicarbonate (5 mM) solution used as column eluent was purged with N_2 (1 hour per 1 L) to minimize nZVI oxidation by dissolved oxygen in the column influent. Twenty pore volumes of 5 mM sodium bicarbonate were flushed initially to provide uniform pH and electrolyte conditions throughout the column. After the column was flushed with 5 mM sodium bicarbonate for 20 pore volumes (PV), a tracer test was conducted using 10% deuterium oxide (D_2O) as a conservative tracer (Irene Man-Chi Lo 2007). The water and deuterium oxide were purged with nitrogen for 1 hour per liter of liquid to remove dissolved oxygen and the pH and ionic strength was adjusted with 5mM sodium bicarbonate (pH 8.6 ± 0.1). The effluent samples were collected in a fraction collector, filtered using a 0.02 μm syringe filter, and analyzed on a Waters 2410 refractive index (RI) detector (Waters Corporation, Milford, MA). The samples (80 μL) were injected into the RI detector at a flow rate of 1 mL/min. Calibration of the RI detector was done using 1, 2.5, 5, and 10% D_2O (by volume) in 5 mM sodium bicarbonate.

PCE at a constant concentration of 6.6 mg /L in deoxygenated 5 mM sodium bicarbonate (< 0.4 mg/L of O_2 , pH = 8.6 ± 0.1) was prepared and stored in a 20 L stainless reservoir. This PCE tank was continuously stirred with a magnetic bar and the head space of the tank was pressurized with nitrogen (3 psi) to maintain anaerobic conditions. The PCE solution (contaminated water) was introduced into the columns at a constant flow rate for the each velocity condition using an FMI piston pump. Throughout the column experiments, flow rates were periodically monitored and adjusted so that the seepage velocity fluctuations for each velocity condition were within 5 % of their average values. The PCE dechlorination rate was

determined by measuring the PCE concentration of influent and effluent samples. Influent sampling was taken directly from the 20 L PCE tank through a gastight valve attached to the tank. Effluent samples were collected using a gas tight syringe connected directly to the effluent line to limits volatile losses. The collected influent or effluent samples (0.8 mL) were transferred to 2 mL vials filled with 0.8 mL of hexane containing 5 mg/L of 1,1,1 trichloroethane as an internal standard. Samples were vortexed for 2 minutes to extract the PCE into the hexane phase. The hexane was transferred to a new GC vial and the PCE concentration was determined by HP 6890 GC/ECD detector. C/C_0 was calculated using effluent and influent PCE concentrations measured within a few minutes of each other. Periodically, PCE, the non-chlorinated reaction products (ethene, acetylene and ethane), and H_2 were measured in column effluent samples. A 2.5 mL effluent sample was collected in a gastight syringe, a 2.5 mL headspace was created and the gas and liquid phases were equilibrated. The headspace was then analyzed using GC/FID for PCE and its reaction products, or GC/TCE for H_2 as described above.

The observed PCE reaction rate constant measured in the reactors was calculated assuming plug flow and eqn 6.9 where,

$$k_{obs} = -\frac{\ln \frac{C}{C_0}}{t} \qquad (6.9)$$

C= PCE concentration along the Fe^0 packed column (mg/L), C_0= initial PCE concentration (mg/L), k_{obs}= first order dechlorination rate constant (h^{-1}), and t = retention time in the column (h).

6.2.13 Flow cell study on effect of NZVI on PCE dechlorination and dissolution from PCE-DNAPL source zone

A custom made glass flow cell that was used in similar studies to investigate effect of bio-activity in DNAPL source zones (Glover et al. 2007) was used in this study as a physical model. The flow cell had a total volume of 15 mL. The flow cell was carefully packed inside an anaerobic chamber, creating a two-zone system where a DNAPL pool could be trapped by a capillary barrier between the coarser and finer materials (this entrapment configuration mimics a DNAPL pool formed at a texture interface in field systems). The lower part of the flow cell was packed with a coarse sand (Unimin # 16; sieve size 1.18 mm) and the upper part, as well as the narrow inflow and outflow sections, were packed with a medium grained sand (Unimin # 50; sieve size 0.3 mm). The flow cells were wet-packed, i.e. adding first the pore water and then the sands to eliminate trapped gas. The pore water was a 10 g/L RNIP solution prepared in the same way as for the batch experiments described above. In this way RNIP was emplaced in the cell from the beginning of the experiments. To create the desired DNAPL distribution first 0.93 mL of PCE was injected at slow rate, which yielded an average PCE saturation of about 70% in the coarse sand layer. PCE was then withdrawn until 0.58 mL remained, which constituted a final average saturation of approximately 40%. No RNIP was observed in the PCE that was extracted. The PCE was dyed red using Sudan IV, 0.01% by weight, allowing the pool zone to be observed visually. A steady flow of de-aired 5 mM $NaHCO_3$ water was established through the cells by pumping this water from an air-free Teflon bag. Experiments were performed at two different flow velocities.

Water samples were collected at the outflow end of the cell, by switching the effluent water stream to go directly into a 5 mL gastight glass syringe and collecting a 1 mL effluent water sample. The syringe was then disconnected, 1 mL of air was drawn into it, and it was capped using a gastight Teflon septum, thus obtaining 50% aqueous phase and 50% headspace. After shaking and a rest period to obtain phase equilibrium the headspace was sampled by inserting a needle through the septum, drawing and injecting directly into the GC with FID as described in Liu et al., 2005b (Liu et al. 2005b). The samples were analyzed for PCE and dechlorination byproducts using the same method as described above.

We developed a detailed model of the three-dimensional flow cell to further analyze the experimental results and their implications for the reactive processes in the DNAPL source zone. The model was developed within the framework of a finite difference groundwater flow code MODFLOW-2000 (Harbaugh et al. 2000) and the reaction module RT3D (Clement 1997), which is an extension of method of characteristics based transport code MT3DMS (Zheng and Wang 1999). Here we implemented a Gilland-Sherwood type model of rate-limited DNAPL dissolution coupled to first order degradation of PCE by the NZVI particles(Saenton and Illangasekare 2007). The model considered mass transfer between the DNAPL and aqueous phase,
using a lumped mass-transfer coefficient for component *i* over the DNAPL-water interface. K_{Li} is contained in a modified Sherwood number $Sh' = K_{Li}\, d_{50}^{2}\, D_{mi}^{-1}$, where d_{50} is the median grain size and D_{mi} is the molecular diffusion coefficient in water of component *i* (Imhoff et al. 1993; Miller et al. 1990). In the system investigated here, many parameters remain constant and assuming that changes in NAPL saturation S_n are negligible during the experiments we formulated a correlation of the form $Sh' = f(Re, Sc_i)$. Here $Sc_i = \mu_a\, \rho_a^{-1}\, D_{mi}^{-1}$ is the Schmidt number of component *i* in the aqueous phase and $Re = v_a\, \rho_a\, d_{50}\, \mu_a^{-1}$ is the Reynolds number for the aqueous phase; μ_a, ρ_a and v_a are the aqueous phase viscosity, density and mean pore-water velocity, respectively. We assumed that the resistance to mass transfer is dominated by processes in the aqueous phase. Additional details of the model and its assumptions can be found in Fagerlund et al., 2012 (Fagerlund et al. 2012).

The dechlorination reactions and simultaneous mass transfer between the DNAPL and the aqueous were coded into the reaction module RT3D (Clement 1997), which was used to calculate reactive transport of components based on flow solutions obtained with MODFLOW-2000 (Harbaugh et al. 2000). The three non-chlorinated degradation end-products: ethane, ethene and acetylene were lumped together in the model and will be referred to as ETH. The degradation of PCE to by-products was described by first order kinetics. By simultaneously solving for the dechlorination reactions and the dissolution of DNAPL PCE to the aqueous phase, the reactions were allowed to influence the rate of dissolution through its influence on the aqueous phase PCE concentration and therefore the driving force for dissolution.

6.2.14 Intermediate scale tests to determine the effect of NZVI emplacement on treatment efficiency

A two-dimensional intermediate scale tank (2.4m x 1.2m x 0.05m) was used to represent a heterogeneous confined test aquifer with access ports on the horizontal and vertical axes (Figure 6.3). To create uniform inflow and outflow, 15 cm channels were created with Unimin sand # 8. An impermeable layer 35 cm deep was created at the bottom of the tank using Unimin sand # 250. A coarse lens (Unimin sand # 16) of 10 cm x 5 cm x 5 cm was created for DNAPL source. Water saturated conditions were maintained while packing the tank with sand by

maintaining water level at least 5 cm above sand level. To create homogenous packing, the sand was hand compacted using a wooden bar for every 2 cm increase in sand level. A pair of brass tubes (Small Parts Inc.) with an inner diameter of 3/16" each with a single hole were placed 10 cm downstream from the edge of the source with their holes aligned with the center of the source zone for nanoparticle injection. A glass tube was place in the source zone for DNAPL PCE injection extending to the top of the tank. The glass tube was connected with Teflon tube connected to a three way Teflon valve which was kept closed all times except during PCE injection. After packing the tank with sand, 10 cm of clay was placed on top of the sand to create confined conditions. Six vertical sampling arrays were created on the back side of the tank for aqueous sampling. Each array had 11 ports each spaced 5 cm apart vertically, named as row 1-6. Dissolved PCE concentration measured at the 11 points for each row along with the average flow velocity (20 cm/d) in the tank was used to calculate the mass flux at different distances away from the source. Changes in measured mass flux of PCE were determined for the two NZVI treatments. To create the desired PCE DNAPL distribution, 77 mL of free phase PCE stained with Sudan IV (0.01% by wt.) was very slowly injected in the small coarse lens at through the glass tube placed in the source zone to yield an average saturation of 70%. Then 55 mL of PCE was withdrawn from a back port on the tank, providing a final average saturation of 21.5%. MRNIP2 was injected into the tank though the brass tubes using a peristaltic pump. Water samples were collected from sampling ports on the back of the tank and analyzed for PCE concentration and by-product formation using GC-FID to monitor for non-chlorinated products, and by GC-ECD to monitor PCE loss and the production of chlorinated by-products.

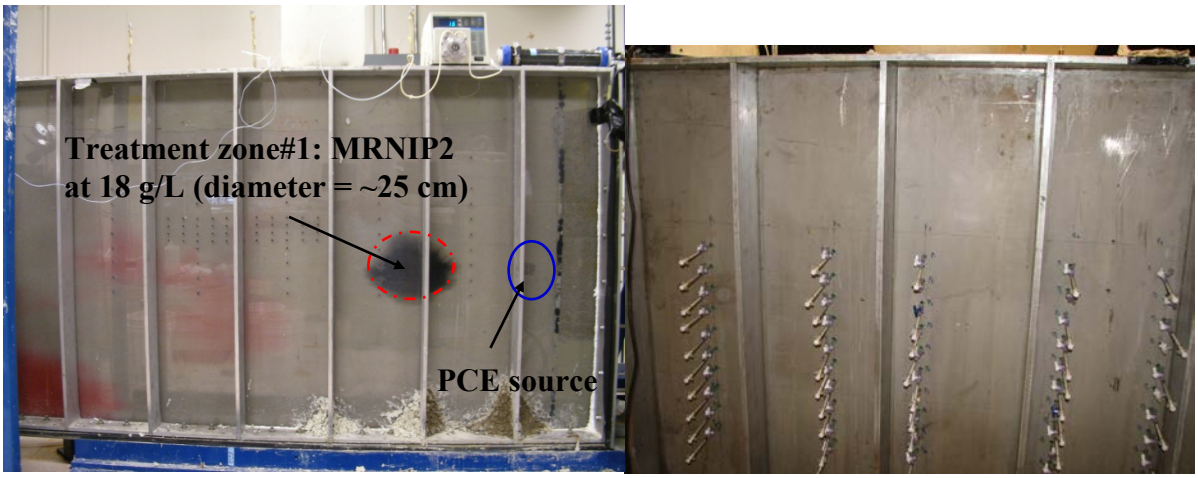

Figure 6.3. Front (left) and back (right) of large tank used to determine the effect of NZVI emplacement on the mass emission from a PCE source zone.

6.2.15 Delivery of polymer modified NZVI in field-scale porous media

Two types of polymer modified NZVI, Z-Loy and CMC-NZVI were used in this study. The dimensions of the aquifer tank are 10m x 10m x 3m deep. Sandy soil was used to pack the tank. The injection and extraction wells had 0.75m screened intervals spanning the distance between two horizontal confining layers. To monitor hydraulic gradient between the wells, pressure monitoring points were installed 0.5 meters from the injection and extraction wells (i.e., 1.5m apart) and instrumented with submersible pressure transducers. Five discrete-level sampling

points were located on the center line between the injection and extraction wells. An additional injection and extraction well pair was installed on either side of the well pair. The purpose of the additional wells was to constrain the lateral spreading of the NZVI plume and to help maintain a high velocity between the wells. The controlled nature of this experiment allowed detailed monitoring of a wide range of parameters in groundwater to track NZVI distribution, including 1) total iron; 2) dissolved oxygen (DO), 3) oxidation/reduction potential (ORP), 4) pH, 5) specific conductance, 6) light transmittance, and 7) dynamic light scattering. To ensure that transport of the polymer modified NZVI was accurately represented, direct measurement of particulate iron concentrations was used as the indicator of NZVI transport.

Table 6.3. Physical properties of the sand used for the field-scale injection experiments.

Property	Value
Hydraulic conductivity (cm/s)	0.03
Organic carbon content (% wt)	0.3%
Sieve analysis (% wt retained)	
0.5 mm	0.00%
0.3 mm	14.08%
0.25 mm	40.41%
0.175 mm	40.61%
0.145 mm	3.27%
0.125 mm	0.82%
0.106 mm	0.41%
0.09 mm	0.20%
0.075 mm	0.06%
0.063 mm	0.04%
<0.063 mm	0.14%
Surface area (m^2/g)	1.316+-0.008
Colloids (settling, % wt)	0.30%

7. RESULTS AND DISCUSSION

This section present the results and major findings for each set of experiments that were conducted under each project component. While the results are not necessarily presented in the chronological order in which they were conducted, the topics are presented to promote the flow of logic. The section presents the following results in order including:

- Particle, porous media, and hydrogeochemcial factors affecting mobility of polymer modified NZVI in porous media
- Effect of physical and chemical heterogeneity on emplacement of polymer modified NZVI
- Numerical models for predicting the emplacement of polymer modified NZVI in porous media
- Targeting polymer modified NZVI to DNAPL
- Factors influencing the reactivity of polymer modified NZVI with TCE and PCE
- Effect of NZVI emplacement on mass emission from entrapped DNAPL
- Environmental considerations for reactivity and emplacement of NZVI in real aquifer media
- Methods for NZVI detection in porous media

The relationship between the SERDP project tasks and the topics in this results and discussion are provides in a Table in Appendix A.

7.1 Particle, porous media, and hydrogeochemcial factors affecting mobility of polymer modified NZVI in porous media.

This section summaries studies conducted to evaluate effect of important particle, solution chemistry, and porous media properties on NZVI transport in porous media. We start with a basic understanding of the factors controlling NZVI dispersion stability against aggregation, then discuss the effect of polymeric coatings on aggregation. Finally, the effect of coatings and media heterogeneity on NZVI transport is presented. These studies identified the most important particle and media properties affecting transport in porous media.

7.1.1 Effect of particle surface chemistry on NZVI aggregation

The aggregation of NZVI decreases its transport in porous media due to enhanced deposition and straining, both of which lead to pore clogging. Therefore, understanding the aggregation behavior of bare particles and using particle surface modification to improve NZVI dispersion stability is essential for understanding and improving their mobility in porous media. Complete details of these studies can be found in Phenrat et al., 2007 (Phenrat et al. 2007).

7.1.1.1 Aggregation and sedimentation of uncoated NZVI particles

Magnetic attraction originated by Fe^0 of NZVI is the main driving force for rapid aggregation and poor mobility of bare NZVI in porous media. To illustrate this, we compared the aggregation and sedimentation of uncoated NZVI (using RNIP which are magnetic Fe^0/Fe_3O_4 core-shell iron nanoparticles) with other iron oxides including magnetite (magnetic, but less so than RNIP), and

hematite (non-magnetic). The surface charge and particle sizes are similar for all three particles (Table 7.1.1). The primary difference between the particle types is their saturation magnetization (M_s) (Table 7.1.1). The saturation magnetization (M_s) of RNIP (570 kA/m) lies between that of magnetite (330 kA/m) and Fe^0 (1226 kA/m), consistent with its Fe^0/Fe_3O_4 core-shell structure and the low Fe^0 content (14%) of the aged particles. The M_s of hematite is very low as it is not ferromagnetic.

Table 7.1.1. Physical properties of \iron-based nanoparticles and sispersions in 1 mM $NaHCO_3$ at pH=7.4.

Sample	composition	average diameter	average density	zeta potential	saturation magnetization
		(nm)	(g/cm^3)	(mV)	(kA/m)
RNIP	14.3 / 85.7% (Fe^0/ Fe_3O_4)	40[a]	6.15[b]	-31.7±0.8[d]	570
Magnetite	98+% (Fe_3O_4)	27.5[c]	4.95[c]	-38.2±1.1	330
Hematite	98+% (α-Fe_2O_3)	40[c]	5.24[c]	-39.0±0.6	14

[a] Nurmi et al. ES&T (2005).
[b] Reported by Toda Kogyo (Japan).
[c] Reported by Nanostructured and Amorphous Materials Inc (USA).
[d] Errors bars represent one standard deviation based on 3 measurements.

Dynamic light scattering (DLS) was used to investigate the rapid aggregation of RNIP from single nanoparticles to micron size aggregates. In addition, optical microscopy and sedimentation studies were used to monitor the formation of inter-connected fractal aggregates. The rate of aggregation was a function of the particle concentration and the saturation magnetization of the particles (Figure 7.1.1). For RNIP with 14.3% Fe^0 primary particles (average radius = 20 nm) aggregated to micron-size aggregates in only 10 minutes, with average hydrodynamic radii ranging from 125 nm to 1.2 μm at a particle concentration of 2 (volume fraction($ø=3.2 \times 10^{-7}$) and 60 mg/L ($ø = 9.5 \times 10^{-6}$), respectively. Subsequently, these aggregates assembled themselves into fractal, chain-like clusters (Figure 7.1.2). At an initial concentration of just 60 mg/L, cluster sizes reach 20 to 70 μm in 30 minutes and rapidly sediment from solution. After 7 hrs of sedimentation, only small fraction (~4 %) of RNIP remained in the dispersion.

According to extended DLVO calculations which take into account the long-range magnetic attractive and van der Waals (Hamaker constant of RNIP = 10^{-19}) forces against electrostatic repulsion, the attraction overcomes repulsion, and no energy barrier to aggregation exists. Thus, rapid aggregation is predicted. This is in good agreement with experimental results. On the other hand, for hematite, only electrostatic repulsions and van der Waals are important (i.e. no magnetic attractions due to non-magnetism of hematite). Electrostatic repulsions overcome van der Waals attraction, and energy barrier to aggregation exists. Thus, a stable dispersion is predicted which is in good agreement with the experimental result. Therefore, we can conclude that magnetic attraction originated from magnetic Fe^0 of NZVI is the main driving force for rapid aggregation and is partly responsible for poor mobility of bare NZVI.

These findings have several important implications for NZVI transport. First, the rapid aggregation to large micron sized gelled aggregates will prevent transport in porous media. Second, M_s is proportional to the Fe^0 and Fe-oxide ratio for RNIP. Therefore, the oxidation of Fe^0 by water to more oxidized iron oxide phases such as Fe_3O_4 (dominant), γ-Fe_2O_3, and γ-

FeOOH in the aquifer could produce more mobile particles. It would also mean that smaller fully oxidized particles in the slurry would transport better than those that are larger and contain a larger fraction of Fe(0). This can affect the ability to measure the movement of NZVI in porous media since transport is generally determined by measuring total Fe in samples recovered from down gradient wells. One alternative is to use ORP measurements to assess NZVI transport. This is discussed later in the report. The very rapid and unavoidable aggregation of uncoated NZVI particles required that they be coated with various polymers to prevent aggregation and to increase transport. The effect of various polymeric coatings on the aggregation of NZVI is discussed next.

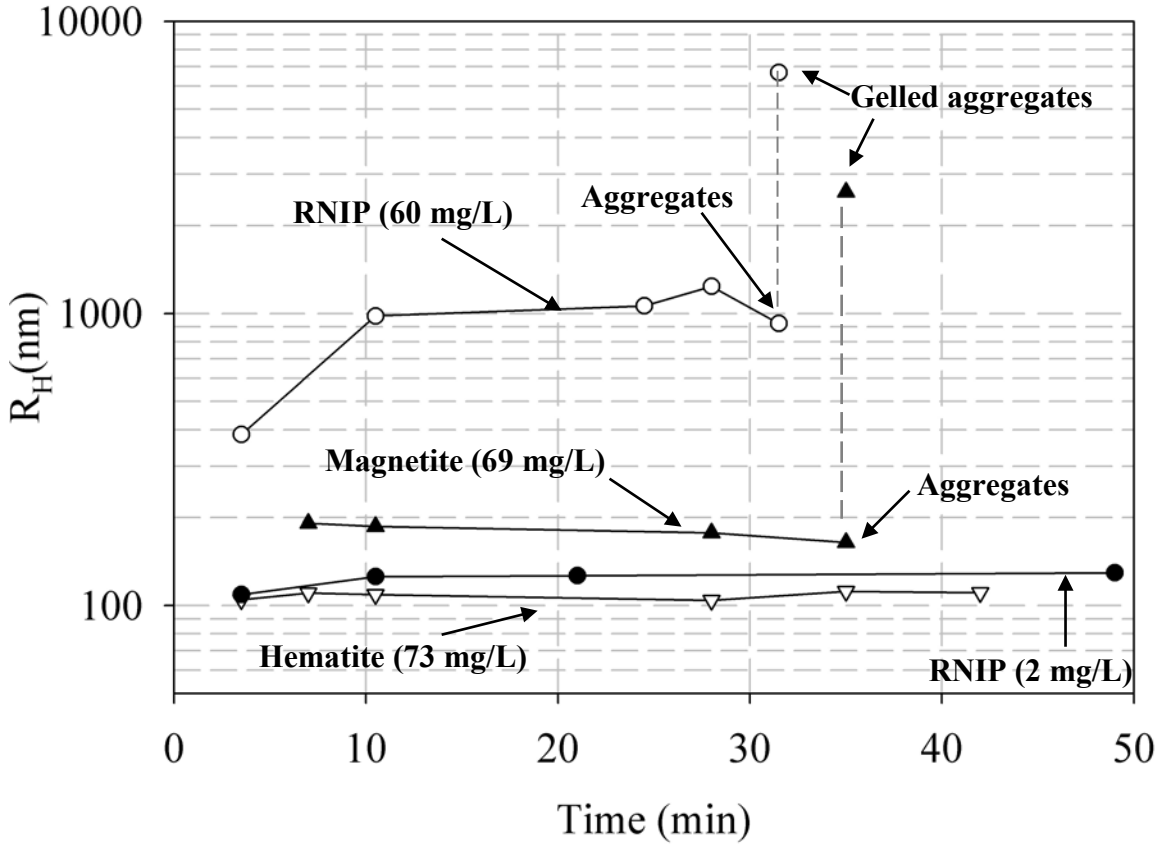

Figure 7.1.1. Evolution of average R_H of dominant size class as a function of time for RNIP (14.3% Fe^0 and M_s = 570 kA/M), magnetite (M_s = 330 kA/M), and hematite(M_s = 14 kA/M). Last measured points for RNIP and magnetite become bimodal distribution with larger size due to gelation of aggregates.

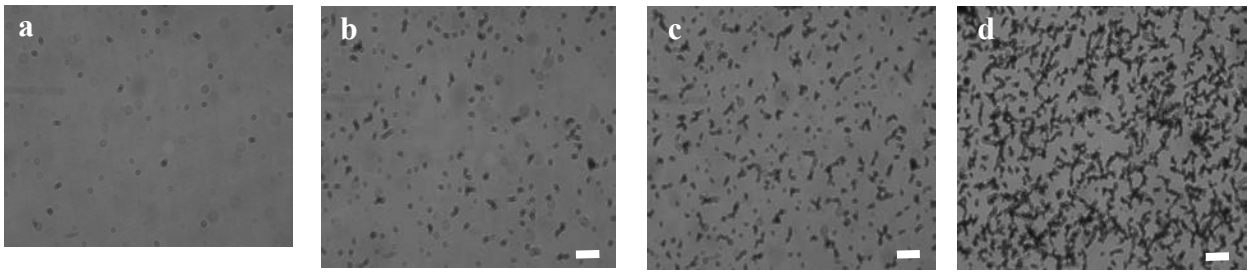

Figure 7.1.2. In-situ micrographs illustrating aggregation kinetics of the dispersion of RNIP (14.3% Fe^0) at 60 mg/L (Φ=$10^{-5.02}$): (a) time (t) = 1 min; (b) t = 3.75 min; (c) t = 9 min; and (d) t = 30 min. Scale bar = 25 µm.

7.1.1.2 Effect of polymer surface modification on NZVI aggregation and sedimentation

To resist rapid aggregation and sedimentation, the surfaces of RNIP were modified by physisorption of various polyelectrolytes such as poly(styrene sulfonate) (PSS), carboxymethyl cellulose (CMC), polyaspartate (PAP). PAP can CMC are used because they are "biopolymers" with no inherent ecotoxicity and thus are attractive choices if they provide the necessary surface properties. The factors affecting the ability of each type of stabilizer, including molecular weight and monomer type) were determined in order to select the polymer coatings that provide NZVI suspensions that are most resistant to aggregation, and that therefore will increase mobility in porous media. Complete details of these studies can be found in Phenrat et al., 2008 (Phenrat et al. 2008).

The adsorbed polyelectrolyte layer provides additional electrosteric repulsion to counter long-ranged magnetic and short range van der Waals attractions. Characteristics of the adsorbed layer such as the mass of each polyelectrolyte onto RNIP (Γ_{max}), thickness of adsorbed layer (d), and electrical potentials affect the magnitude and extent of electrosteric repulsion (Napper 1983; Zhulina et al. 2000). These parameters were measured for RNIP modified with poly(styrene sulfonate) with molecular weight of 70,000 g/mole (PSS70K), carboxymethyl cellulose with molecular weight of 90,000 and 700,000 g/mole (CMC90K and CMC700K), and polyaspartate with molecular weight of 2,000-3,000 and 10,000 g/mole (PAP2.5K and PAP10K). The maximum surface excess concentration for each of these polyelectrolytes adsorbed on RNIP was ~ 1 to 2 mg/m^2. The layer thicknesses estimated using electrophoretic mobility and Ohshima's soft particle analysis were ~7 nm for CMC90K, ~ 40 nm for CMC90K, PAP2.5K, and PAP10K, ~67 nm for PSS70K, and ~198 nm for PSS1M. To determine the ability of each polymer to stabilize the dispersion against aggregation, particle size distributions were determined over time by dynamic light scattering. The order of effectiveness to prevent rapid aggregation and stabilize the dispersions was PSS70K(83%)>≈PAP10K(82%) >PAP2.5K(72%)>CMC700K(52%), where stability is defined operationally as the volume percent of particles that do not aggregate after one hour. CMC90K and PSS1M could not stabilize RNIP relative to bare RNIP. A similar trend was observed for their ability to prevent sedimentation, with 40 wt%, 34 wt%, 32 wt%, 20 wt%, and 5 wt%, of the PSS70K, PAP10K, PAP2.5K, CMC700K, and CMC90K modified RNIP remaining suspended after 7 hours of quiescent settling, respectively. The stable fractions with respect to both aggregation and sedimentation correlate with the adsorbed mass and layer thickness (Figure 7.1.3), indicating that both of these properties must be considered when predicting the stability of polyelectrolyte-stabilized NZVI.

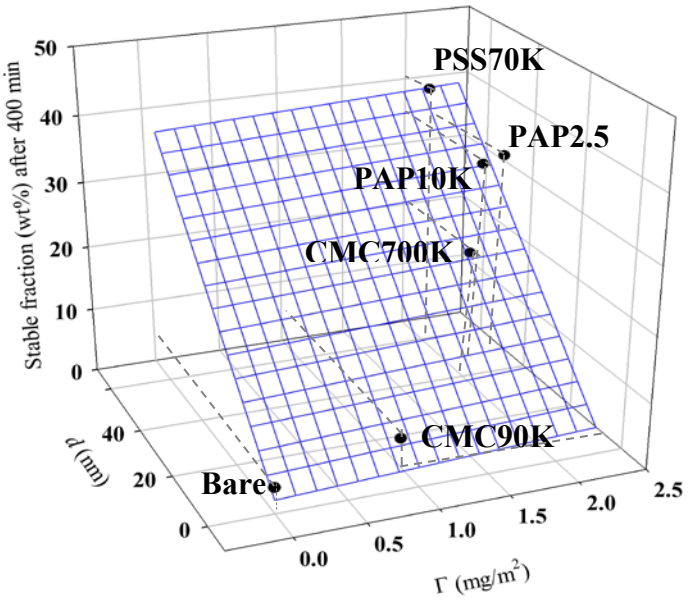

Figure 7.1.3. Correlation between the colloidally stable fraction (wt %) of nanoparticles and the measured surface excess (Γ, mg/m^2) and layer thickness (*d*, nm) of each adsorbed polyelectrolyte.

Importantly, the Fe(0) content of the RNIP and resulting magnetic attraction results in a fraction of the particles that cannot be stabilized by any modifier. This fraction rapidly agglomerates to micron sized aggregates, as was observed for unmodified RNIP. This implies that a fraction of the polymer modified-RNIP will aggregate in the porous media thereby limiting transport. This is what has been observed with nearly all of the modified NZVI evaluated to date, even very small (10nm) CMC coated particles as discussed later in the large scale 3-D tank studies.

7.1.2. Assess the effect of NZVI surface modification on mobility in sand packed columns

The mobility of NZVI in porous media is affected by particle deposition, aggregation/agglomeration, straining, and pore clogging. Agglomeration increases deposition by increasing straining which ultimately leads to pore clogging. Polymeric surface modification provides NZVI with electrosteric repulsions which decreases both NZVI agglomeration and attachment onto porous media. We investigated the effect of polymeric surface modification on deposition onto porous media at both low particle concentration (deposition only) and high particle concentration (deposition plus straining). These studies provide a qualitative assessment of the processes controlling NZVI transport in porous media. A quantitative discussion is provided in section 7.3.

7.1.2.1 Effect of polymer surface modifiers on RNIP transport.

Seven types of modified RNIP were characterized in terms of size, electrophoretic mobility, and dispersions stability. The modifiers include two triblock copolymers with different PSS block sizes (MW=91k (PSS 466) or 125 k g/mol (PSS 650)), polyaspartate (MW=2 to 3k) supplied by Toda Kogyo Corporation (MRNIP) or synthesized from RNIP plus 2 to 3 k MW sodium polyaspartate, sodium dodecylbenzene sulfonate (SDBS) surfactant, polystyrene 70K MW homopolymer, and carboxymethyl cellulose (CMC) 700k MW. The mobility of a 3 g/L solution of triblock copolymer- and SDBS-modified RNIP and MRNIP was measured in water

saturated and packed columns at pH-7.4 and an ionic strength of 1mM ($NaHCO_3$). This particle concentration is in the range of concentration used in field application. The fraction of particles that eluted through a 12.5 cm column for each type of modified particle is shown in Figure 7.1.4 (Saleh et al. 2007). RNIP with surface modifiers transported through porous media much better than uncoated NZVI (% elution is close to zero). Enhanced transport is due to electrosteric repulsions afforded by surface modifiers that minimize aggregation and prevent deposition. The type of modifier used impacts the relative mobility of the particles. High molecular weight polyelectrolytes such as polyaspartate (MW=2k to 3k, MRNIP) and very large molecular weight polyelectrolytes such as the triblock copolymer (MW=50k to 60k) provided the greatest mobility enhancement. It should be noted that at high NZVI concentration (3 g/L), both agglomeration and deposition of NZVI affect NZVI transport. To try and understand which process is more important we conducted experiments at both low NZVI concentration where aggregation is minimal, and at high NZVI concentration where NZVI aggregation is significant.

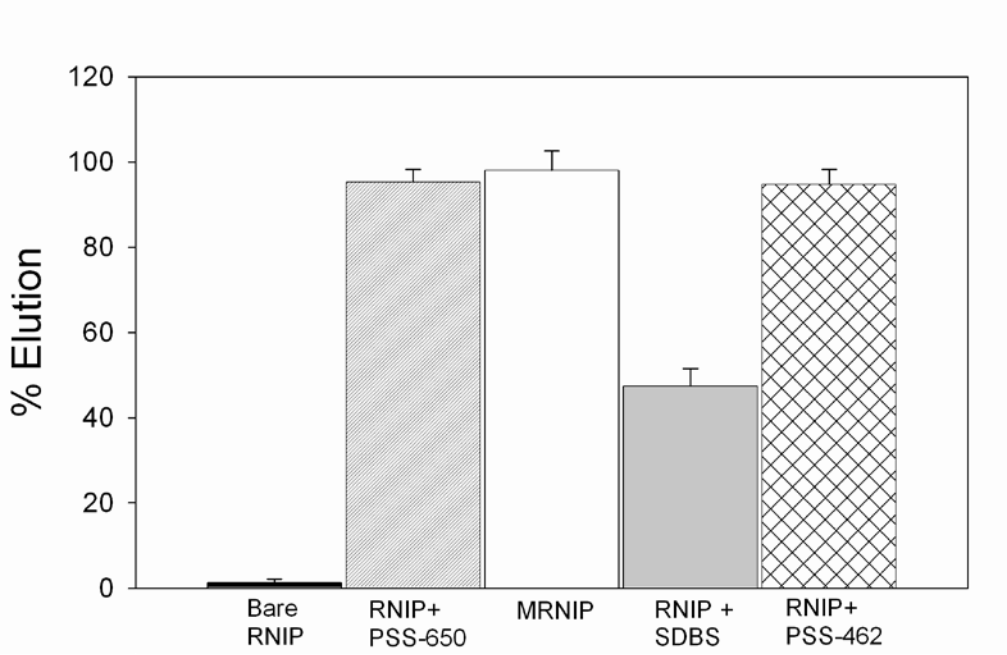

Figure 7.1.4. Percent mass of bare and modified RNIP eluted through a 12.5-cm silica sand column with porosity of 0.33. RNIP was 3 g/L and modifying agents i.e. PMAA-PMMA-PSS triblock copolymers or SDBS were added at 2g/L concentration in each case. MRNIP was supplied by Toda Kogyo, Inc. The approach velocity was 93 m/d.

7.1.2.2 Effect of NZVI surface modification, particle concentration, and particle size distribution on agglomeration and deposition in porous media

The application of polymer modified NZVI particles for in situ subsurface remediation occurs at high particle concentration (1-10 g/L). At this high particle concentration, agglomeration and filter ripening can become significant and will increase the filtration efficiency and decrease particle mobility. We designed experiments to evaluate the relative contribution of the two phenomena in preventing NZVI transport. This understanding allows for

optimizing NZVI transport through polymeric coatings that either prevent aggregation, or deposition, or both. We determined that agglomeration of NZVI in porous media is a function of particle concentration, magnetic attraction, and particle size distribution. Agglomeration in porous media subsequently promotes particle deposition which limits NZVI deliverability (Phenrat et al. 2009a).

NZVI modified by physisorption of poly(styrene sulfonate) with molecular weight of 70 kg/mol (PSS70K) was used in this study. Bench-scale column experiments were performed at various particle concentrations (0.03 to 6 g/L) at environmentally relevant ionic strength, 10 mM Na^+, a pore water velocity of 3.2 x 10^{-4} m/s, and an average sand grain size of 300 μm. To elucidate the importance of particle size and distribution, transport of PSS-modified NZVI particles with three different particle size distributions (-F1, -F2, and –F3, see Table 7.1.2) were compared. We hypothesized that the larger particles, which has greater magnetic attraction and therefore greater Fe(0) content and more significant aggregation would transport less well than smaller particles. The influence of intrinsically magnetic particle-particle interaction of PSS-modified NZVI on deposition in porous media was assessed by comparing the deposition behavior of PSS-modified NZVI with PSS-modified hematite (nonmagnetic) of the similar surface properties. Table 7.1.2 summarizes the particle characteristics of PSS70K-modified RNIP and hematite dispersions. PSS70K-RNIP-F1 contains a greater amount of large-sized particle fraction in comparison to PSS70K-RNIP-F2 while PSS70K-RNIP-F3 contains only small-sized particle fraction. PSS70K-RNIP-F1 also has significantly higher Fe^0 content than PSS70K-RNIP-F2 and –F3. However, the adsorbed layer characteristics (surface excess (Γ) and layer thickness (d)) of these three fractions are the same.

Transport and deposition of concentrated polyelectrolyte-modified nanoparticles in porous media are affected by: 1) particle-sand interaction that will lead to particle deposition and 2) particle-particle interaction that will result in aggregation and collector ripening/blocking. PSS70K-RNIP-F1 and-F2 with larger particles and higher Fe^0 content agglomerated more rapidly and aggregation was less reversible than PSS70K-RNIP-F3. This was confirmed with a sedimentation study showing that 50 % of PSS70K-RNIP-F3 remained stable after 300 minutes of quiescent sedimentation while only 3-4% of PSS70K-RNIP-F1 and-F2 remained stable in the same condition (10mM Na^+ and 1 g/L particle concentration, Table 7.1.2). The importance of magnetic attraction on RNIP agglomeration and transport is further demonstrated using non-magnetic hematite particles with the same surface properties. Without magnetic attractive forces, the PSS-hematite particles were highly stable against aggregation (Table 7.1.2). These particles transported will regardless of concentration because they do not aggregate or deposit readily on the sand surfaces. This suggests that delivery of particles in the subsurface is feasible provided one can prevent their aggregation and attachment.

Table 7.1.2 Physical properties of PSS70K-modified RNIP and hematite

Particle	Fraction	mode	Average R_H nm :% by Vol.		Γ (mg/m^2)	d (nm)	Fe^0 (%)	Stable fraction with respect to sedimentation (% by mass)
			1st peak	2nd peak				
PSS70K-RNIP	F1	Vol.	45:6	328:94	2.1±0.4	67±7	62.6±5.1	3
		No.	26:98	263:2				
	F2	Vol.	25:40	367:60			9.6±0.5	4
		No.	15:100	-				
	F3	Vol.	24:100	-			4±0.1	50
		No.	16:100	-				
PSS70K-He	F1	Vol.	155:100	-	1.5±0.7	32±4	-	80
		No.	81:100	-				
	F2	Vol.	62:100	-			-	90
		No.	38:100	-				

The transport of PSS-modified RNIP and hematite at low particle concentration (30 mg/L) was conducted to investigate the importance of particle deposition without agglomeration. At low particle concentration where aggregation is minimal all polymer modified particles can transport effectively through porous media (C/C_0>0.95). Under these conditions particle attachment can indeed be predicted by clean bed filtration as hypothesized and the deposition characteristics are solely controlled by particle-collector interaction (see section 7.3.1 for the development of a model to predict the deposition of polymer modified nanoparticles without agglomeration). In contrast, agglomeration and attachment of PSS70K-modified RNIP is sensitive to particle size/polydispersity (Figure 7.1.5). Interestingly, transport is less sensitive to total concentration than to size/aggregation for concentrations between 1-6 g/L. C/C_0 of PSS70K-RNIP-F1, -F2, and –F3 are ~0.6, 0.8, and 0.95, respectively, regardless of particle concentrations (from 1 to 6g/L). Because the adsorbed layer properties of PSS70K-RNIP-F1,-F2, and –F3 and thus particle-collector interaction are similar, the difference in deposition behavior of different RNIP fractions is attributed to agglomeration of the particles within the porous media (Table 7.1.2). Because the magnitude and extent of van der Waals attraction is proportional to the size of clusters(Evans and Wennerstrom 1999), the larger the cluster, the deeper the secondary minimum energy well, the higher the attachment probability, and the poorer the mobility of particles. These findings suggest that the transport of polymer modified NZVI with high Fe^0 and large particle sizes (e.g. 100's on nm) may not be readily described by deep bed filtration model which assume that particles are not aggregating. In contrast, models that account for agglomeration and the effects of agglomeration on particle deposition are needed.

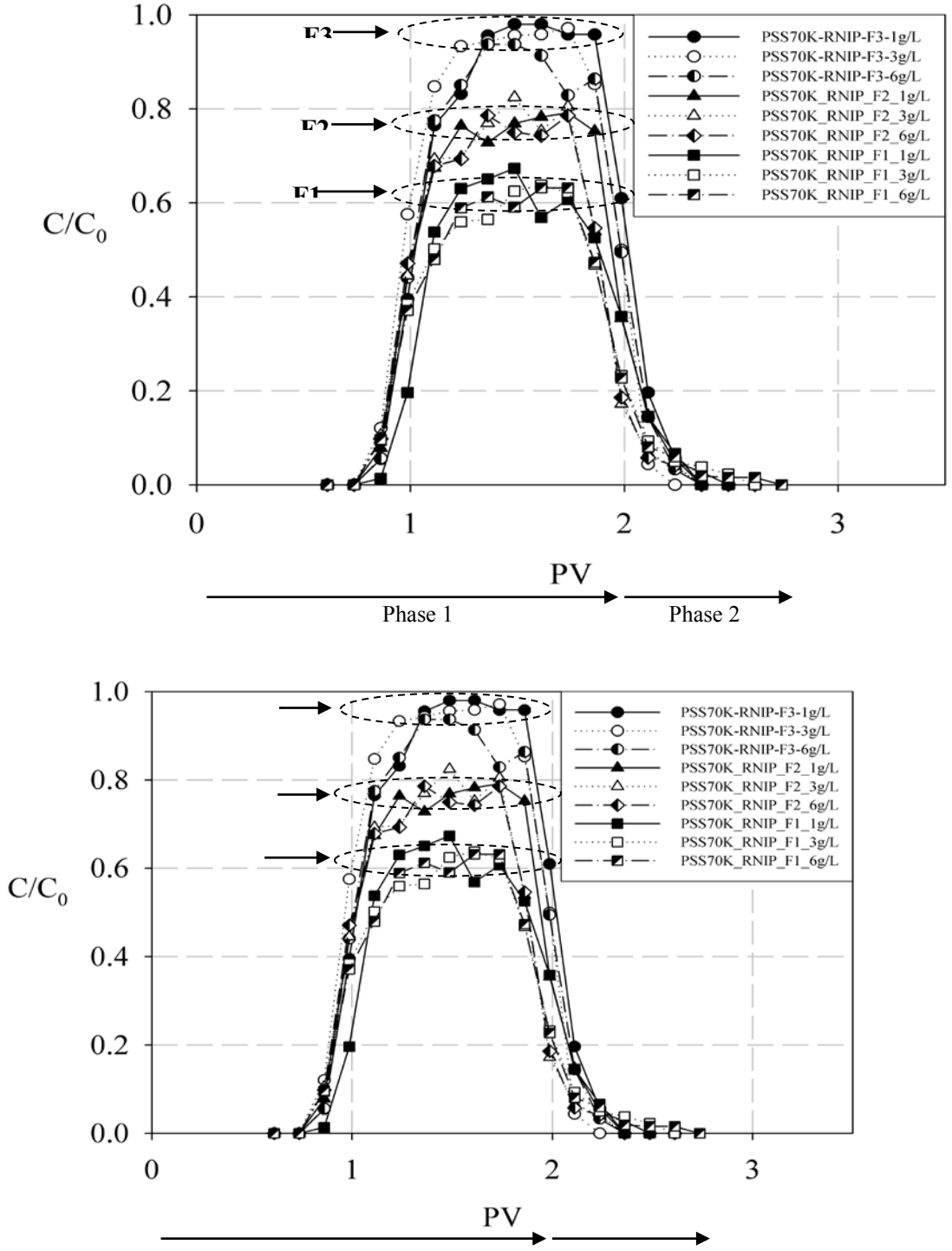

Figure 7.1.5. Breakthrough curves of different fractions of PSS70K-RNIP of particle concentrations from 1-6 g/L.

7.1.3 Assess the effect of fluid velocity on mobility of polymer modified NZVI through homogeneous sand columns.

Fluid velocity is a very important engineering parameter which can affect aggregation of NZVI and its deposition to porous media (Figure 7.1.6). The fluid velocity can be controlled via

NZVI injection rate and therefore understanding exactly how flow velocity influences deposition and transport of NZVI is needed to design an injection/emplacement strategy.

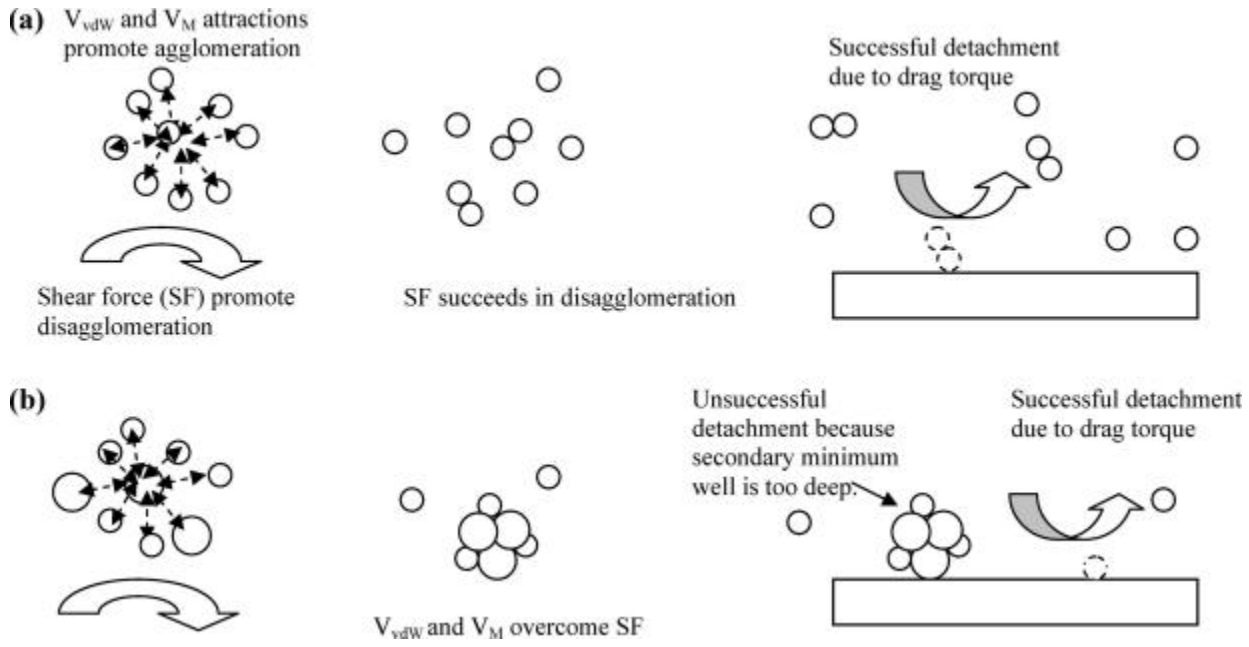

Figure 7.1.6 Conceptual model of agglomeration of polydisperse PSS-modified RNIP followed by deposition of clusters under a secondary minimum. This model considers the balance of shear force (which is a function of fluid velocity) and total attraction energy between particles and/or aggregates (which is a function of ionic strength, van der Waals attraction, magnetic attraction, and electrosteric repulsions) on agglomeration and disagglomeration, together with the balance between secondary minimum between clusters and collectors and drag torque on attachment and detachment: (a) small less polydisperse particles with low Fe0 content and (b) large more polydisperse particles with higher Fe0 content.

For a modified NZVI dispersion at high particle concentration and fixed collector (sand grain) size and ionic strength, the higher the approach velocity, the lower the observed attachment efficiency, i.e. higher transportability. We observed the inverse relationship between the attachment efficiency (sticking coefficient) calculated using filtration theory, α_{CF}, and the approach velocity (u_s) for PSS70K modified RNIP in 10 mM Na^+ and 50 mM Na^+ as a background electrolyte and an average collector size (d_g) of 300 μm. This trend contradicts

classical filtration theory which contends that attachment efficiency is independent of approach velocity (Bai and Tien 1999; Elimelech 1992).

However, this finding is consistent with a revised conceptual model of agglomeration and subsequent deposition on as proposed above (Figure 7.1.6). At higher approach velocity, fluid shear promotes disagglomeration of polyelectrolyte modified NZVI and the size of stable aggregates formed in the flow field are smaller than those at the low approach velocity. The smaller sized agglomerates deposit under a shallower secondary minimum well and are more easily disagglomerated than larger agglomerates. The higher seepage velocity also results in higher drag force that promotes greater detachment of the deposited agglomerates (Bergendahl and Grasso 2000; Torkzaban et al. 2007). In summary, assuming agglomeration and subsequent deposition, the higher seepage velocity promotes NZVI disagglomeration and detachment, both of which result in the lower observed attachment efficiency and higher transportability of polymer modified NZVI in porous media. This suggests that high injection velocities can enhance transport distances and enable emplacement.

7.1.4. Effect of pH and ionic strength on polymer modified NZVI mobility through homogeneous sand columns.

7.1.4.1 Effect of pH.

Solution pH is an important environmental factor which can affect transport of polymer modified NZVI via alteration of surface charge (particle and collector) and adsorbed polymer confirmation. Our work had demonstrated that solution pH can affect transport in several ways. First, the solution pH can change the charge density and polarity (negative to positive) since the pH_{iep} is around 6.3 for RNIP. This means that at pH>>6.3 the particles are highly negatively charged. At pH<<6.3 the particles are positively charged. At pH near 6.3 the total charge is low. These affect deposition onto porous media through changes in the electrosteric repulsion between the particles and the sand grains. This is also affected by the conformation of the adsorbed polymer layer on the particles, which tends to flatten at low pH when the particle and the polymer are of opposite charge and extends at high pH when the polymer and the particle are of the same charge (Kim et al., 2012). Second, the low pH can lead to positively charged patches on the sand surfaces, leading to electrostatic attraction between the negatively charged NZVI and the sand surface. The latter is discussed below in the section describing the impacts of media heterogeneity on NZVI transport.

We evaluated the effect of pH on NZVI transport in porous media from pH 5 to 8 using a particle concentration of 300 mg/L. We evaluated both washed particles (no excess free polymer in suspension) and with excess (free) polymer in the injected particle solution. The first condition used washed particles (i.e. without excess polymer in solution) in order to determine if with the presence of excess free polymer in solution could enhance transport. RNIP was modified by triblock copolymer and polyaspartate (MRNIP). The results from each condition are described below.

Solution pH has significant effect on the transport of polymer modified NZVI in the absence of excess polymer in the solution. Without excess polymer, the elution of MRNIP decreased from 72% at pH=8 to <1% at pH=6 (Figure 7.1.7). Triblock copolymer ($PMAA_{42}$-$PMMA_{26}$-PSS_{462})-modified RNIP also showed same trend. At pH 8, 70% of triblock copolymer modified NZVI were eluted while only 50% and almost none were eluted at pH 7 and pH 6, respectively

(Figure 7.1.7). This behavior provides insight regarding the mechanisms by which the NZVI is being filtered in the porous media.

The low mobility of MRNIP and triblock modified NZVI at pH=6 and pH=7 compared to pH=8 is a result of both aggregation and higher deposition of the particles in the column. The effect of aggregation is evident when comparing the transport of modified RNIP (which aggregates) and modified hematite which does not. The greater mobility of modified hematite compared to either modified RNIP indicates that aggregation is having an effect on transport. Further, MRNIP and triblock copolymer modified NZVI both showed an increase in their particle size distribution when the pH decreased from pH=8 to pH=6. At pH=8 MRNIP average agglomerate size was ~1.1 μm. At pH=6, the average MRNIP size doubled to ~2 □m. This increase is the likely reason for the lower mobility at pH=6 compared to pH=8. The impact of enhanced deposition at pH=6 on NZVI transport is indicated by the strong pH effect of modified hematite which does not aggregate. The greater deposition at pH=6 compared to pH=8 must be attributed to enhanced deposition.

The presence of excess polymer in the injection solution prevented deposition of all particles at pH=6 (Figure 7.1.8). The excess free polymer in solution adsorbed to the positively charged sand surfaces, making them negatively charged which prevented deposition (Kim et al. 2012). This result indicates that excess free polymer in suspension is a good mechanisms to enhance NZVI transport in porous media.

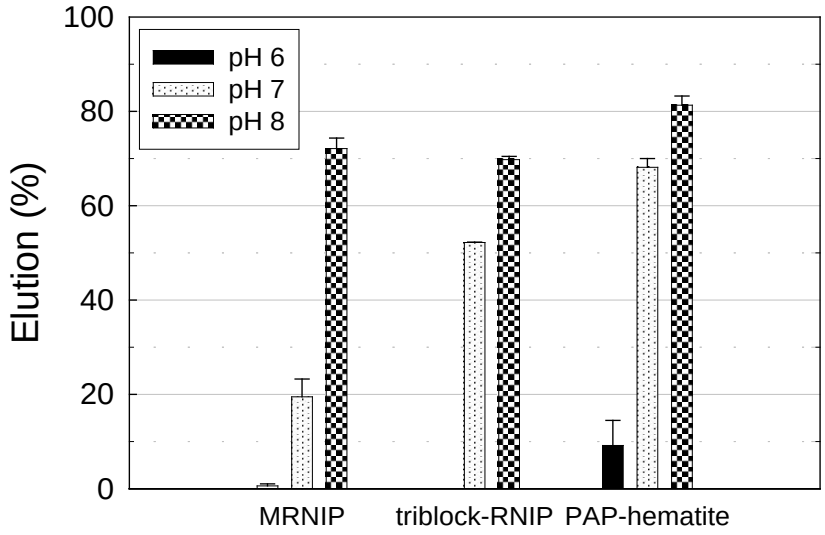

Figure 7.1.7. Percent of mass eluted for MRNIP, triblock-RNIP, and PAP-hematite eluted through 15 cm columns filled with silica sand at pH 6, pH 7 and pH 8. The eluted mass of triblock-RNIP was near zero at pH=6. The initial RNIP or hematite particle concentration was 300 mg/L, porosity of 0.33, linear pore water velocity was 3.2×10^{-4} m/s and ionic strength was controlled at 10 mM NaCl plus 1 mM $NaHCO_3$.

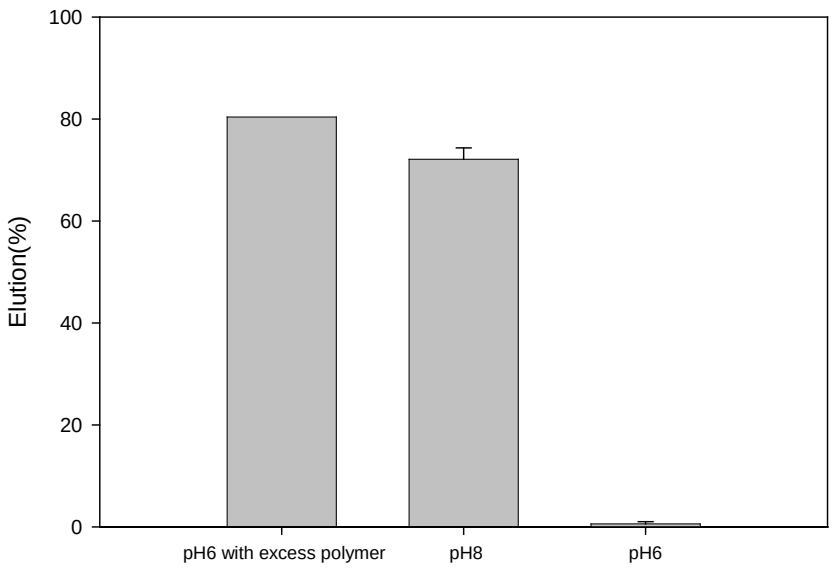

Figure 7.1.8. Effect of pH on mobility of polyaspartate modified RNIP under low particle concentration (with excess polymer) and high particle (without excess polymer) concentration at pH=6 and pH=8. L=15 cm I=10mM NaCl, U=3.2 x 10^{-4} m/s.

7.1.4.2 Effect of ionic strength and composition

Ionic strength (concentration of cations and anions) and the types of ions present affects transport of polymer modified NZVI. In the presence of cations (which is the case for most groundwater), the electrostatic double layer (EDL) repulsion of uncoated NZVI is screened by the counter-ions, resulting in agglomeration, deposition, and filtration (Evans and Wennerstrom 1999). Surface modifiers can overcome the effect of increased ionic strength on EDL screening by providing steric repulsions that are not greatly affected by ionic strength (Fleer et al. 1993; Napper 1983). Similar to the study of pH effect, we evaluated two transport conditions, low (30 mg/L) and high (6 g/L) NZVI concentration. The transport of MRNIP (electrosteric stabilization) and RNIP modified by triblock copolymers (electrosteric stabilization) and Na^+ and Ca^{2+} concentration ranging from 1 to 1000mM and 0.5 to 2 mM, respectively, was studied in water saturated sand columns. Experiments at low particle concentration (30 mg/L) where aggregation was inconsequential, and at more realistic application concentrations (6 g/L) where aggregation could be significant were tested. The transport of polymer modified RNIP was compared with surfactant (SDBD) modified RNIP (electrostatic stabilization) under otherwise identical conditions to compare the effectiveness of these types of modifiers. RNIP dispersions modified by PSS, CMC, and PAP were used for transport at high particle concentration (6 g/L). The results at low and high particle concentration were compared and discussed as follows.

Low particle concentration. In general, increasing ionic concentration decreased mobility of modified NZVI in porous media, and Ca^{2+} had a greater effect than Na^+ as expected from the principles of colloid science. However, there were significant differences in the ability of each

modifier to enhance the mobility of NZVI at varying ionic strength and composition. Triblock copolymers provided the greatest resistance to increases in ionic concentration followed by MRNIP and SDBS. The breakthrough data and the classical filtration model were used to calculate α for each ionic strength evaluated (Table 7.1.3), and the resulting log α values were plotted vs. ionic concentration C_s to obtained critical deposition concentration (CDC) and slope of the deposition curves (β) values via the best fit of these data (Table 7.1.4) according to Eq 7.1.1 (Chen and Elimelech 2007; 2008; Elimelech et al. 1995).

$$\alpha_{CF} = \frac{1}{1+\left(\frac{CDC}{C_S}\right)^{\beta}} \qquad (7.1.1)$$

The CDC is the ionic concentration where all collisions result in attachment, and the slope of the deposition curves describes the sensitivity of the particles to increase in ionic concentration. As shown in Table 7.1.4, the triblock copolymer provided the greatest resistance and lowest sensitivity to increases in the ionic concentration. Polyaspartate i.e. MRNIP showed second best performance followed by SDBS in case of Na^+, however for Ca^{2+} both SDBS and MRNIP showed similar resistance and sensitivity. This is in good agreement with theoretical expectation in that in the presence of ionic species, electrosterically stabilized NZVI can transport better than electrostatically stabilized NZVI (Phenrat et al. 2010d; Zhulina et al. 2000), and electrosteric stabilization with a large layer thickness (triblock copolymer d=~60 nm) is more effective than a small layer thickness (d =~ 40 nm MRNIP) (Fritz et al. 2002; Phenrat et al. 2010d).

Table 7.1.3. Calculated sticking coefficients and filtration length for RNIP with different modifiers.

	Na^+		Ca^{2+}	
Modifier	**Conc. (mM)**	**Log α_{CF} (--)**	**Conc. (mM)**	**Log α_{CF} (--)**
Triblock Co-polymer (MW=125 kg/mol)	10	-3.6	0.5	-3.15
	100	-2	5	-1.89
Aspartate (MW=2 to 3 kg/mol)	10	-2.5	0.5	-1.77
	100	-0.96	1	-0.96
SDBS (MW=350 g/mol)	10	-2.7	0.5	-1.33
	100	-0.6	1	-0.89

Table 7.1.4 Critical deposition concentration (CDC) and β determined from column studies.

	Na^+		Ca^{2+}	
Modifier	**CDC (mM)**	**Slope β**	**CDC (mM)**	**Slope β**
Triblock Copolymer	4040±290[a]	1.44±0.15	4540±3670	0.46±0.1
MRNIP	770±80	1.06±0.08	4.3±0.6	1.42±0.25
SDBS	350±40	1.04±0.13	3.5±0.36	1.45±0.24

a. Reported errors are one standard deviation for the data fits.

High particle concentration. The effect of ionic concentration and species on transport of polymer modified NZVI at high particle concentration were similar to that of low particle concentration. The trends were identical (Figure 7.1.9), but the measured attachment efficiencies were larger than at lower particle concentration, indicating greater deposition and lower mobility. The greater effect of ionic strength and cation type on transport of RNIP dispersions at high particle concentration is a result of agglomeration of particles and subsequent deposition. At the high particle concentration agglomeration is significant compared to the low particle concentration. The higher the electrolyte concentration, the larger the sizes of stable agglomerates formed, and the deeper the secondary minimum well between deposited agglomerates and a collector. These two effects lead to the poor mobility as experimentally observed with increasing ionic strength. Overall, these data indicate that groundwaters having high ionic strength and high concentrations of divalent cations (e.g. marine sites) may limit NZVI mobility significantly. The use of these waters for injecting NZVI should be avoided. It should be noted however, that NZVI dispersed in low ionic strength water may be injectable into an aquifer of higher ionic strength or with high divalent cations since mixing between the injected water and the aquifer water will likely be limited. After injection, the presence of divalent cations would help prevent any unwanted mobilization of emplaced NZVI.

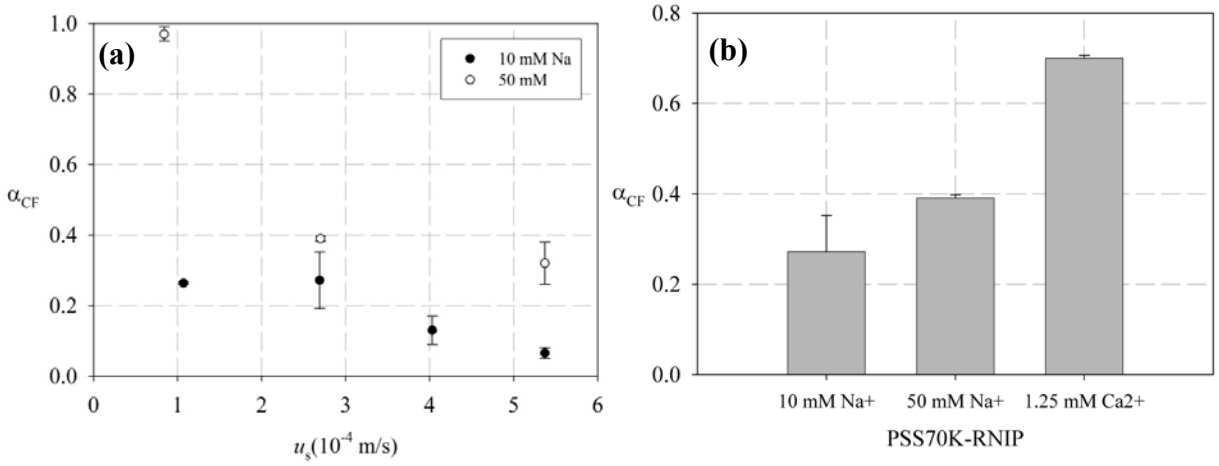

Figure 7.1.9. (a) Relationship between α_{CF} and approach velocity (u_s) for PSS70K modified RNIP in 50 mM Na^+ (open circles) as background electrolyte and in 10 mM Na^+ (filled circles) as background electrolyte with an average collector size = 300 µm. (b) α_{CF} values of PSS70K-RNIP in 10 mM Na^+, 50 mM Na^+, and 1.25 mM Ca^{2+} for an average collector size = 300 µm and the approach velocity (u_s) of 2.7x10-4 m/sec.

7.1.5. Effect of sand grain size on polymer modified NZVI mobility through homogeneous sand columns.

For transport of a concentrated polyelectrolyte-modified NZVI dispersion through porous media with fixed average approach velocity, cation type, and ionic strength, the attachment efficiency calculated using filtration theory, α_{CF}, increased with increasing collector size, d_g (Figure 7.1.10). This trend contradicts filtration theory which predicts that α_{CF} should decrease with increasing collector size due to a lower surface area for deposition on the larger collectors. This contradiction is explained by considering the effect of hydrodynamic forces on agglomeration and disagglomeration and deposition and detachment as proposed in Figure 7.1.6 (Phenrat et al. 2010b). The local fluid shear in the pores of porous media can affect both agglomeration and disagglomeration. For a fixed approach velocity, the smaller the average diameter of collectors, the higher the apparent shear in pores. This shear promotes disagglomeration. Therefore, for the same adsorbed layer properties, ionic strength, and seepage velocity, the size of stable agglomerates formed in the pores of porous media packed with small diameter collectors should be smaller than for larger diameter collectors due to the higher magnitude of local shear in the pores. The smaller sized agglomerates formed for the smaller collector particle size travel farther than the larger sized agglomerates formed for larger collector particles.

In addition to affecting the size of the agglomerates formed, fluid shear can affect deposition and detachment (Johnson et al. 2006; Torkzaban et al. 2007). The hydrodynamic drag torque acting on the deposited NZVI agglomerates is locally lower for agglomerates deposited on larger sized collectors compared to the smaller sized collectors while the adhesive (attachment) torque originating from the secondary minimum well (DLVO forces) is unaffected by fluid shear.

Therefore, for a fixed agglomerate size, the probability for detachment is higher for smaller diameter collectors in comparison to larger diameter collectors. In summary, for transport of concentrated nanoparticle suspensions with reversible agglomeration and deposition expected for polymer coated NZVI and at a fixed approach velocity, smaller diameter collectors increase the average shear force acting on deposited particles, promoting disagglomeration and detachment which results in the higher observed transportability in porous media.

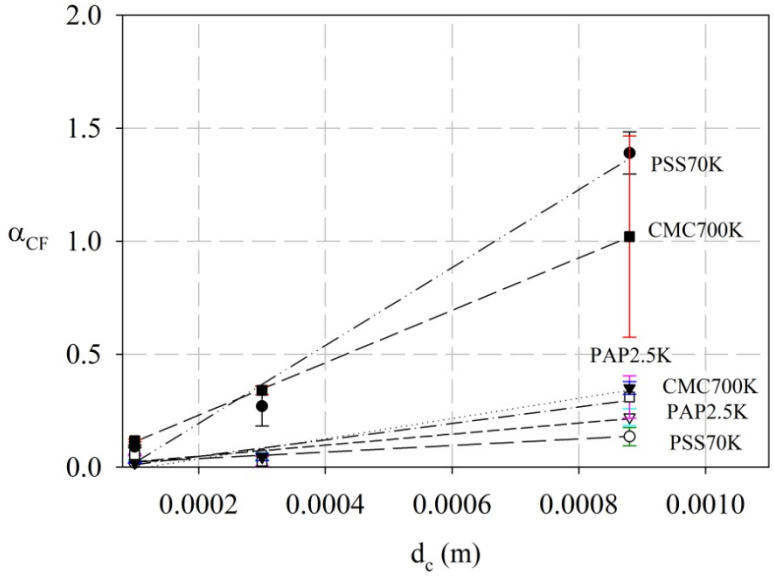

Figure 7.1.10. (a) α_{CF} vs. collector size (d_c) for different polyelectrolyte modified RNIP at various transport conditions. Open symbols are in 1mM Na^+ background electrolyte and porewater velocity = $5.5x10^{-4}$ m/s. Closed symbols are in 10mM Na^+ background electrolyte and approach velocity = $2.7x10^{-4}$ m/s. Each trend line illustrates the measurement of the effect of d_c on α_{CF} for a given polyelectrolyte modified NZVI transported at high particle concentration at a fixed ionic strength and seepage velocity.

7.2 Effect of physical and chemical heterogeneity on emplacement of polymer modified NZVI

Section 7.1 provides a fundamental understanding of the processes and system variables affecting polymer modified NZVI transport in homogeneous porous media. However, natural aquifer media is never homogeneous. Rather, an aquifer is both chemically and physically heterogeneous. Chemical heterogeneity includes the presence of minerals (such as iron oxide) and organic (such as particulate organic matter) patches on soil grains and the presence of e.g. clay particles in aquifer media which have unique surface properties. Physical heterogeneity includes layer formation in aquifers by various sizes of soil grains which can result in high hydraulic conductivity and low conductivity regions and therefore preferential flow paths. We determined the effect of both chemical and physical heterogeneity on transport and emplacement of polymer modified NZVI.

7.2.1 Effect of chemical heterogeneity of porous media on transport of polymer modified NZVI

Chemical heterogeneity of porous media evaluated in this section involves collector scale heterogeneity such as oxide patches on sand grain and porous scale heterogeneity such as the presence of fine particles and clay particles.

Natural aquifer materials typically contain metal oxide surface impurities (e.g. Fe-oxides or Al-oxides) that have a relatively high isoelectric point (pH_{iep} = pH 7 ~ 9.5) (Litton and Olson 1994; Song et al. 1994) compared to silica (pH_{iep} 2 ~ 3). Metal oxide impurities on mineral surfaces can behave as favorable deposition sites that limit nanoparticle mobility through the porous media at low pH (Song et al. 1994). These favorable sites originate from metal oxide impurities with relatively high pH_{iep}, resulting in positively charged surface patches at lower pH. To evaluate effect of these metal oxide impurities on transport of polymer modified NZVI, we compared column experiments using untreated sand (containing 0.14% Fe_2O_3 and 0.49% Al_2O_3 by weight) and acid washed sand (i.e. no metal oxide impurities) for the transport of PAP modified hematite (300 mg/L). Hematite nanoparticles were used instead of NZVI in this study to avoid particle agglomeration promoted by magnetic attraction of NZVI which would complicate the result interpretation. As evident in Figure 7.2.1, PAP modified hematite eluted through acid washed sand better than sand with metal oxide surface impurities over the range of pH 6-8, confirming that positively charge patches of metal oxides limit transport of polyanion modified nanoparticles. Because in an actual field scale application we cannot remove all surface metal oxide impurities from sand or soil by acid washing, an implementable engineering approach to reduce adverse effect on particle transport by these impurities is necessary. As shown above in this report, this is achieved by transporting polymer modified NZVI with excess polymer in the injection solution. Excess polymer preferentially adsorbs onto metal oxide patches and eliminates positively charge site favorable for particle attachment.

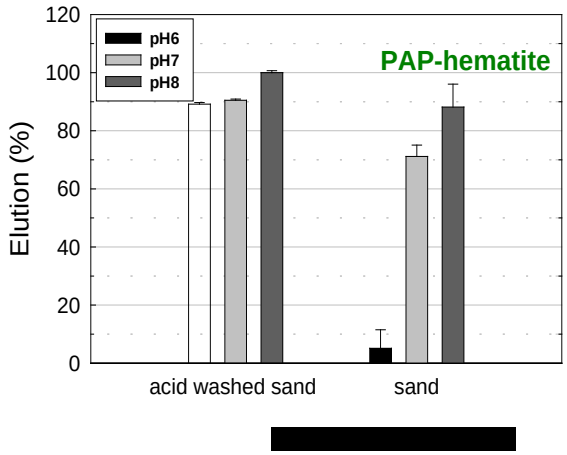

Figure 7.2.1 Percent mass of PAP hematite eluted through 15 cm columns filled with sand and acid washed sand at pH=6, pH=7 and pH=8 with porosity of 0.33. The initial hematite particle concentration was 300 mg/L, linear pore water velocity was 3.2 x 10-4 m/s and ionic strength was controlled at 10 mM NaCl + 1 mM NaHCO3.

Real aquifer media typically has a large range of particle sizes. The smallest particles, clay particles, are distributed throughout the porous media and reside in the interstitial pore spaces between the larger pores. This small fraction of clay can have a big impact on mobility of polymer modified NZVI due to pore plugging and as a result of charge heterogeneity of the clay. Clays such as kaolinite can have both a permanent negative charge on the basal plane because of isomorphic substitution of minerals (Si, Al) for lower positive valent ions and pH dependent edge charge due to surface hydroxyl groups (Al-OH, Si-OH) created from broken bonds which can protonate or deprotonate depending on the pH in the solution (Itami and Fujitani 2005; Tombacz and Szekeres 2006). The reported pH_{pzc}-edge of kaolinite edge sites ranges from pH 5.8 to 7.5 (Kretzschmar et al. 1998; Tombacz et al. 1999; Tombacz et al. 2004; Tombacz and Szekeres 2006). The positively charged edge sites on clay may serve as deposition sites for NZVI similar to the case of metal oxide surface impurities. In addition, kaolinite clay can undergo "edge to face heteroaggregation" to form large aggregates which can fill pore throats in the porous media. This occurs predominantly at low pH where the positive edge sites are attracted to the negative face sites of the clay particles. This process will be more significant if the nanoparticles also aggregate to larger sized particles. To evaluate the importance of the presence of clay particles in the porous media on transport of polymer modified NZVI, comparative transport experiments of polymer modified NZVI (including MRNIP, triblock modified RNIP, and PAP modified hematite) through columns packed with clean sand, sand with silica fines (1-2 μm), and sand with clay (kaolinite, also 1-2 μm)) were conducted. As shown in Figure 7.2.2 (using MRNIP as an example), even a small fraction of clay (2 wt% kaolinite) substantially limited transport of all polymer modified NZVI. The effect of clay is more severe than silica fines when present at the same mass fraction. This implies the importance of charge heterogeneity of clay on NZVI attachment. In addition, the effect of clay is more severe for particle transport at low pH where NZVI agglomeration also occurs. This suggests that not only attachment of polymer modified on positively charged sites on clay but also edge-to-face heteroaggregation of clay which can promote mechanical filtration of NZVI agglomerates plays important role. Similar to the case of metal oxide surface impurities, we can decrease adverse effect on particle mobility due to the presence of clay by transporting polymer modified NZVI with excess polymer. Excess polymer preferentially adsorbs onto positively charged edge of clay and eliminates positively charge sites or prevents edge-to-face heteroaggregation of clay. Identical trends were observed for triblock modified RNIP and for PAP modified hematite (Kim et al. 2012).

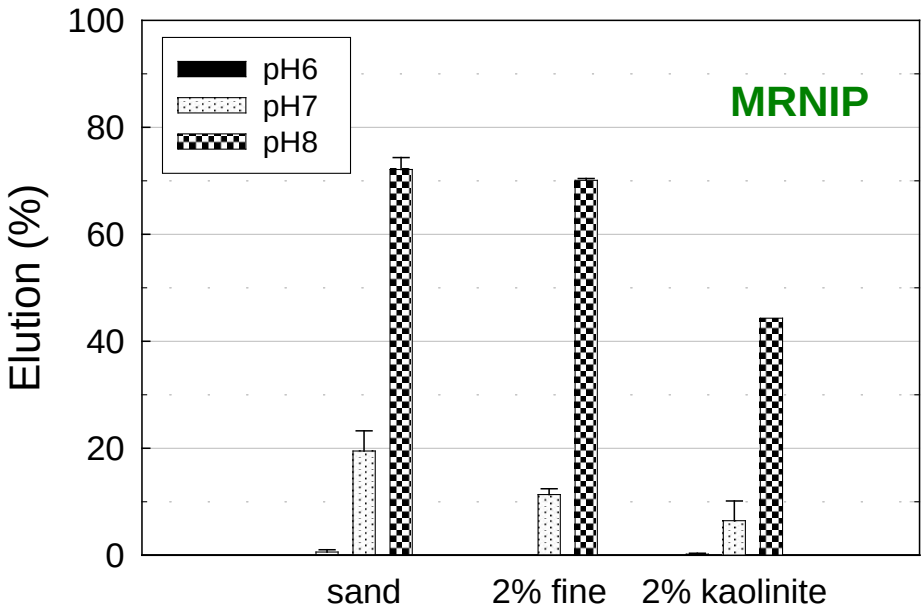

Figure 7.2.2. Percent of mass eluted for MRNIP (300 mg/L) through a 15 cm column filled with silica sand, sand + 2 wt. % silica fines (1.7 µm), or sand + 2 wt. % clay (1.36 µm) at pH 6, pH 7 and pH 8. The porosity was 0.33, the linear pore water velocity was 3.2 x 10-4 m/s, and ionic strength was controlled at 10 mM NaCl + 1 mM NaHCO3.

7.2.2 Effect of physical heterogeneity of the porous media on transport of polymer modified NZVI

Physical heterogeneity of the subsurface including aquifer permeability/hydraulic conductivity, collector size, and non-uniform flow fields may substantially affect NZVI transport. Since hydrodynamic shear affects transport of NZVI in porous media by breaking NZVI agglomerates formed during the transport and detaching deposited NZVI from a collector, spatial variation of seepage velocity due to heterogeneity will likely affect NZVI transport. Ultimately, the NZVI properties, solution chemistry, subsurface heterogeneity, and flow pattern together will determine NZVI transport and deposition in the subsurface. Porous media heterogeneity and non-constant flow velocity cannot be easily studied in a column experiment. Therefore, we used a two-dimensional (2-D) flow cell with more realistic physicall and hydrological conditions to assess the effect of heterogeneity on NZVI transport in porous media. To evaluate the effect of physical heterogeneity of porous media together with other physicochemical properties of NZVI including particle concentration, Fe^0 content, and adsorbed polymer layer thickness on transport of NZVI (which are evaluated in previous section for one dimensional flow), we conducted a transport and emplacement study of MRNIP2 in a two dimensional (2-D) aquifer cell which was packed using three different sizes of sand to create layered heterogeneity of hydraulic conductivity (Figure 7.2.3). To evaluate effect of NZVI particle concentration, we compared transport of MRNIP2 at three different particle concentration (0.3, 3, and 6 g/L). To evaluate effect of Fe^0 content, we compared transport of fresh and oxidized MRNIP2.

As shown in Figure 7.2.4, preferential flow paths created by heterogeneity in hydraulic conductivity had a significant impact on the transport and deposition of NZVI. Although injected into the middle layer of fine sand, due to the lower hydraulic conductivity of the fine sand, the tracer and polymer modified NZVI (regardless of particle concentration and Fe^0 content) preferentially moved through the upper medium grain sand and lower coarse grain sand layers which have a higher hydraulic conductivity. MRNIP2 followed the same transport pattern as a tracer, suggesting that density driven transport phenomenon as observed for another type of polymer modified NZVI (Kanel et al. 2008) is not significant for MRNIP2 under the transport conditions studied here. Polymer modified NZVI deposited in the regions where fluid shear is insufficient to prevent NZVI agglomeration and deposition (Figure 7.2.5). NZVI transported in heterogeneous porous media better at low particle concentration (0.3 g/L) than at high particle concentrations (3 and 6 g/L) due to greater particle agglomeration at high concentration. However, MRNIP2 at 3g/L transported better than at 6 g/L. This contrasts a previous finding that particle concentration (from 1 to 6 g/L) did not impact polyelectrolyte modified NZVI in homogeneous porous media in columns (section 7.1.2.2). This is a result of the 2-D flow field. In one dimensional flow (i.e. a column) fluid is forced to flow through pores with NZVI particles deposited on porous media; therefore, shear can effectively disaggregate and detach NZVI from porous media regardless of deposited particle concentration. In two dimensional flow like that used here fluid can more easily be diverted to take paths with less resistance, (i.e. in areas where NZVI has not deposited). Thus, in 2-D system, the shear force in areas of deposited NZVI is insufficient to diagglomerate and detach them. Injecting MRNIP2 at 6 g/L in heterogeneous porous media yielded a greater mass of deposited MRNIP2 than for 3 g/L as determined from measurements of Fe retained in the 2-D flow cell. This resulted in greater flow resistance through the zones of deposited MRNIP2 for the 6 g/L case compared to the 3 g/L. The lower flow resulted in a greater number of deposited particles at 6g/L compared to 3 g/L. Similar to findings in the column studies, MRNIP with lower Fe^0 content transports better due to a decrease in aggregation compared to particles with high Fe^0 content. Complete details of this study can be found in Phenrat et al., 2010 (Phenrat et al. 2010a).

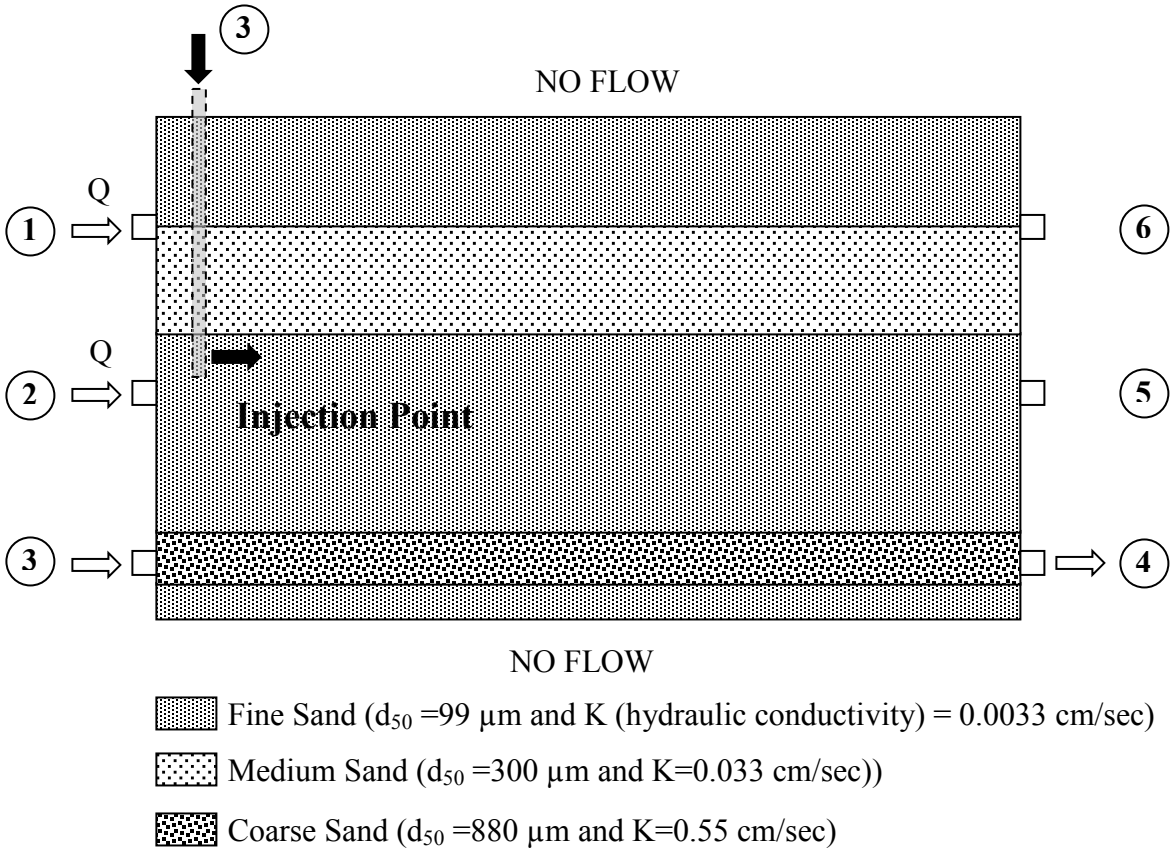

Figure 7.2.3 Schematic of 2-D flow-through cell (18cm x30cm x2.5 cm) with heterogeneous layered packing. Polymer modified NZVI and tracer were injected through the injection well while background flow was supplied through ports 1 to 3 and exited the tank through ports 4 to 6.

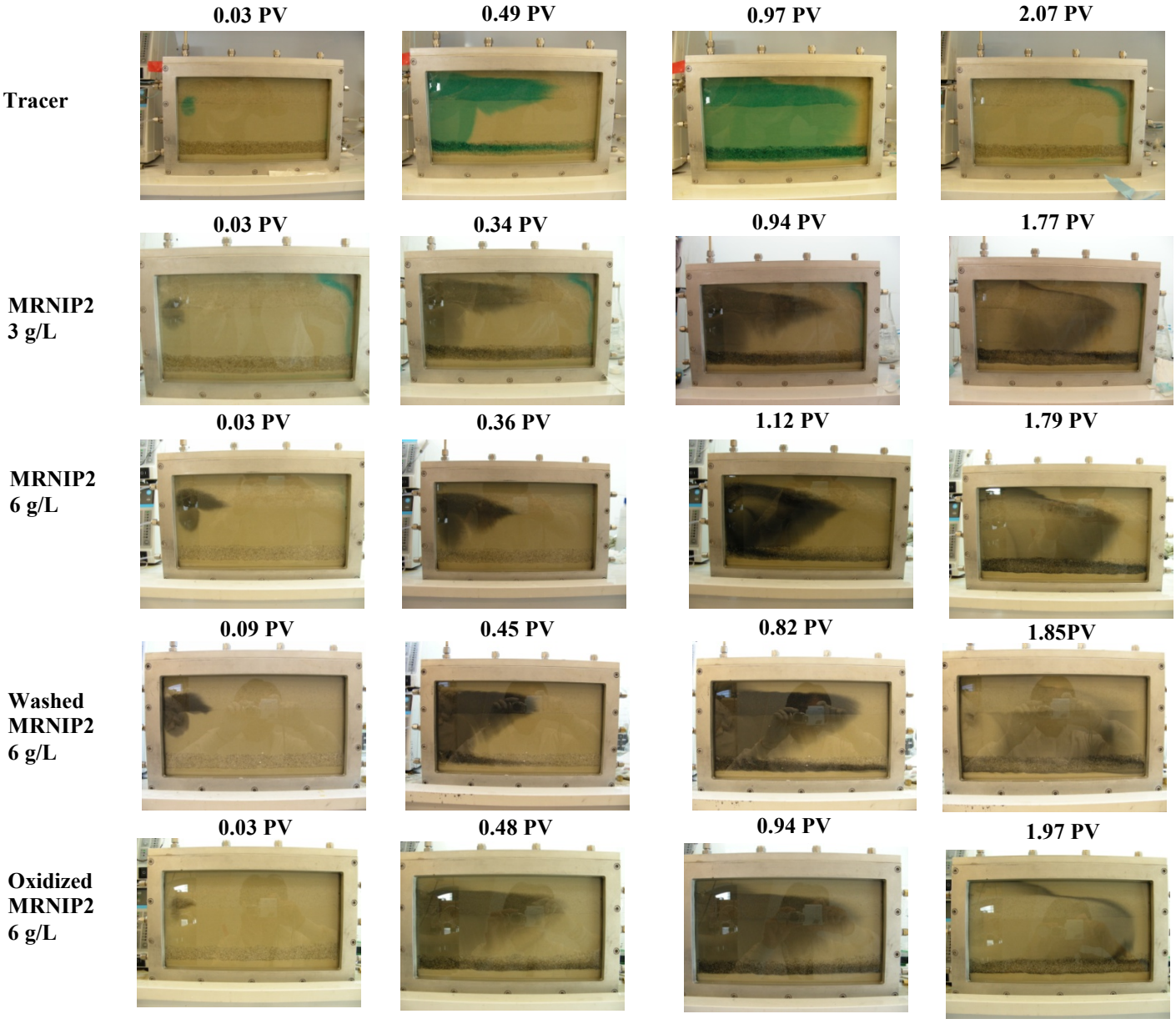

Figure 7.2.4. Representative photos illustrating the transport of a tracer, fresh MRNIP2 at 3 g/L and 6g/L, washed MRNIP2 at 6 g/L, and oxidized MRNIP2 at 6 g/L.

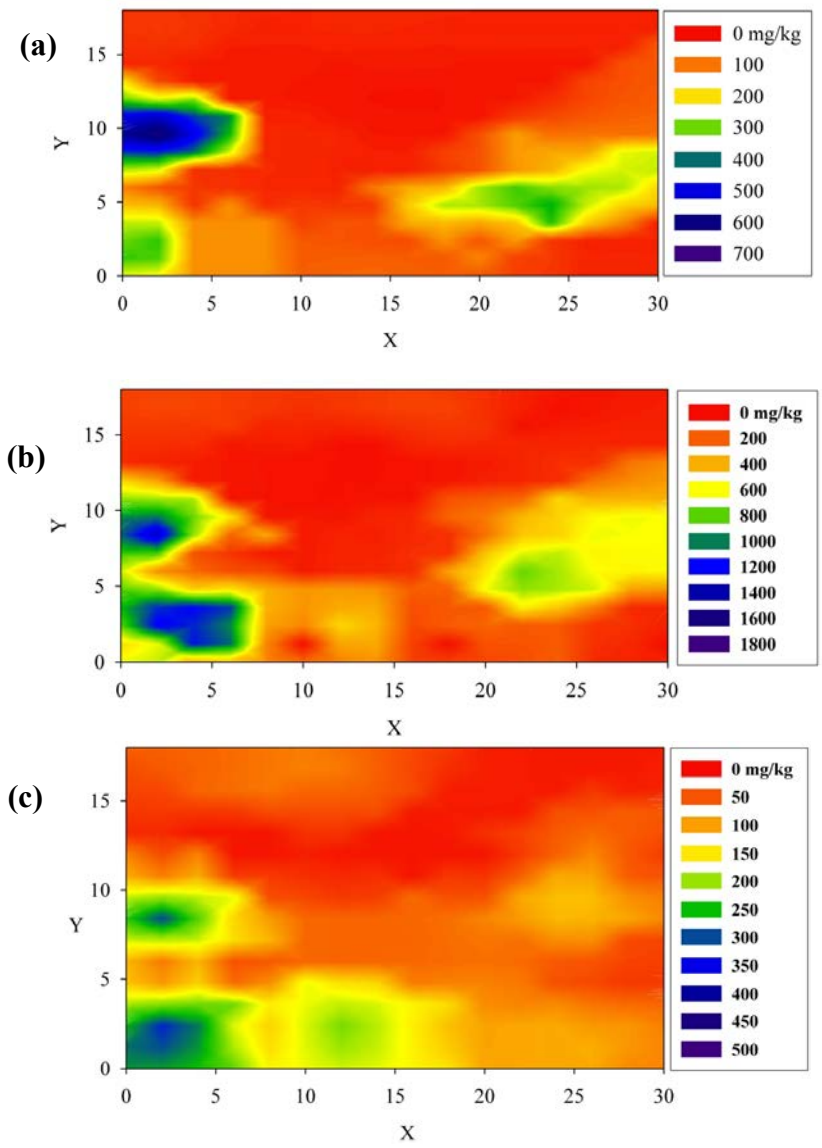

Figure 7.2.5 Contour maps illustrating MRNIP2 deposited onto sand grains (mg of nanoparticles per kg of sand). Maps are interpolated from 30 measurements of deposited MRNIP2 distributed across the cell. (a) Unwashed MRNIP at 3g/L. (b) Unwashed MRNIP2 at 6g/L. (c) Oxidized MRNIP2 at 6g/L. MRNIP2 significantly accumulates in three regions: 1) the region at the injection point (X from 0 to 7.5 cm and Y from 7 to12 cm); 2) the stagnation zone in the leftmost coarse sand layer (X=0 to 8 cm and Y from 1 to 4 cm); and 3) the region far from the injection in the fine sand (X from 17 to 30 cm and Y from 4 to 8 cm). MRNIP2 was injected to flow down gradient (i.e. from left to right with the groundwater flow). However, due to the relatively low hydraulic conductivity of the fine sand, MRNIP2 flowed backward (from right to left) at the injection point to migrate through the upper layer with medium sand and the lower layer with the coarse sand, both of which have higher conductivity. This flow field created regions with low pore water velocity where deposition occurred. This illustrates the importance of subsurface heterogeneity and the resulting flow pattern on the transport and deposition of NZVI in porous media.

7.3 Numerical models for predicting the emplacement of polymer modified NZVI in porous media

In sections 7.1 and 7.2, we qualitatively or semi-quantitatively discussed effects of particle properties, environmental factors, and hydrodynamic properties on transport and emplacement of polymer modified NZVI in homogeneous and heterogeneous porous media. In this section, we use this fundamental understanding to develop a quantitative model to predict NZVI transport and emplacement in heterogeneous porous media. As discussed earlier, transport of polymer modified NZVI at low particle concentration is different from at high particle concentration. Therefore, in this section, we first develop a model for transport of polymer modified NZVI at low concentration when deposition dominates the mobility. Then, we develop a model for NZVI at high particle concentration when both agglomeration and deposition affect particle mobility. The model for low particle concentration is more relevant for risk assessment of NZVI while the model for high particle concentration is essential as a preliminary tool for delivery of NZVI in subsurface for in situ environmental remediation.

7.3.1 A Semi-empirical model for predicting attachment of polymer modified NZVI in porous media at low particle concentration.

For low particle concentration where agglomeration and aggregation is trivial, attachment efficiency (α) of nanoparticles determines particle mobility in porous media and is solely affected by particle-collector (physicochemically and hydrodynamically) interfacial interaction (Elimelech et al. 1995; Phenrat et al. 2009a; Saleh et al. 2008). Magnetic attraction of NZVI does not affect NZVI-collector interactions because a collector (sand) is non-magnetic. Therefore, for polymer modified NZVI, the main driving forces affecting deposition are electrosteric repulsion, van der Waals attraction, and hydrodynamic forces. For this reason, the transport behavior of polymer modified NZVI is governed the same underlying forces as other polymer and natural organic matter (NOM) modified nanoparticles (Amirbahman and Olson 1993; Franchi and O'Melia 2003; Pelley and Tufenkji 2008). Thus, a model was developed for polymer and NOM modified nanoparticles to predict the attachment efficiency of polymer modified NZVI based on the characteristics of the adsorbed polymer layer.

We first investigated whether existing empirical correlations developed for electrostatically stabilized particles (proposed by (Bai and Tien 1999; Elimelech 1992)) can predict attachment efficiency for NOM- or polymer-coated nanoparticles. These empirical correlations are given in equations 7.3.1 and 7.3.2. The dimensionless parameters are given in Table 7.3.1.

$$\alpha = 2.57x10^{-2} N_{col}^{1.19} \tag{7.3.1}$$

$$\alpha = 2.527x10^{-3} N_{Lo}^{0.7031} N_{E1}^{-0.3121} N_{E2}^{3.5111} N_{DL}^{1.352} \tag{7.3.2}$$

As shown in Figure 7.3.1a, neither Elimelech's nor Bai and Tien's correlation adequately predicts the collision efficiencies of NOM- or polymer-coated particles. This is because these models account only for only van der Waals attraction and electrostatic repulsion, neglecting the electrosteric repulsions resulting from the adsorbed NOM or polyelectrolytes.

To develop a model that can better predictability of the collision efficiency of polymer modified nanoparticles, we develop a dimensionless number, N_{LEK}, and corresponding empirical

correlation for predicting the attachment efficiency, α_{pre} that includes electrosteric repulsions and the decrease of the friction force afforded by the adsorbed macromolecules. Steric repulsions are a function of particle and adsorbed layer properties including dp, d_M, Γ, ρ_p, and M_W. The rolling and detachment which is promoted by the reduction of the friction force is a function of fluid viscosity (μ) and fluid velocity (u_s) in addition to the particle and adsorbed layer properties mentioned above. The dimensionless Layer-Electrokinetic Parameter (N_{LEK}), representing both electrosteric repulsions and the decrease in friction force can be expressed as a function of dp, d_M, Γ, ρ_p, and M_W, μ, and u_s. Using the Buckingham-Π approach, N_{LEK} is expressed as,

$$N_{LEK} = \frac{d_p d_M^2 u_s \Gamma N_a \rho_p}{\mu M_W} \tag{7.3.3}$$

where N_a is Avogadro's number. Details of this analysis can be found in Phenrat et al., 2010 (Phenrat et al. 2010d). We use Ohshima's approach to determine the adsorbed layer thickness, d_{M0}, and adjust the layer thickness (d_M) for a particular salt concentration (I) using eqn 7.3.4.

$$d_M = d_{M0}\left[\frac{I}{I_{ave}}\right]^{-2/3} \tag{7.3.4}$$

Multiplying N_{LEK} with the dimensionless parameters for electrostatic repulsion (i.e. N_{E1}, N_{E2}, and N_{DL}) represents the relative influences of electrosteric repulsions at the particle-collector interface and the fluid velocity on the particle deposition rate due to interception.

To test the significance of N_{LEK} on the prediction of attachment efficiency of surface coated nanoparticles, "stepwise" multiple regression analyses using SPSS for Windows (Version 12; SPSS Inc., Chicago, U.S.) were conducted with N_{LEK} together with N_{Lo}, N_{E1}, N_{E2}, and N_{DL}. The same eighty data points used to test Elimelech's and Bai and Tien's correlations were used again here to test N_{LEK} inclusion. The data set (α_{exp}, N_{Lo}, N_{E1}, N_{E2}, N_{DL}, and N_{LEK}) was linearized using a common logarithm prior to regression analysis. The resulting correlation for surface coated nanoparticles based on the regression is given in eqn 7.3.5.

$$\alpha_{pre} = 10^{-1.35} N_{LO}^{0.39} N_{E1}^{-1.17} N_{LEK}^{-0.10} \tag{7.3.5}$$

The (unstandardized) exponent for N_{LEK} is negative (-0.10) indicating that steric repulsions originated from adsorbed macromolecule layers inhibit deposition as theoretically expected. The standardized coefficient for N_{LEK} (-0.24) is similar to that for N_{Lo} (0.32), suggesting that the steric repulsions afforded by adsorbed NOM or polyelectrolyte are as important for predicting particle deposition as are van der Waals forces under the conditions tested. The coefficient of determination (r^2) of this model is 0.8. (Figure 7.3.1b). The relatively high value of r^2 implies that this model captures the majority of the important independent parameters for predicting the deposition of NOM- and polyelectrolyte-modified nano-particles in porous media.

Table 7.3.1. Dimensionless parameters used in equations 7.3.1, 7.3.2, and 7.3.5.

Notation	Definition	Formula
N_{col}	Stability parameter	$\frac{\kappa H}{\varepsilon_o \varepsilon_r \zeta_p \zeta_g}$
N_{Lo}	London number	$\frac{4H}{9\pi\mu d_p^2 u_s}$
N_{E1}	1st electrokinetic parameter	$\frac{\varepsilon o \varepsilon r(\zeta_p^2 + \zeta_g^2)}{3\pi\mu u_s d_p}$
N_{E2}	2nd electrokinetic parameter	$\frac{2\zeta_p \zeta_g}{(\zeta_p^2 + \zeta_g^2)}$
N_{DL}	Double layer force parameter	κd_p
N_R	Aspect ratio	$\frac{d_p}{d_c}$
N_{Pe}	Peclet number	$\frac{u_s d_c}{D_\infty}$
N_{vdW}	Van der Waals number	$\frac{H}{k_b T}$
N_A	Attraction number	$\frac{H}{3\pi\mu d_p^2 u_s}$
N_G	Gravity number	$\frac{d_p^2(\rho_p - \rho_f)g}{18\mu u_s}$
As	Porosity-dependent parameter	$\frac{2(1-\gamma^5)}{2-3\gamma+3\gamma^5-2\gamma^6}$

Note: d_p is particle diameter, d_c is collector diameter, D_∞ is the bulk diffusion coefficient (described by Stokes-Einstein equation), ε_0 and ε_r are permittivity of vacuum and dielectric constant, respectively, g is the gravitational acceleration, H is the Hamaker constant, k_b is the Boltzmann constant, κ is the Debye parameter, ρ_p and ρ_f, are the density of particle and fluid, respectively, T is fluid absolute temperature, u_s is fluid superficial velocity, μ is viscosity of fluid, ζ_p and ζ_g are electrical surface potential of particle and collector, respectively, γ is $(1-f)^{1/3}$, where f is porosity.

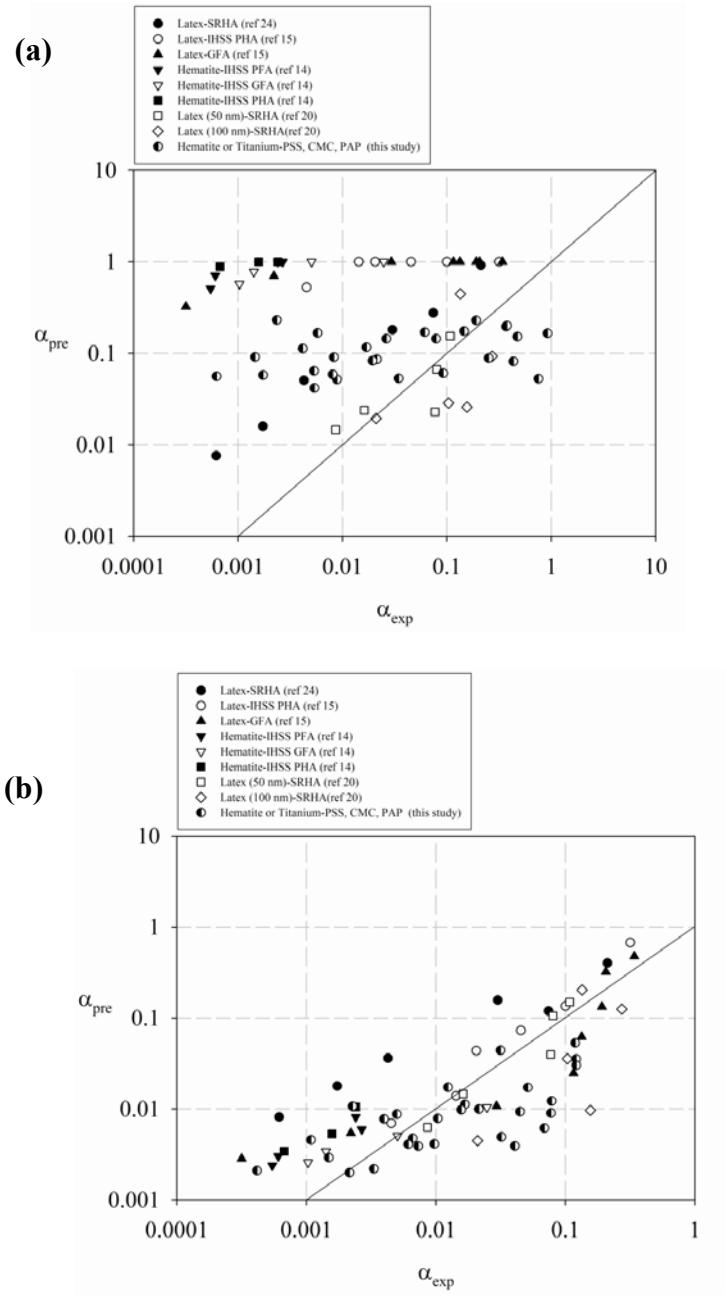

Figure 7.3.1. (a) α_{pre} from Bai and Tien's correlation vs. αexp for latex particles coated with SRHA (Franchi and O'Melia 2003), latex particles coated with GFA and PHA (Amirbahman and Olson 1993), hematite particles coated with GFA, PFA, and PHA (Amirbahman and Olson 1995), hematite particles coated with GFA, PFA, and PHA (Amirbahman and Olson 1995), latex particles coated with SRHA(Pelley and Tufenkji 2008), and hematite and titanium dioxide nanoparticles coated with PSS, CMC, and PAP. Solid line represents the 1:1 correlation for α_{pre} vs. α_{exp}. (b) α_{pre} vs. α_{exp} for all NOM- and polymer-coated nanoparticles and colloids examined in this study using eq. 7.3.5 (with N_{LEK}). Solid line represents the 1:1 correlation for α_{pre} vs. α_{exp}.

7.3.2 Empirical correlations to estimate agglomerate size and deposition during injection of a polyelectrolyte-modified Fe^0 nanoparticle at high particle concentration in saturated sand.

In section 7.3.1, we presented the development and verification of a semi-empirical model to predict attachment efficiency of polymer modified nanoparticles in saturated porous media. This is valid for transport of polymer modified NZVI at low particle concentration. However, agglomeration due to strong magnetic attraction of NZVI particles and high collision frequency expected for concentrated NZVI dispersions used for in situ remediation suggests that classical filtration (CF) theory (taking into account only particle attachment and ignoring agglomeration) may in fact not be reliable for quantitative estimation of attachment efficiency, α, for NZVI dispersions at high particle as suggested in sections 7.1.2-7.1.5. Evidence suggesting that the CF model is inappropriate for predicting the transport of polyelectrolyte-modified NZVI at high particle concentration includes of the dependency of the attachment efficiency determined using the CF model, α_{CF}, on the seepage velocity and the inverse correlation between collector size and α_{CF} observed in this study. Further, α_{CF} values are greater than 1 in several cases (see section 7.1.4 and 7.1.5) which are physically impossible for the NZVI-collector interactions without agglomeration during transport. Thus, we modify CF theory to allow for steady state agglomeration and subsequent deposition of agglomerates formed during transport. We then develop a model for predicting α for NZVI transport at high particle concentration in porous media. The details of this model are available in Phenrat et al., 2010 (Phenrat et al. 2010b). We briefly describe the important findings from this model.

For a system that has reached a steady-state agglomerate size (d_{agg}) the observed single collector removal efficiency (η') of the agglomerate in a porous media is a result of the transport and attachment of the agglomerate (rather than the individual particle) and is experimentally determined from C_{PT}/C_o of a breakthrough curve using Eq. 7.3.6.

$$\eta' = -ln\left(\frac{C_{PT}}{C_o}\right)\frac{4a_c}{3(1-\varepsilon)L} = \eta_o'\alpha' \qquad (7.3.6)$$

The observed single collector removal efficiency can be expressed as the product of the single-collector collision frequency of the agglomerate (η_0') and the attachment efficiency of the agglomerate (α') (Eq.7.3.6). Please note that the "prime" notation on η', η_0' and α' is used to distinguish between filtration theory that assumes no aggregation and the modified filtration theory presented in this study which assumes rapid steady state agglomeration. Both η_0' and α' are a function of d_{agg} and are determined by iterating Eqns. 7.3.7 and 7.3.8 to yield the observed attachment η' in the column.

$$\eta_0' = \left[\frac{67.39H^{0.05}A_s^{1/3}}{(k_BT)^{-0.66}d_c^{0.63}u_s^{0.72}}\right]d_{agg}^{-0.796} + \left[\frac{0.985H^{0.12}A_s}{u_s^{0.12}d_c^{1.68}}\right]d_{agg}^{1.425} + \left[\frac{3.16x10^{-5}H^{0.05}d_c^{0.24}}{(k_BT)^{0.05}u_s^{1.11}}\right]d_{agg}^{1.98} \qquad (7.3.7)$$

$$\alpha' = \left[\frac{6.29x10^{7}H^{0.39}u_s^{0.68}\eta_v^{0.88}M_W^{0.10}}{\rho_{poly}^{0.10}\Gamma^{0.10}d_M^{0.20}\left(\zeta_p^2+\zeta_g^2\right)^{1.17}}\right]d_{agg}^{0.29} \qquad (7.3.8)$$

Here H is the Hamaker constant between a particle and a collector, A_s is a porosity-dependent parameter, u_s is approach velocity, d_c is the diameter of a collector. Γ is the surface excess of

macromolecule on NZVI (in kg/m^2), d_M is adsorbed layer thickness (in m), M_W is molecular weight (in kg/mole) and ρ_{poly} is density (in kg/m^3) of adsorbed polymer, η_v is viscosity (in Pa-s), ζ_p and ζ_g are zeta potentials of particles and collectors, respectively (in V). Eq. 7.3.7 is derived from Eq.6.8 but uses d_{agg} instead of initial particle size to represent the transport of a particle with diameter d_{agg} to a collector via diffusion, interception, and gravity. Eq. 7.3.7 is specific for the transport of NZVI particles with the density of 6.5 g/cm^2 in water. It is assumed that aggregation of polymer modified NZVI affects d_{agg} but not the other parameters.

Solving Eqs. 7.3.6 to 7.3.8 for d_{agg} using C_{PT}/C_o of a breakthrough curve together with particle properties and transport conditions obtained from column experiments of polymer modified NZVI at 6 g/L (summarized in section 7.1.2 to 7.1.5) results in the *apparent* diameter of NZVI agglomerates (d_{agg}) for different transport conditions and types of surface modifiers. The calculated values of d_{agg} demonstrate trends with parameters affecting agglomeration in porous media such as adsorbed particle layer properties, particle size, size of porous media, and approach velocity, suggesting that it is possible to develop an empirical correlation to predict d_{agg} from a set of parameters that describe the physics of the system. Using regression analysis of the set of column data we propose an empirical model to predict a dimensionless agglomerate size (d_{agg}/d_p) as a function of the transport conditions, NaCl concentration, shear rate in porous media (sec^{-1}), and properties of the polymeric surface modifiers (Eq. 7.3.9).

For NaCl

$$\frac{d_{agg}}{d_p} = 4.24x10^{-15}\frac{\mu_o^{1.28} M_s^{2.55} M_w^{0.10}}{\eta_v^{2.26} N_{avo}^{0.3} d_{M0}^{1.2} \gamma_s^{0.3} [NaCl]^{*0.2}} \qquad (7.3.9)$$

Where μ_0 is magnetic permeability in vacuum (1.25x10^{-6} N/A^2), and N_{avo} is Avogadro's number (6.03x10^{23} mole^{-1}). [NaCl]* in this equation is in mole/m^3. M_S (in A/m) is NZVI saturation magnetization. d_{M0} (in m) is adsorbed polymer layer thickness determined from Ohshima's soft particle analysis. M_W is molecular weight of polymeric surface modifier and η_v is fluid viscosity. The empirical unit of the constant in Eq.7.3.9 is kg$^{-0.88}$ m$^{4.13}$ mole$^{-0.3}$.

Eq.7.3.9 allows the prediction of d_{agg} formed in porous media during the transport of polymer modified NZVI at high particle concentration. Fig. 7.3.2a illustrates the accuracy of Eq. 7.3.9 in predicting d_{agg} while Fig. 7.3.2b illustrates the accuracy of using Eq.7.3.9 together with Eqns. 7.3.7 and 7.3.8 in predicting η' (i.e. comparing predicted η'_{pre} with η calculated from column experiments).

Some general conclusions can be made about the particle properties and the hydrogeochemical parameters found to be significant in assessing NZVI attachment, i.e. those included in Eq. 7.3.9. 1) Higher fluid shear γ_s, yields a smaller d_{agg} because fluid shear breaks the agglomerates. 2) Larger NZVI primary particles, d_p, yield greater d_{agg} because magnetic attraction scales with d_p to the sixth power. 3) A larger d_{M0} yields a smaller d_{agg} because d_{M0} is proportional to extent of electrosteric repulsions which prohibits agglomeration. 4) A greater saturation magnetization, M_s, yields a larger d_{agg} because M_s promotes magnetic attraction which drives agglomeration. 5) A higher [NaCl]* yields a smaller d_{agg} because NaCl screens electrostatic attraction between particles and collapses the adsorbed polymer layer thickness, both of which promote formation of "dense" agglomerates with higher fractal dimension and a smaller apparent d_{agg}. 6) A polyelectrolyte with a higher M_w yields a larger d_{agg} because a polymer with large M_w better resists charge screening by salt than a polymer with a low M_w. Thus, large M_w decreases the potential of forming dense agglomerates.

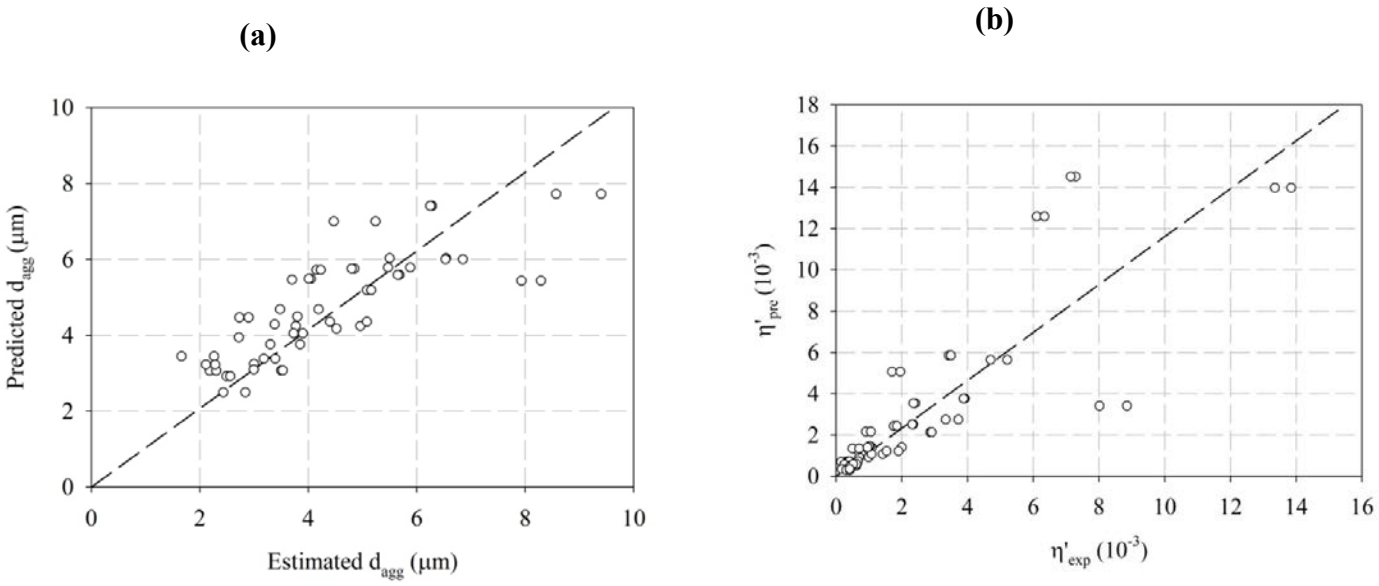

Figure 7.3.2. (a) a comparison between predicted d_{agg} using Eq. 7.3.9 and estimated d_{agg} from column experiments. (b) a comparison between predicted η' based on the predicted d_{agg} in (a) and experimental η'. R^2=0.87 for the data fit for both cases. The fits statistics are the same since they are transformed from the same data set.

7.3.3 COMSOL-based particle transport model for predicting the emplacement and transport of polymer-modified NZVI in heterogeneous porous media

In the previous two sections we described the development of an empirical model that allows for the prediction of polymer modified NZVI transport in porous media at high particle concentration. However, it was validated only for homogeneous sand and one dimension flow. To enable the model to predict the transport and deposition of NZVI in heterogeneous porous media with varying flow velocities we coupled the semi-empirical correlations for estimating stable aggregate sizes and their deposition in porous media (Eq.7.3.7 to 7.3.9) with a two dimensional flow field simulation using COMSOL. To evaluate the performance of the model, we compared the measured transport and deposition of polymer modified NZVI transport in 2-D heterogeneous porous media (section 7.2.2) with modeled results using the same hydrogeochemical conditions as in the experiment. This experiment is described in detail in Phenrat et al., 2010 (Phenrat et al. 2010a). Figure 7.3.3 shows the experimental and modeling results of MRNIP2 transport at different pore volumes (PV) of transport. The experimental and modeling results of MRNIP2 transport are similar. This suggests that the COMSOL-based model using the semi-empirical correlations for estimating stable aggregate sizes and of those aggregates in porous media is a promising tool for designing delivery schemes for polymer modified NZVI in porous media *when the nanoparticle properties and subsurface properties are known*. We also tried to couple other available colloidal transport models (such as standard and modified filtration models (Eq.7.3.2) that account for steric effects on deposition but ignores agglomeration (Eq. 7.3.5)) with the COMSOL model. However, these models could not simulate the experimental results. Assuming a filtration model alone (ignoring steric effect and agglomeration) underestimates MRNIP2 transport while assuming a modified filtration model

with the effects of steric repulsions on deposition but ignoring agglomeration overestimates the transport.

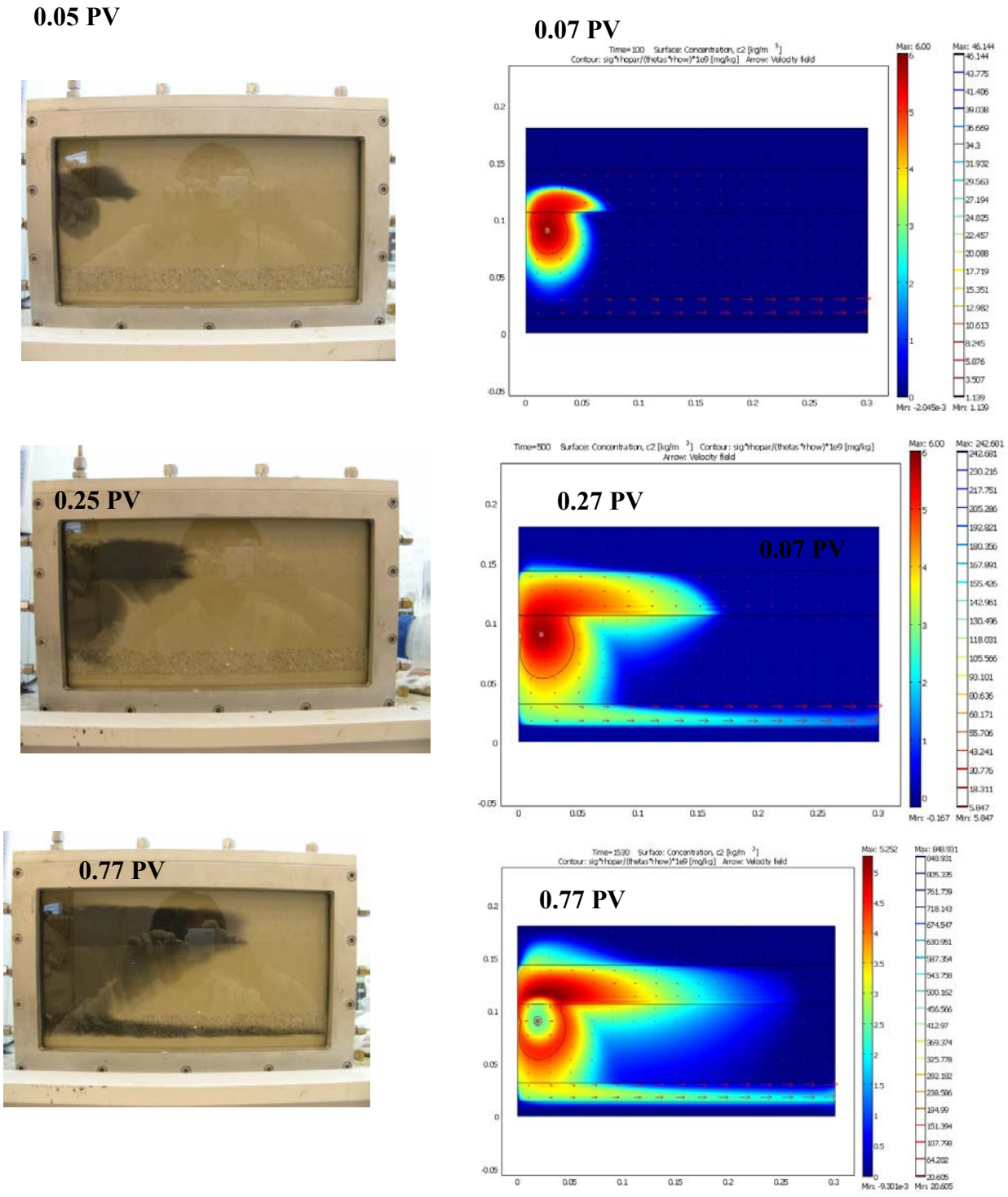

Figure 7.3.3 A comparison between experimental and modeling results of MRNIP2 transport in 2-D heterogeneous porous media at similar PV.

7.4 Targeting polymer modified NZVI to DNAPL

Emplacing **N**ZVI directly in the source zone may provide NAPL mass reduction and subsequently speed up time to the site closure. Delivering polymer modified NZVI to NAPL source zones can be done two ways; 1) interfacial targeting of NAPL-water interface using polymer modified NZVI and 2) controlling the delivery of NZVI to NAPL source zone. This section will discuss what was found about the potential for these two possible approaches.

7.4.1 Interfacial targeting of NAPL-water interface using polymer-modified NZVI.

To achieve interfacial targeting of NAPL source zones, polymer modified NZVI must have affinity to target the interface, and the hydrodynamic conditions must allow the delivery of NZVI to NAPL-water interface. We conducted batch tests to screen various polymers for their ability to target the NAPL-water interface and 2-D tank experiments to evaluate the mechanisms by which NZVI can be targeted to entrapped NAPL in situ.

7.4.1.1 Screening of NZVI affinity to target NAPL-water interface via ex Situ (batch) targeting test

The ability of an amphiphilic triblock copolymer to target the TCE/water interface was demonstrated previously by our group (Saleh et al. 2005b). This particular triblock copolymer is not commercially available, but various diblock and triblock copolymers are now commercially available with prices ranging from about $10/kg to $1000's/kg depending on the architecture and the amount being produced. We also used batch experiments to evaluate the ability of commercially available inexpensive polyelectrolytes (e.g. $2/kg for bulk polystyrene) adsorbed to NZVI (i.e. MRNIP2) to target NAPL-water interface. Overall, the polymer cost will likely be low compared to other costs given that very little is needed to coat the NZVI. One exception would be if polymer is injected along with the injection solution to improve transport.

For MRNIP2, three particle concentrations (0.5, 3, and 15 g/L MRNIP2) were evaluated for their ability to target NAPL-water interface. At all particle concentrations MRNIP2 was capable of targeting NAPL/water interface via the formation of Pickering emulsions as evident by 1) the flat interface formed between dodecane and MRNIP2 at 3 g/L and 15 g/l (Figure 7.4.1a), suggesting either interfacial tension lowering or spontaneous partitioning of MRNIP2 to dodecane phase and 2) rapid accumulation of MRNIP2 at the NAPL interface rather than being dispersed in the aqueous phase (Figure 7.4.1b), and 3) dodecane was emulsified.

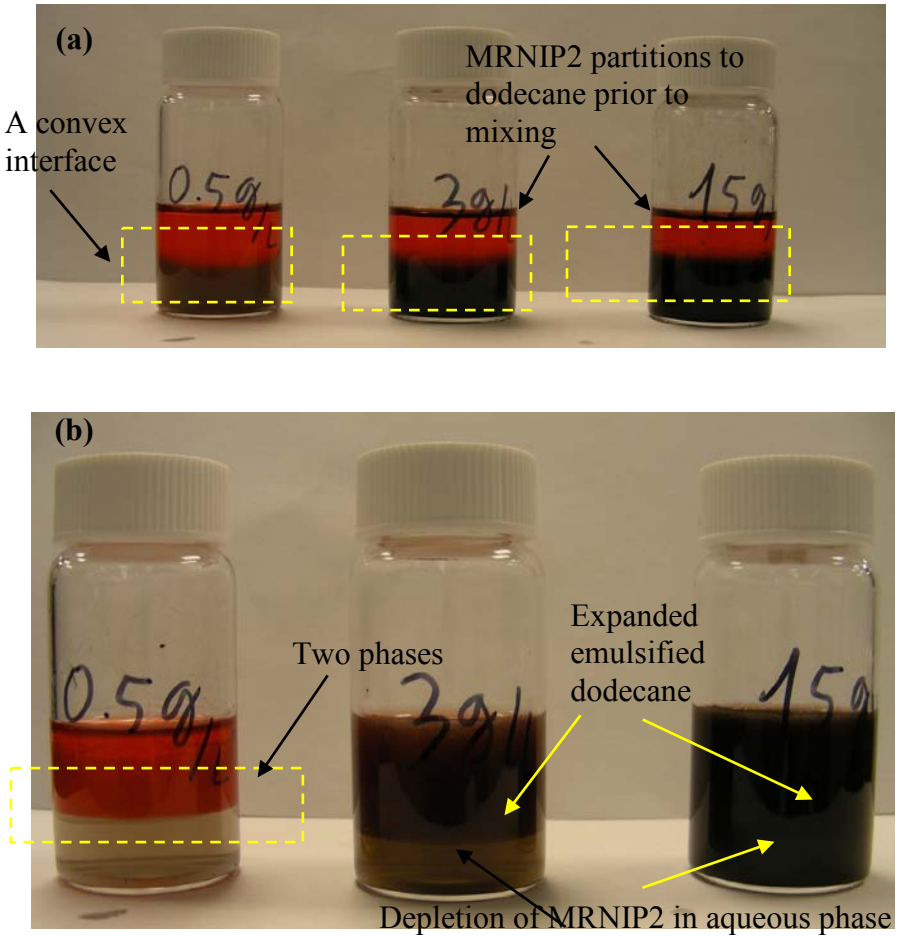

Figure 7.4.1. The mixture of 5 mL washed MRNIP2 (0.5 g/L, 3 g/L, and 15 g/L) (black) and 5 mL dodecane (red) (a) prior to hand shaking and (b) after hand shaking when Pickering emulsion was formed.

Similar emulsification experiments were conducted for the three different kinds of polyelectrolyte-modified RNIP (3 g/L) including CMC, PSS, and PAP modifiers both with and without excess polymer to determine the potential for targeting RNIP to the water/TCE interface. All of the modifiers (in the absence of RNIP) except PAP could emulsify TCE, demonstrating their amphiphilic behavior. PSS-modified RNIP was capable of targeting RNIP to the TCE/water interface with and without excess free polymer in solution. CMC-modified RNIP created an emulsion phase, but did not promote contact between RNIP and TCE DNAPL as with PSS. The PAP-modified RNIP did not create an emulsion when excess free polymer was present, but could do so when the particles were washed and there was no excess free polymer in the solution.

Based on these studies, MRNIP2 has affinity for NAPL-water interface even at low particle concentration. CMC does not appear to be a promising RNIP surface modifier, but PSS and PAP without excess free polymer appear to provide the potential for enhancing contact between TCE DNAPL and modified RNIP in situ.

7.4.1.2 In situ NAPL targeting by polymer-modified NZVI in two dimensional, heterogeneous porous media.

The targeting of NZVI to entrapped NAPL in 2-D heterogeneous porous media was evident. NAPL targeting using polymer modified NZVI is affected by NAPL saturation (S_n), particle concentration, and the injection strategy. MRNIP2 was used in this study, and dodecane was used as a model NAPL. The details are summarized below. Complete details of this study can be found in Phenrat et al., 2011 (Phenrat et al. 2011).

Figure 7.4.2 illustrates NAPL source zones in heterogeneously packed 2-D flow through cell used in an *in situ* targeting study as described in Section 6.2.9. Two MRNIP2 delivery strategies were evaluated here. Strategy#1 simply involved the injection of MRNIP2 in porous media, followed by flushing with 1 mM $NaHCO_3$. MRNIP2 interacted with NAPL/water interfaces during the flow of the dispersion through the source zone. Strategy#2 included additional 24 hrs of the interaction between MRNIP2 and NAPL/water interface under a no-flow condition in addition to the similar delivery and flushing procedure of Strategy#1. The hypothesis behind Strategy#2 is that the extra interaction time might increase NAPL targeting by MRNIP2. Three different MRNIP2 concentrations were evaluated (0.5, 3, and 15 g/L). Because NAPL targeting is an interfacial phenomenon, a NAPL targeting index (Γ_{SA}) was determined for each source zone by normalizing the MRNIP2 remaining in the source zone with a theoretically calculated NAPL/water interfacial area (IFA) in the source zone (g of MRNIP2/m^2 of NAPL/water interface in source zone)

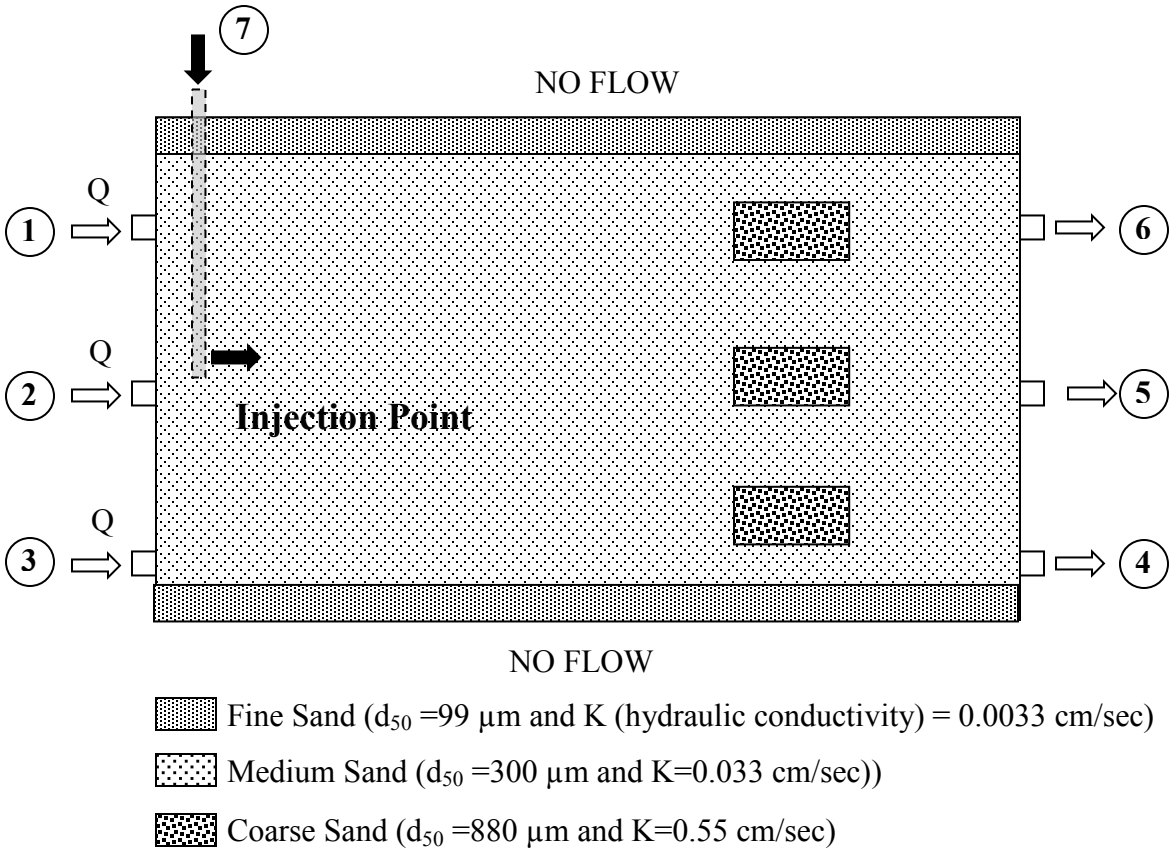

Figure 7.4.2. Schematic of 2-D flow-through cell (18cm x30cm x2.5 cm) with heterogeneous packing to create three NAPL source zones. MRNIP2 and tracer were injected through the injection well while background flow (to simulate groundwater flow) was supplied through ports 1 to 3 and exited the tank through ports 4 to 6.

Due to polymer surface modification, MRNIP2 was mobile in porous media and able to access NAPL source zones when S_n < 100%. As shown in Figures 7.4.3a, c, and e as an example, MRNIP2 at 15 g/L was deliverable through porous media (using delivery Strategy#1) and able to access NAPL source zones of S_n=50 and 75%. The same behavior was observed for NAPL source zones of S_n = 13 and 27%. On the other hand, the flow of groundwater carrying MRNIP2 bypassed the NAPL source zone with S_n =100% (Figure 7.4.3b) and consequently, MRNIP2 could interact with NAPL just at the boundary of the source zone (Figure 7.4.3g). After flushing with 3 PVs of 1mM $NaHCO_3$, most MRNIP2 was eluted from the main porous media domain, leaving only a small fraction attached to Unimin sand#50. On the other hand, even after flushing, MRNIP2 still resided at NAPL-water interfaces in the source zones (Figure 7.4.3d, f, h). Obviously, most MRNIP2 in the source zones were accumulated at NAPL/water interfaces while only a small amount was on the Unimin sand#16. This is also confirmed by a micrograph of a cored sample from a NAPL source zone, indicating that MRNIP2 accumulated at NAPL/water interfaces. These results indicate that NAPL targeting by MRNIP2 is mainly promoted by

physicochemical interactions between dodecane and MRNIP2 rather than a deposition or sedimentation of MRNIP2 on NAPL. While MRNIP2 at moderate and high particle concentrations both demonstrate NAPL accessibility and targeting, the quantitative NAPL targeting depended strongly on NAPL saturation and particle concentration as summarized below.

- Particle concentration effect. MRNIP2 at low particle concentration (0.5 g/L) could not target NAPL source; however, MRNIP2 at moderate and high particle concentrations (3 g/L and 15 g/L) was shown to accumulate preferentially at sites of NAPL entrapment, *i.e.*, that it was capable of *in situ* targeting.
- NAPL saturation effect. The amount of MRNP2 that targets a NAPL source is a function of NAPL saturation (S_n) (Figure 7.4.4) presumably because the saturation controls the available NAPL/water interfaces for targeting. The flow field through the NAPL source is affected by the NAPL saturation and also plays a role on NAPL targeting by MRNIP2. At effective S_n close or equal to 100%, MRNIP2 flow bypassed the source and could target only the boundary of the source zone. However, the ability of MRNIP2 to target the NAPL source (Γ_{SA}) is relatively constant (~0.8 g/m^2 for MRNIP2 = 3g/L) from S_n = 13 to ~100, suggesting that the interfacial affinity of MRNIP2 to adhere onto NAPL/water interface is also an important factor controlling targeting.
- Delivery strategy effect. At high MRNIP2 particle concentration (15 g/L), the interaction between MRNIP2 and NAPL/water interface during the residence time of the NZVI in the NAPL source area is sufficient to achieve source zone targeting. Providing additional time (24 hrs under no flow condition) for MRNIP2 to sediment or diffuse to the NAPL/water interface only slightly improves targetability (Figure 7.4.4)

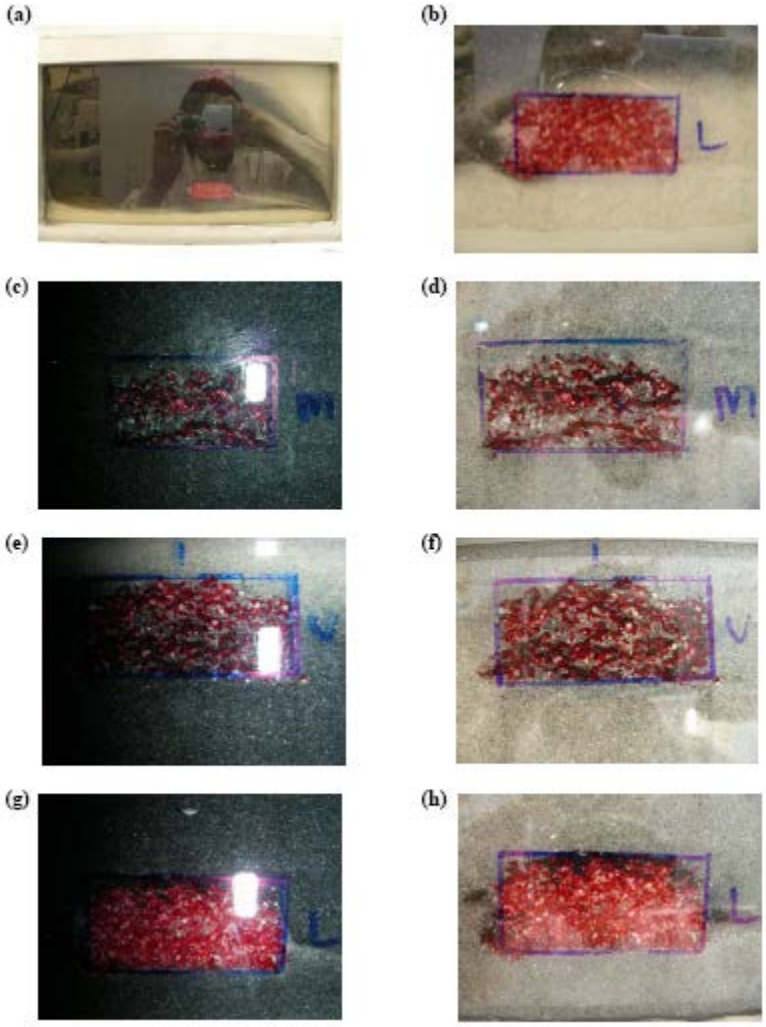

Figure 7.4.3. (a) MRNIP2 (15 g/L) transported to the NAPL sources during the injection Strategy#1. (b) MRNIP2 flowed bypass the source of S=100%. (c) MRNIP2 in the source zone of S=50%, (e) S=75%, and (g) S=100%. MRNIP2 remaining in the source zone of (d)S=50%, (f) S=75%, and (h) S=100% after flushing.

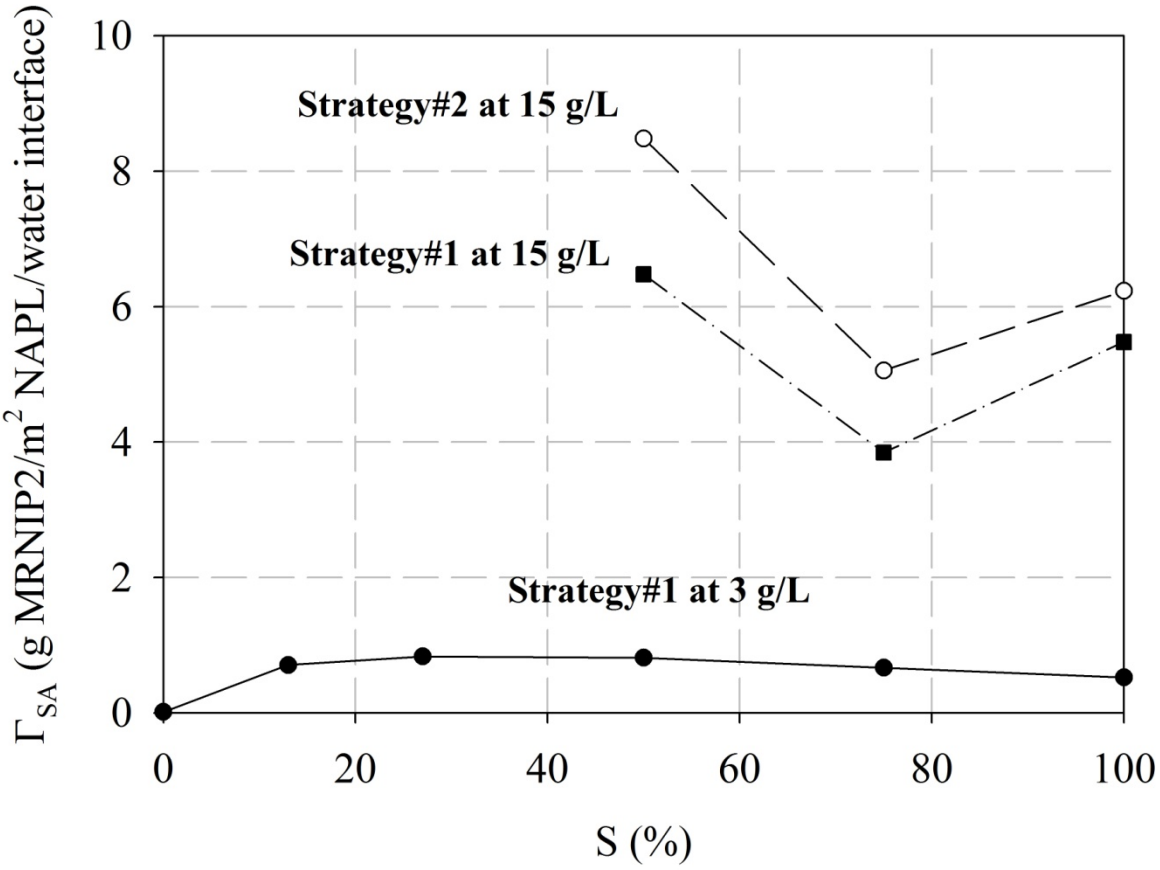

Figure 7.4.4. NAPL targetability by MRNIP2 at different particle concentration and delivery strategy and NAPL saturation.

7.4.2 Determine the potential for NAPL targeting by NZVI destabilization

NAPL targeting by NZVI destabilization (or destabilization targeting) requires that the surface modifier be released upon contact with NAPL. To assess the potential for destabilization targeting, the desorption of polyelectrolytes adsorbed to RNIP were measured including polyaspartate (2.5k and 10k molecular weight), PSS homopolymer (70k and 1M molecular weight) and carboxymethyl cellulose (90k and 700k molecular weight). The mixtures of RNIP and polyelectrolytes were equilibrated for 5 days at 25°C using an end-over-end rotator at 30 rpm, then centrifuged and the supernatant analyzed to determine the adsorbed mass of polymer. The sorbed mass was determined by difference between the added polyelectrolyte and the equilibrium concentration. Complete experimental details can be found in Kim et al., 2009 (Kim et al. 2009).

After sorption equilibrium is attained (about 4 days), the particles are washed to remove any excess polymer in solution and then allowed to equilibrate in polymer free solution for up to four months. Desorption of polyelectrolytes was monitored by centrifuging the particles after 2 weeks, 4 weeks, 8 weeks, and 16 weeks, and measuring the concentration of desorbed polymer in solution at each time step to determine the kinetics of release of each polymer. Over the 16 week period, only 10~26% of each polymer was desorbed. Higher molecular weight polymers

were desorbed less than the lower molecular weight polymer with in the same structure, i.e. PAP 2.5K, CMC 90K, and PSS 70K which are the lower molecular weight polyelectrolytes showed ~2 to 9% more desorption than PAP 10K, CMC 700K, and PSS 1M. PSS had lowest desorption rate among three polyelectrolytes evaluated, and the desorption rate of PAP and CMC were similar. Considering the larger molecular weight of CMC relative to PAP, CMC appears to desorb most easily of the three polyelectrolytes evaluated, however, very little of any of the modifiers desorbed after 16 weeks, indicating that large MW polymers and polyelectrolytes that are required to enhance mobility are not likely to desorb from the particles on time scales that can make them appropriate for destabilization targeting. It does, however, indicate that polymer desorption and subsequent NAPL mobilization is unlikely.

7.5 Factors influencing the reactivity of polymer modified NZVI with TCE and PCE

The reactivity of the NZVI in situ is an important factor affecting its ability to mitigate release of contaminants from the source. In this section, we evaluate impact of practical factors affecting in situ dechlorination rates of dissolved and NAPL phases. These factors include surface modifier properties, NZVI mass loading, flow velocity, and contaminant loading, i.e. reactivity in the presence of entrapped NAPL.

7.5.1 Effect of surface modifiers on reactivity with dissolved TCE

Polymeric surface modification is necessary for delivering NZVI in porous media and targeting NZVI to NAPL-water interface. However, surface modification may decrease NZVI reactivity. The reactivity of uncoated and surface modified RNIP with TCE was determined in batch studies to determine the effect of surface modification on reactivity. The TCE dechlorination rates of RNIP modified by PSS70K, PSS1M, CMC700K, CMC90K, PAP2.5K, and PAP100K become 5.6, 11.2, 13.4,17.9, 18.2, and 20.4 times slower than that of the uncoated RNIP. It was demonstrated that adsorbed modifiers could be decreasing decrease TCE dechlorination rate by 1) blocking surface sites and 2) by decreasing the concentration of TCE at the particle surface due to partitioning to the adsorbed layer (Figure 7.5.1a). It was also determined that the adsorption of polymer did not decrease the reactivity of the NZVI with water to form H_2. To distinguish between these two effects, the TCE dechlorination rate, reaction products formed, and H_2 evolution was measured as a function of the mass of polyelectrolytes sorbed onto RNIP surface. Three commercially available polyelectrolytes, poly(styrene sulfonate) (PSS), carboxymethyl cellulose (CMC), and polyaspartate (PAP), were used as representative modifiers. For all modifiers, the TCE dechlorination rate constant decreased non-linearly with increasing surface excess, but the TCE dechlorination pathways were not affected (Figure 7.5.1b). TCE dechlorination by β-elimination remains the dominant dechlorination pathway and yields acetylene as a reaction intermediate together with ethane and ethene as the major reaction by-products. Surface modification did not significantly affect the rate of H_2 evolution from RNIP. Based on the Scheutjens-Fleer theory for polymer sorption, the nonlinear relationship between the dechlorination rate and the surface excess of sorbed polyelectrolytes suggests that adsorbed polymers block reactive surface sites at low surface excess (Region I) where they adsorb relatively flat onto the NZVI surface, while at high surface excess the polymers adsorb in an extended configuration and develop a polymeric layer around the NZVI particles which blocks sites and decreases the concentration of TCE available for reaction at the

particle surface (Region II) (Figure 7.5.1a). This conceptual model is consistent with the measured surface excess of sorbed polyelectrolyte, the estimated layer thickness from Ohshima's soft particle analysis, and the measured partition coefficient of TCE into the polyelectrolytes. Additional details for this work, including detailed mechanisms, can be found in Phenrat et al., 2009 (Phenrat et al. 2009b).

These findings have several implications regarding polymeric surface modifiers for NZVI. In most applications the polyelectrolyte will be adsorbed at the maximum surface excess to enhance the colloidal stability and transport in the subsurface. The $k_{TCE\text{-}obs}$ for all the polyelectrolyte-modified RNIP at the maximum amount of sorbed polyelectrolyte are summarized in Table 7.5.1. The effect of the modifier depends on the type of modifiers used, but the differences amongst modifier types is small and is not likely to influence the choice of modifier. Rather, the governing criteria might be the ability of the modifier to enhance transport (Saleh et al. 2008) and potentially to increase the contact between NZVI and TCE as described earlier in this report. It should be noted, however, that the conformation of the adsorbed polyelectrolyte will affect the polymer density at the surface and therefore their effect on reactivity. The conformation can be affected by groundwater constituents such as Ca^{2+} and Mg^{2+}, and from Fe^{2+}. For example, Ca^{2+} and Mg^{2+} in groundwater can screen the charge of ionized groups in the polyelectrolyte or promote dehydration of both the ions and the polyelectrolyte chains. This would cause the adsorbed polyelectrolyte layer to collapse onto the particle surface, thereby increasing polymer density at the NZVI surface. This is especially true for weak polyelectrolytes such as PAP and CMC. While the effect of Fe^{2+} from Fe^{0} oxidation is accounted for in this study, the effect of Ca^{2+} or Mg^{2+} is not and should be evaluated.

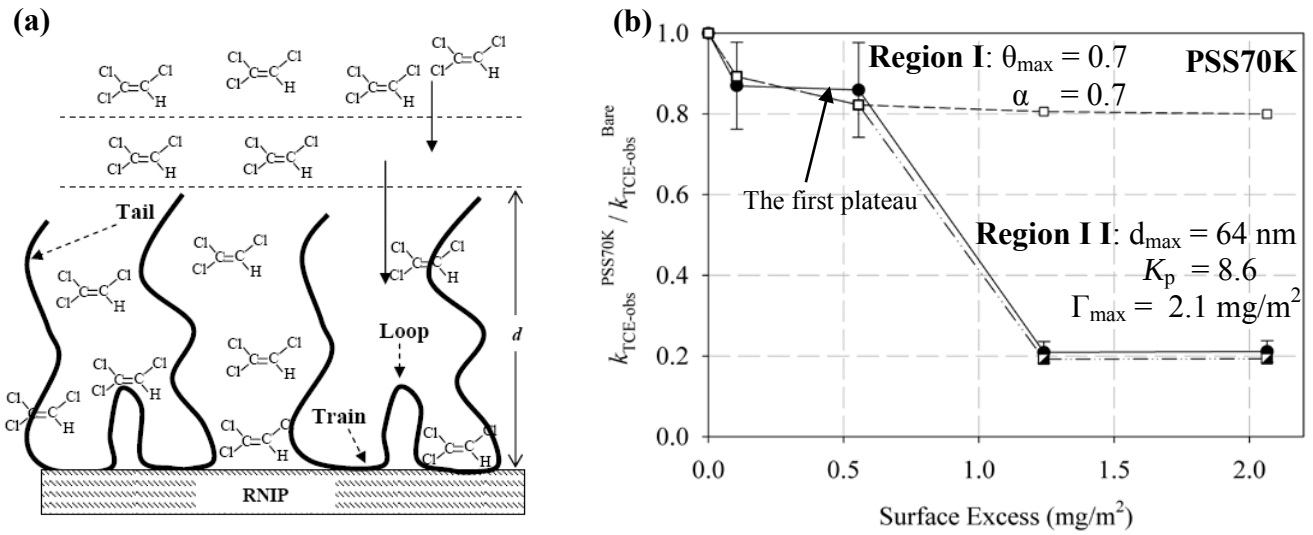

Figure 7.5.1. (a) A schematic diagram illustrating the site blocking effect and mass transfer resistance on TCE dechlorination due to trains, loops, and tails of sorbed polyelectrolytes onto RNIP surface; (b) filled-symbols for normalized $k_{TCE\text{-}obs}$ for PSS70K-modified RNIP as a function of surface excess, open symbols for the k_{TCE} simulated using site blocking by trains, and half-filled symbols for k_{TCE} simulated using site blocking by trains coupled with mass transfer by loops and tails.

Table 7.5.1 Measured Fe^0, estimated characteristics of sorbed layer, dechlorination rate, and calculated lifetime (τ) of TCE for each polyelectrolyte-modified RNIP

Code	Fe^0 content (%)	Γ_{max} (mg/m^2)	d[a] (nm)	$k_{TCE\text{-}obs}$ at Γ_{max} (10^{-3} L m^{-2} hr^{-1})	τ[b] (day)
Bare	26 ±0.4	0	0	3.51±0.42	0.4
PSS70K	15±0.0	2.1±0.3	67±7	0.73±0.03	1.9
PSS1M	15±0.5	1.9±0.2	198±30	0.44±0.04	3.2
CMC90K	24±0.2	1.0±0.2	7.2±3.2	0.31±0.02	4.5
CMC700K	29±1.0	2.0 ±0.1	40±6.5	0.38±0.03	3.7
PAP2.5K	24±0.4	2.3±0.2	40±12	0.15±0.01	9.3
PAP10K	25±0.9	2.2±0.4	44±13	0.14±0.01	9.9

[a] Based on Ohshima's soft particle analysis at the maximum surface excess.
[b] Assume that 2 g/L of RNIP in porewater is available for TCE dechlorination

7.5.2 Effect of NZVI mass loading on PCE reaction rate and H_2 evolution rate.

Large tank experiments described later in this report used PCE NAPL because its solubility is lower than for TCE and it is better suited for the large tank experiments investigating

the effect of NZVI treatment on mass emission of PCE from an entrapped PCE NAPL source. Additionally, the reaction rates with PCE were needed for models used to predict the effect of NZVI on mass emission from a PCE source. Therefore we measured the effect of NZVI loading on the PCE dechlorination rate and on the H2 evolution rate suing six different NZVI particle concentrations (1 g/L, 2 g/L, 5 g/L, 10 g/L 15 g/L or 20 g/L MRNIP2) in batch reactors with dissolved PCE (29 μM) in 5 mM $NaHCO_3$. The batch experiments were conducted as described in section 6.2.10

The kinetics of PCE dechlorination by MRNIP2 was adequately fit assuming the pathways proposed for TCE dechlorination by bare RNIP. The primary reaction products were ethene and ethane. Chlorinated by-products such as vinyl chloride, cis or trans DCE and 1,1 DCE were not detected during the reaction. The surface area normalized PCE dechlorination rate constants (k_{SA}) for the various MRNIP2 mass loadings are shown in Figure 7.5.2a. The surface area normalized PCE dechlorination rates using MRNIP2 ranged from 2.0 to 3.8×10^{-4} $Lh^{-1}m^{-2}$ over the MRNIP 2 concentration range from 1 g/L to 20 g/L. The surface area normalized PCE dechlorination rate constants (k_{SA}) ($Lh^{-1}m^{-2}$) are expected to be constant if the reaction is first order with respect to iron mass loading. However, the reactivity (k_{SA}) of MRNIP2 over the range of 1 g/L to 20 g/L particle concentrations was not constant. A first order relationship between MRNIP2 dosage and PCE reactivity was valid only for iron mass loadings above 10 g/L. Below 10 g/L, k_{SA} decreases as the mass loading decreases (Figure 7.5.2a).

The initial H_2 evolution rate also depended on the NZVI mass loading (Figure 7.5.2b). The surface area normalized zero order hydrogen evolution rate was independent of NZVI mass loading above 10 g/L, but increased 3 fold for nZVI mass loadings below 5 g/L. This trend at low particle loading is opposite to the trend observed for the PCE dechlorination rate. Overall, however, the maximum difference in the reactivity of PCE and hydrogen evolution within the rage of NZVI dosage from 1 g/L to 20 g/L was less than a factor of 3, which is likely small compared to the other uncertainties encountered in planning groundwater remediation strategies, e.g. heterogeneity of the subsurface, or equal to those expected due to variations in ionic composition and organic matter.

The effect of NZVI loading on the PCE degradation rate might be attributed to the change of pH and E_h due to different NZVI mass loading. Increasing MRNIP2 mass loading increased pH and also decreased E_h (Figure 7.5.2) so it is unclear whether the PCE dechlorination rate was controlled by E_h or pH, or both. In both cases PCE reactivity increased when pH increased. However, controlling pH at a constant mass loading (Figure 7.5.3 closed circles) showed four times less effect than when mass loading also increased (Figure 7.5.3 open circles). This result suggests that the increase in the PCE dechlorination rate constant is only partially due to the elevated pH. The other possibility is that higher NZVI mass loading provides a lower E_h and therefore driving force for PCE dechlorination. PCE dechlorination rates from various NZVI mass loading conditions (Figure 7.5.3 open circles) and from different pH conditions at a fixed NZVI mass loading (2 g/L) (Figure 7.5.3 closed circles) with respect to E_h are shown in Figure 7.5.4. Generally, the variation in the measured k_{SA} is explained by variation in measured E_h regardless of the Fe(0) content of the iron. Overall PCE dechlorination correlated better with E_h rather than pH.

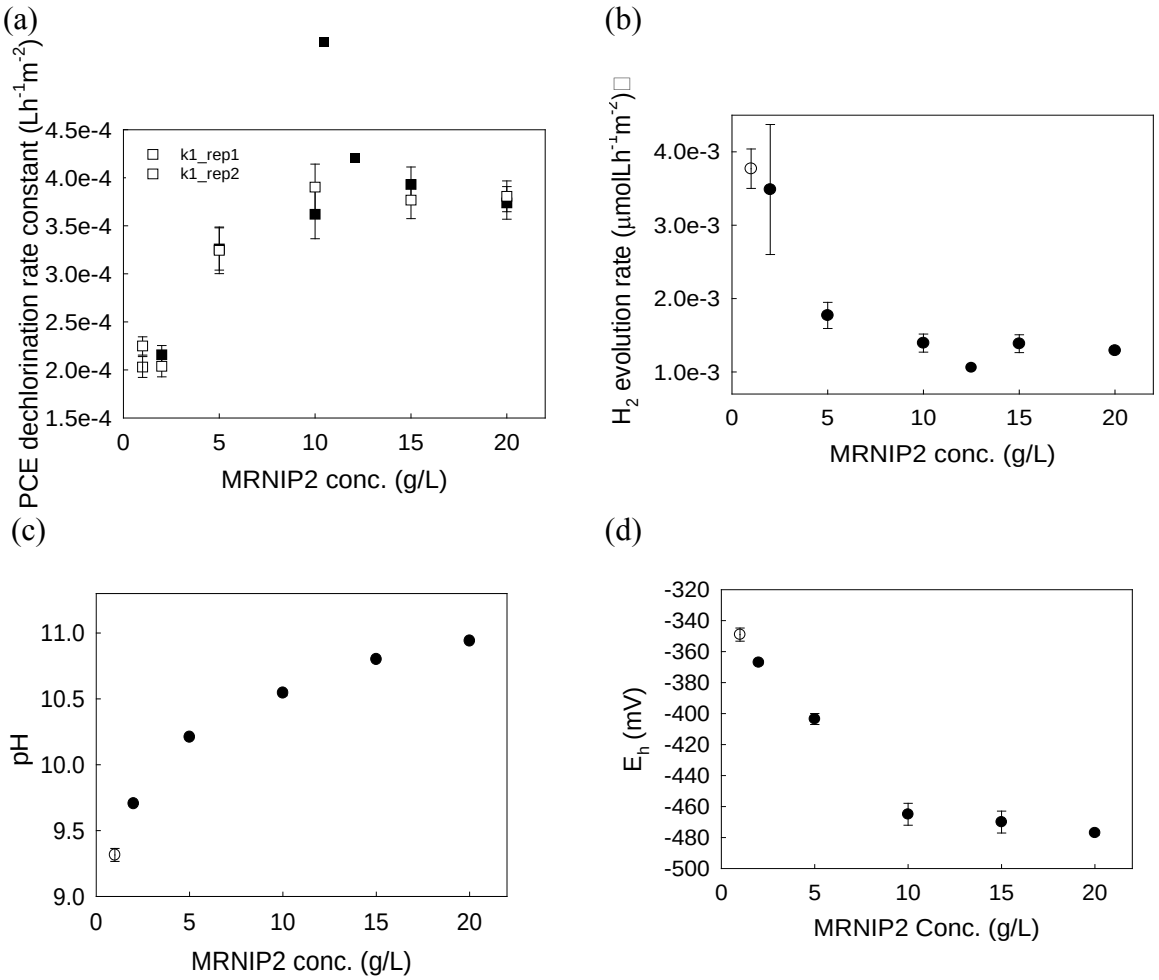

Figure 7.5.2. **(a) PCE dechlorination rate constant normalized with MRNIP2 concentration (1, 2, 5, 10, 15 and 20 g/L) and surface area (15 m^2/g). □ and ● represent the rate constants derived from the model fit for duplicate experimental results and each error is in 95 % confidence interval. Fe^0 content of MRNIP2 was 47 % when the reactivity was tested. (b) The hydrogen evolution rate constant normalized with MRNIP2 concentration (1, 2, 5, 10, 15 and 20 g/L) and surface area (15 m^2/g). (c) The final pH after the reaction (d) The standard potential after the reaction.**

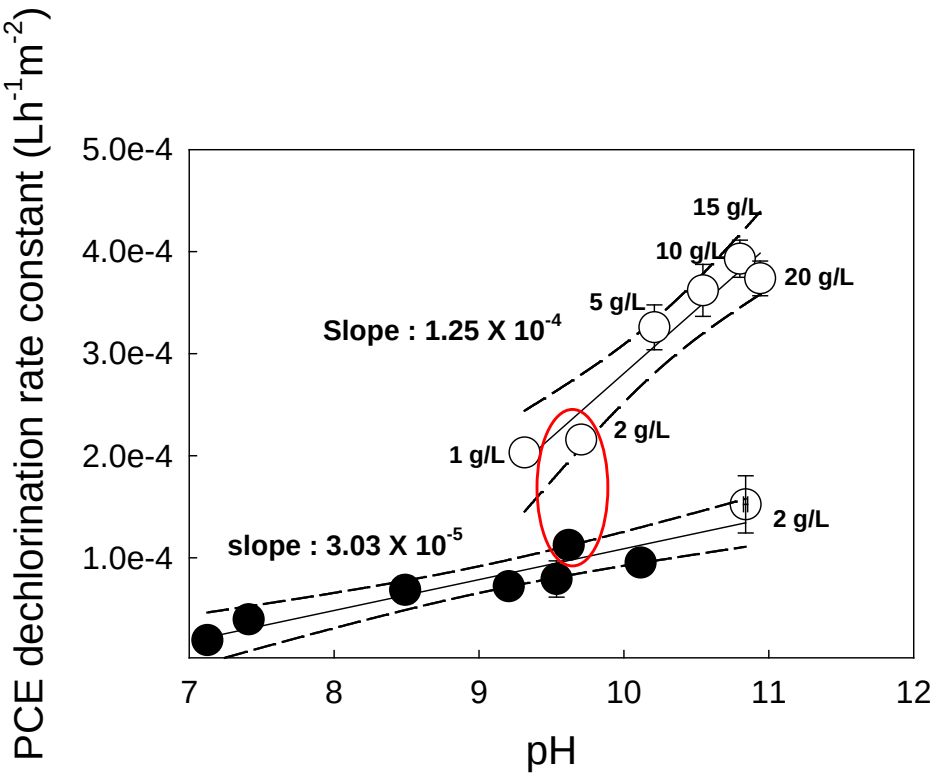

Figure 7.5.3. **PCE dechlorination rate constant normalized with MRNIP2 concentration and surface area (15 m^2/g) depending on pH change. Open circle (○) represents the rate constants derived from batch reactors for the range of MRNIP2 mass loading (1, 2, 5, 10, 15 and 20 g/L). ● represents the rate constants derived from batch reactors with constant MRNIP2 concentration (2 g/L) under different pH condition. The solid line represents linear regression fit to the experimental data and dashed lines represent 95 % confidence intervals for each data set.**

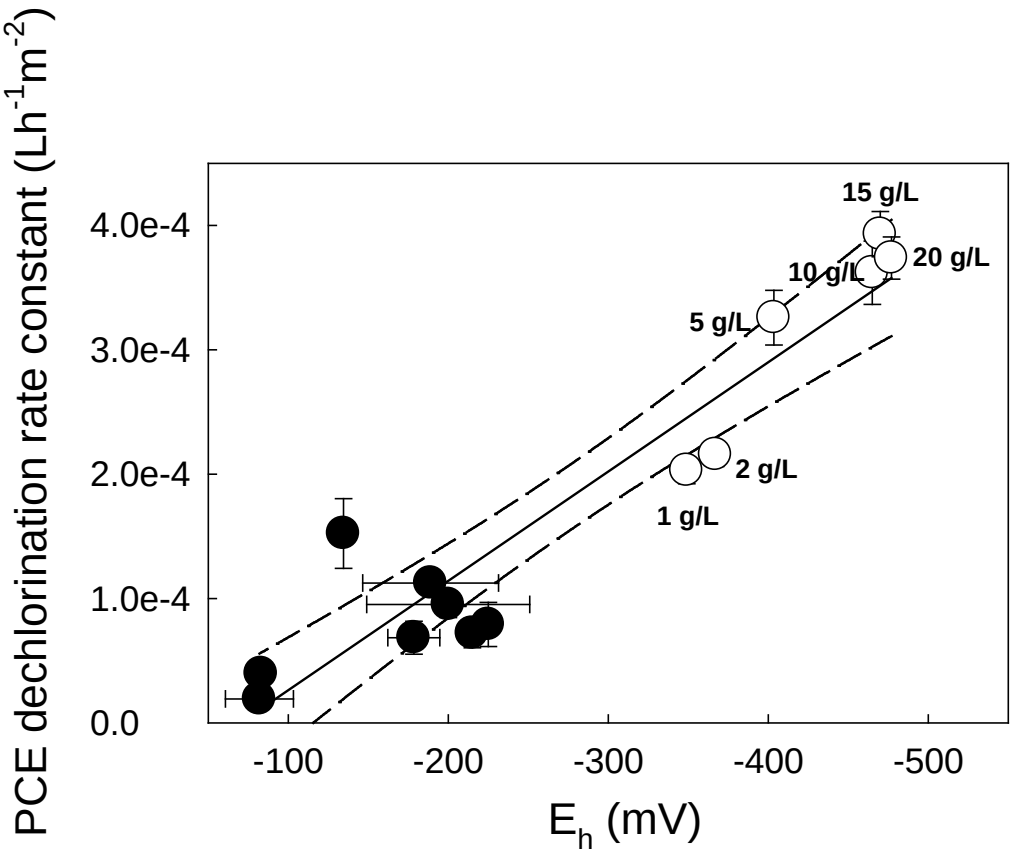

Figure 7.5.4. **PCE dechlorination rate from MRNIP2 depending on E_h (mV). One set (○) represents the rate constants at different MRNIP2 mass loading (1, 2, 5, 10, 15 and 20 g/L) in 5 mM sodium bicarbonate buffer without adjusting pH and the other set (●) shows the rate constants with constant mass loading (2 g/L) at differently adjusted pH. Line is linear fit of the data with 95 % confidence interval.**

These findings have several implications for the effectiveness of NZVI to treat NAPL sources or dissolved plumes. First, the reaction rates in areas where only a small NZVI loading is achieved may be lower than predicted from batch studies using higher NZVI concentrations. Second, the rate of reaction with TCE decreases at lower NZVI concentration while the reaction with water to form H2 increased. This suggests that areas where NZVI loadings are lower will be less efficient in their use of NZVI for the target compound. Finally, these data suggest that emplaced NZVI concentrations should be as high as possible, and greater than 10g/L. This will be difficult to achieve in the field because it becomes increasingly difficult to inject NZVI as the concentration increases. Most field studies have used NZVI concentrations closer to 1 g/L to facilitate transport.

7.5.3 Effect of flow velocity on PCE dechlorination using polymer modified NZVI in columns with homogeneous porous media.

Flow velocity through a reactive zone containing NZVI determines the retention time of within the zone, and hence the extent of dechlorination. Therefore, flow velocity is another important factor to consider in the design of NZVI emplacement strategies that will yield the desired treatment efficiency. Column reactivity studies were performed (see section 6.2.12 for the details of experimental setup) at different flow velocities to determine the effect of groundwater flow rate on the rate of PCE dechlorination by MRNIP2 (10 g/L) emplaced in a water saturated sand column. The surface area normalized PCE dechlorination rate constants determined under the range of linear pore water velocity are shown in Figure 7.5.5. Two sets of data are plotted on Figure 7.5.5 because during the time that the column experiments were conducted, there was a change in the color at the front end of the column from black (fresh MRNIP2) to greenish brown which is presumed to be due to the oxidation of NZVI. The front of discoloration of the column moved uniformly through the column over the course of the experiment, accounting for approximately 60 % of the column mass by the end of the experiment. Given this change in color, it was difficult to know with certainty whether changes in reactivity were due to changes in velocity or changes in the MRNIP2 reactivity due to aging of the NZVI. Thus, we bounded the effects by calculating the observed rate constant using two methods; one assuming complete oxidation of the iron in the column where the line of discoloration was, and a second assuming that the reactivity of MRNIP2 in the column remained unchanged despite the color change. Increasing the velocity from 7 cm/day to 113 cm/day increased the PCE reaction rate 2.8 times. When the reacted zone was not considered (i.e. assuming that total length of the column remains reactive despite the discoloration of the NZVI), the PCE dechlorination rate increased 4.7 times when the linear pore water velocity increased under the range tested. This suggests that the reaction was mass transfer limited since increasing the pore water velocity should decrease the boundary layer on the MRNIP surface and increase the rate of PCE diffusion to the particle surface, and hence the reaction rate.

The observed PCE dechlorination reaction rate constant (k_{obs}) can be limited by either mass transfer of PCE to the NZVI surface or by the reaction itself (Eq. 7.5.1) where k_L (m s^{-1}) is the mass transfer coefficient and a is the specific surface area of the particles (m^{-1}). Based on estimates of time scales for mass transfer and for reaction (See Kim et al., 2012 for detailed calculations) mass transfer of PCE across the boundary layer at the particle surface should not be the rate limiting step under the conditions evaluated. However, k_{obs} decreased as the flow velocity decreased suggesting that reactivity of PCE was indeed mass transfer limited. A possible explanation for this is the presence of a H_2 gas layer at the NZVI surface that builds up at low flow rates but does not at the higher flow rates tested. This gas layer may inhibit mass transfer of PCE to the NZVI surface or make portions of the NZVI inaccessible to flow thereby decreasing the observed reactivity. Overall, the effects of mass loading and velocity on the observed dechlorination rate of PCE were a factor of 4 to 5 and can be accounted for in models and in design calculations for designing the length a reactive zone needed to achieve a desired degradation.

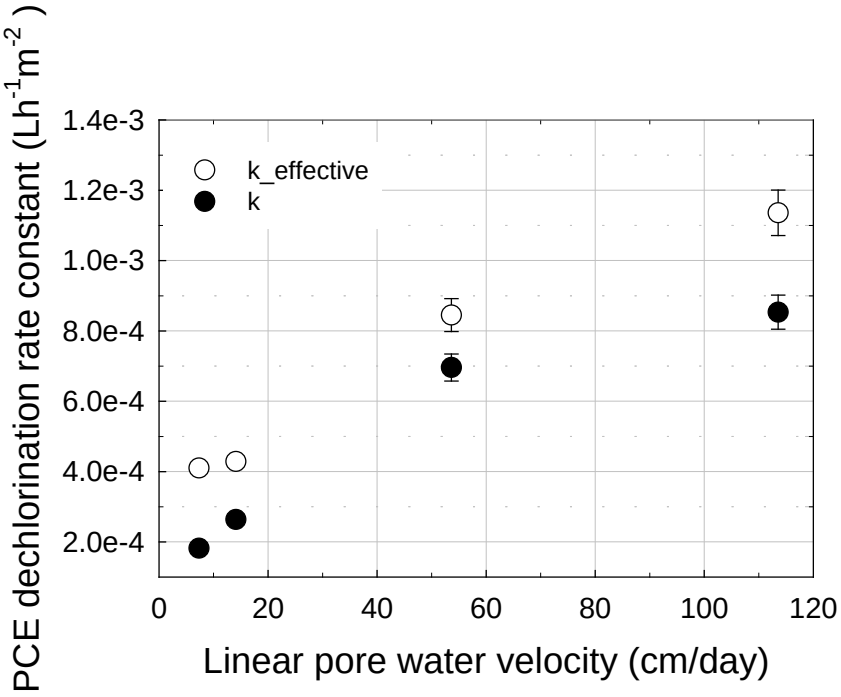

Figure 7.5.5. The influence of linear pore water velocity on PCE dechlorination rates in the sand column packed with 10 g/L of MRNIP2. k_effective is the PCE dechlorination rate for the effective reactive zone (by considering only the non oxidized zone as a effective length) and k is the PCE dechlorination rate calculated based on the assumption that the total length of column is still reactive after the front column end oxidation.

7.5.4 Effect of NZVI emplaced directly in the NAPL source zone

The benefits of delivering NZVI directly to NAPL source zones have been speculated by several previous studies (Gavaskar et al. 2005; Liu et al. 2005b; Saleh et al. 2005a; Tratnyek and Johnson 2006; Zhang 2003) but has never been demonstrated. Delivering reactive NZVI particles in situ to reductively dechlorinate entrapped DNAPL has been expected to provide DNAPL mass reduction and provide residual treatment capacity to mitigate mass flux from diffusion-controlled low permeability zones. Here we evaluated the effect of NZVI treatment on NAPL mass depletion and decrease of mass emission under the ideal conditions where NZVI is emplaced directly into and surrounding entrapped NAPL.

To evaluate this possibility, we first conducted experiments in a small (15 mL) flow cell, where emplaced (uncoated) NZVI particles (10 g/L) (dissolved PCE dechlorination rate obtained from a batch experiment =7.1 x 10^{-4} $L \cdot h^{-1} \cdot m^{-2}$) were allowed to react and interact with a PCE DNAPL pool, while steady groundwater flow was maintained through the flow cell. The flow cell had a total volume of 15 mL. The detail of flow cell setup is described in section 6.2.13 and is shown pictorially and schematically in Figure 7.5.6a. Additional details can be found in (Fagerlund et al. 2012). The PCE was dyed red using Sudan IV, 0.01% by weight, allowing the pool zone to be observed visually, as seen in Figure 7.5.6b, showing the flow cell after creating the DNAPL PCE pool. Experiments were conducted at two different groundwater flow

velocities, i.e. the controlled flow rate = 0.0864 mL/min (81 cm/day) for experiment 1 and 0.0010 mL/min (9.4 cm/day) for experiment 2. We also developed a model to evaluate simultaneous dissolution and dechlorination of PCE-DNAPL source in the presence of NZVI as discussed in section 6.2.13.

(a)

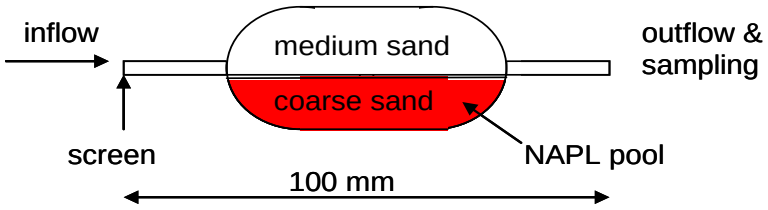

(b)

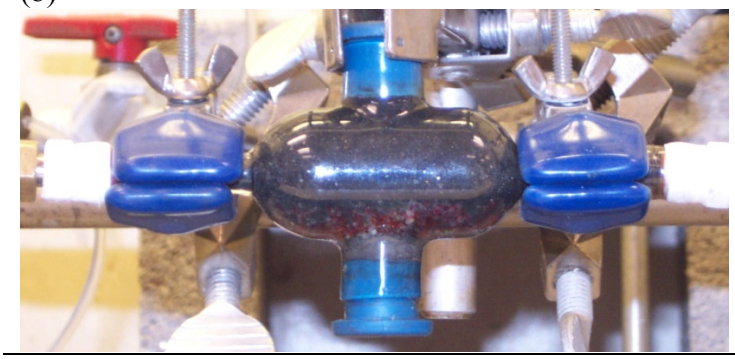

Figure 7.5.6. Flow cell. (a) Schematic experiment setup. (b) Photograph taken after packing the cell and creating the DNAPL PCE pool (red).

The main by-products of PCE dechlorination is acetylene, ethane, and ethene (all together called ETH), as was the case for dechlorination of dissolved PCE in a column experiment discussed in the previous section. Due to different resident times, the by-product concentrations were much lower for experiment 1 (flow velocity = 81 cm/day) than for experiment 2 (flow velocity=9.4 cm/day). For both experiments, a correlation between PCE and total by-product concentrations can be observed, as can be expected for 1st order dechlorination reaction kinetics (Figure 7.5.7). The modeled effluent concentrations (using $D_{m,PCE}$ = 8.2E-10 m^2/s, Sc_{PCE} = 1.2E-3, a_0 = 0.23, and a_1 = 0.87, see section 6.2.13) for experiments 1 and 2 are also shown in Figure 7.5.7. The total dissolved concentration is the sum of PCE and byproduct (ETH) molar concentrations, corresponding to the total mass-transfer from the DNAPL source to the groundwater.

Even though conventional wisdom may suggest that the most effective way to remediate NAPL source is to place the RNIP as close as possible to the sources, the findings of this section suggest DNAPL mass depletion will not be significantly enhanced by NZVI-mediated dechlorination by placing NZVI directly in the DNAPL source zone. The cumulative effluent mass as a function of time for models with no dechlorination reactions is shown in Figure 7.5.8.

When comparing the results from these models with the average total mass-transfer rate during the quasi steady state periods, it can be seen that the dechlorination reactions only have a minor impact on the total mass-transfer rate. In experiment 1 the dechlorination by RNIP is predicted to produce a difference in mass-transfer rate of less than 0.5%. For experiment 2, in which more than 25% of the total dissolved PCE was reacted to non-chlorinated byproducts, the predicted difference in total mass-transfer due to RNIP reactions is still only 3.5% (4.2 μmol/day with reactions and 4.06 μmol/day without). Comparing experiments 1 and 2 it can be concluded that for slower groundwater flow through the DNAPL source zone (experiment 2) there is more time for dechlorination reactions to occur and the presence of NZVI can have a larger effect on the DNAPL mass-depletion rate compared to faster flow (experiment 1). However, at a slower flow rate, the mass-transfer is in any case smaller than that for the faster flow rate, the limiting case being stagnant groundwater when the transport of PCE away from the DNAPL-water interface is purely diffusive.

The case considered here is a scenario when a high-concentration (10 g/L) of NZVI has been emplaced directly in the DNAPL source zone, everywhere surrounding the DNAPL-water interfaces. However, despite this what may be considered to an "optimal" emplacement to target the source, very little enhancement of the source depletion rate can be seen. This finding is logical because the dechlorination reactions occur in the aqueous phase (as they require water to take place) and the mass-transfer of PCE from DNAPL to the aqueous phase is generally rate-limited. Thus, significant acceleration of the DNAPL mass-depletion rate is unlikely. Additionally, the NZVI closest to the DNAPL source (i.e., with the highest oxidant loading) is rapidly oxidized. The scenario fairly quickly becomes a reactive barrier one in which dissolved PCE is degraded as it moves through the NZVI that is farther from the interface and remains reactive. This can result in a decrease in mass emission from the source provided that the retention time in the reactive zone is sufficient, however, it is not likely to speed up source depletion.

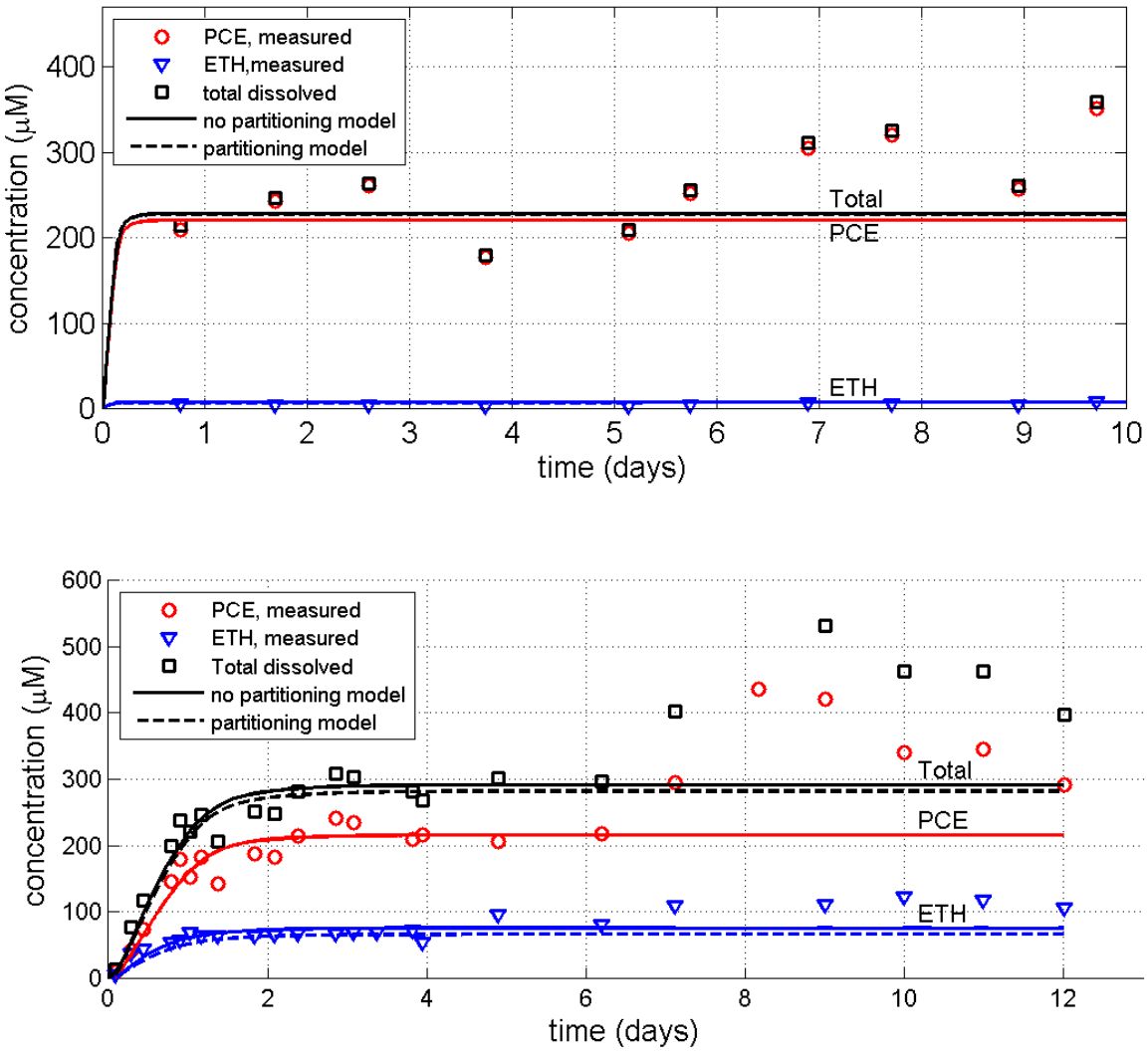

Figure 7.5.7. (a) Measured effluent concentrations (symbols) and modeled concentrations without (base case) and with partitioning of byproducts into the DNAPL (solid and dotted lines, respectively) for (a) Experiment 1 and (b) Experiment 2.

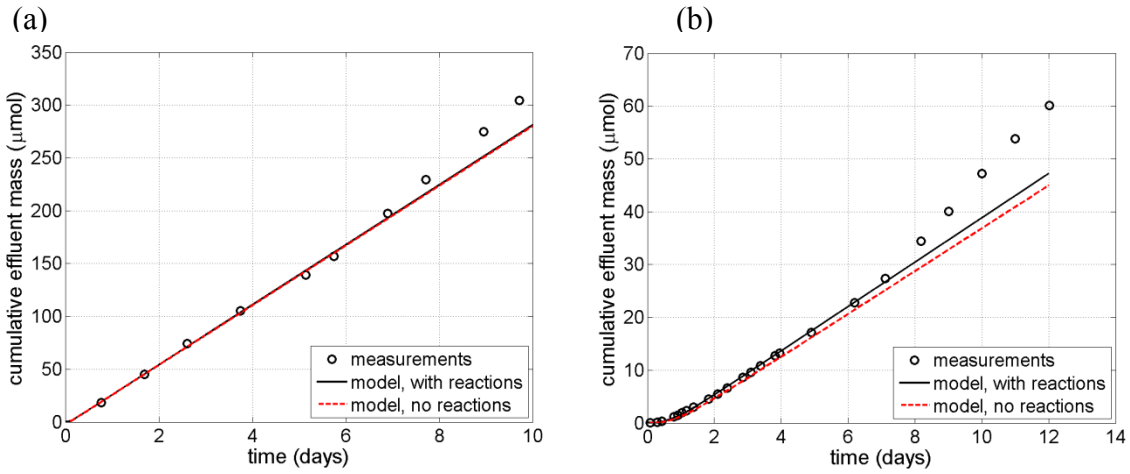

Figure 7.5.8. Measured and modeled cumulative total effluent molar mass for (a) experiment 1 and (b) experiment 2.

7.6 Effect of PCE NAPL source zone treatment by injected polymer modified NZVI in an intermediate-scale experiment

In light of the result that emplaced NZVI is most likely to sever as a reactive barrier for treating dissolved phase contaminants, and that this could reduce mass emission from the source zone we performed an intermediate scale experiment where we use a well to deliver polymer modified NZVI to create a reactive area immediately downstream of entrapped tetrachloroethene (PCE) DNAPL. We also test again the scenario where NZVI is injected directly within the entrapped PCE DNAPL in a heterogeneous confined environment in a two dimensional intermediate tank. From this intermediate scale experiment, we observed the importance of partial pore clogging and flow bypass due to NZVI emplacement. Thus, an additional experiment was preformed in a small 2-D cell to investigate this important issue.

7.6.1 Effect of emplacement location on treatment efficiency at intermediate scale

Figure 7.6.1 illustrates the experimental setup that is also described in detail in section 6.2.14. Six vertical sampling arrays were created on the back side of the tank for aqueous sampling. Each array had 11 ports spaced 5 cm apart vertically, referred to as row 1-6 (R1-R6) (Figure 7.6.1). Dissolved PCE concentration measured at the 11 points for each row along with the average flow velocity (20 cm/d) in the tank was used to calculate the mass flux at different distances away from the source. Changes in measured mass flux of PCE were determined for the two NZVI treatments as discussed next. A PCE source zone with the final average saturation of 21.5% was emplaced. Figure 7.6.2a shows the source zone in the tank with residual PCE DNAPL. The dissolved PCE concentration was measured downstream of the DNAPL source zone for 30 days prior to NZVI injection to achieve a baseline steady-state dissolution and mass emission down gradient from the PCE DNAPL source. The effect of NZVI treatment was determined from changes in measured mass flux before and after NZVI treatment. Mass flux was calculated using Eq. 7.6.1.

$$\Gamma = \frac{C_{aq} V}{MW} \qquad (7.6.1)$$

Where Γ is the mass flux (mmole/cm^2 d), C in the concentration (mg/L) measured in the porewater, V is the porewater Velocity (cm/d), and MW is the compound molecular weight (mg/mmole)

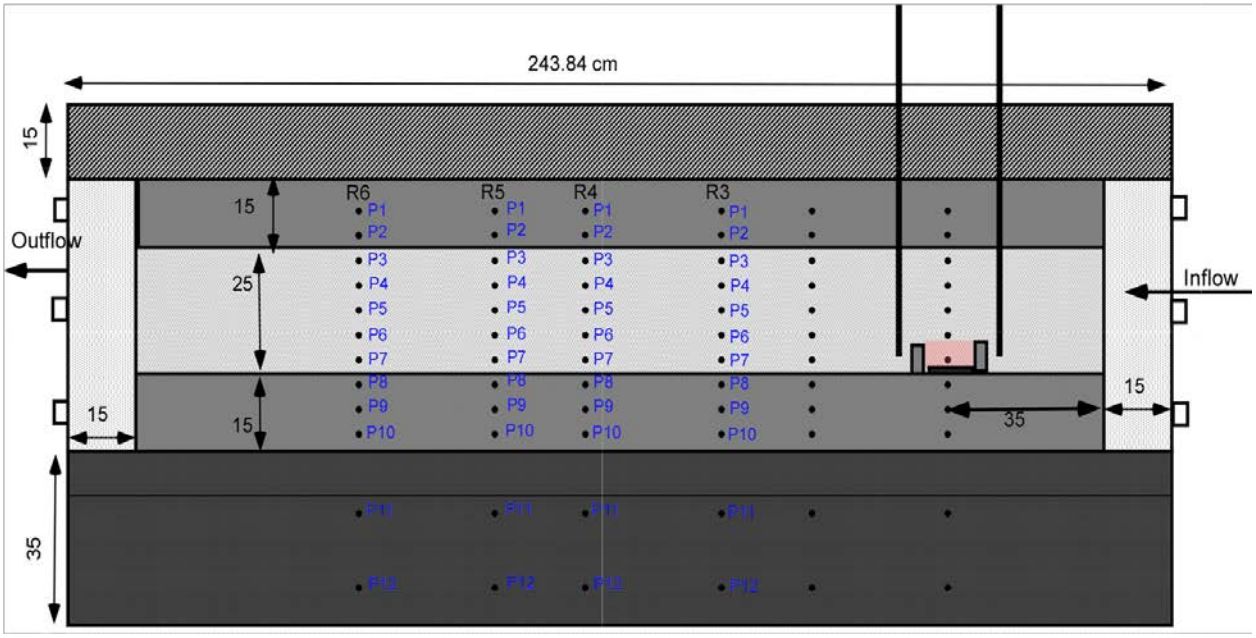

Figure 7.6.1 Schematic diagram of the two-dimensional tank used.

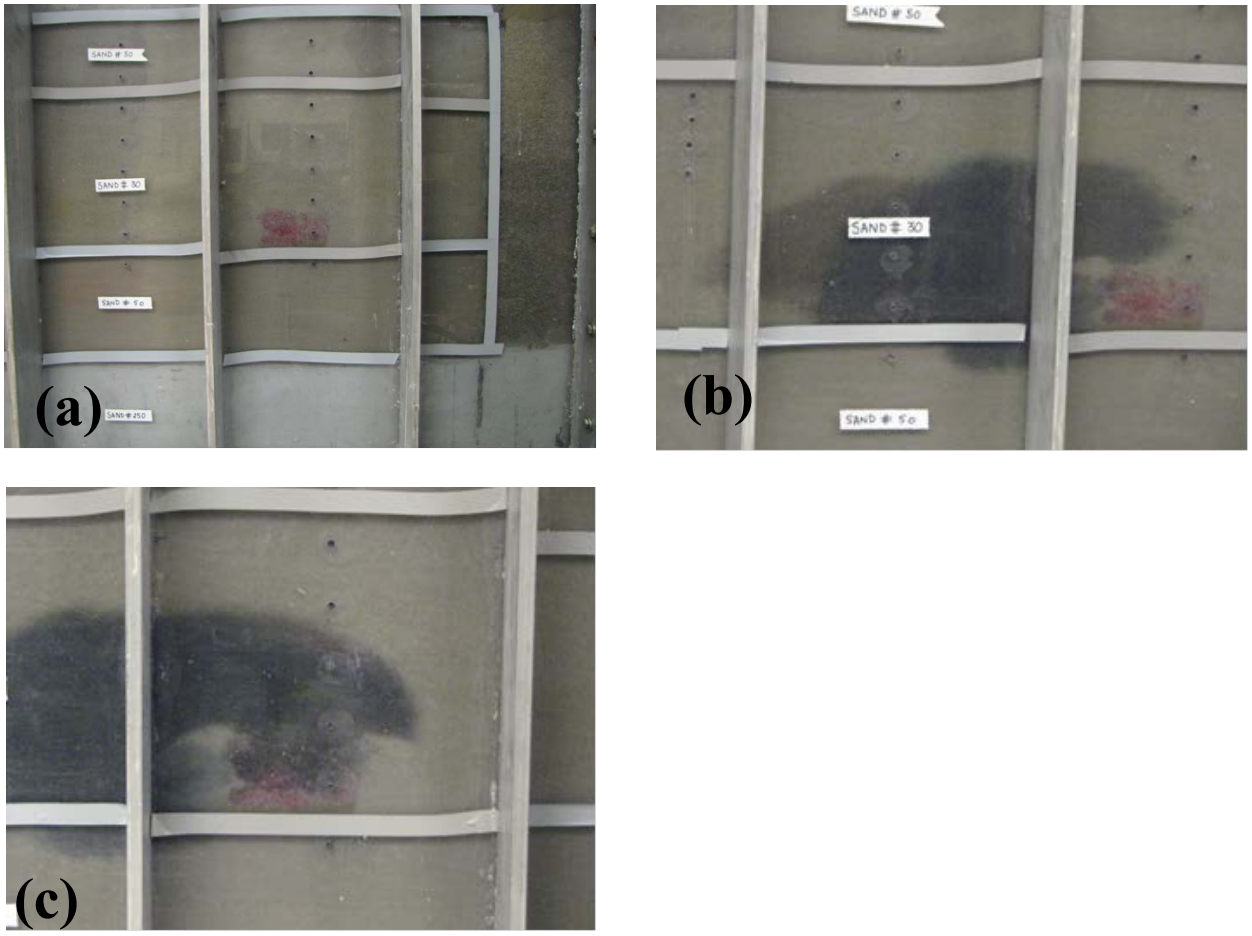

Figure 7.6.2. Photos of source zone area a) after DNAPL PCE injection, b) after NZVI particles emplaced in the area immediate downstream of the DNAPL PCE source zone and c) after emplacement of NZVI particles in the source zone.

MRNIP2 with an initial Fe^0 content of ~40% was used in this study. The aqueous dispersion (990 mL) at 10 g/L (9.9g) was injected at a total flow rate of 290 ml/min into the tank through two injection wells using a peristaltic pump. For the first NZVI injection NZVI particles were injected to create a reactive zone of ~25 cm x 25 cm x 5 cm containing 10.4g of MRNIP2 particles adjacent to and down gradient from the PCE DNAPL source (Figure 7.6.2b). A second injection of MRNIP2 was performed after the PCE mass flux from the source had reached a new steady state due to the degradation afforded by the first injection. In this injection, 185 mL of 10.5 g/L of MRNIP2 particles (1.9g) was injected directly into the DNAPL source to determine if NZVI within the source would have a significant impact on the mass emission from the source (Figure 7.6.2c).

Prior to the NZVI injection PCE mass flux at Row 2 is highest as it is closest to the DNAPL source zone and decrease at Rows 3 through 6 as the distance from the source increases. Mass flux increased rapidly in the first 4 days, followed by a more gradual increase. A *pseudo* steady state of 0.06 mmole/cm^{2}d was achieved after 27 days. At that time NZVI particles were injected just down gradient of the DNAPL source. An approximately 85% reduction in PCE mass flux was observed after emplacing reactive zone of NZVI particles in the area immediately downstream of the entrapped PCE DNAPL (Figure 7.6.3). This reduction in PCE mass flux from the source could be a result of either reductive dechlorination of PCE or a change in the rate of dissolution of PCE after the emplacement of NZVI particles, or both. Formation of non-chlorinated by-products such as ethylene, acetylene and ethane was observed with ethylene being the most abundant product. No chlorinated reaction by-products (e.g. tricholorethene, dichlorethene, or vinyl chloride) were observed. The reaction products accounted for an average ~50% of the total mass that had been released from the source prior to injection of NZVI. This indicates that degradation by NZVI only accounts for a portion of the observed flux reduction. The remaining decrease in flux reduction must therefore be due to a decrease in the rate of dissolution of PCE resulting from NZVI injection. Since no NZVI was placed directly into the DNAPL source, the decrease in dissolution rate is most likely from a change in the flow field through the source as discussed later. PCE mass emission and flux in the plume reached pseudo steady state ~33 days after emplacement of NZVI particles immediately downstream of the source zone and remained stable or perhaps continued to decrease slightly over the next 30 days (Figure 7.6.3). This behavior is consistent with reports of significant decreases in contaminant flux upon injection of NZVI in the field (e.g. Waddle and Henn, 2006). In this case the NZVI is acting as a reactive barrier between the source and the down gradient well. It also suggest that some flux reduction observed in the filed may also be due to pore plugging and flow diversion around the source. Dilution may also be a factor.

At day 65 a second mass of NZVI particles were injected directly into the DNAPL source to determine if direct contact between NZVI particles and free phase PCE would further decrease the mass emission of PCE from the source. No significant additional decrease in PCE mass flux was achieved beyond that observed for the first injection of NZVI particles (Figure 7.6.3). This may be because the reactive lifetime of the NZVI is the presence of DNAPL is short (hours to a day) (Liu et al. 2007) and the limited mass of NZVI (1.9 g or approximately 12 mmol Fe(0)) injected into the PCE DNAPL source containing approximately 220 mmol PCE. Theoretically it requires 6 electrons to reduce PCE to acetylene and 8 electrons to reduce PCE to ethene (the primary product observed), or 3 mol Fe(0)/mole PCE and 4 mol Fe(0)/mole PCE, respectively. Regardless, the lack of a significant impact of adding NZVI directly into the source zone is consistent with observations in the smaller flow cell described previously.

The 50% carbon mass balance for degradation products suggested that the reduced downgradient PCE flux from the PCE DANPL source could be from flow bypassing the source area. This would occur if emplacement of NZVI decreased the permeability of the formation within or down gradient of the source. This was qualitatively evaluated using a tracer test (food dye). The results of tracer test indicated that indeed flow was diverted around the source to some degree (Figure 7.6.4), which could be partially responsible for the decrease of mass emission from the source downgradient. It is likely that the pores were partially occluded by emplaced NZVI forcing a greater amount of flow over the top of the source area rather than through it. Some flow continued to move through the source and into the reactive zone as green food dye

was recovered in ports 6 and 7 in column 2; however, their arrival time was longer than for the flow path over the top of the DNAPL source.

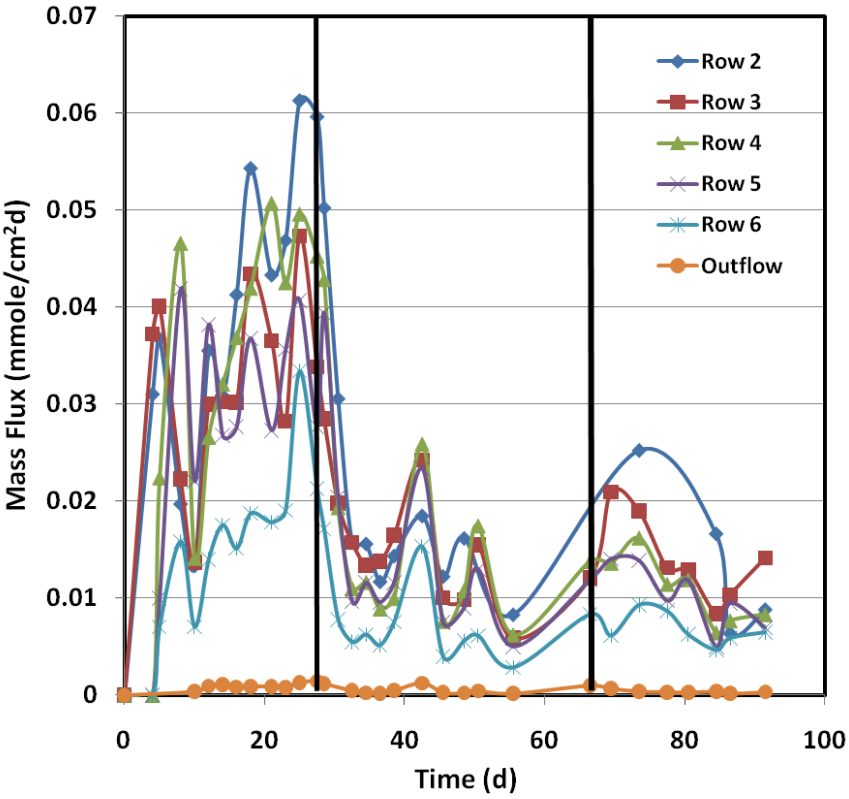

Figure 7.6.3. Mass flux of dissolved PCE in the downstream plume at five different cross sections. The first black line from left represents the first MRNIP injection in the area immediate downstream of the source zone and second black line represents the second MRNIP injection in the source zone.

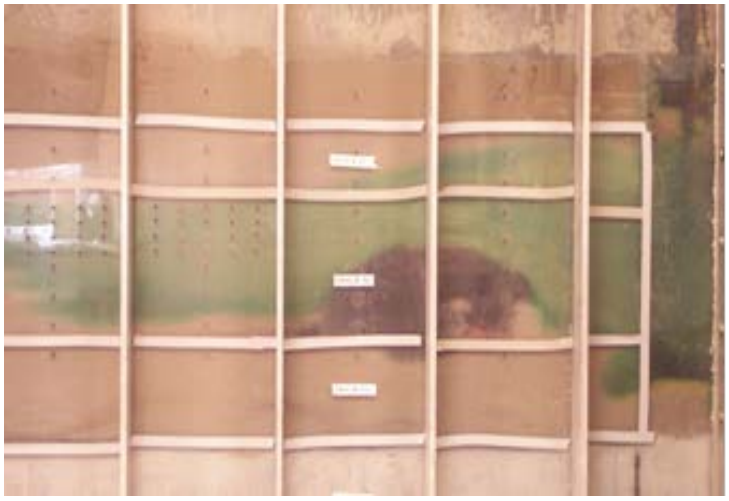

Figure 7.6.4. Partial isolation of the DNAPL source zone after emplacement of NZVI particles in the source zone as shown by dye test.

7.6.2 Pore clogging due to NZVI emplacement

The finding in the previous section suggests that pore clogging may affect the treatment efficiency of a NAPL source zone using NZVI. Pore clogging can occur if the mass of NZVI particles deposited in porous media is large enough to decrease the hydraulic conductivity of the area, causing resistance to flow. If this occurs, dissolved contaminants may bypass the reactive NZVI zone and therefore not be degraded. We evaluated how the properties of NZVI (polymer layer thickness) and how the mass of injected NZVI mass affect clogging by NZVI.

7.6.2.1 Effect of adsorbed polymer layer on pore clogging

Uncoated NZVI aggregates rapidly due to strong magnetic attraction, making injection impossible. Polymeric surface modification is used to enhance NZVI dispersion stability against aggregation and deposition and enhance injectability. As discussed earlier in this report, the adsorbed polymer layer thickness greatly affects NZVI dispersion stability and mobility in porous media. We demonstrated that not all polymeric coatings provide the same resistance against pore clogging, and that poor clogging is more significant for polymers with smaller extended layers.

To illustrate the importance of adsorbed polymer layer thickness on NZVI transport and pore clogging we compared the pore plugging observed for MRNIP2 (with a 90nm adsorbed layer thickness according to Ohshima's method) and PSS-RNIP (with a 30nm adsorbed layer thickness according to Ohshima's method). For the latter, RNIP was modified by physisorption of PSS, but allowing only 30 min for adsorption of PSS to obtain the smaller adsorbed layer thickness. NZVI delivery in heterogeneous porous media was conducted with 6g/L suspensions of each particle type following the methods discussed in the previous section in the report (Figure 7.2.4).

PSS-RNIP with the 30nm adsorbed layer thickness showed significant clogging of the porous media. As shown in Figure 7.6.5, PSS-RNIP did not appear on the wall of the middle layer (fine sand #140) as had MRNIP2 discussed previously. PSS-RNIP appeared in the layer of coarse sand (sand#16) after 0.21 pore volumes (PV) and barely broke through at around 0.75 PV. As shown in the deposition mapping of PSS-RNIP (Figure 7.6.6), ~16 g/kg of PSS-RNIP deposited

right at the injection point in the middle layer of fine sand. This amount is around ten times greater than the case of washed MRNIP2 at the similar location (Figure 7.2.5). This deposition was enough to cause pore clogging in sand #140 (d_{50} = 99 μm) as suggested by the change of the tracer flow path measured after PSS-RNIP deposition (Figure 7.6.7) in comparison to the flow path of tracer in pristine sand layers (Figure 7.2.4). Flow bypassing resulting from pore clogging can potentially decreases the *in situ* treatment efficiency of NZVI as shown in the next section.

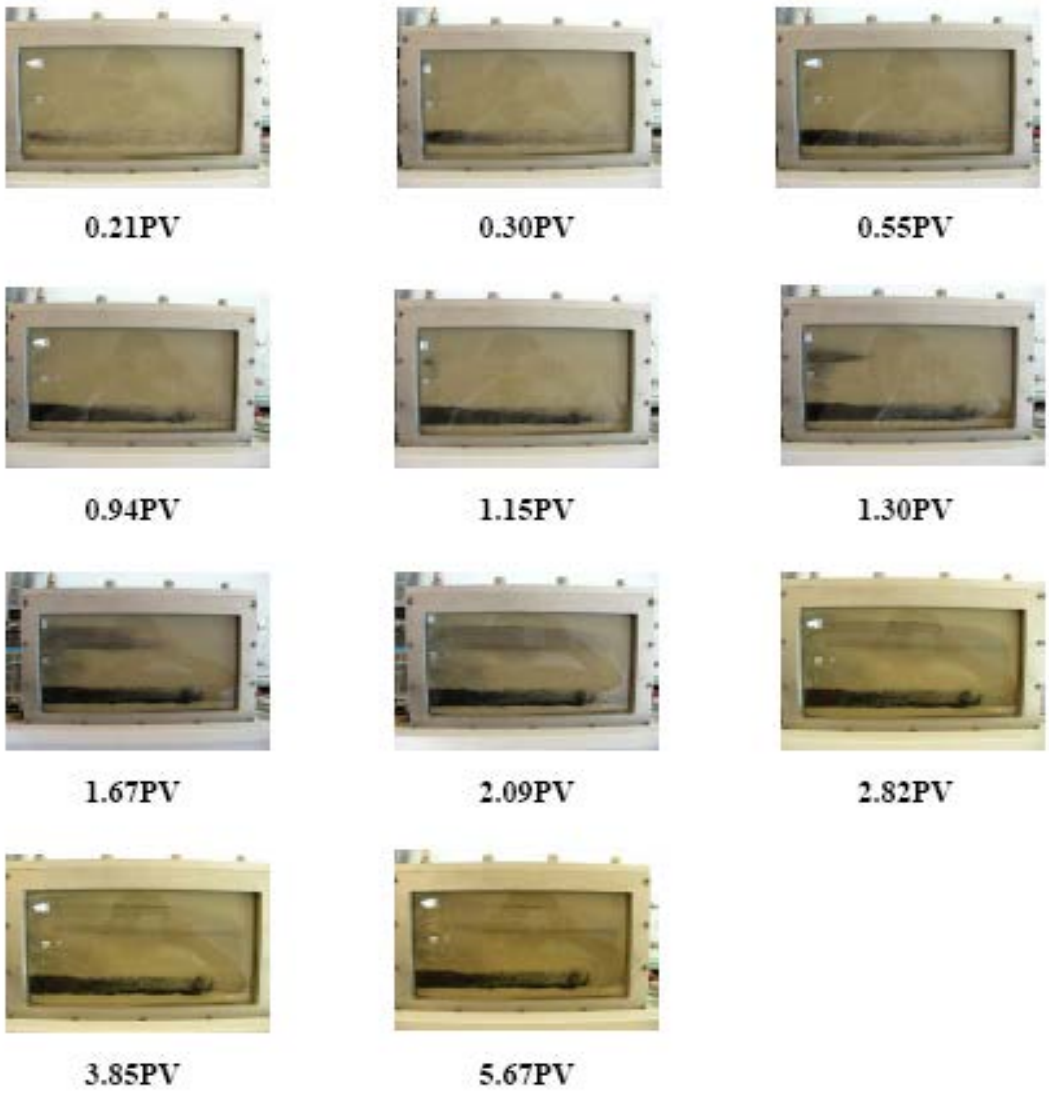

Figure 7.6.5 Selected Photos illustrating the transport of fresh, washed PSS-RNIP at 6 g/L as a function of time (as PV).

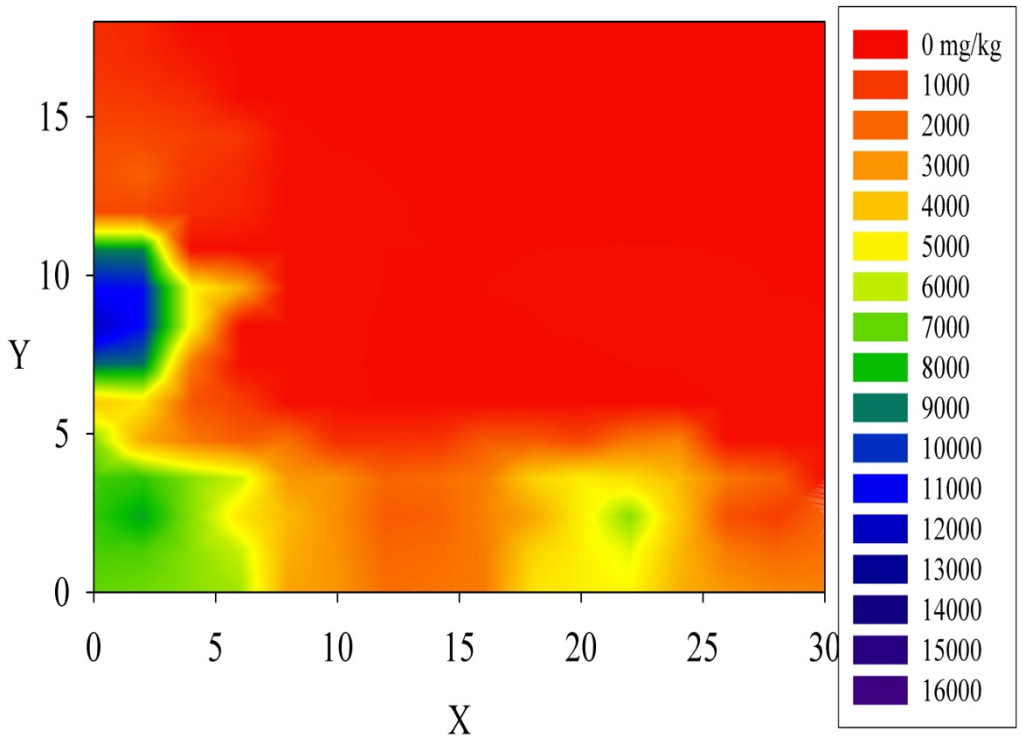

Figure 7.6.6. The contour maps illustrating the amount of fresh, unwashed PSS-RNIP (6 g/L) deposited on sand grain, reported as mg of nanoparticles per kg of sand

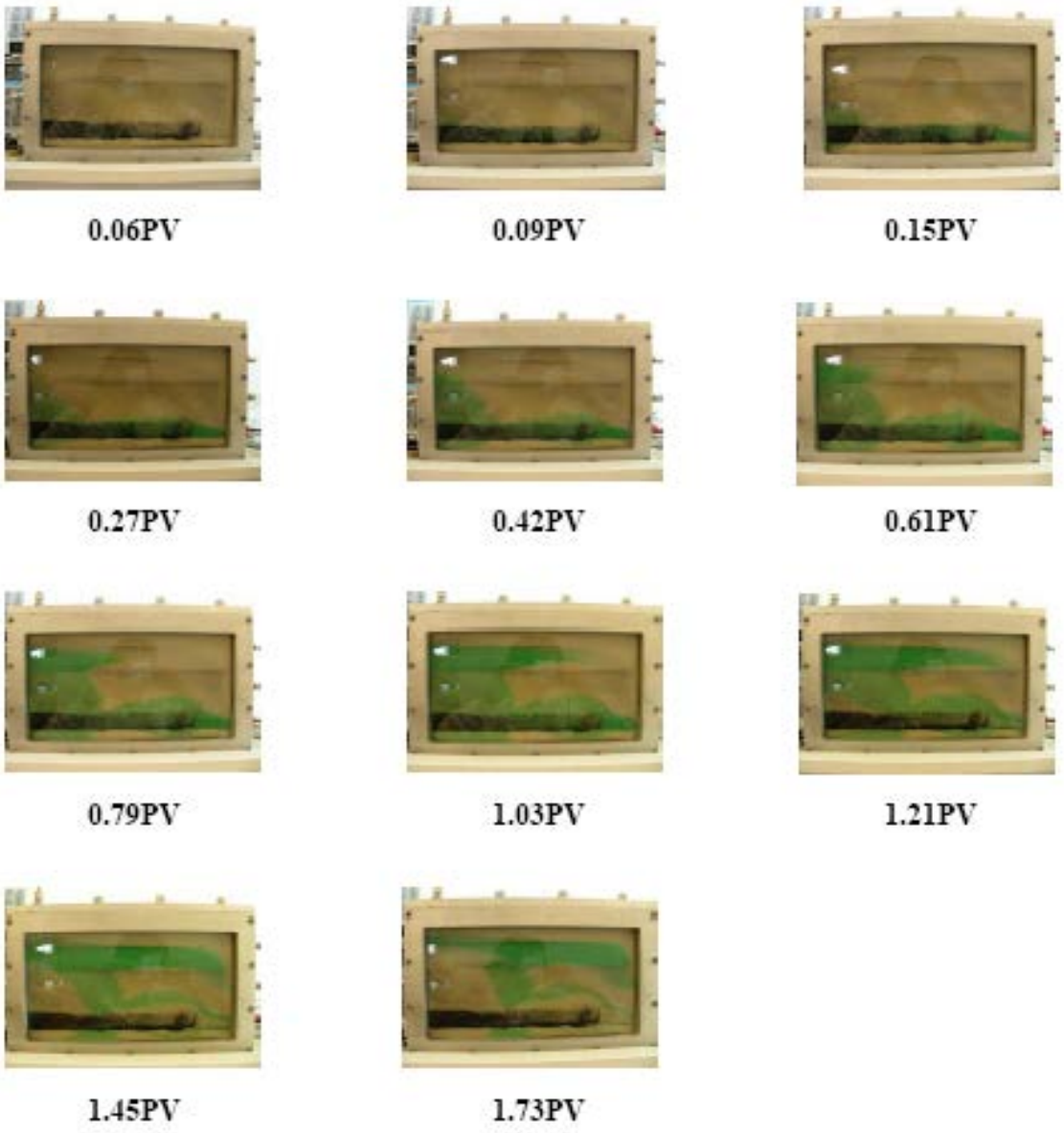

Figure 7.6.7. Selected Photos illustrating the transport of food dye (a conservative tracer) as a function of time (as PV) after the deposition of fresh, washed PSS-RNIP at 6 g/L

7.6.2.2 Effect of pore clogging on degradation of dissolved contaminants by emplaced NZVI.

Intuitively, a greater mass of NZVI emplaced in a reactive zone should increase the degradation rate of NAPL in the source. Therefore, operationally one might try to inject as much NZVI as possible for in situ remediation. However, pore clogging by injected NZVI can divert flow and dissolved contaminants around the reactive zone and greatly diminish the effectiveness of the NZVI.

The effect of pore plugging on dissolved PCE degradation was demonstrated in the small 2D flow cell (Figure 7.6.8). Four different silica sands were used in the flow cell. A PCE DNAPL source zone (5 cm x 5cm) was created using coarse sand (Unimin # 16). The central part of the tank was packed using medium grained sand (Unimin # 50). To create the desired PCE DNAPL distribution 20.3 mL was injected at a very slow rate using a syringe pump yielding an average PCE saturation of about 80%. Then 10.1 mL of PCE was withdrawn, constituting a final average saturation of 40%. A peristaltic pump with a constant flow rate of 1.5 mL/min of 5 mM $NaHCO_3$ was used to provide flow through the cell. Water samples were collected downstream of the DNAPL source zone in a vertical profile from top to bottom through ports located at the back of the tank and from the outflow. These were analyzed for PCE concentration using GC with ECD. PCE concentrations measured up gradient and down gradient of the emplaced NZVI were used to determine the degradation observed across the reactive zone containing NZVI.

5 mL of 50 g/L of MRNIP2 was injected in the flow cell downstream of the DNAPL source zone using the back ports to create a barrier of NZVI down gradient of the plume as shown in Figure 7.6.9. MRNIP2 at this high concentration and without continuous sonication during injection caused pore clogging. Pore clogging and diversion of flow around the reactive zones was observed using a tracer test (5 mL of food dye) as shown in Figure 7.6.10.

Due to pore clogging, even with a high emplaced NZVI concentration, no PCE dechlorination was observed across the barrier. This is a result of complete pore clogging in the location of the NZVI which caused water containing PCE to flow around the emplaced NZVI (Figure7.6.10). This suggests that there will be an optimal mass of NZVI that can be emplaced to achieve sufficient reaction (the reaction rate constant is approximately proportional to the emplaced NZVI mass as described above), but to avoid flow bypassing. The mass of NZVI the leads to this flow bypassing will depend on the properties of the porous media, and therefore site specific, but also will depend on the polymer coating used.

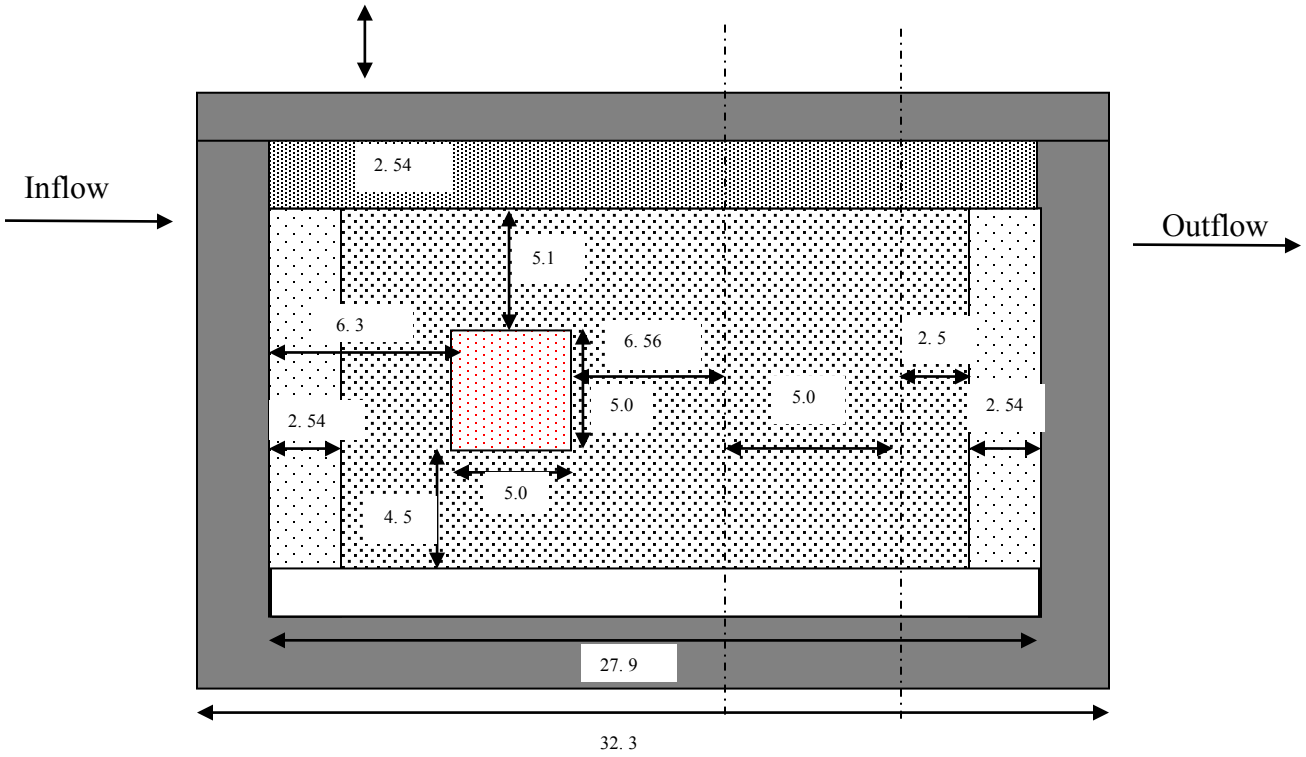

Figure 7.6.8. Schematic diagram of the small 2D flow cell. All dimensions are in cm.

- Outer frame
-
- Screen, Unimin sand # 8 (d_{50} = 1510 μm)
- Homogenous mixture of Unimin sand # 50 (d_{50} = 300μm)
- Upper fine layer of Unimin sand # 140 (d_{50} = 99μm)
- PCE source zone, Unimin sand # 16 (d_{50} = 880 μm)

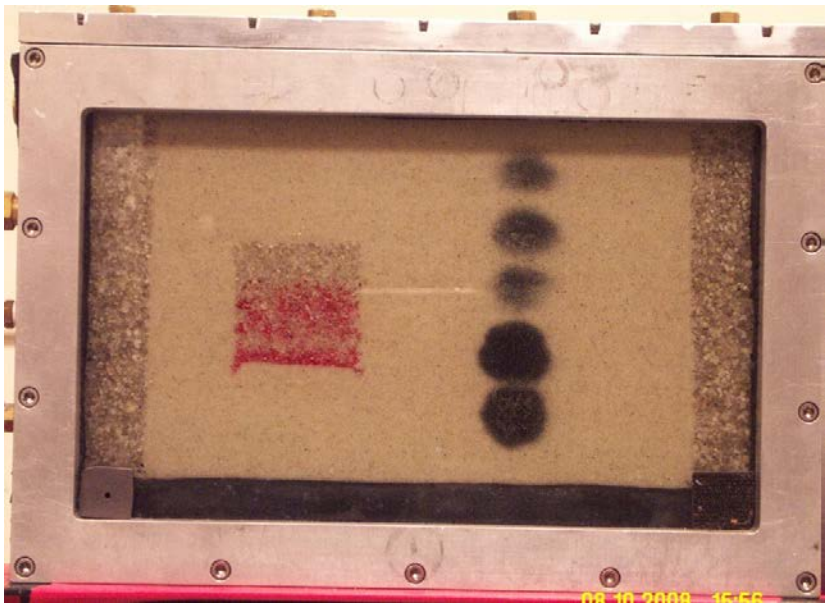

Figure 7.6.9. Creation of MRNIP2 barrier downstream of the PCE DNAPL pool.

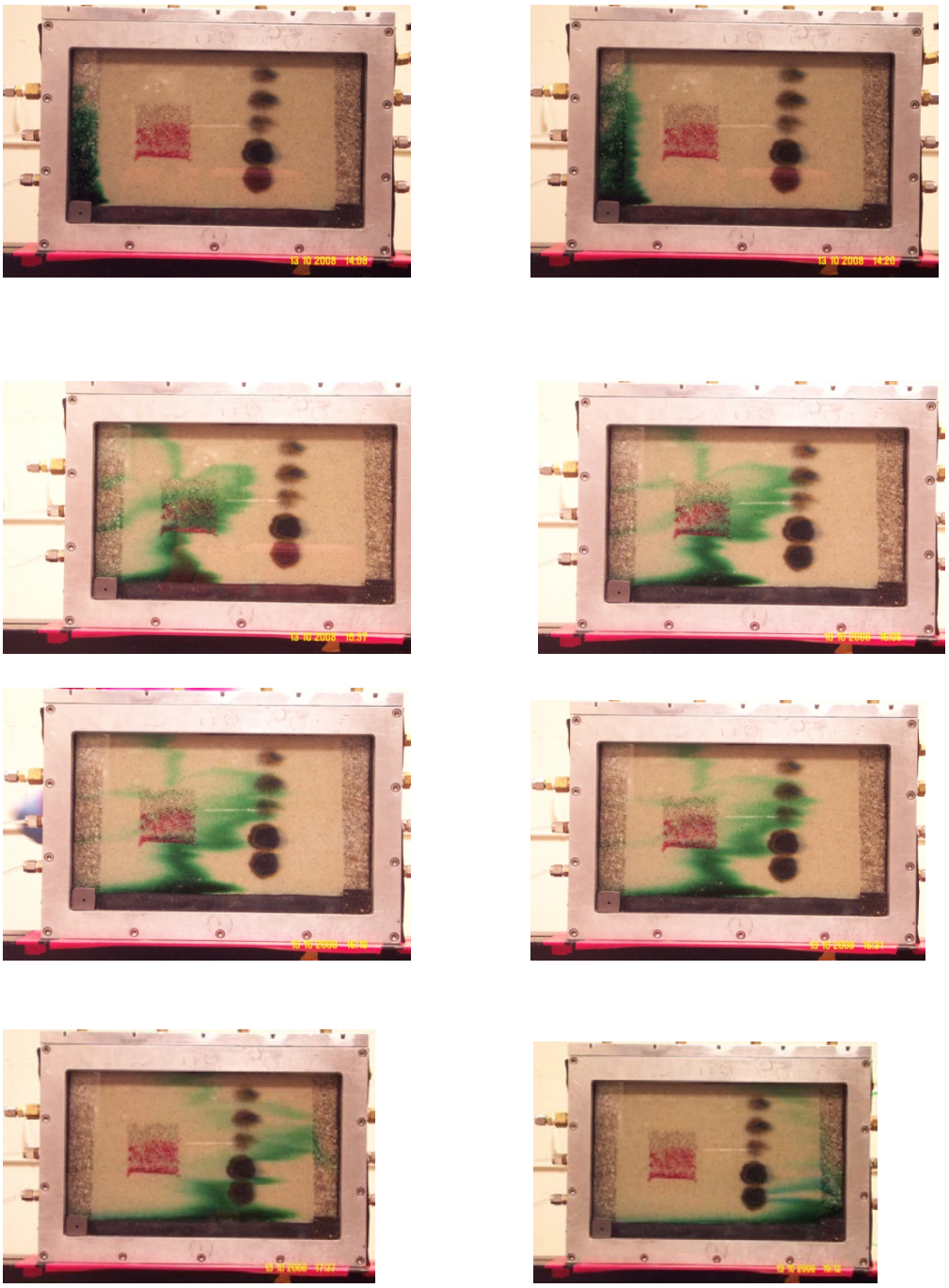

Figure 7.6.10. Selected photos illustrating the flow pattern when a food dye was used as a tracer.

7.7 Reactivity and transport of polymer modified NZVI in natural aquifer materials

In the previous sections, we identified important factors affecting NZVI transport and reactivity, but these used neither real groundwater nor real soil. The complexity of natural soils can affect reactivity and transport of NZVI so we evaluated both reactivity and mobility of various types of polymer modified NZVI in soil and groundwater samples from contaminated sites. We determined that real groundwater affects reaction rates, reactive lifetime, and mobility as described next.

7.7.1 Treatability study for a TCE contaminated area using nanoscale-zerovalent iron particles: Reactivity and reactive life-time

Several types of NZVI are commercially available, each made by different processes, having different surface properties, and therefore likely to perform differently as remedial agents. We conducted a treatability study using groundwater and soil from a former naval air base in a marine location in California to ensure the suitability of a specific type of NZVI for that site's geochemical conditions. Table 7.7.1 summarizes important physicochemical properties including particle size, surface area, structure/composition, and surface modifier of these NZVI products evaluated in this section.

Table 7.7.1 Manufactures and important physicochemical properties of NZVI products

Particle Type	Manufacture	Structure/Composition	Size (nm)	Surface Area (m^2/g)	Modifier
RNIP	Toda Koygo Corporation (Onada, Japan)*	Fe^0 core surrounded by a Fe_3O_4 shell	20 to 70 nm in diameter	~15-25 m^2/g as measured by BET	none
MRNIP-1					Polyaspartate, weak polyelectrolyte
MRNIP-2					poly(olefin maleic acid) weak polyelectrolyte
RNIP-R		Fe^0 core surrounded by a Fe_3O_4 shell coated with a proprietary catalyst			none
Z-Loy™	OnMaterials	zero-valent iron decorated ceramic core	<250 nm diameter	~15m^2/g	proprietary modifier

* Note that at the time of this report it appears that Toda Koygo was no longer producing or selling the RNIP product for remediation purposes.

This laboratory study determined the rates of tricholoethylene (TCE) degradation, propensity to form chlorinated intermediates, the mass of TCE degraded per mass of NZVI added, and the effect of NZVI addition on the site geochemistry for the NZVI products in Table 7.7.1. Reactivity studies were done in sealed 70 mL serum bottles containing 30 mL of deoxygenated groundwater with aquifer material and 40 mL headspace. The aquifer material contained 40% solids by mass. 50 mg/L of TCE was spiked in a reactor. TCE dechlorination rate per mass of NZVI was quantified and reported. Additional details of this work can be found in (Phenrat et al. 2010c).

Table 7.7.2 summarizes the efficiency of using each type of NZVI. Unfavorable geochemical conditions (high DO, neutral to acidic pH, and a high nitrate concentration) of the site groundwater contributed to the relatively short reactive life times and low TCE dechlorination rates using NZVI products. The range of NZVI lifetimes was vast, ranging from 3 days to ~60 days with experimental TCE degradation half-life times that varied from ~1 hour to ~90 hours. Z-Loy™ has the greatest TCE dechlorination rate (301 $\pm 115 \times 10^{-3}$ L g^{-1} hr^{-1}). The high rate of reactivity comes at the cost of a relatively short reactive lifetime which was only 3-4 days. RNIP-R has the second greatest TCE dechlorination rate (56.4 $\pm 14.7 \times 10^{-3}$ L g^{-1} hr^{-1}) due to the noble metal on its surface which presumably accelerates the dechlorination via catalytic pathway. The main by-products of TCE dechlorination using RNIP-R were ethene and ethane as expected for bimetallic NZVI particles. However, RNIP-R also has relatively short reactive life time (~6 days). Uncoated RNIP provided moderate TCE dechlorination rates (17.4 ±5.5 and 22.1 $\pm 6.7 \times 10^{-3}$ $Lg^{-1}hr^{-1}$ for the first and second spikes, respectively). The reactive life time of RNIP is greater than 18 days. The major by-products are acetylene, ethene, and ethane, indicating β elimination as the major TCE dechlorination pathway(Liu et al. 2005a). All of the NZVI materials evaluated produced small amounts of chlorinated intermediates including 1,1-DCE, t-DCE, and c-DCE. GC measurements confirmed that 0.6 mol% to 5 mol% of the TCE degraded was present as chlorinated intermediates at their maximum. Z-Loy™ produced the highest quantity at 5 mol% whereas the other NZVI produced less than 1.8 mol%. In many cases, the chlorinated products appeared at the beginning of the reaction and were slowly degraded as long as the NZVI was still available to react.

The influence of solution chemistry and the presence of aquifer material on NZVI performance in site water and aquifer solids can be evaluated by comparing the TCE dechlorination rate and life time of NZVI in site water and aquifer solids with that in DI water. The TCE dechlorination rate in microcosms with site water and solids using RNIP is around 4 times slower than the dechlorination of RNIP in DI water at a similar pH (81×10^{-3} L g^{-1} hr^{-1}). In addition, the life time of RNIP (18 days) in the aquifer materials from the site is significantly shorter than that observed in DI water (~6 months at pH ~8.9). The relative short life time and low TCE dechlorination rate are in good agreement with expectation when considering that the site water is buffered by aquifer solids at near neutral pH, and has high nitrate concentration. Nitrate is reduced by NZVI to ammonia and consumes 8 mmol of electrons per mmol of nitrate reduced.

The ratio of NZVI added/ TCE degraded (kg/kg) for different NZVI products can be used as a preliminary criteria for evaluating the cost effectiveness of TCE dechlorination at a particular site condition by each NZVI product. This is calculated from the amount of TCE degraded over the duration of the particle's reactive lifetime, assuming an initial Fe^0 content of 50% Fe^0. The mass of NZVI added per mass of TCE degraded ranged from 17 kg/kg for RNIP-R to 121 kg/kg for MRNIP-2 (Table 7.7.3) while the ratio between NZVI added/ TCE degraded (kg/kg) for Z-Loy, RNIP, and MRNIP-1 is similar, i.e.~30. It also suggests that NZVI with the lowest Fe^0/TCE mass ratio are more efficient than those with higher Fe^0/TCE ratios. The ratio between NZVI added/ TCE degraded (kg/kg) of RNIP in aquifer material and groundwater is much higher than the ratio of 1:1 for RNIP added/ TCE degraded (kg/kg) calculated from a batch study of TCE dechlorination by RNIP in DI water. This suggests that environmental conditions decrease the efficiency of the reaction, and that field application requires approximately 17-28 times more RNIP than the theory predicts from reactions in DI water.

Table 7.7.2. TCE reduction rate constants, primary reaction products, lifetime, Fe^0 product required for TCE degradation measured in groundwater and aquifer solids slurry, and Half-life times for 2 g/L concentration of each NZVI.

Material	Mass added (g/L)	Measured Rate constant (L g-1 hr-1)*1000	Reaction products observed	Lifetime (days)	NZVI added/ TCE degraded (kg/kg)	TCE t1/2 for 2 g/L (hr)
MRNIP-1	10	7.4 ±2.6a 6.4 ±2.2 11.9 ±2.1 17 ±5.1	Acetylene, ethene and ethane	30-60	28	20-54
Z-Loy™ (w/ dispersant)	3	301 ±115	Ethane, minor ethene	3-4	30	1.2
RNIP	4	17.4 ±5.5 22.1 ±6.7	Acetylene, ethene and ethane	≥18	27	16-20
MRNIP-2	10	3.9 ±1.8 8.5 ±1.9	Acetylene and ethene	8-14	121	41-89
RNIP-R	3	56.4 ±14.7	Ethane and some ethane/ acetylene.	6	17	6

7.7.2 Evaluate injection of polymer modified NZVI in a controlled field-Scale aquifer model packed with natural aquifer materials

We conducted a well-controlled, field-scale demonstration of polymer modified NZVI transport in a natural, well-sorted medium sand ("Field sand"). Two types of polymer modified NZVI based materials were used including Z-Loy (see Table 7.7.1) and CMC-modified NZVI (He et al. 2007). In this experiment we were interested in transporting NZVI on a scale that was relevant to remediation systems (e.g., 2-3 meters). To accomplish this, and maximize the likelihood of transport, we installed an NZVI delivery system that included injection and extraction wells separated from one another by 2.5m. Figure 7.7.1 illustrates the experimental setup used in this section (also described in section 6.2.15)

For the first experiment, Z-Loy™ was injected at 2 gallons per minute (with comparable volumes of water injected in the adjacent wells) and a corresponding amount was withdrawn from the extraction wells.

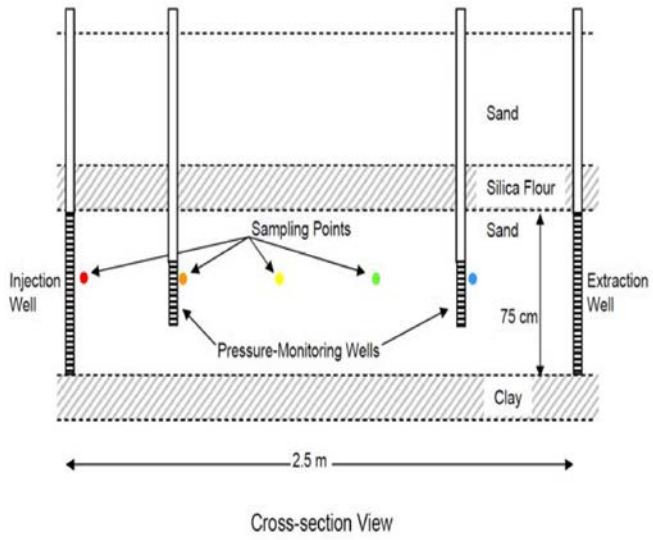

Figure 7.7.1. Cross section showing the injection and extraction wells, pressure monitoring wells and sampling points.

Contrary to the laboratory data and the use of a simple filtration model, approximately 60% of the particles were filtered from the injected water within 5 cm of the well, and by the end of the experiment that value may have risen to as much as 90% of the injected mass (Figure 7.7.2). This removal indicates that there must have been significant deposition immediately around the well. Deposition likely caused "filter ripening" that increased the NZVI removal efficiency as a function of time, and could have caused pore plugging and changes in flow patterns around the injection well. Both of these processes resulted in much lower transport distances than were predicted in column studies with Z-Loy™. It should be noted that MRNIP2 was not used in these studies because the manufacturer no longer produced the materials.

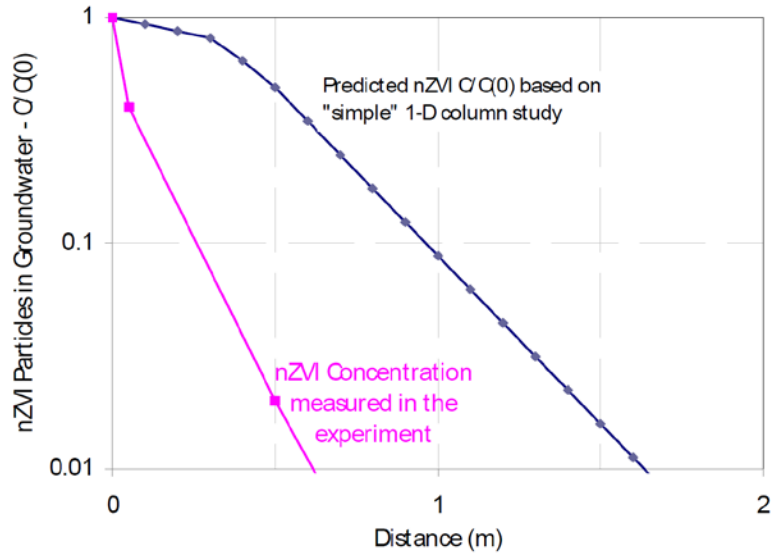

Figure 7.7.2. NZVI transport distance based on filtration models and column transport studies and transport distance measured in the field-scale experiment.

To confirm that filter ripening and pore plugging were responsible for the decreased transport of Z-Loy^{TM}, we conducted a column experiment in which up to 100 pore volumes of Z-Loy^{TM} (based on a 10-cm long column) could be injected to approximate near-well conditions during the injection. The linear velocity in the column was 0.167 cm/s, which is comparable to conditions near the well in the field-scale experiment. Both effluent iron concentration and injection pressure in the column were monitored. The iron concentrations in the column effluent (normalized to the injection concentration) are shown in Figure 7.7.3. As expected, Z-Loy^{TM} breakthrough occurred at about 1 pore volume. It rose to a C/C_o value of ~0.36, which is consistent with both our earlier laboratory experiments and the observed field-scale experiment.

The injection pressure for the column, which remained relatively constant during the first ~18 pore volumes, then rose dramatically and exceeded the capacity of our pumping and monitoring systems before 25 pore volumes had been injected. The iron effluent data for the column do not show a significant decrease in concentration with increasing number of pore volumes (although the column experiment could not be operated for as long a period as the field-scale experiment [>100 pore volumes] due to the dramatic pressure increase). This is consistent with the conclusion that the reduced concentration at the 5 cm location in the field-scale experiment was due to plugging near the injection well, and changes in flow pathways that resulted in less in contact with the sampling point than had been the case at the outset of the experiment. This conclusion is further supported by the observation of "daylighting" of the NZVI at several surface locations around the experiment. For this to have occurred, pathways must have been created through the low-permeability silica flour layer above the injection depth (possibly at locations where instrumentation was installed).

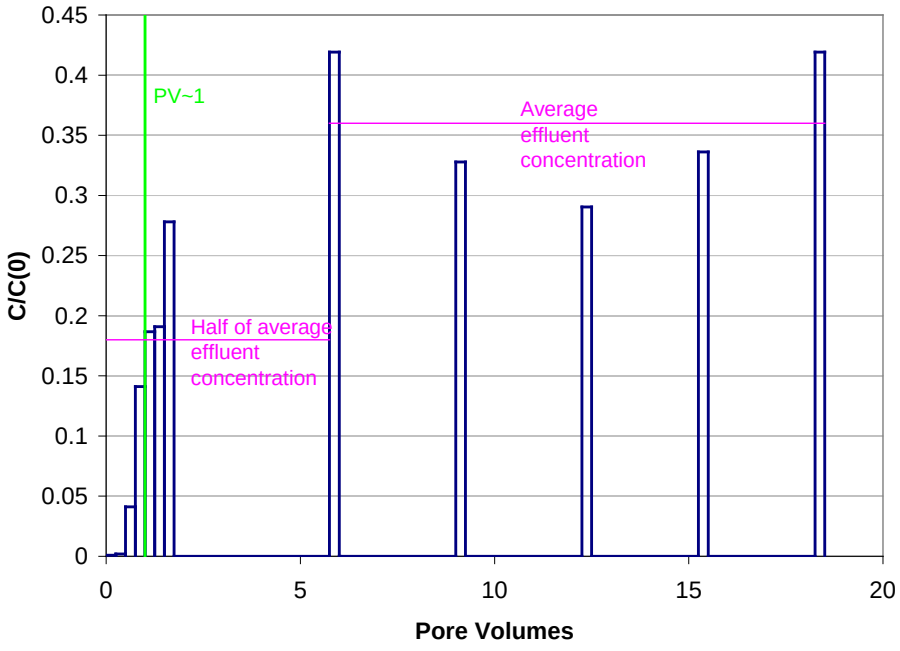

Figure 7.7.3 Normalized iron concentrations measured column effluent samples (blue rectangles indicate the pore volume intervals for each water sample)

7.7.3 Factors affecting Z-Loy transport through field sand

The mobility of Z-Loy in the field scale tank experiment using was less than expected. Evidence of pore clogging was observed, suggesting the importance of near-well effects on transport. Systematic experiments were conducted to determine the cause of the poor deliverability of Z-Loy in the field test. This systematic study demonstrated the importance fines and clay particles in sandy soil. Fine particles and clays are typically present in natural media but only in a small amount (by weight). However, as revealed below, their impact on transport is profound. This finding is consistent with the column studies that showed that clay particles in the porous media decreased transport of NZVI. Column experiments (discussed in section 6.2.3) using Field sand were conducted to evaluate the effects of aggregation and the presence of clay and fine particles as discussed next.

7.7.3.1 Effect of aggregation on Z-Loy transport

Both the injection rate and the type of surface modifier used could impact the time available for aggregation and the ultimate size of the aggregates formed. This would in turn affect transport. In the field scale experiment, the injection rate of Z-Loy was only 2 gpm. It is possible that the flow rate was not high enough to keep Z-Loy from significant aggregation and from forming large aggregates. If this hypothesis is correct, Z-Loy transport can be improved at higher flow rates because the higher flow rate decreases the time available for aggregation and the size of the aggregates formed. To test this possibility, we conducted column experiments of Z-Loy at 1 g/L and 2% modifier in 10 mM Na^+ (pH 8) at five different approach velocities (u_s) (from 0.2 to 0.025 m/sec). In a 25-cm column C/C_0 values ranged from 0.66 to 0.8, leading to α of 0.15 to 0.32 calculated using classic filtration theory (Figure 7.7.4). This suggests that aggregation of Z-Loy in the porous media is not significant over this range of velocity, and that an increase in the Z-Loy injection rate is not likely to improve Z-Loy mobility in Field sand.

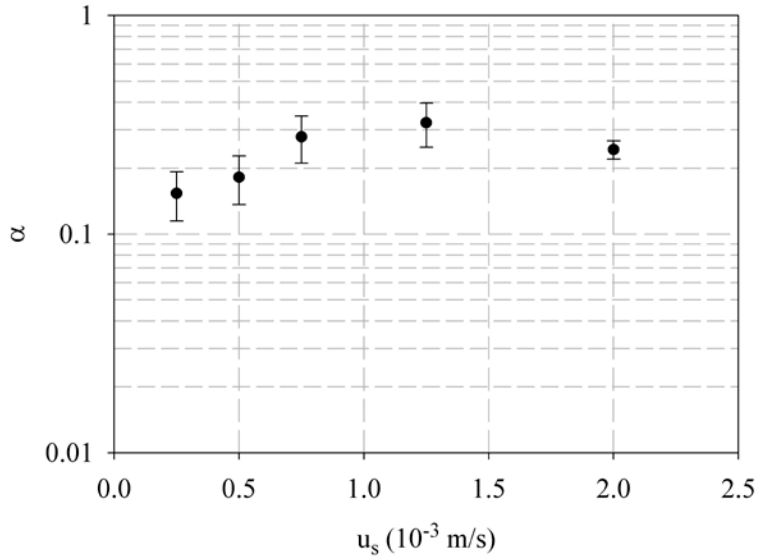

Figure 7.7.4 Sticking coefficients (α) of Z-Loy in "Field sand" columns as a function of approach velocity (u_s).

We tested the hypothesis that a different surface modifier might increase transport by preventing aggregation. We monitored sedimentation of Z-Loy modified by various polymeric surface modifiers as a way to assess the effect of those modifiers on aggregation of Z-Loy. This test method was used previously for testing the effect of various modifiers on RNIP (Phenrat et al. 2008). Figure 7.7.5 shows sedimentation curves of Z-Loy modified by various polymeric modifiers (with excess polymer). All surface modified Z-Loy consisted of 1 g/L Z-Loy and 1g/L polymer. All surface modifiers improved Z-Loy dispersion stability as expected. Most surface modifiers performed similarly under the range of resident times in column experiments conducted in this study (i.e. 3.2 min to 25.5 min for the approach velocity of 0.2 to 0.025 cm/sec). Z-Loy modified by carboxymethyl cellulose (CMC) and xanthan gum (xanthan) provided excellent stability, however, this is due to the high viscosity of CMC and xanthan. The transport of Z-Loy modified with CMC and xanthan gum were evaluated in column experiments but did not transport any better than Z-Loy modified with the proprietary modifier used by OnMaterials. This suggests that it was not aggregation that impacted transport of Z-Loy in the field-scale experiments. Rather, the issue appeared to be a result of the sand properties. The specific property of the sand that resulted in poorer transport than clean, relatively monodisperse sand was determined experimentally as described next.

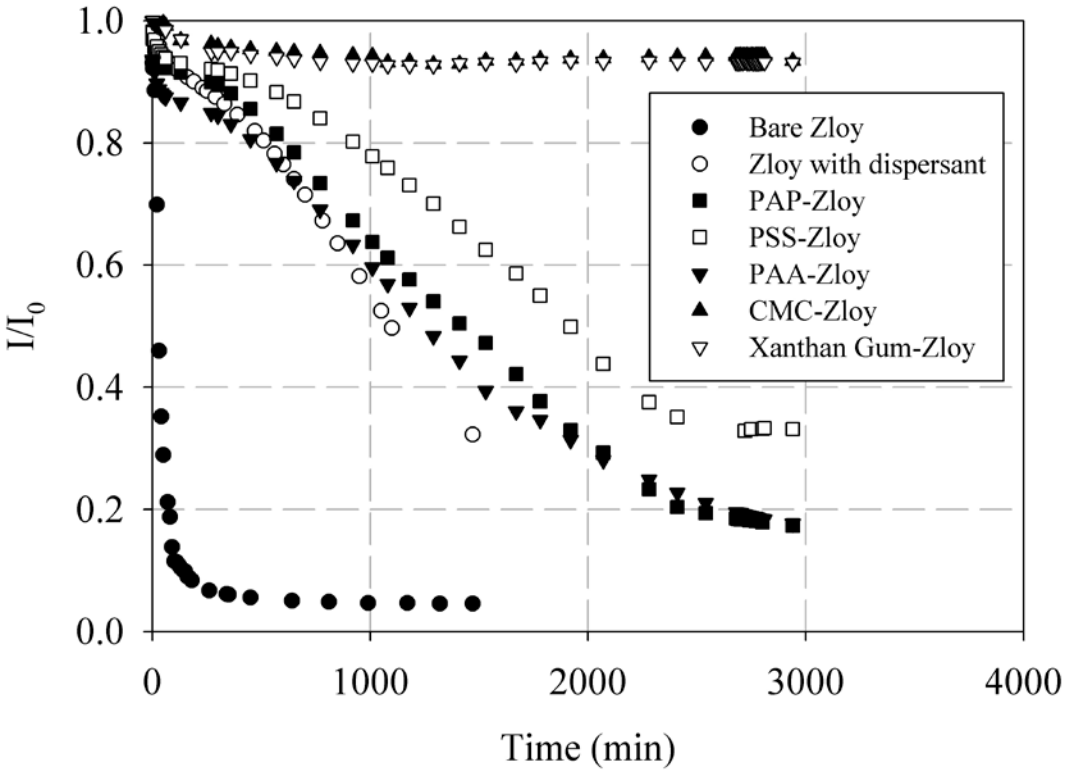

Figure 7.7.5 Sedimentation curves of Z-Loy modified with various macromolecules

The sand used in the field-scale experiments is more chemically and physically complex than silica sand typically used for a laboratory transport study of nanoparticles. We hypothesized that the angularity of the sand grains, its NOM content, or its fine and clay fraction could be responsible for the pore plugging and poorer than expected field-scale transport. These three factors were tested systematically as follows.

To evaluate the effect of grain angularity on transport of Z-Loy in porous media, we conducted column experiments using a 24.5 cm column packed with glass bead (spherical) and Unimin sand#50 (angular sand) and 10 mM Na^+ at the approach velocity of $1.25x10^{-3}$ m/s. Both the beads and the sand have a similar d_{50} (~250 to 300 μm), and are similar to the d_{50} of Field sand. As shown in Table 7.7.4, C/C_0 values of Z-Loy through glass bead (0.92) and Unimin sand#50 (0.95) were similar, and were greater than C/C_0 (0.67) through Field sand under the same conditions. This indicates that grain angularity is not likely the cause of poor mobility of Z-Loy through Field sand.

Natural organic matter (NOM) coated on aquifer materials may affect the transport of the Z-Loy as NOM will alter the surface chemistry of the sand. To evaluate the role of NOM on transport of Z-Loy through sand, we removed the NOM from Field sand using 10 mM KCl and 1 g/L polyethylene glycol (PEG). We flowed 4 PVs of 10 mM KCl and 1 g/L polyethylene glycol (PEG) (pH 4.5) through a column packed with Field sand, then allowed 30 min for adsorption, followed by flushing the column with 10 mM KCl and 1 g/L polyethylene glycol (PEG) (pH 11.5) to remove the NOM from Field sand. We kept flushing until the effluent turned clear again (around 500 mL) prior to injection Z-Loy through the column at the same condition as above. As shown in Table 7.7.4, C/C_0 is only 0.45, indicating that removing NOM from soil decreased Z-Loy mobility through the sand. This agrees with several recently published works (Johnson et al. 2009) reporting enhanced transport of NZVI in the presence of NOM in porous media. The adsorbed NOM likely made the surface more negatively charged at neutral pH which increases the repulsive forces between the Z-Loy and the sand surface, preventing deposition.

Table 7.7.4 Mobility of Z-Loy in Column Experiments at Various Transport Conditions (Approach Velocity = $1.25x10^{-3}$ m/s).

Particle	Treatment	Porous Media	C/C_0
Z-Loy modified with 1 g/L CMC (in excess)	10 mM Na^+/No	Field sand	0.58
Z-Loy modified with 1g/L xanthan gum (in excess) in Field sand	10 mM Na^+/No	Field sand	0.26
MRNIP2	10 mM Na^+/No	Field sand	0.64
Z-Loy (base case)	*10 mM Na^+/No*	*Field sand*	*0.67*
Z-Loy	10 mM Na^+/No	Glass bead	0.92
Z-Loy	10 mM Na^+/No	Unimin sand#50	0.95
Z-Loy	10 mM Na^+/10 mM KCl and 1 g/L polyethylene glycol (PEG) to remove NOM	Field sand	0.4
Z-Loy	10 mM Na^+/No	Washed Field sand	0.93
Z-Loy	DI/ 20-PV flushing with DI	Field sand	0.48
Z-Loy	5 mM Ca^{2+} to decrease clay swelling	Field sand	0.74
Z-Loy	PEG (1g/L) with 10 mM K^+ to decrease clay swelling	Field sand	0.70
Z-Loy	10 mM Na^+/500 mg/L SDBS	Field sand	0.77
Z-Loy	10 mM Na^+/500 mg/L PSS	Field sand	0.74

Sand grain angularity and NOM were not the reasons for poor transport of Z-Loy. Based on this, and on the column studies indicating that the presence of clay particles can dramatically decrease transport of NZVI, it appears that the presence of fines and clays in the interstitial spaces between the sand grains is likely responsible for the poorer than expected transport. To confirm this, we conducted column experiments using a 24.5 cm column packed with washed Field sand and 10 mM Na^+ at the approach velocity of $1.25x10^{-3}$ m/s. Field sand was washed with water and sieved with the opening size of 180 μm to remove the fine particles. Any soil fraction smaller than 180 μm was discarded. As shown in Table 7.7.4, C/C_0 of Z-Loy transport through washed Field sand is 0.93, as high as that through glass bead and Unimin sand, indicating that fine and clay fraction in Field sand was responsible for poor mobility of Z-Loy in this sand and therefore for poorer than expected transport of Z-Loy in the field-scale study.

Several attempts were made to remove fines in situ prior to injection of Z-Loy to improve transport. This included 1) a 20 PV flush with DI water. 2) Flushing with Ca^{2+} and PEG together with K^+ to inhibit clay swelling (Kjellander et al. 1988; Liu et al. 2004). Ca^{2+} (5 mM) and PEG (1g/L) with 10 mM K^+ were used to flush the columns for 4 PVs and allowed to react for 30 min. prior to inject Z-Loy dispersion (in DI water) at the approach velocity of $1.25x10^{-3}$ m/s. 3) Flushing with an anionic surfactant (SDBS) and anionic polyelectrolyte (PSS). A solution of 10 mM Na+ and 500 mg/L solutions of either SDBS or PSS were eluted through the column prior to introducing Z-Loy. None of these treatments could mobilize a sufficient amount of the fine fraction in the sand column to significantly increase transport (Table 7.7.4).

7.7.4 Injection of CMC/NZVI

A second field-scale injection was conducted using NZVI that was pre-synthesis stabilized with carboxymethyl cellulose (CMC). The experimental setup was similar to the Z-Loy experiment and is further described in Johnson et al., 2012. The CMC/NZVI had a nominal ZVI concentration of 1 g/L and the injection rate was ~6 liters per minute. The duration of the NZVI injection period was 100 minutes, which was followed by 60 minutes of water injection.

Prior to injection of the CMC/NZVI, in order to demonstrate that the hydraulics of the pumping system were working as expected, a non-reactive tracer was injected under the same conditions used for the NZVI injection. The data in Figure 7.7.6 indicate that breakthrough occurred in the expected sequence and at time intervals that were expected based on preliminary modeling. The tracer was injected for a period of 60 minutes, and as the data suggest, concentrations remained elevated during that period. Initial breakthrough of the tracer at the closest sampling port occurred after only ~5 minutes and reached injection concentrations within ~10 minutes.

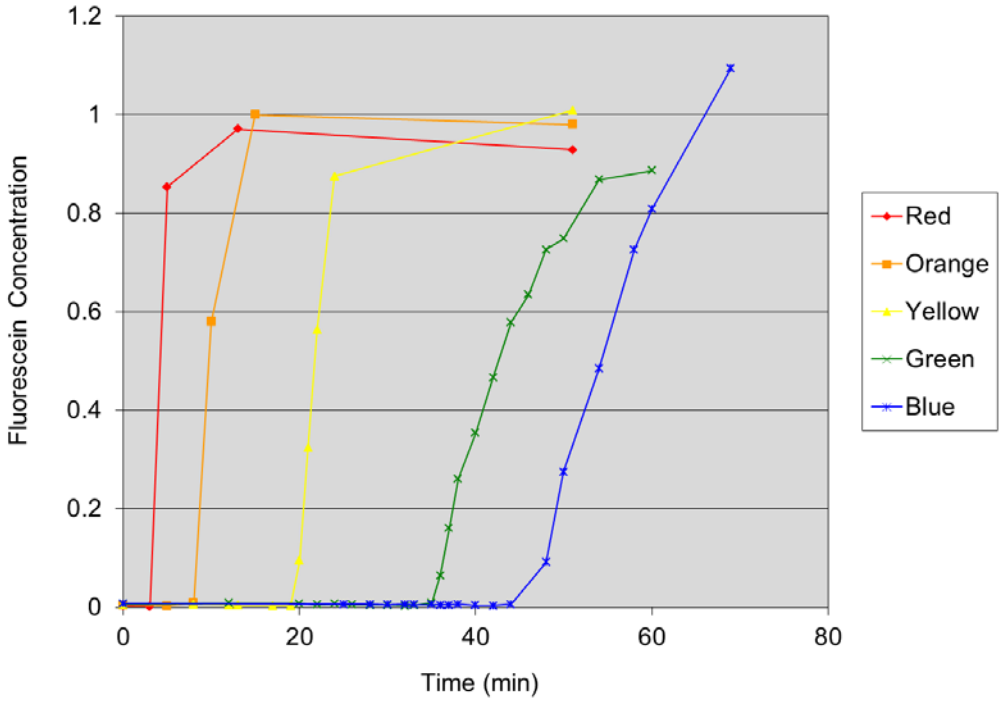

Figure 7.7.6. Normalized fluorescence concentration data at 5 monitoring points along the injection/extraction center line.

For the CMC/NZVI injection the hydraulic gradient was again maintained at about 0.5, which resulted in a velocity of ~0.03 cm/s. Unlike the previous experiment with Z-Loy, no increases in pressure due to plugging near the injection well were observed during injection. Breakthrough began at about 5 minutes and reached a peak at 10-15 minutes. However, the magnitude of that peak was only about half of the injection concentration (Figure 7.7.7). This suggests that a significant amount of NZVI deposition was occurring in the vicinity of the injection well, even though it was expected that the high velocity of the injected water would minimize deposition. Essentially no NZVI was observed at any of the other sampling points.

Surprisingly, after reaching a C/C(0) value of ~0.5 at 15 minutes, the total iron concentration began to drop, even though injection was on-going. This decrease could have occurred for either of two reasons. It could have been that: 1) removal of the NZVI by filtration could have increased with time, or 2) there could have been changes in flow that caused the NZVI to be directed along some other pathway due to plugging by the NZVI or by the production of hydrogen gas.

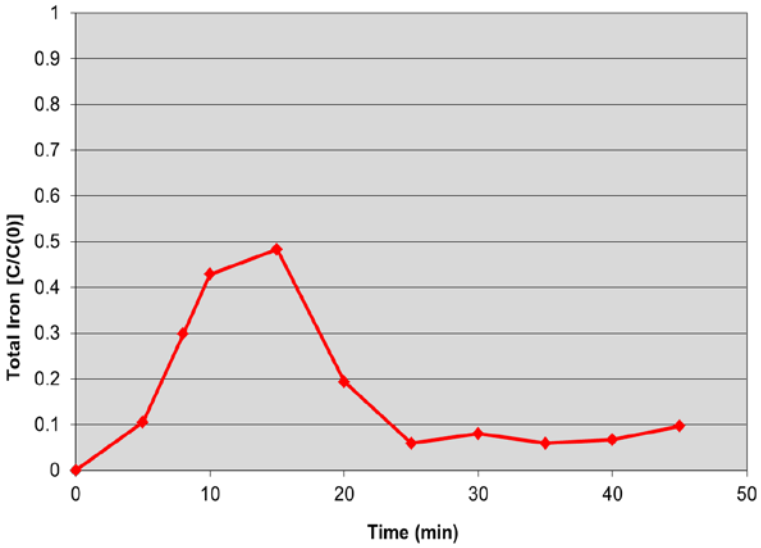

Figure 7.7.7. Normalized total iron concentration measured at the first downgradient sampling port (0.25m from the injection well)

During the course of the injection, specific conductance was measured at each of the samples collected from the monitoring locations. The data in Figure 7.7.8 are from the same location as Figure 7.7.8, and show that specific conductance exhibits the same "rise and fall" behavior as the total iron data. Calculations indicate that species contributing to the measured specific conductance are primarily dissolved ions, and as such they should not be affected by filtration and should flow with the injected water. This suggests that a change in flow patterns, rather than filtration, was the cause of the observed behavior. To confirm this, a conservative tracer (boron) within the injection cocktail was analyzed in each of the samples.

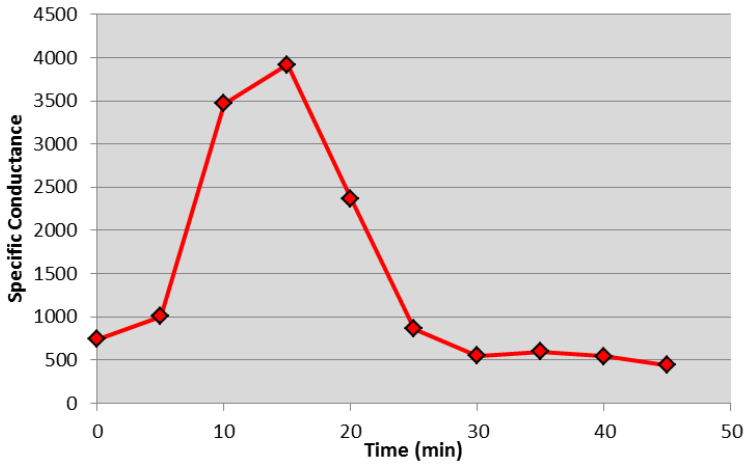

Figure 7.7.8. Specific conductance of water samples measured in samples collected at the first downgradient sampling point (0.25m) from the injection well

The source of the boron in the injection mixture is borohydride used in the NZVI synthesis process. Reduction of iron during synthesis produced borate ion, however traditional synthesis methods use borohydride in excess, so un-reacted borohydride can remain in the injection mixture until it reacts with water or other species (usually within ~48 hours). During the injection process all of the residual borohydride likely reacts with oxidized species in the subsurface (oxygen, mineral surfaces, etc.). In the context of discussions below it is also important to point out that oxidation of the borohydride results in the production of molecular hydrogen which, if present at above saturation concentrations, can result in pore blockage due to bubble formation. The total boron concentration in each of the samples discussed above was analyzed using the spectrophotometric "Carmine" method (Hach Corporation).

The data in Figure 7.7.9 indicate that the boron behaves in a similar manner to both the total iron and specific conductance. This confirms that decrease in iron concentration is not primarily the result of losses due to filtration, but does result from changes in flow caused by plugging of the formation during the injection process. The two most likely causes for plugging of the formation are the NZVI itself and the formation and entrapment of hydrogen bubbles resulting from oxidation of the borohydride or the NZVI.

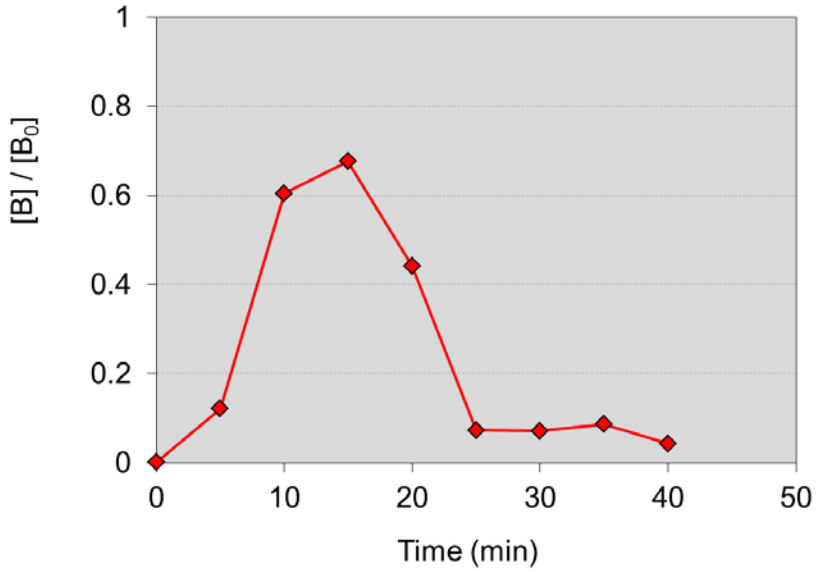

Figure 7.7.9. Normalized total boron concentrations in water samples collected during the C<C/NZVI injection process.

To further evaluate the mechanism of plugging, approximately 6 days after injection a second fluorescein tracer test was conducted to determine if the observed changes in flow were permanent or transient. Our working hypothesis was that plugging caused by deposition of the NZVI would persist over that period of time, while flushing by hydrogen-free groundwater could remove the trapped hydrogen. Figure 7.7.10 shows results from the second tracer test and indicates that flow conditions were very similar to those prior to NZVI injection. We believe this strongly suggests that hydrogen bubbles formed during the injection process significantly impacted flow during the injection process.

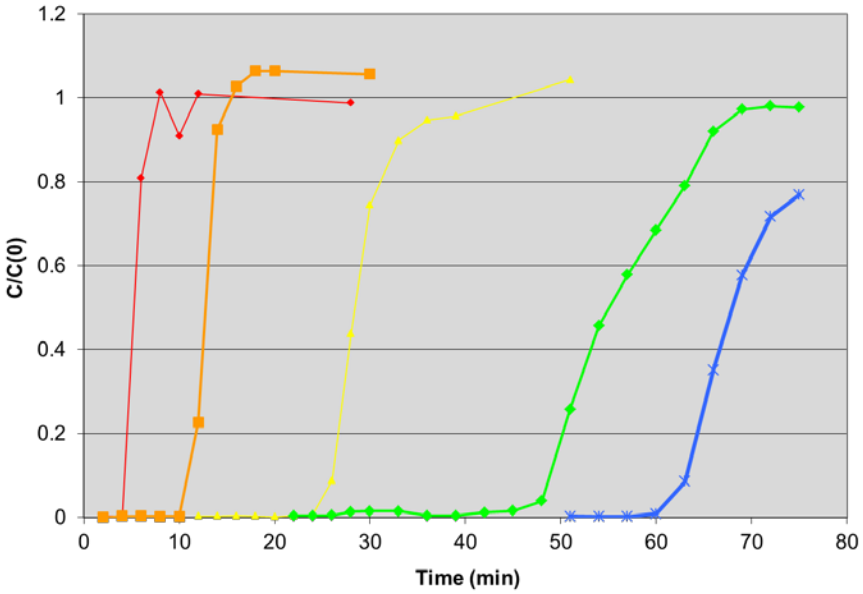

Figure 7.7.10. Normalized fluorescein concentrations from water samples collected at 5 monitoring locations downgradient from the injection well. This test was conducted ~6 days after NZVI injection.

It is important to note that, while we believe hydrogen bubbles were the cause of changes in flow, we also believe that NZVI concentrations were significantly reduced within 0.5 meters of the injection location as the result of filtration. As a consequence, we believe that, under the conditions of this test, the ability to deliver significant quantities of NZVI to a specific target location at field-relevant distances (e.g., >1 m) is very limited.

7.8 Evaluate methods for NZVI detection in the field.

Among all measurement methods, ORP measurement is a traditional electrochemical method to detect the redox condition change due to the iron corrosion reactions, which reduce the oxidants and release H_2 gas. The injection of NZVI can significantly decrease the ORP to very low values (e.g. < -500 mV), which may be an important indicator for the reactivity of injected NZVI particles(Elliott and Zhang 2001; Quinn et al. 2005). Currently assessing the results of injecting NZVI into the subsurface for groundwater remediation relies heavily on measuring ORP of water samples. Although the ORP measurement is a routine measurement in the field, how the NZVI injection affects ORP under various natural conditions has never been studied. The NZVI particles are highly reactive and charged, and they tend to undergo complex physical processes (e.g. aggregation/sedimentation) and chemical reactions (e.g., depassivation/corrosion). The ORP method may measure the mixed potential due to different redox couples, and the measurement is influenced by a number of factors, including nZVI properties (e.g. NZVI particle size/aggregation, concentration, and aging time), the water chemistry (e.g., Fe^{2+}, H_2, and natural organic matter (NOM)), and electrodes deployed.

We systematically investigated the impact of NZVI injection on the ORP measurement under various conditions, including (i) NZVI particle aggregation, settling, and aging; (ii)

various NZVI concentrations; and (iii) varying other chemistry parameters such as NOM, background electrolyte, and H_2 gas. We employed both a stationary batch reactor and a rotating disc electrode (RDE) system to study ORP evolution upon NZVI injection. Both Pt and GC working electrodes are being used to continuously monitor ORP of NZVI suspensions. Complete details of experimental procedures can be found in Shi et al., 2011(Shi et al. 2011).

7.8.1 Aging effects

The effect of aging on ORP is presented in Figure 7.8.1. For the short aging time (2 h), the ORP changed little after NZVI injection, indicating the NZVI particles were not depassivated. After 2 d aging, upon injection of NZVI stock solution, the ORP dropped quickly and was below -600 mV after about 1 h. The results are consistent with the previous aging study (Sarathy et al. 2008), which demonstrated that it usually took more than 12 h to depassivate the NZVI particles and the NZVI reactivity increased within 2 d. For the rest of our experimental results, all NZVI stock solutions were aged for 2 d in the background electrolytes.

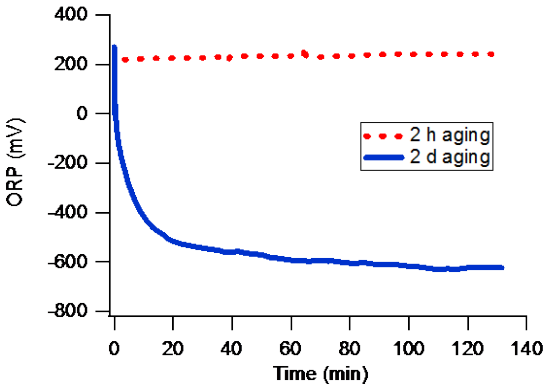

Figure 7.8.1. Temporal evolution of ORP (Pt vs. Ag/AgCl) of NZVI suspensions diluted from the NZVI stock solutions aged for different time (shown in the legend). [nZVI] = 200 mg/L. The electrodes were located at the mid level of the suspensions.

7.8.2 NZVI particle aggregation/size effect

The NZVI particles tend to aggregate and form larger size of particles in solutions(Phenrat et al. 2007). Ultra-sonication is often used to break large aggregates. Without sonication, the ORP of the NZVI suspension dropped much more slowly, compared with the NZVI suspension diluted from the sonicated NZVI stock solution (Figure 7.8.2). For the NZVI sample without sonication, the NZVI particles quickly aggregated and settled down to the bottom of the reactor, which may cause much slower NZVI corrosion reactions. Furthermore, the NZVI concentration in solution close to the electrode may decrease significantly due to NZVI particle settling as the electrode response depends on NZVI particle concentrations. (See discussion in the next section "settling effect"). For the remaining results, the NZVI stock solutions were sonicated for 30 min before use.

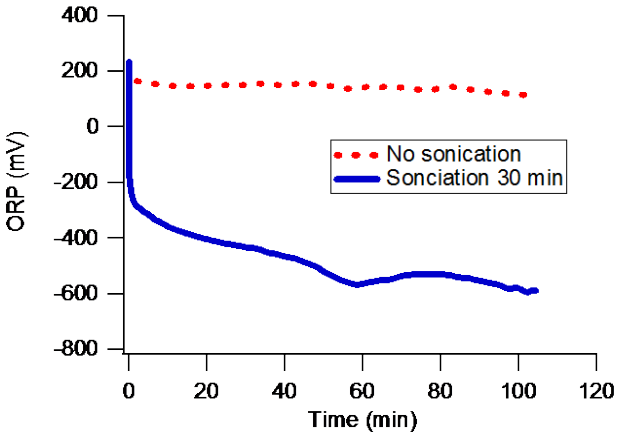

Figure 7.8.2. Temporal evolution of ORP (Pt vs. Ag/AgCl) of NZVI suspensions diluted from the NZVI stock solutions with or without sonication. [NZVI] = 200 mg/L. The electrodes were located at the mid level of the suspensions.

7.8.3 Settling effects

The rates of NZVI particle aggregation and settling depend on the NZVI concentrations(Phenrat et al. 2007). We investigated how the ORP measured by the electrodes responds to NZVI particle settling as this may affect in situ measurements. In batch experiments, after the initial quick drop the ORP tended to rebound, probably caused by the settling of NZVI particles (Figure 7.8.3). The ORP measured by the Pt electrode located at the top level of the suspensions rebound faster compared with that measured by Pt electrode located at the bottom (Figure 7.8.3a). Furthermore, both Pt and GC electrodes (located at the mid level of the suspension) showed similar ORP rebound behavior (Figure 7.8.3b). These observations suggested that the electrode responses, for both Pt and GC, were greatly affected by NZVI particle settling, which decreased NZVI particle concentrations in the water column. So it is likely that the charged NZVI particles contributed to the electrode responses directly rather than solely through dissolved species.

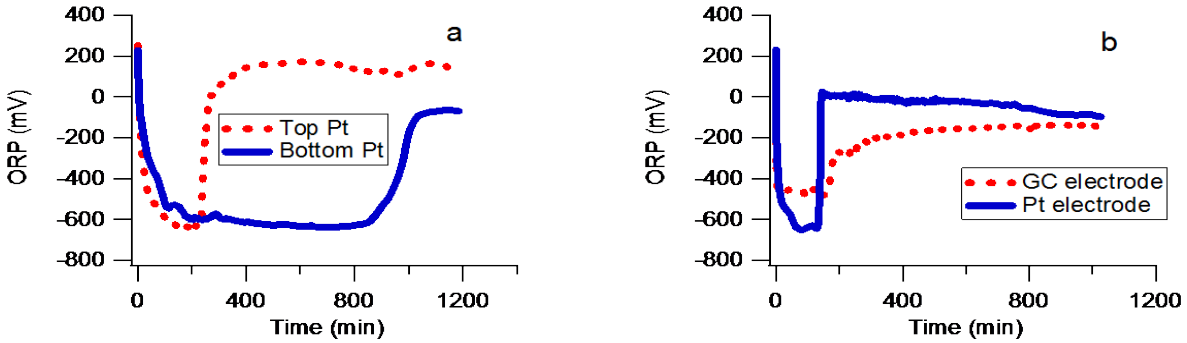

Figure 7.8.3. Temporal evolution of ORP of NZVI suspensions measured by (a) Pt electrodes at top and bottom levels of the suspension ([NZVI] = 50 mg/L); and (b) GC and Pt electrodes located at the mid level of the suspension ([NZVI] = 200 mg/L).

7.8.4 H_2 effect

The measurement of ORP could be complicated by the presence of H_2 since Pt electrode response is affected by H_2 gas concentration. Even without the presence of NZVI, purging the $NaHCO_3$ solution with mixed gas (5% H_2 and 95% Ar) significantly reduced ORP values measured by Pt electrode (Figure 7.8.4a). The steady state ORP value for the Pt electrode is close to the value based on theoretical calculations with the hydrogen electrode (-646 mV vs. Ag/AgCl reference electrode at pH 8.4 and 5% H_2 partial pressure). The amount of time needed to reach steady state is dependent on the rate of purging. In contrast, the ORP measurement by the GC electrode was not affected by the presence of H_2, indicating that the GC electrode is inert to the H_2.

When the NZVI suspension was continuously purged with the mixed gas, the ORP measured by Pt electrode stayed low even after 15 h due to the presence of H_2 (Figure 7.8.4b). By contrast, the ORP measured by GC electrode slowly rebound with time, consistent with the previous observation on the effect of NZVI particle settling. This suggests that H2 evolved from NZVI can impact ORP readings using a Pt electrode as the working electrode to monitor NZVI reactivity. The H_2 may be much more mobile in the subsurface environment compared with the NZVI particles and suggest greater spatial distribution than actually exists. The GC electrode appeared to be a good alternative to eliminate the H_2 effect for ORP measurement.

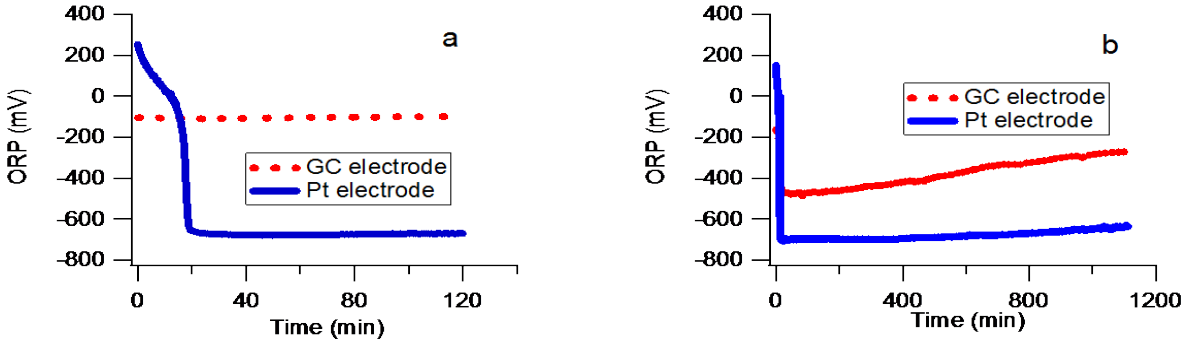

Figure 7.8.4. Temporal evolution of ORP measured by GC and Pt electrodes (located at the mid level of the suspension) under the effect of H2 gas purging. (a) no NZVI added; (b) [NZVI] = 200 mg/L. Note that the time scales are different for plots a and b.

7.8.5 Effect of background electrolytes

The corrosion rate of NZVI varied according to different background electrolytes. The overall effects of background electrolytes on ORP of NZVI suspensions (Figure 7.8.5) are consistent with previous findings(Nurmi et al. 2005). In borate buffer, the decrease of ORP with time was small (about 200 mV), while the ORP decrease in bicarbonate solution was more than 700 mV. In DI water, the ORP decrease is smaller than that in bicarbonate solution, indicating a slower NZVI corrosion rate in DI water than $NaHCO_3$. It is interesting that the ORP drop in the site water was smaller compared with both DI water and $NaHCO_3$ solution, which may be due to high concentration of calcium bicarbonate observed in this solution. The precipitation of calcite enhanced the settling of NZVI particles and also blocked the reactive sites of NZVI by forming precipitates on the NZVI particle surface (Wu et al. 2009).

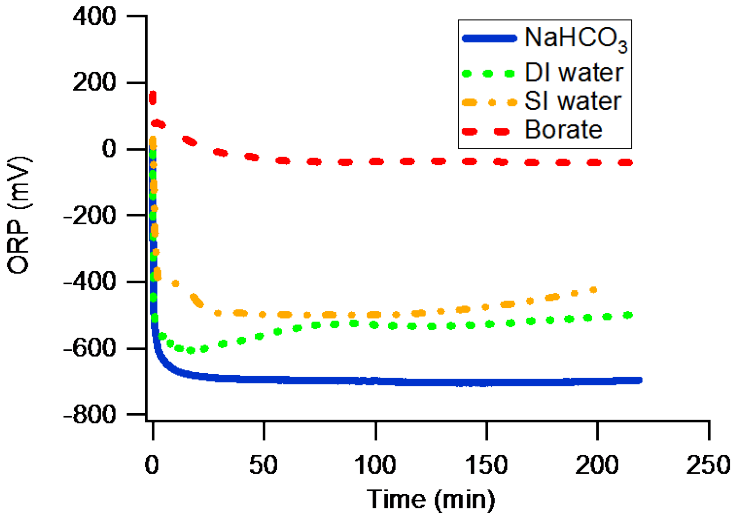

Figure 7.8.5. Temporal evolution of ORP (Pt vs. Ag/AgCl) of NZVI suspensions in various background electrolytes (electrolyte names are presented in the legend). [NZVI] = 200 mg/L. RDE rotating speed = 4000 rpm.

7.8.6 Effect of RDE rotating speed

The measurement of ORP by the RDE could be affected by mass transfer in the diffusion layer on the electrode surface. As discussed previously, the NZVI particles aggregate and settle down with time. With higher rotation speed of the RDE, the thickness of the diffusion layer is reduced which enhanced the overall mass transfer. Further, the settling of nZVI particles may also slow down due to mixing from the rotating electrode. Increasing the rotation speed resulted in more negative ORP limiting values (the lowest ORP observed in each RDE experiment) (Figure 7.8.6). The stable ORP limiting values were reached after 1h for the 200 mg/L NZVI suspensions at 4000 rpm in both $NaHCO_3$ and borate buffer electrolytes. Based on visual observations, the NZVI particles settled down faster at lower rotating speeds, which may account for the slow ORP rebound at 200 rpm in $NaHCO_3$ solution (Figure 7.8.6b). At the 4000 rpm, the NZVI particles appeared to be well dispersed in the solutions during our experiments and the ORP limiting values remained stable.

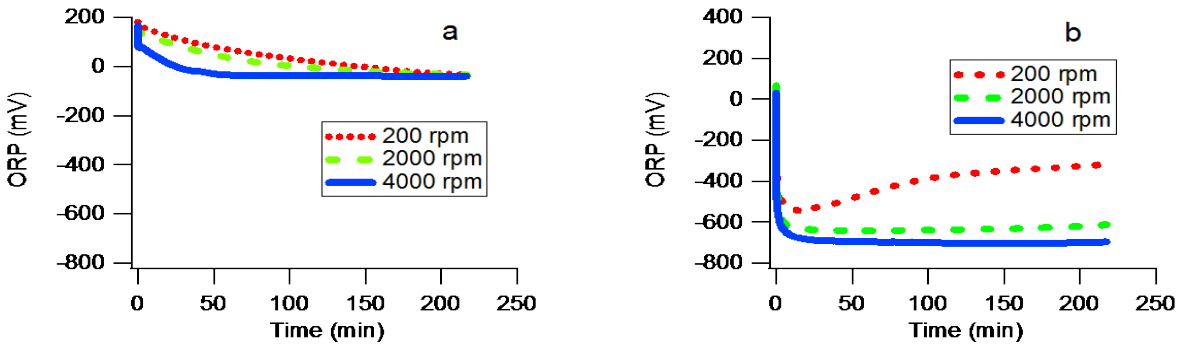

Figure 7.8.6. Temporal evolution of ORP (Pt vs. Ag/AgCl) of NZVI suspensions at various RDE rotating speeds (presented in the legend). (a) Borate buffer; (b) NaHCO3 solution. [NZVI] = 200 mg/L.

7.8.7 Effect of NZVI concentration

The ORP measured by the electrodes is a mixed potential due to various redox couples. The solution chemistry such as Fe^{2+} and H_2 concentrations may affect the mixed potential. Since NZVI particles are charged particles they may adsorb onto the electrode surface and affect the electrode responses directly. We performed the ORP measurement using a Pt electrode over a wide range of NZVI concentrations (10 mg/L to 950 mg/L) in $NaHCO_3$ background electrolyte. Generally with the injection of NZVI, the ORP values dropped quickly and reached the limiting value within 1 h (Figure 7.8.7). The ORP stabilized at the low limiting values for higher NZVI concentrations but, at lower NZVI concentrations (less than 50 mg/L), the ORP rebounded. The ORP limiting values are more negative with increasing NZVI concentration.

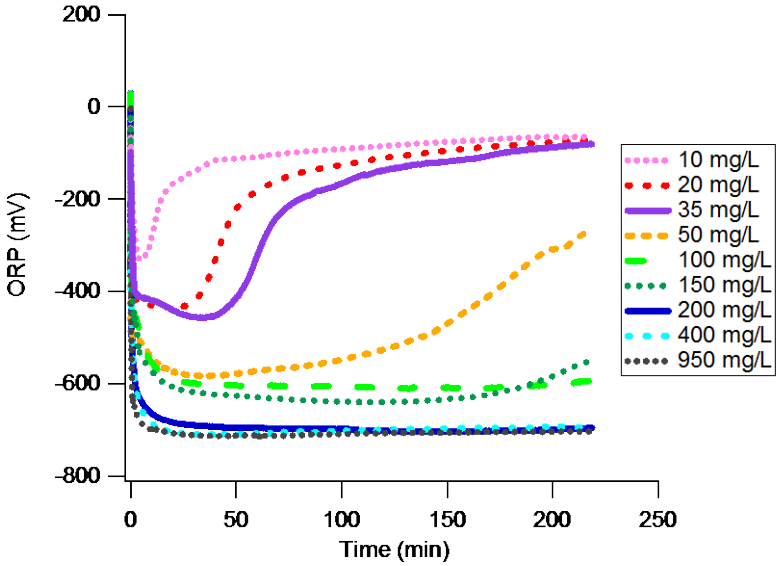

Figure 7.8.7. Temporal evolution of ORP (Pt vs. Ag/AgCl) of NZVI suspensions at various NZVI concentrations (presented in the legend). RDE rotating speed = 4000 rpm. $NaHCO_3$ was the background electrolyte.

7.8.8 Effect of natural organic matter (NOM)

Generally, the increase in NOM concentrations resulted in less negative ORP (Figure 7.8.8). This is probably due to the adsorption of NOM to NZVI particles which may block reactive sites and affect the corrosion potentials. A similar result was found for MRNIP2 vs. RNIP, where the MRNIP2 (which is polymer coated) was approximately 200 mV higher in ORP than for the uncoated RNIP. This again is likely due to the coating in the NZVI surface decreasing its reactivity.

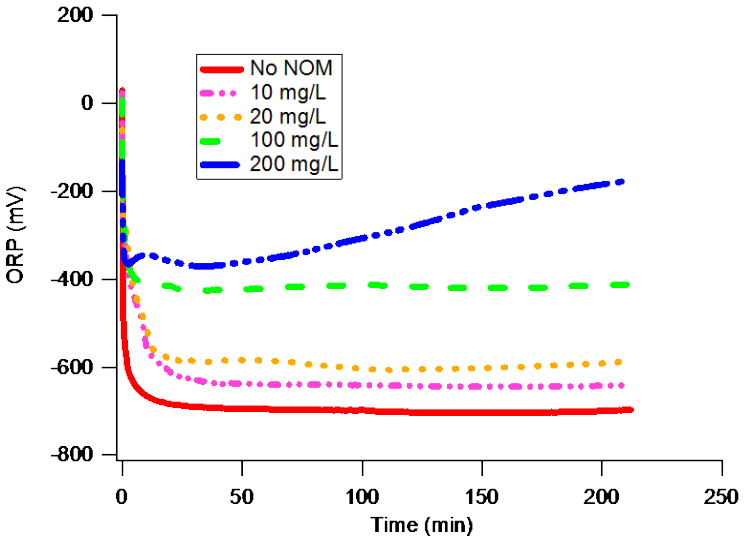

Figure 7.8.8. Temporal evolution of ORP (Pt vs. Ag/AgCl) of NZVI suspensions at various NOM concentrations (presented in the legend). RDE rotating speed = 4000 rpm. [nZVI] = 200 mg/L. NaHCO3 was the background electrolyte.

Overall, these results indicate that the response of ORP electrodes to suspensions of NZVI is not a simple function of NZVI concentration. At high concentrations of NZVI, ORP is dominated by direct interaction between the electrode and the NZVI particles, but this response is nonlinear and saturates with increased coverage of the electrode surface with adsorbed particles. Under these conditions, the presence of NZVI is visually apparent, and ORP measurements add little additional information about the concentration or condition of the particulate material. At low NZVI concentrations, the measured ORP is a mixture of contributions that includes adsorbed NZVI and the dissolved H_2 and Fe(II) species that arise from corrosion of NZVI. Since all of these redox active species give potentials that fall in the same range, ORP measurements cannot distinguish their concentrations. This lack of specificity is compounded for field applications because of the possibility that NZVI and its corrosion products will be affected differently by transport, resulting in partial separation of these species into zones. Conversely, however, ORP measurements may provide useful information when applied in combinations (e.g., Pt vs. GC electrodes) or with complementary characterizations (e.g., concentrations of dissolved iron or hydrogen).

8. Conclusions and Implications for Future Research/Implementation

This project was initiated in April 2006. A combination of laboratory studies across multiple scales, and modeling were used to determine the physicochemical properties of polymer coated NZVI (RNIP), and environmental factors that affect NZVI transport in porous media and reactivity with chlorinated organic solvents. Uncoated RNIP rapidly aggregates in water due to magnetic attractive forces between particles. The rate and extent of RNIP aggregation increased with increasing concentration. This aggregation limits mobility in porous media and thus surface modifiers are essential to making RNIP mobile in water saturated porous media. Surface modification with large molecular weight polyelectrolytes can stabilize a large fraction of RNIP

against aggregation. The ability of a modifier to inhibit aggregation depends on the adsorbed mass and the extended layer thickness of the adsorbed polyelectrolyte. RNIP is a polydisperse mixture of particles and the surface modifiers cannot stabilize the largest particles due to their strong magnetic attractive forces since the saturation magnetization of the particles, M_s, increases as r^6. Generally, small particles with the lowest saturation magnetization, and polymers affording the greatest extended layer thickness and adsorbed mass will resist aggregation the best. However, the small particle size will lead to a shorter reactive lifetime and the coating will decrease reactivity with chlorinated solvents so these factors must be considered in selecting an NZVI with the best resistance against aggregation and greatest transport.

Surface modification enhances the mobility of RNIP in porous media due to electrosteric repulsions afforded by adsorbed polymer layer. These forces decrease aggregation and can prevent deposition in model sand columns, leading to enhanced transport relative to uncoated NZVI. The extent of enhancement depends on 1) the type of modifier, the extended layer thickness, and the adsorbed mass, 2) particle/dispersion properties including particle concentration, particle polydispersity, Fe^0 content, 3) solution chemistry including ionic strength and composition, pH, 4) the physical properties of the porous media including collector size and flow velocity. The transport of polymer modified NZVI at high particle concentration (1-20 g/L) (relevant for in situ remediation) is limited by particle agglomeration in the pores and subsequent attachment on a collector. We developed models for estimating transport distances of polymer modified NZVI at high particle concentration where the properties of adsorbed polymer layer, NZVI, solution chemistry, and porous media are known. Laboratory and modeling studies demonstrated that for transport of high concentration NZVI dispersions minimizing the agglomerate size (d_{agg}) formed can decrease deposition and improve transport. To maximize transport in porous media, one will need to inject NZVI of the smallest size possible (that still provides acceptable reactive lifetime) with the most extended layer thickness, and at as high of an injection rate as possible for the media.

Chemical and physical heterogeneity of the porous media including the presence of clay particles (kaolinite), surface charge heterogeneity, and preferential flow paths can greatly decrease NZVI transport in porous media. However, the use of excess free polymer in the injection solution can lessen these impacts. The presence of 2 wt% of silica fines or clay (kaolinite) fines substantially decreased the mobility of polymer modified NZVI. Clay had a greater effect than silica at the same wt% due to increased deposition to the positively charged edge sites on the clay. The presence of positive charges on the sand surfaces also enhanced deposition of the NZVI and decreased transport. This effect was greater at pH=6 than at pH=8. An engineering approach to mitigate the adverse of clay and charge heterogeneity on NZVI transport is to use low amounts of excess polyanion in the dispersion of polymer modified NZVI. Excess polyanion adsorbs onto the positively charged edges of clay or sand and decrease the attachment of polymer modified NZVI. In two-dimensional flow cells NZVI transported primarily through less resistant flow paths and accumulated at stagnation zones, i.e. low pore water velocity zones. Increasing the injected particle concentration from 0.3 to 3 g/L decreased NZVI transport. The presence of high excess polymer concentration (~3 wt%) caused depletion flocculation and decreased transport while a lower amount of excess polymer (0.1 wt%) increased mobility. High Fe^0 content promoted NZVI agglomeration in porous media and decreased the transport. The increase of adsorbed polymer layer thickness enhanced the transport and prevented pore clogging due to the excess deposition of NZVI in porous media. These findings are consistent with those determined from the column studies and modeling so a

COMSOL based model utilizing the semi-empirical models (described above) was developed to model NZVI agglomeration and deposition in the 2-dimensional flow cells and compared with the experiments. This model successfully modeled the observed transport and deposition of polymer modified NZVI at high particle concentration (6g/L).

In situ targeting of entrapped NAPL was observed in 2-D flow cells due to the affinity of the polymeric coating for the NAPL-water interface. Targeting increased as the NAPL saturation decreased because more particles could contact the NAPL-water interface at lower NAPL saturations. This suggests that targeting a fraction of injected NZVI to entrapped NAPL is possible, however, the attached NZVI is quickly oxidized. Furthermore, the presence of NZVI at the NAPL water interface did not enhance NAPL dissolution. Therefore, NZVI delivered near entrapped NAPL (and away from entrapped NAPL) essentially serves as a reactive barrier that degrades dissolved phase contaminants as they move through the reactive NZVI zone. Therefore, NZVI reactivity and its reactive lifetime are important factors affecting its ability to decrease mass emission from a NAPL source area and must be determined for the site of interest.

Given that the emplaced NZVI will effectively serve as a reactive barrier, the reactivity of that barrier will determine the size and extent of a reactive zone needed to decrease contaminant concentrations to the desired level. We evaluated factors affecting NZVI reactivity including the polymer modifier, concentration of emplaced NZVI, pore plugging, and the presence of groundwater solutes on NZVI reactivity and reactive lifetime. Surface modification required for mobility decreases the reactivity of RNIP for TCE dechlorination by a factor of 5 to 24 depending on the type of surface modifier used. The lower reactivity is due to a combination of reactive site blocking and a decrease in availability of TCE from the bulk solution to the RNIP surface due to the presence of the hydrophobic adsorbed layer. The PCE dechlorination rate increased approximately linearly with increasing concentration of NZVI for concentrations greater than 10g/L, but was non-linear for NZVI concentrations less than 10g/L. In a flow through experiment, the dechlorination rate constant of dissolved PCE increased 2.8 times when the average pore-water velocity in the column increased from 7 cm/d to 113 cm/day, indicating that mass transfer may have limited the reaction. Emplacement of too much NZVI, or NZVI that is not stable against aggregation, lead to pore clogging. This subsequently causes flow (and dissolved contaminants) to bypass the NZVI reactive zone and not to degrade. NZVI reactivity and reactive lifetime was lower in real groundwater and in the presence of aquifer solids than in NZVI/water reactors. NZVI reactive lifetimes ranged from relatively short (3-4 days) to as much as 60 days. In general, there was a tradeoff between reactivity and reactive lifetime, with the more reactive material having a shorter reactive lifetime. This is a result of the poor specificity of the NZVI for the contaminant, and oxidation by water to form H_2. The efficiency of NZVI, i.e. the total mass of TCE degraded per mass of NZVI added to the reactors ranged from ~1:17 to 1:30 for a range of NZVI evaluated. This is much larger than the theoretical amount (1:1 for TCE to acetylene) and was due to additional oxidant demand from nitrate in the groundwater.

The effect of NZVI treatment on down gradient mass flux of contaminants was determined in a two dimensional intermediate-scaled tank study. Emplacement of NZVI (10 g/L) just down gradient of the PCE DNAPL source decreased mass flux up to 85%. Reaction products accounted for approximately 50% of the total decrease in PCE flux, suggesting that flow bypassing the source zone due to permeability reduction from emplaced iron was partially responsible for the decrease in mass emission. A second injection emplacing NZVI directly into the PCE-DNAPL source did not accelerate source zone depletion and had little effect on mass emission.

The transport of NZVI and methods to detect NZVI in field samples was evaluated. We conducted a field scale injection of two types of polymer modified NZVI; Z-Loy and CMC-carboxymethylcellulose (CMC) coated NZVI produced by reduction of ferrous sulfate by borohydride just prior to injection. The mobility in the field scale tank was less than expected based on bench scale column experiments. Injected Z-Loy™ was detected 75 cm from the injection well, about ½ of the distance predicted based on a column experiment. However, pore clogging near the injection well was observed, and approximately 60% of the particles were filtered from the injected water within 5 cm of the well. For injection of CMC-coated NZVI in the same system no increase in pressure due to plugging near the injection well was observed. Transport of CMC-NZVI was greater than 1m, however, the concentration of NZVI as a function of distance from the injection point dropped significantly. At 0.25m, 0.5, and 1m from the injection point the NZVI concentration was about 45%, 25%, and 5% of the injected concentration, respectively. The lower than expected transport was due to the presence of fine particles in the sand used in the tank experiments, consistent with findings from column studies showing that fine particles and clay particles in the interstitial spaces of the larger sand grains significantly decreased transport. We also demonstrated that ORP measurements alone could not be used to determine NZVI concentrations in water samples because it is non-specific and the measurement is confounded by the presence of solutes including H_2 and dissolved Fe. ORP measurements may provide useful information on NZVI concentration when applied with complementary characterizations (e.g., concentrations of dissolved iron or hydrogen).

There are several data gaps remaining where future research may lead to innovations that improve the ability of NZVI to be emplaced in situ, and provide NZVI with sufficient reactive lifetime to make it useful as a reactive barrier technology. With respect to improving emplacement, research is needed to determine if pre-injection or co-injection of a polymer solution can improve NZVI transport. Evidence in this study suggests that this is the case, but this needs to be systematically evaluated in a field scale experiment. Additionally, innovation in the injection techniques is needed to enable use of particle-based remediation technologies. Particles (NZVI are only one type of particle) are a condensed form of material that can deliver concentrated remediation agents to contaminants in situ, and provide slow release of remedial agents where needed. As such, this approach should not be abandoned. Rather, innovation in injection strategies and testing those strategies in real field soils for a variety of particle types is needed. Determining mobility in real heterogenous field soils is best accomplished at the pilot scale. With regard to NZVI, there is a need for better materials than are currently available. NZVI with greater selectivity for the contaminants of interest, and lower reactivity with water, are needed such that they remain reactive for long enough times to be an effective barrier. Additional types of materials (e.g. slow release biostimulants) should also be considered. Determining the optimal size, reactivity, and transport tradeoffs also must be determined.

Appendix A. List of acronyms

1,1-DCE	1,1-Dichloroethylene
ATRP	Atom transfer radical polymerization
CDC	Critical deposition concentration
c-DCE	cis-Dichloroethylene
CMC-	Carboxymethyl cellulose
CMC700k	Carboxymethyl cellulose-700k Molecular weight
CMC90k	Carboxymethyl cellulose-90k Molecular Weight
DI	Deionized
DLVO	Derjaguin-Landau-Verwey-Overbeek
DNAPL	Dense nanaqueous phase liquid
EDL	Electrostatic double layer
EPM	Electrophoretic mobility
GC	Gas chromatograph
GC-ECD	Gas chromatograph-Electron capture detector
GC-FID	Gas Chromatograph-Flame ionization detector
GFA	Georgetown Fulvic Acid
MRNIP	Modified nanoscale iron particles
MRNIP2	Poly(olefin maleic acid)-modified reactive nanoscale iron particles
NAPL	Nonaqueous phase liquid
NOM	Natural organic matter
NZVI	Nanoscale zerovalent iron
ORP	Oxidation-reduction potential
PAP	Poly(aspartate)
PAP10k	Poly(aspartate)-10k Molecular weight
PAP2.5k	Poly(aspartate)-2.5k Molecular weight
PCE	Perchloroethylene
PEG	Poly(ethylene glycol)
PHA	Peat Humic Acid
PMAA	Poly(methylmethacrylate)
PMMA	Poly(methylmethacrylate)
PSS	Poly(styrene sulfonate)
PSS1M	Poly(styrene sulfonate)-1M molecular weight
PSS-70K- poly(styrene sulfonate)	Poly(styrene sulfonate)-70k molecular weight
PV	Pore volume
PVA	Poly(vinyl alcohol)
PZC	Point of zero charge
RDE	Rotating disc electrode
RNIP	Reactive nanoscale iron particles
RNIP-R	Catalyst-modified reactive nanoscale iron particles
SDBS	Sodium dodecylbenzene sulfonate
SQUID	Superconducting quantum interference device
SRHA	Suwnaee River humic acid
TCE	Trichloroethylene

t-DCED	trans-Dichloroethylene
TEM	Transmission electron microscopy
VC	Vinyl chloride

Appendix B. Relationship between SERDP tasks and sections in this report

Task #	Task Description	Topic #	Topic Description
1	Determine the relative effects of flow velocity, aquifer permeability, particle surface chemistry, pH, ionic strength, and heterogeneity on nanoparticle transport.		
1.1	Assess the effect of nanoiron surface modification on mobility in 1-D bench scale columns	7.1.1 and 7.1.2	- Effect of Particle Surface Chemistry on NZVI Aggregation -Assess the effect of NZVI surface modification on mobility in 1-D bench scale columns
1.2	Assess the effect of pore fluid velocity (approach velocity) on mobility of nanoiron through homogeneous sand columns	7.1.3	Assess the Effect of Fluid Approach Velocity on Mobility of Polymer modified NZVI through Homogeneous Sand Columns.
1.3	Assess the effect of pH, ionic strength, and aquifer media grain/pore size on modified nanoiron mobility through homogeneous sand columns	7.1.4 and 7.1.5	-Assess the Effect of pH and Ionic Strength on Polymer modified NZVI mobility through homogeneous sand columns. - Assess the Effect of Collector Size on Polymer modified NZVI mobility through homogeneous sand columns.
1.4	Develop and validate 2-D flow cell experimental methods including methods to image iron nanoparticles, methods to monitor mass emission from TCE DNAPL source, and nanoparticle injection methods	7.2	Determine Effect of Aquifer Heterogeneity on Transport and Emplacement of Polymer modified NZVI in Porous Media
1.5	Assess the effect of geochemistry on nanoiron transport in 2-D flow cells.	7.2.1	Effect of Chemical Heterogeneity of Porous Media on Transport of Polymer modified NZVI
1.6	Assess the effects of soil heterogeneity on nanoiron migration in 2-D cells	7.2.2	Effect of Physical Heterogeneity of Porous Media on Transport of Polymer modified NZVI
2	Determine the particle surface properties and hydrodynamic conditions necessary to achieve nanoiron targeting to the DNAPL-water interface in situ.		
Task #	**Task Description**	**Topic #**	**Topic Description**
2.1	Ex Situ targeting of the NAPL-water interface	7.4.1.1	Screening of NZVI affinity to target NAPL-water Interface via Ex Situ (batch) Targeting Test
2.2	Determine the potential for destabilization targeting ex situ	7.4.2	Determine the Potential for NAPL Targeting by NZVI Destabilization
2.3	In situ targeting in 1-D columns	7.4.1.2	In Situ NAPL Targeting by Polymer-modified NZVI in One Dimensional, Homogeneous Porous Media.
2.4	In situ targeting in 2-D cells and nanoiron imaging to determine emplacement	7.4.1.3	In situ NAPL Targeting by Polymer-modified NZVI in Two Dimensional, Heterogeneous Porous Media.
2.5	Determine the effect of injection conditions on the ability to deliver nanoiron to the DNAPL		

	source area		
2.6	Evaluate methods for pre and post-treatment characterization to determine treatment effectiveness	7.6	Determine Effect of PCE NAPL Source Zone Treatment by Deliverable Polymer Modified NZVI in Intermediate-Scale Experiment
2.7	Measure the effect of nanoiron treatment on flow field in and around the DNAPL source, and on net mass emission from source	7.6.2	Determine the effect of Pore Clogging due to NZVI Emplacement
3	Determine the effect of adsorbed polymers and surfactants on nanoiron reactivity	7.5.1	Effect of Surface Modifiers on Reactivity with Dissolved TCE
4	Modeling and scale-up in a large scale tank experiment		
4.1	Design and set up of large tank experiments	7.6.1	Effect of Emplacement Location on Treatment Efficiency in Intermediate Scale
4.2	Transport and DNAPL targeting at intermediate scale and effect of nanoiron treatment on DNPAL source architecture and strength.		
4.3	Evaluation and selection of codes for particle transport	7.3.2	Empirical Correlations to Estimate Agglomerate Size and Deposition during Injection of a Polyelectrolyte-modified Fe^0 Nanoparticle at High Particle Concentration in Saturated Sand.
Task #	**Task Description**	**Topic #**	**Topic Description**
4.4	Validate particle transport and upscaling methods and models	7.3.3	Evaluate Ability of Particle Transport COMSOL-based Model for Predicting the Emplacement and Transport of Polymer-modified NZVI in Heterogeneous Porous Media
6	Selection and Preparation of nZVI	7.7.1	Treatability Study for a TCE Contaminated Area using Nanoscale-Zerovalent Iron Particles: Reactivity and Reactive Life Time
7	Evaluate Optimal Conditions for Transport with Respect to Particle Concentration, Polymer Stabilizer Type, and Aquifer Pretreatment with Polymer Stabilizer	7.1.2.2 and 7.7.3	-Effect of NZVI Surface Modification, Particle Concentration, and Particle Size Distribution on Agglomeration and Deposition in Porous Media -Improving Z-Loy Transport through Field Sand
8	Methods for Monitoring NZVI Transport and Reactivity in situ		
8.1	Identify Methods and Test in Lab Reactors/columns	7.8	Identify and Evaluate Geophysical Methods for NZVI Detection in the Field.
8.2	Measure in Large Tanks	7.7.2	Evaluate Injection of Polymer modified NZVI in a Controlled Field-Scale Aquifer Model Packed with Natural Aquifer Materials
9	Test and Validate Semi-Empirical Models for Predicting Emplacement	7.3.3	Evaluate Ability of Particle Transport COMSOL-based Model for Predicting the Emplacement and Transport of Polymer-modified NZVI in Heterogeneous Porous

			Media
10	Pilot Scale Injection Testing and Characterization		
10.1	Set up and Evaluation of Potential Injection Methods	7.7.2	Evaluate Injection of Polymer modified NZVI in a Controlled Field-Scale Aquifer Model Packed with Natural Aquifer Materials
10.2	Injection Testing with Optimal Particle Types and Properties		

Appendix C. "Lessons Learned"

The efficacy of nanoscale zerovalent iron (NZVI) treatment of chlorinated solvent contaminant source areas containing entrapped dense non-aqueous phase liquid (DNAPL, either as residuals, ganglia or pools) requires the delivery and placement of a significant mass of NZVI into the vicinity of the source, and requires that the emplaced NZVI remain reactive with the contaminants for extended times. This can decrease the down-gradient concentrations of chlorinated solvent emanating from the entrapped DNAPL so long as the NZVI remains reactive and is emplaced near the source. This document outlines the lessons learned from a series of experiments, ranging from laboratory to field scales to identify factors affecting the efficacy of NZVI treatment. Specifically, these experiments identified factors influencing the ability to deliver NZVI in situ to the vicinity of the source, to decrease the DNAPL mass and mass emission from the source, and to evaluate the impact of NZVI on native microbial communities including dehalogenators. This document draws on scientific findings from these experiments to provide general guidance to site managers and remediation professionals who are considering the use of NZVI for in situ treatment of a DNAPL source zone. It also provides guidance on the types of sites where NZVI treatment may be an appropriate option once site specific and feasible injection methods and strategies have been established and once NZVI products with sufficient reactive lifetimes become available.

Summary of important lessons learned in this study:

Effectiveness of Treatment

- Direct placement of NZVI into the source zone with DNAPL is not feasible or desirable. The strategy should be to place the NZVI downstream of the source in an optimal manner so that the plume generated from the dissolution of entrapped NAPL is intercepted as close to the source as possible before the plume spreads by dispersion. Hence, injected NZVI principally should serve as a reactive barrier localized near the source and strategies to utilize NZVI should be informed by knowledge of other reactive barrier technologies (e.g. PRBs with ZVI)
    - Reactive barriers made from emplacing NZVI just down-gradient from an entrapped PCE DNAPL source significantly decreases mass emission from the source, without producing significant amounts of chlorinated reaction products.
    - NZVI emplaced immediately at the DNAPL-water interface (at 10g/L) is rapidly oxidized, but does not enhance DNAPL dissolution compared to the absence of NZVI and thus does not accelerate source mass loss.

- Polymeric coatings and constituents in groundwater including dissolved organic matter and inorganic ions generally decreases the reactivity of NZVI, but it still remains reactive enough to serve as a reactive barrier.
    - Polymer coating used on NZVI are not readily desorbed and decrease NZVI reactivity with chlorinated solvents by up to a factor of 20 compared to uncoated NZVI depending on the polymer used.
    - NZVI reactivity generally scales with NZVI concentration (above ~2g/L) and is relatively unaffected by pH.

- Reactive lifetime of NZVI depends on the groundwater pH, and the concentration of contaminants and competing oxidants
    - Reactive lifetime of NZVI depends significantly on groundwater pH and the presence of reducible ions like dissolved oxygen, nitrate, and chromium. Reactive lifetimes of NZVI (~30 nm sized) is not expected to be more than 12 to 18 months in ideal conditions (i.e. in the absence of competing oxidants other than groundwater that is buffered by the iron at relatively high pH=10 to 11). Reactive lifetime generally decreases with decreasing NZVI particle size.
    - NZVI to TCE mass ratios much greater than the stoichiometric amount are required (as much as 20:1 for one site evaluated) due to consumption for Fe(0) by dissolved oxygen, other reducible substrates (nitrate, hexavalent chromium, heavy metals) and generation of H_2. Reductant demand will be site-specific and must be determined.
    - Polymeric coatings did not protect NZVI against oxidation by water.
    - NZVI reactive lifetime is short in the immediate vicinity of free phase DNAPL.

- NZVI is not detrimental to total microbial abundance, but can shift the microbial community due to creation of a reducing environment and generation of H_2 from the reduction of water.
    - Sulfate reducers and methanogens are enhanced.
    - Dehalogenators can also be enhanced, but to a lesser degree.

Implications of these findings for treatability testing and application of NZVI

NZVI can serve as an in situ reactive barrier to decrease down-gradient flux of contaminants. Both the NZVI properties and groundwater constituents will affect the reactivity and lifetime of the reactive barrier formed through emplacement of NZVI. The performance of such a barrier can be predicted using the same tools developed for PRBs made from ZVI. Treatability studies must consider the NZVI being used, any applied coatings, and groundwater geochemistry. Safety factors of 10 or more should be considered when estimating the NZVI to contaminant ratios needed based on stoichiometry. Impacts of NZVI on microbial ecology are likely to be limited and its use should not preclude the ability to employ monitored natural attenuation (MNA) as part of the remediation strategy.

NZVI emplacement in porous media and DNAPL targeting

- Achieving good distributions of NZVI injected at concentrations (several to 10's of g/L) needed for in situ treatment of a source zone containing residual DNPAL is extremely difficult using standard wells and pressure injection methods.
    - Transport is limited by both aggregation and deposition of the NZVI near the injection well, and transport distances decrease with increasing concentration of NZVI in the injected slurry. Repeated injections of NZVI can lead to pore plugging, changes in the flow field around the DNAPL source area, and the inability to deliver additional NZVI to the source area.
    - For non-fracture-based injection methods, there are no field data that directly show significant NZVI transport over distances of more than about 1 meter.

- Heterogeneity in the hydraulic conductivity field significantly impacts NZVI transport and emplacement.
  - Transport of NZVI is highest in paths having the high hydraulic conductivity, and limited into low conductivity regions where groundwater flow is slow.
  - The presence of clay and other fine particles, and the grain shape decreases NZVI transport in porous media in a pH dependent manner.
  - Empirical models developed to predict transport of NZVI in heterogeneous porous media must be parameterized for the specific NZVI being used and for the site-specific porous media.
  - Excess free polymer in solution can potentially enhance transport of NZVI relative to the absence of free polymer.
- Demonstration of NZVI emplacement should be made by direct observation of the NZVI, rather than by indirect indicators such as ORP or [H_2]
  - Concentrations of NZVI are readily visible at <<1 g/L.
  - Measurements of Fe(0) on the collected particles can indicate whether or not the transported material remains active.
  - If possible, this should be accomplished with nests of wells with short screened intervals (or via direct-push profiling or coring) in order to assess the vertical distribution as well as the lateral distribution.

Implications of these findings for emplacement and application of NZVI

The ultimate distribution of NZVI into a specific formation cannot easily be predicted using bench scale and intermediate scale testing of injections, even using site specific soils. Stability against aggregation, i.e. a highly stable NZVI suspension, does not guarantee good mobility in porous media. Simple filtration models are not good indicators for the distribution of NZVI in the subsurface. More complex models are needed, but must be calibrated for each site and each NZVI type and must take into account the heterogeneity of the site and potential confounding factors (e.g., the presence of fine – e.g., clay – particles). Methods need to be developed to determine the effective parameters of these models at the application scales. Evaluations of injectability should be piloted at the site of interest.

Overall, there remains a need for innovative methods to introduce NZVI slurries into porous media. This may involve the use of free polymer in solution to facilitate mobility, fracturing followed by injection of NZVI into the fractures formed, or other yet to be determined methods. There is also a need to develop NZVI with a greater reactive lifetime. The former will require innovation with respect to hydraulic or potentially pneumatic emplacement of NZVI. The latter will require innovation with respect to NZVI dopants or coatings that are selective for specific compounds and decrease the activity of water at the NZVI-water interface. It may also be achieved through manipulation of particle size to optimize emplacement, reactivity, and reactive lifetime. As this summary suggests, while NZVI remains a promising technology, there are still a number of important technical challenges remaining regarding its effective implementation. Pilot tests should, in most cases, be viewed from the perspective of possible “red flags” for implementation.

Appendix D. Technology performance evaluation matrix

The following technology performance evaluation chart is intended to provide guidance on the hydrogeochemical conditions that are favorable for emplacement of nanoscale zerovalent iron (NZVI) as an in situ remediation technology. The green coloring indicates relatively favorable conditions for the implementation of NZVI and suggests conditions where injection and a moderately long-term reactivity of the injected iron may be likely. Yellow indicates that it may be feasible but perhaps should be avoided. Red indicates a poor chance of success. Since the effect of many of these variables will depend on the type of NZVI, its size, and its coating, including values or ranges of values for many of these parameters is not possible. Parameters in bold are the most critical factors influencing the potential success of NZVI as a remediation alternative.

Hydrogeochemical Condition	**Range of Values**		
Impact on Emplacement			
Porous matrix material	Sand/cobble	Silt	Clay
Hydraulic conductivity	High	Medium	Low
Sorting of aquifer material	Well	Moderate	Poorly
Ionic strength (salt content)	Low	Medium	High
Divalent Cation	None	Low	Med
Groundwater flow	Low	Med	High
Impact on Reactivity/Lifetime			
Groundwater flow	Low	Med	High
Groundwater chemistry	Reducing	Oxidizing	Strongly oxidizing
Co-contaminants			
Dissolved oxygen	Zero	Low	Medium
Nitrate	Zero	<0.5mM	>0.5mM
PotentialEffectiveness			
Chlorinated organic concentration	>>2ppm	<2ppm	ppb
Longevity of source	Yr	>yrs	Decades

Overall, the optimal site conditions for the application of nanoparticulate phase reductants like NVZI are those that allow for emplacement of a significant mass of NZVI in and around the entrapped DNAPL source. Emplacement is most feasible in relatively high conductivity regions or strata within an aquifer without fine of clay particles filling pore spaces, and potentially within fractured media (untested). Conditions that favor the longevity of reactivity of emplaced NZVI will have greatest utility. Longevity will be best in the absence of competing oxidants like nitrate, chromate, or dissolved oxygen, and in poorly buffered groundwater where the pH of water flowing through the reactive barrier is buffered at a relatively high pH by the corrosion of NZVI. The ability of any of these strategies to be effective is the advent of innovative technologies to emplace NZVI, and more selective and longer lasting reactive materials.

Appendix E. List of technical publications

Peer-reviewed Journals

Liu, Y., Lowry, G.V. (**2006**). "Effect of Particle Age (Fe^0 content) and Solution pH on NZVI Reactivity: H_2 Evolution and TCE Dechlorination". *Environ. Sci. Technol.*, 40 (19) 6085-6090.

Saleh, N., Sirk, K., Liu, Y., Phenrat, T., Dufour, B., Matyjaszewski, K., Tilton, R., Lowry, G. V. (**2007**) "Surface Modifications Enhance Nanoiron Transport and DNAPL Targeting in Saturated Porous Media." *Environ. Eng. Sci*. 24 (1) 45-57.

Phenrat, T., Saleh, N., Sirk, K., Tilton, R., Lowry, G. V. (**2007**) "Aggregation and Sedimentation of Aqueous Nanoiron Dispersions." *Environ. Sci. Technol. 41(1) 284-290.*

Liu, Y., Phenrat, T., Lowry, G.V. (**2007**). Effect of TCE concentration and dissolved groundwater solutes on NZVI-promoted TCE dechlorination and H_2 evolution. *Environ. Sci. Technol.* 41(22) 7881-7887.

Phenrat, T., Saleh, N., Sirk, K.; Kim, H.-J., Tilton, R., D., Lowry, G., V. Stabilization of aqueous nanoscale zerovalent iron dispersions by anionic polyelectrolytes: adsorbed anionic polyelectrolyte layer properties and their effect on aggregation and sedimentation. *Journal of Nanoparticle Research 10* **(2008)** 795-814.

Navid Saleh, Hye-Jin Kim, Krzysztof Matyjaszewski, Robert D. Tilton, and Gregory V. Lowry. (**2008**). Ionic Strength and Composition affect the mobility of surface-modified NZVI in water-saturated sand columns. *Environ. Sci. Technol.* 42 (9) 3349-3355.

Phenrat, T., Long, T. C., Lowry, G.V., Veronesi, B. Partial Oxidation ("Aging") and Surface Modification Decrease the Toxicity of Nanosized Zerovalent Iron. *Environmental Science and Technology* 43 **(2009)** 195–200.

Phenrat, T., Liu, Y., Tilton, R.D., Lowry, G.V. Adsorbed Polyelectrolyte Coatings Decrease Fe(0) Nanoparticle Reactivity with TCE in Water: Conceptual Model and Mechanisms. *Environmental Science and Technology* 43 (**2009**) 1507–1514

Sirk, K.M., Saleh, N.B., Phenrat, T., Kim, H.-J., Dufour, B., Ok, J., Golas, P.L., Matyjaszewski, K., Lowry, G.V., Tilton, R.D. Effect of Adsorbed Polyelectrolytes on Nanoscale Zero Valent Iron Particle Attachment to Soil Surface Models. *Environmental Science and Technology* **(2009)** 43 (10), 3803-3808

Kim, H.-j., Phenrat, T., Tilton, R.D., Lowry, G.V. Fe0 Nanoparticles Remain Mobile in Porous Media after Aging Due to Slow Desorption of Polymeric Surface Modifiers. *Environmental Science and Technology* (**2009**) 43 (10), 3824–3830.

Phenrat, T., Kim, H.-J., Fagerlund, F., Illangasekare, T., Tilton, R.D., Lowry, G.V. Particle Size Distribution, Concentration, and Magnetic Attraction Affect Transport of Polymer- modified Fe0 Nanoparticles in Sand Columns. *Environmental Science and Technology* (**2009**) 43 (13), 5079–5085.

Kirschling, T., Gregory, K., Minkley, N., Lowry, G., Tilton, R. (**2010**). Impact of Nanoscale Zero Valent Iron on Geochemistry and Microbial Populations. *Environ. Sci. Technol.* 44 (9) 3474-3480

Phenrat, T., Song, J., Cisneros, C., Schoenfelder, D., Tilton, R., Lowry, G. (**2010**). Estimating Attachment of Nano- and Submicrometer-particles Coated with Organic Macromolecules in

Porous Media: Development of an Empirical Model. *Environ. Sci. Technol.* 44 (12) 4531-4538.
Reinsch, B. C., Forsberg, B., Penn, R. L., Kim, C. S., Lowry, G. V. Chemical transformations during aging of zero-valent iron nanoparticles in the presence of common groundwater dissolved constituents. *Environ. Sci. Technol*. 44 (9) 3455-3461 .
Li, Zhiqiang; Greden, Karl; Alvarez, Pedro; Gregory, Kelvin; Lowry, Gregory. (**2010**). Adsorbed polymer and NOM limits adhesion and toxicity of nano scale zero-valent iron (NZVI) to E. coli. *Environ Sci. Technol.* 44 (9) 3462-3468.
Phenrat, Tanapon, Hye-Jin Kim, Fritjof Fagerlund, Tissa Illangasekare, Gregory V. Lowry (**2010**). Empirical Correlations to Estimate Agglomeration, Deposition, and Transport of Polyelectrolyte-modified Fe(0) Nanoparticles at High Particle Concentration in Saturated Porous Media. *J. Contam. Hydrol.* 118 (3-4), 152-164.
Phenrat, Tanapon, Abdullah Cihan, Hye-Jin Kim, Menka Mital, Tissa Illangasekare, Gregory V. Lowry (**2010**). Transport and Deposition of Polymer-modified Fe0 Nanoparticles in 2-D Heterogeneous Porous Media: Effects of Particle Concentration, Fe0 Content, and Coatings. *Environ. Sci. Technol.* 44, 9086–9093.
Phenrat, Tanapon, Fritjof Fagerlund, Tissa Illangasekare, Gregory V. Lowry, Robert D. Tilton. (**2011**). Polymer-modified Fe0 Nanoparticles Target NAPL Source Zones in Two Dimensional Porous Media: Effect of Particle Concentration, NAPL Saturation, and Delivery Strategy. *Environ. Sci. Technol.*45 (14) 6102-6109.
Shi, Z., Nurmi, J. T., Tratnyek, P. G. (**2011**). Effects of Nano Zero-Valent Iron on Oxidation-Reduction Potential. *Environ. Sci. Technol. 45,* 1586–1592.
Kim, H-J., Tanapon Phenrat, Robert D. Tilton, and Gregory V. Lowry (**2012**). Clay Fines and pH Affect Aggregation, Deposition and Transport of Zero Valent Iron Nanoparticles in Heterogeneous Porous Media. *J. Colloid Interface Sci*. 370 1-10.
Fagerlund F., Illangasekare, Phenrat T., Kim H.-J., Lowry G.V (**2012**). PCE dissolution and simultaneous dechlorination by nanoscale zero-valent iron particles in a DNAPL source zone. *J. Contam. Hydro*l. 131 9-28.
Kim, H-J., Megan Leitch, Robert D. Tilton, Tissa Illangasekare, Gregory V. Lowry. Effect of emplaced nZVI mass and seepage velocity on PCE dechlorination and hydrogen evolution in water saturated porous media. *Environ. Sci. Technol.* (in revision)
Johnson, R.L., J. T. Nurmi, G. O'Brien Johnson, D. Fan, R. O'Brien Johnson, Z. Shi, G.V. Lowry and P. G. Tratnyek, 2012, "Field-Scale Transport of Carboxymethyl Cellulose Stabilized Nano Zerovalent Iron" Environ. Sci. Technol. (in prep).

Published technical abstracts

Lowry, G. and Liu, Y. (**2006**) "Lifetime and Reactivity of NZVI in Groundwater". Partners in Environmental Technology Technical Symposium & Workshop, Washington, D.C. November 28-30, 2006.
Lowry, G.V., Navid Saleh, Tanapon Phenrat, Hye-Jin Kim, Kevin Sirk, Robert D. Tilton, Tissa Illangasekare (**2006**). "Effects of Polymeric Surface Coatings on NZVI Mobility in Saturated Porous Media and Reactivity with TCE." Partners in Environmental Technology Technical Symposium & Workshop, Washington, D.C. November 28-30, 2006.
Lowry, G.V., Saleh, N., Phenrat, T., Liu, Y., Kim, H., Sirk, K., Matyjaszewski, K., Tilton, R. (**2006**). "Delivering Polymer-modified Fe^0 Nanoparticles to Subsurface Chlorinated Organic

Solvent DNAPL." US EPA Nanotechnology and the Environment: Applications and Implications Progress Review Workshop III, Washington D.C., November 8-9, 2006.
Lowry, G.V. (**2006**). Environmental Fate and Transport of Nanomaterials. In the Proceedings of the "Nanotechnology and OSWER: New Opportunities and Challenges". US EPA OSWER. Jul7 12-13, 2006.
Gregory V. Lowry, N. Saleh, Y. Liu, T. Phenrat, K. Sirk, B. Dufour, T. Sarbu, K. Matyjaszewski, R. Tilton. **(2006)**. Nanoiron Treatment of DNAPL Source Zones: Efficient Delivery and DNAPL Targeting. The Fifth International Conference on Remediation of Chlorinated and Recalcitrant Compounds, Monterey, CA. May 22-25, 2006.
Tanapon Phenrat, Yueqiang Liu, Hye-Jin Kim, Navid Saleh, Kevin Sirk, Robert D. Tilton, Gregory V. Lowry. (**2007**). Effect of adsorbed polyelectrolytes on TCE dechlorination and product distribution by Fe^0/Fe-oxide nanoparticles. In the Proceedings of the Division of Environmental Chemistry for the 233rd ACS National Meeting, Chicago, IL March 25-29, 2007.
Yueqiang Liu and Tanapon Phenrat, Gregory V. Lowry (**2007**). Effect of Groundwater Constituents on H_2 evolution and TCE reduction by reactive Fe^0/Fe-oxide nanoparticles. In the Proceedings of the Division of Environmental Chemistry for the 233rd ACS National Meeting, Chicago, IL March 25-29, 2007.
Gregory V. Lowry, Hye-Jin Kim, Yueqiang Liu, Tanapon Phenrat1, Kris Matyjaszewski, Navid Saleh, Kevin Sirk, Robert D. Tilton. (**2007**). Functionalized Fe^0 nanoparticles for targeted in situ degradation of entrapped DNAPL. Division of Industrial Engineering & Chemistry for the 233rd ACS National Meeting, Chicago, IL March 25-29, 2007.
Tanapon Phenrat, Navid Saleh, Kevin Sirk, Hye-Jin Kim, Yueqiang Liu, Robert D. Tilton, Gregory V. Lowry (**2007**). Polyelectrolyte-Modified Nanoscale Zerovalent Iron: Characteristics of the Adsorbed Polyelectrolyte Layer and Dispersion Stability. Division of Colloid and Surface Chemistry for the 233rd ACS National Meeting, Chicago, IL March 25-29, 2007.
Saleh, N. B., Phenrat, T., Tilton, R.D., Lowry, G. V. (**2007**). Porewater velocity and collector grain size affects the mobility of surface-modified nanoiron in water-saturated porous media. Division of Colloid and Surface Chemistry for the 233rd ACS National Meeting, Chicago, IL March 25-29, 2007.
Kevin M. Sirk, Navid B. Saleh, Tanapon Phenrat, Hye-Jin Kim, Gregory V. Lowry, and Robert D. Tilton (**2007**). Amphiphilic Block Copolymer Surface Modification of Nanoscale Zero Valent Iron (NZVI) for Source Zone DNAPL Remediation. *ACS Division of Colloid and Surface Science*, 81st Colloid & Surface Science Symposium. University of Delaware, Newark, DE, June 24-27.
Tanapon Phenrat, Hye-Jin Kim, Navid Saleh, Kevin Sirk, Robert D. Tilton, and Gregory V. Lowry (**2007**). Polyelectrolyte-Modified Nanoscale Zerovalent Iron : Characteristics of the Adsorbed Polyelectrolyte Layer and Dispersion Stability. *ACS Division of Colloid and Surface Science*, 81st Colloid & Surface Science Symposium. University of Delaware, Newark, DE, June 24-27.
Hye-Jin Kim, Tanapon Phenrat, Navid Saleh, Kevin Sirk, Robert D. Tilton, Gregory V. Lowry (**2007**). Desorption of Polyelectrolyte Coatings from Nanoscale Fe^0 Used for Environmental Remediation ACS Division of Colloid and Surface Science, 81st Colloid & Surface Science Symposium. University of Delaware, Newark, DE, June 24-27.

Lowry, G.V. (**2007**). "Hydrogeochemical Parameters Controlling the Emplacement, Reactivity, and Longevity of Nanoscale Zerovalent Iron (NZVI) for in-situ Groundwater Remediation". Keynote Lecture at the 3rd International Symposium on Permeable Reactive Barriers and Reactive Zones, Rimini, Italy, November, 8-9, 2007.

Gregory V. Lowry, Tanapon Phenrat, Fritjof Fagerlund, Hye-Jin Kim, Navid Saleh, Tissa Illangasekare, Robert D. Tilton (**2007**). "Delivering Reactive Nanoparticles to Subsurface DNAPL Source Zones". Presented at the SERDP Partners in Technology Symposium, Washington, D.C., December 4, 2007.

Tanapon Phenrat, Hye-Jin Kim, Robert Tilton, Fritjof Fagerlund, Tissa Illangesakera, Gregory V Lowry (**2007**). Polyelectrolyte-Modified Nanoscale Zerovalent Iron: Characteristics of the Adsorbed Polyelectrolyte Layer and Their Effects on Dispersion Stability and TCE Dechlorination. SERDP Partners in Technology Meeting, Washington, DC, December 4-6.

Hye-Jin Kim, Navid Saleh, Tanapon Phenrat, Robert D. Tilton, Fritjof Fagerlund, Tissa Illangasekare, Gregory V. Lowry (**2007**). Effect of pH, pore water velocity, grain size, and clay content on the transportability of surface-modified NZVI in saturated sand columns. SERDP Partners in Technology Meeting, Washington, DC, December 4-6.

Gregory V. Lowry, T. Phenrat, D. Schoenfelder, Mark Losi and June Yi, Steven A. Peck (**2007**). NZVI Treatability Study for a TCE Source Area at Alameda Point, CA SERDP Partners in Technology Meeting, Washington, DC, December 4-6.

Fritjof Fagerlund, Tanapon Phenrat, Hye-Jin Kim, Tissa Illangesakera, Gregory V Lowry (**2007**). Nanoscale zero-valent iron treatment of a DNAPL source zone in sandy soils SERDP Partners in Technology Meeting, Washington, DC, December 4-6.

Gregory V. Lowry, Tanapon Phenrat, Fritjof Fagerlund, Hye-Jin Kim, Navid Saleh, Tissa Illangasekare, Robert D. Tilton (**2007**). "Controlled placement of polyelectrolyte modified engineered nanomaterials in the subsurface: Correlating modifier layer properties and geochemistry with mobility". Invited keynote lecture at the American Geophysical Union Fall Meeting, Hydrology Division, San Francisco, CA, December 10-14.

Tanapon Phenrat, Fritjof Fagerlund, Hye-Jin Kim, Tissa Illangasekare, Robert D. Tilton, Gregory V. Lowry (**2007**). Effect of Nanoparticle Aggregation, Polydispersity, and Concentration on Transport of Surface-Modified Nanoscale Zerovalent Iron (NZVI) Particles in Saturated Porous Media. Hydrology Division, American Geophysical Union Fall Meeting, San Francisco, CA December 10-14.

Gregory V. Lowry, T. Phenrat, Dan Schoenfelder, Mark Losi, June Yi, Steven A. Peck (**2008**). NZVI Treatability Study for a TCE Source Area at Alameda Point, CA. Sixth International Conference on Remediation of Chlorinated and Recalcitrant Compounds, Monterey, CA, May 19-22.

Gregory V. Lowry, Tanapon Phenrat, Fritjof Fagerlund, Hye-Jin Kim, Tissa Illangasekare, Robert D. Tilton (**2008**). Effect of Nanoparticle Aggregation, Polydispersity, and Concentration on Transport of Surface-Modified NZVI in Saturated Porous Media. Sixth International Conference on Remediation of Chlorinated and Recalcitrant Compounds, Monterey, CA, May 19-22.

Gregory V Lowry, Daniel Schoenfelder, Tanapon Phenrat, Mark Losi, Jun Yi, Steven Peck (**2008**). NZVI treatability study for a TCE source area at Alameda Point, CA. Sixth International Conference on Remediation of Chlorinated and Recalcitrant Compounds, Monterey, CA, May 19-22.

Fritjof Fagerlund, Tanapon Phenrat, Hye-Jin Kim, Tissa Illangasekera, Gregory V Lowry (**2008**). "Effect of nanoscale zero-valent iron treatment on the characteristics of a DNAPL source zone in sandy soils. Sixth International Conference on Remediation of Chlorinated and Recalcitrant Compounds, Monterey, CA, May 19-22.

Kim, Hye-Jin, Phenrat, T., Tilton, R. Lowry, G. (**2008**). Desorption of adsorbed polyelectrolytes from Fe0 nanoparticles. In the Proceedings of the Division of Environmental Chemistry for the 234th ACS National Meeting, New Orleans, LA April 6-10, 2008.

F Fagerlund *, TH Illangasekare, T Phenrat, H-J Kim, G Lowry. (**2008**). Simultaneous DNAPL dissolution and dechlorination by nanoscale zero-valent iron particles. Presented at MODFLOW and More: Ground Water and Public Policy. Colorado School of Mines, Golden Colorado, May 19-21, 2008.

Tissa Illangasekare, Fritjof Fagerlund, Menka Mittal, Pinar Cihan, Tanapon Phenrat, Hye-Jin Kim, Gregory V. Lowry (**2008**). Effects of DNAPL source morphology on contaminant mass transfer and the zone of effective treatment using nano-scale zero-valent iron. AGU Fall Meeting, San Francisco, CA December 15-19.

Tanapon Phenrat, Fritjof Fagerlund, Hye-Jin Kim, Tissa Illangasekare, Gregory V. Lowry (**2008**). Two-Dimensional Transport of Concentrated Dispersions of Polyelectrolyte-modified Fe0 Nanoparticles in Saturated Sand. AGU Fall Meeting, San Francisco, CA December 15-19.

Gregory V. Lowry, Tanapon Phenrat, Charlotte M. Cisneros, Daniel P. Schoenfelder, Fritjof Fagerlund, Hye-Jin Kim, Tissa Illangasekare, Robert D. Tilton (**2008**). Correlation to Predict Collision Efficiency of Natural Organic Matter (NOM)- and Polymer-coated Nanoparticles in Porous Media. AGU Fall Meeting, San Francisco, CA December 15-19.

Gregory V. Lowry, Tanapon Phenrat, Hye-Jin Kim, Fritjof Fagerlund, Tissa Illangasekare (**2008**). Effect of Aggregation, Hydrogeochemistry, and Clay on NZVI Emplacement in the Subsurface. SERDP Partners in Technology Meeting, Washington DC. December 2-4.

Brian Carl Reinsch, Greg V. Lowry, and Christopher S. Kim (**2009**). E XAFS investigation of the oxidation and Fe-oxide speciation of Fe0 Nanoparticles (NZVI) under geochemically relevant conditions. Division of Colloid Science and Environmental Chemistry for the 235th ACS National Meeting, Salt Lake City, UT March 22-26, 2009.

Tanapon Phenrat, Fritjof Fagerlund, Hye-Jin Kim, Tissa Illangasekare, Robert D. Tilton, Gregory V. Lowry (**2009**). Transport Characteristics of Polyelectrolyte-modified Fe0 Nanoparticles at High Particle Concentration in Sand Columns. Presented at RemTec 2009, Atlanta, GA March 3-5, 2009.

Phenrat, T., Tilton, R., Lowry, G. (**2009**) Semi-empirical Correlation to Predict the Collision Efficiency of Natural Organic Matter (NOM) - and Polymer-coated Nanoparticles in Porous Media, International Conference on the Environmental Implications and Applications of Nanotechnology, UMASS, June 9-11, 2009.

Tissa Illangasekare, Tanapon Phenrat, Menka Mittal, Sidika Pinar Turkbey Cihan, Hye-Jin Kim, Fritjof Fagerlund, Gregory V. Lowry **(2009**). In Situ PCE Remediation using Polymeric Modified Nanoscale Zerovalent Iron in an Intermediate-scaled Aquifer System: Effect of Repeating NZVI Injections on Treatment Efficiency and Differential Mobility of Particles, AGU 2009 Joint Assembly, Toronto, Ontario, Canada, May 24-27, 2009.

Phenrat, T., Kim, H., Illangesekare, T., Abdullah, Lowry, G. Insights to the Influence of Adsorbed Organic Macromolecules on Nanoparticle Attachment Efficiency in Porous

Media. *Eos Trans. AGU, 90 (52),* Fall Meet. Suppl., Abstract H41I-03, December 14-18, **2009**.

Li, Z., Alvarez, P., Gregory, K., Lowry, G. Polymeric coatings eliminate the bactericidal effects of Nanoscale zero-valent iron to Escherichia coli. *Eos Trans. AGU, 90 (52),* Fall Meet. Suppl., Abstract H43B-1012 December 14-18, **2009**.

A. Cihan; T. Phenrat; S. P. Cihan; G. V. Lowry; T. H. Illangasekare. Modeling Tools to Design In Situ Nanoscale Zerovalent Iron (NZVI) Emplacement Strategies. *Eos Trans. AGU, 90 (52),* Fall Meet. Suppl., Abstract H41I-07 December 14-18, **2009**.

T. H. Illangasekare; M. Mittal; T. Phenrat; F. Fagerlund; H. Kim; A. Cihan; G. V. Lowry Use of an Intermediate-Scale Tank to Study Strategies for Modified NZVI Emplacement for Effective Treatment of DNAPL Source Zones . *Eos Trans. AGU, 90 (52),* Fall Meet. Suppl., Abstract H43B-1028 December 14-18, **2009**.

Gregory V. Lowry, Tanapon Phenrat, Abdullah Cihan, Tissa Illangasekare. Modeling Tools to Design In Situ Nanoscale Zerovalent Iron (NZVI) Emplacement Strategies. SERDP 2009 Partners in Technology Meeting, Washington DC. Nov 30-Dec 2, **2009**.

Hye-Jin Kim, Tanapon Phenrat, Robert D. Tilton, Fritjof Fagerlund, Menka Mittal, Sidika Pinar Turkbey Cihan, Tissa Illangasekare, Gregory V. Lowry. Nonlinear relationship between kobs and nZVI dose for PCE dechlorination in batch and flow through columns at realistic seepage velocity in porous media. SERDP Partners in Technology Symposium, Nov 30-Dec 2, **2009**, Washington DC.

Paul G. Tratnyek, Richard L. Johnson, James T. Nurmi, Peter Langren, Gregory V. Lowry, Yuxin Wu, Kenneth H. Williams. Injection of Nano Zero-valent iron for subsurface remediation: A field scale test of materials, methods, and models. SERDP Partners in Technology Symposium, Nov 30-Dec 2, **2009**, Washington DC.

Fritjof Fagerlund, Menka Mittal, Tissa H. Illangasekare, Sidika Turkbey Cihan, Tanapon Phenrat, Hye-Jin Kim and Greg Lowry. Evaluation of the concept of effective reactivity zone for optimum placement of nano-scale zero-valent iron for treatment of aquifers contaminated with DNAPLs. SERDP Partners in Technology Symposium, Nov 30-Dec 2, **2009**, Washington DC.

Published text books, book chapters, and theses.

Lowry, G.V. and Wiesner, M. R. Environmental Considerations: Occurrences and Fate of Nanomaterials in the Environment. In *Nanotoxicology: Characterization, Dosing, and Health Effects.* Eds. N. Monteiro-Riviere and C. Long Tran. Informa Health Care USA, Inc., New York, NY 2007 p. 369-390.

Lowry, G. V. *Groundwater Remediation Using Nanoparticles.* In *Environmental Nanotechnology: Applications and Impacts of Nanomaterials*. Eds. M. Wiesner and F. Bottero, McGraw-Hill, New York, NY, 2007 p.297-333.

Saleh, N. (2007). An Assessment of Novel Polymeric Coatings to Enhance Transport and In Situ Targeting of Nanoiron for Remediation of Non-aqueous Phase Liquids (NAPLs). Ph.D. Thesis, Carnegie Mellon University, Department of Civil and Environmental Engineering, Pittsburgh, PA.

Phenrat, T. (2008). Effect of polymeric surface modification on nano-sized zerovalent iron (NZVI) aggregation, transport of concentrated NZVI dispersions in porous media, and reactivity with trichloroethylene. Ph.D. Thesis, Carnegie Mellon University, Department of Civil and Environmental Engineering, Pittsburgh, PA.

Phenrat, T. and Lowry, G. V. Physicochemistry of Polyelectrolyte Coatings that Increase Stability, Mobility, and Contaminant Specificity of Reactive Nanoparticles used for Groundwater Remediation. In *Nanotechnology for Water Quality*, William Andrews Publishing. (in press)

Lowry, G. V. and Casman E. A. (2009). Nanomaterial Transport, Transformation, and Fate ion the Environment: A Risk-based Perspective on Research Needs. In *Risk, Uncertainty and Decision Analysis for Nanomaterials: Environmental Risks and Benefits and Emerging Consumer Products*. Eds. Igor Linkov and Jefferey Stevens. Springer Verlag. pp. 125-139.

Tanapon Phenrat, Daniel Schoenfelder, Mark Losi, June Yi, Steven A. Peck, and Gregory V. Lowry. Treatability Study for a TCE Contaminated Area at Alameda Point, CA using Nanoscale- and Microscale-Zerovalent Iron Particles: Reactivity and Reactive Life Time. ACS Publications. (in press).

Other Outreach and/or presentations

Lowry, G.V. "The role of surface coatings on the fate and mobility of nanomaterials in the Environment". Duke University, Civil and Environmental Engineering, February 21, 2007.

Lowry, G. "Occurrences and fate of nanomaterials in the groundwater". Presented at the US EPA National Health and Environmental Effects Research Laboratory in RTP, NC. February 22, 2007.

Lowry, G. "Functionalized Reactive Nanoscale Fe0 (NZVI) for in situ DNAPL Remediation: Opportunities and Challenges". Presented as part of the EPA/HIEHS Webinar series on Nanotechnology. March 15, 2007.

Lowry, G.V. "Surface Functionalized Reactive Nanoparticles for in situ DNAPL Source Zone Treatment". Stanford University, Civil and Environmental Engineering, March 16, 2007.

Lowry, G. V., "Assessing the Fate and Mobility of Nanomaterials in the Environment". American Bar Association Section of Energy, Environment, and Resources. July 11, 2007.

Lowry, G.V. "Nanoparticle and Geochemical Properties Controlling the Mobility of Surface-Modified Nanomaterials in the Environment". Department of Civil and Environmental Engineering at the Pennsylvania State University, October 3, 2007.

Lowry, G.V. "Optimizing the Reactivity and Mobility of Reactive Nanomaterials for In Situ Groundwater Remediation". Department of Civil and Environmental Engineering at the University of Illinois-Urbana Champaign, November 2, 2007.

Lowry, G. V., Correlating nanoparticle surface coating properties and geochemistry with nanoparticle reactivity, transport, and potential for exposure". National Science Foundation, December 6, 2007.

Lowry, G. V., Reactive Nanomaterials for In Situ Remediation of Contaminated Groundwater Aquifers and Sediments". Chevron ETC, Richmond, CA December 11, 2007.

Lowry, G. V. Reactive NPs for GW Remediation: Optimizing emplacement and mitigating risks through surface modification, NanoEco, Ascano, Switzerland, March 7, 2008.

Lowry, G. V. Transport of Surface Modified Nanoparticles (Colloids): Physical and Chemical Processes. Presented at the Gordon Conference on Transport in Porous Media, Oxford, UK. July 16, 2008.

Lowry, G. V. Reactive Nanomaterials for In Situ Aquifer Remediation: Effect of Surface Coatings on Reactivity, Transport, and Emplacement. Presented at the Bren School of Environment, UCSB, Santa Barbara, CA. October 17, 2008.

Lowry, G. V. Potential Impacts of Nanotechnology on the Environment. Keynote lecture presented at Remtech 2009 Atlanta, GA March 3-5, 2009.

Lowry, G. V. Reactive Nanoparticles for In Situ Groundwater Remediation: Optimizing the Benefits and Mitigating the Risks with Surface Coatings, OECD, Paris France, July 16, 2009.

Lowry, G. V. Environmental Remediation Potential of Engineered Nanoparticles: Benefits, Challenges, and Risks (Keynote), Soil Science Society of America (SSSA) Fall Meeting, Nov 2, 2009.

Lowry, G. V., Groundwater Remediation with Nanomaterials: What applications tells us about implications, Franco-American Young Environmental Scientist Symposium (YESS), Paris, France Nov. 17, 2009.

Appendix F. References

Amirbahman, A., and Olson, T. M. (1993). "Transport of humic matter-coated hematite in packed beds " *Environ. Sci. Technol.*, 27(13), 2807-2813.

Amirbahman, A., and Olson, T. M. (1995). "The role of surface conformations in the deposition kinetics of humic matter-coated colloids in porous media." *Colloids Surf., A*, 95(2-3), 249-259.

Bai, R., and Tien, C. (1999). "Particle Deposition under Unfavorable Surface Interactions:." *J. Colloid Interface Sci.*, 218(2), 488-499.

Bear, J. (2007). *Hydraulics of Groundwater* Dover Publications, New York.

Bergendahl, J., and Grasso, D. (2000). "Prediction of colloid detachment in a model porous media: hydrodynamics." *Chem. Eng. Sci.*, 55, 1523-1532.

Brant, J., Labille, J., Bottero, J.-Y., and Wiesner, M. R. (2007). "Nanoparticle transport, aggregation, and deposition." In: *Environmental Nanotechnology: Applications and impacts of nanomaterials*, M. R. Wiesner and J.-Y. Bottero, eds., McGraw-Hill, New York.

Cayer-Barrioz, J., Mazuyer, D., Tonck, A., and Yamaguchi, E. (2009). "Frictional rheology of a confined adsorbed polymer layer." *Langmuir*, 25(18), 10802-10810.

Chen, K. L., and Elimelech, M. (2007). "Influence of humic acid on the aggregation kinetics of fullerene (C60) nanoparticles in monovalent and divalent electrolyte solutions. ." *J. Colloid Interface Sci.*, 309, 126-134.

Chen, K. L., and Elimelech, M. (2008). "Interaction of Fullerene (C60) Nanoparticles with Humic Acid and Alginate Coated Silica Surfaces: Measurements, Mechanisms, and Environmental Implications " *Environ. Sci. Technol.*, 42(20), 7607–7614.

Chibowski, S., and Wisniewska, M. (2002). "Study of electrokinetic properties and structure of adsorbed layers of polyacrylic acid and polyacrylamide at Fe2O3-polymer solution interface." *Colloid Surf. A.*, 208, 131-145.

Clarke, J., and Braginski, A. I. (2004). *The SQUID Handbook: Fundamentals and Technology of SQUIDs and SQUID Systems*, Wiley-VCH, New York.

Clement, T. P. (1997). "RT3D A modular computer code for simulating reactive multi-species transport in 3-dimensional groundwater systems." Pacific Northwest National Laboratory, Richland, WA, USA.

de Vicente, J., Delgado, A. V., Plaza, R. C., Durán, J. D. G., and González-Caballero, F. (2000). "Stability of cobalt ferrite colloidal particles: Effect of pH and applied magnetic fields." *Langmuir*, 16, 7954-7961.

Elimelech, M. (1992). "Predicting collision efficiencies of colloidal particles in porous media." *Water Res.*, 26(1), 1-8.

Elimelech, M., Gregory, J., Jia, X., and Williams, R. (1995). *Particle Deposition and Aggregation: Measurement, Modeling, and Simulation*, Butterworth-Heinemann, Boston.

Elliott, D. W., and Zhang, W.-X. (2001). "Field assessment of nanoscale bimetallic particles for groundwater treatment." *Environ. Sci. Technol.*, 35, 4922-4926.

Evans, D. F., and Wennerstrom, H. (1999). *The Colloidal Domain: Where Physics, Chemistry, Biology, and Technology Meet* Wiley-VCH, New York.

Fagerlund, F., Illangasekare, T., Phenrat, T., Kim, H.-J., and Lowry, G. V. (2012). "PCE dissolution and simultaneous dechlorination by nanoscale zero-valent iron particles in a DNAPL source zone." *J. Contam. Hydrol.* , in press.

Fleer, G. J., Cohen Stuart, M. A., Scheutjens, J. M. H. M., Cosgrove, T., and Vincent, B. (1993). *Polymers at Interfaces*, Chapman & Hall, London.

Franchi, A., and O'Melia, C. R. (2003). "Effects of Natural Organic Matter and Solution Chemistry on the Deposition and Reentrainment of Colloids in Porous Media " *Environ. Sci. Technol.*, 37(6), 1122-1129.

Fritz, G., Schadler, V., Willenbacher, N., and Wagner, N., J. (2002). "Electrosteric stabilizatoin of colloidal dispersions." *Langmuir*, 18, 6381-6390.

Gavaskar, A., Tatar, L., and Condit, W. (2005). "Cost and performance report nanoscale zero-valent iron technologies for source remediation." Naval Facilities Engineering Command (NAVFAC).

Glover, K., Munakata-Marr, J., and Illangasekare, T. H. (2007). "Biologically-Enhanced Mass Transfer of Tetrachloroethene from DNAPL in Source Zones: Experimental Evaluation and Influence of Pool Morphology." *Environ. Sci. Technol.*, 41(4), 1384-1389.

Harbaugh, A. W., Banta, E. R., Hill, M. C., and McDonald, M. G. (2000). "MODFLOW-2000, the U.S. Geological Survey modular ground-water model – user guide to modularization concepts and the ground-water flow process." U.S. Geological Survey, Reston, VA, U.S.A.

He, F., M. Zhang, T. Qian, and Zhao, D. (2009). "Transport of carboxymethyl cellulose stabilized iron nanoparticles in porous media: Column experiments and modeling " *J Colloid Interf. Sci.*, 334(1), 96-102.

He, F., and Zhao, D. (2005). "Preparation and Characterization of a New Class of Starch-Stabilized Bimetallic Nanoparticles for Degradation of Chlorinated Hydrocarbons in Water." *Environ. Sci. Technol.*, 39(9), 3314-3320.

He, F., Zhao, D., Liu, J., and Roberts, C. B. (2007). "Stabilization of Fe-Pd Nanoparticles with Sodium Carboxymethyl Cellulose for Enhanced Transport and Dechlorination of Trichloroethylene in Soil and Groundwater." *Ind. Eng. Chem. Res.*, 46(1), 29-34.

Illangasekare, T. (1998). "Flow and entrapment of nonaqueous phase liquids in heterogeneous soil formations." In: *Physical Nonequilibrium in Soils: Modeling and Application*, H. M. Selim and L. Ma, eds., Ann Arbor Press, New Jersey, 417-435.

Illangasekare, T. H., Ramsey, J. L., Jensen, K. H., and Butts, M. (1995). "Experimental study of movement and distribution of dense organic contaminants in heterogeneous aquifers." *J. Contam. Hydrol.*, 20, 1-25.

Imhoff, P. T., Jaffe, P. R., and Pinder, G. F. (1993). "An experimental study of complete dissolution of a nonaqueous phase liquid in saturated porous media." *Water Resour. Res.*, 30(2), 307-320.

Irene Man-Chi Lo, R. Y. S., Keith C. K. Lai. (2007). *Zero-valent iron reactive materials for hazardous waste and inorganics removal* ASCE.

Israelachvili, J. N. (1992). *Intermolecular and Surface Forces, Second Edition: With Applications to Colloidal and Biological Systems*, 2nd Ed., Academic Press.

Itami, K., and Fujitani, H. (2005). "Charge characteristics and related dispersion/flocculation behavior of soil colloids as the cause of turbidity." *Colloids and Surfaces a-Physicochemical and Engineering Aspects*, 265(1-3), 55-63.

Johnson, R. L., Johnson, G. O., Nurmi, J. T., and Tratnyek, P. G. (2009). "Natural organic matter enhanced mobility of nano zerovalent iron." *Environ. Sci. Technol.*, 43, 5455-5460.

Johnson, W. P., Li, X., and Assemi, S. (2006). "Deposition and re-entrainment dynamics of microbes and non-biological colloids during non-perturbed transport in porous media in the presence of an energy barrier to deposition." *Adv. Water Resour.*, 30(6-7), 1432-1454.

Kanel, S. R., Goswami, R. R., Clement, T. P., Barnett, M. O., and Zhao, D. (2008). "Two Dimensional Transport Characteristics of Surface Stabilized Zero-valent Iron Nanoparticles in Porous Media " *Environ. Sci. Technol.*, 42(3), 896-900.

Kim, H. J., Phenrat, T., Tilton, R. D., and Lowry, G. V. (2009). "Fe(0) Nanoparticles Remain Mobile in Porous Media after Aging Due to Slow Desorption of Polymeric Surface Modifiers." *Environmental Science & Technology*, 43(10), 3824-3830.

Kim, H. J., Phenrat, T., Tilton, R. D., and Lowry, G. V. (2012). "Clay Fines and pH Affect Aggregation, Deposition and Transport of Zero Valent Iron Nanoparticles in Heterogeneous Porous Media." *J. Colloid Interface Sci.* , 370, 1-10.

Kjellander, R., Marcelja, S., Pashley, R. M., and Quirk, J. P. (1988). "Double-layer ion correlation forces restrict calcium-clay swelling." *J. Phys. Chem.*, 92(23), 6489–6492.

Koziarz, J., and Yamazaki, H. (1999). "Stabilization of polyvinyl alcohol coating of polyester cloth for reduction of bacterial adhesion." *Biotechnology Techniques*, 13(4), 221-225.

Kretzschmar, R., Holthoff, H., and Sticher, H. (1998). "Influence of pH and humic acid on coagulation kinetics of kaolinite: A dynamic light scattering study." *Journal of Colloid and Interface Science*, 202(1), 95-103.

Lecoanet, H. F., and Wiesner, M. R. (2004). "Velocity effects on fullerene and oxide nanoparticle deposition in porous media " *Environ. Sci. Technol.*, 38(16), 4377-4382.

Litton, G. M., and Olson, T. M. (1994). "Colloid deposition kinetics with surface active agents evidence for discrete surface-charge effects." *Journal of Colloid and Interface Science*, 165(2), 522-525.

Liu, S., Mo, X., Zhang, C., Sun, D., and Mu, C. (2004). "Swelling inhibition by polyglycols in montmorillonite dispersions." *Journal of Dispersion Science and Technology*, 25(1), 63 - 66.

Liu, Y., C., C., Dionysiou, D., and Lowry, G. V. (2005a). "TCE hydrodechlorination in water by highly disordered monometallic nanoiron." *Chem. Mat.*, 17, 5315-5322.

Liu, Y., and Lowry, G. V. (2006). "Effect of particle age (Fe0 content) and solution pH on NZVI reactivity: H2 evolution and TCE dechlorination." *Environ. Sci. Technol.*, 40(19), 6085-6090.

Liu, Y., Majetich, S. A., Tilton, R. D., Sholl, D. S., and Lowry, G. V. (2005b). "TCE dechlorination rates, pathways, and efficiency of nanoscale iron particles with different properties." *Environ. Sci. Technol.*, 39, 1338-1345.

Liu, Y., Phenrat, T., and Lowry, G. V. (2007). "Effect of TCE concentration and dissolved groundwater solutes on NZVI-promoted TCE dechlorination and H2 evolution." *Environ. Sci. Technol.*, 41(22), 7881-7887.

Lowry, G. V. (2007). "Nanomaterials for Groundwater Remediation." In: *Environmental Nanotechnology: Applications and Impacts of Nanomaterials*, M. R. Wiesner and J.-Y. Bottero, eds., McGraw-Hill, New York.

Matsson, M. K., Kronberg, B., and Claesson, P. M. (2004). "Adsorption of alkyl polyglucosides on the solid/water interface: Equilibrium effects of alkyl chain length and head group polymerization." *Langmuir*, 20, 4051-4058.

Miller, C. T., Poirer-McNeill, M. M., and Mayer, A. S. (1990). "Dissolution of trapped nonaqueous phase liquids: Mass transfer characteristics." *Water Resor. Res.*, 26(11), 2783-2796.

Nakamae, K., Tanigawa, S., Nakano, S., and Sumiya, K. (1989). "The effect of molecular weight and hydrophilic groups on the adsorption behavior of polymers onto magnetic particles." *Colloid Surf. A.*, 37, 379.

Napper, D., H. (1983). *Polymeric Stabilization of Colloidal Dispersions*, Academic Press, New York.

Nurmi, J. T., Tratnyek, P. G., Sarathy, V., Baer, D. R., Amonette, J. E., Pecher, K., Wang, C., Linehan, J. C., Matson, D. W., Penn, R. L., and Driessen, M. D. (2005). "Characterization and properties of metallic iron nanoparticles: spectroscopy, electrochemistry, and kinetics." *Environ. Sci. Technol.*, 39(5), 1221-1230.

Ohshima, H. (1995). "Electrophoresis of soft particles." *Adv. Colloid Interface Sci.*, 62, 189-235.

Pelley, A. J., and Tufenkji, N. (2008). "Effect of particle size and natural organic matter on the migration of nano- and microscale latex particles in saturated porous media." *J. Colloid Interface Sci.*, 321(1), 74-83.

Phenrat, T., Cihan, A., Kim, H. J., Mital, M., Illangasekare, T., and Lowry, G. V. (2010a). "Transport and Deposition of Polymer-Modified Fe(0) Nanoparticles in 2-D Heterogeneous Porous Media: Effects of Particle Concentration, Fe(0) Content, and Coatings." *Environmental Science & Technology*, 44(23), 9086-9093.

Phenrat, T., Fagerlund, F., Illangasekare, T., Lowry, G. V., and Tilton, R. D. (2011). "Polymer-Modified Fe(0) Nanoparticles Target Entrapped NAPL in Two Dimensional Porous Media: Effect of Particle Concentration, NAPL Saturation, and Injection Strategy." *Environmental Science & Technology*, 45(14), 6102-6109.

Phenrat, T., Kim, H.-J., Fagerlund, F., Illangasekare, T., Tilton, R. D., and Lowry, G. V. (2009a). "Particle size distribution, concentration, and magnetic attraction affect transport of polymer-modified Fe^0 nanoparticles in sand columns." *Environ. Sci. Technol.*, 43(13), 5079-5085.

Phenrat, T., Kim, H. J., Fagerlund, F., Illangasekare, T., and Lowry, G. V. (2010b). "Empirical correlations to estimate agglomerate size and deposition during injection of a polyelectrolyte-modified Fe(0) nanoparticle at high particle concentration in saturated sand." *Journal of Contaminant Hydrology*, 118(3-4), 152-164.

Phenrat, T., Liu, Y., Tilton, R. D., and Lowry, G. V. (2009b). "Adsorbed Polyelectrolyte Coatings Decrease Fe0 Nanoparticle Reactivity with TCE in Water: Conceptual Model and Mechanisms." *Environ. Sci. Technol.*, 43, 1507-1514.

Phenrat, T., Saleh, N., Sirk, K., Kim, H.-J., Tilton, R. D., and Lowry, G. V. (2008). "Stabilization of aqueous nanoscale zerovalent iron dispersions by anionic polyelectrolytes: adsorbed anionic polyelectrolyte layer properties and their effect on aggregation and sedimentation." *J. Nanopart. Res.*, 10, 795-814.

Phenrat, T., Saleh, N., Sirk, K., Tilton, R., D., and Lowry, G., V. (2007). "Aggregation and sedimentation of aqueous nanoscale zerovalent iron dispersions." *Environ. Sci. Technol.*, 41(1), 284-290.

Phenrat, T., Schoenfelder, D., Losi, M., Yi, J., Peck, S., and Lowry, G. V. (2010c). "Treatability Study for a TCE Contaminated Area using Nanoscale- and Microscale-Zerovalent Iron Particles: Reactivity and Reactive Life Time " In: *Environmental Applications of*

Nanoscale and Microscale Reactive Metal Particles, C. L. G. a. K. M. Carvalho-Knighton, ed., American Chemical Society, Washington, DC, 183-202.

Phenrat, T., Song, J. E., Cisneros, C. M., Schoenfelder, D. P., Tilton, R. D., and Lowry, G. V. (2010d). "Estimating attachment of nano- and submicrometer-particles coated with organic macromolecules in porous media: development of an empirical model." *Environ. Sci. Technol.*, 44(12), 4531–4538.

Quinn, J., Geiger, C., Clausen, C., Brooks, K., Coon, C., O'Hara, S., Krug, T., Major, D., Yoon, W.-S., Gavaskar, A., and Holdsworth, T. (2005). "Field demonstration of DNAPL dehalogenation using emulsified zero-valent iron." *Environ. Sci. Technol.*, 39(5), 1309-1318.

Roddick-Lanzilotta, A., and McQuillan, J. (1999). "An in Situ Infrared Spectroscopic Investigation of Lysine Peptide and

Polylysine Adsorption to TiO2 from Aqueous Solutions." *J. Colloid Interface Sci.*, 217, 194–202.

Saenton, S., and Illangasekare, T. H. (2007). "Up-scaling of mass transfer rate coefficient for the numerical simulation of DNAPL dissolution in heterogeneous aquifers." *Water Resour. Res.*, 43, W02428.

Saleh, N., Kim, H.-J., Phenrat, T., Matyjaszewski, K., Tilton, R. D., and Lowry, G. V. (2008). "Ionic Strength and Composition Affect the Mobility of Surface-Modified Fe0 Nanoparticles in Water-Saturated Sand Columns " *Environ. Sci. Technol.*, 42(9), 3349-3355.

Saleh, N., Phenrat, T., Sirk, K., Dufour, B., Ok, J., Sarbu, T., Matyjaszewski, K., Tilton, R. D., and Lowry, G. V. (2005a). "Adsorbed triblock copolymers deliver reactive iron nanoparticles to the oil/water interface." *Nano Lett.*, 5(12), 2489-2494.

Saleh, N., Sarbu, T., Sirk, K., Lowry, G. V., Matyjaszewski, K., and Tilton, R., D. (2005b). "Oil-in-water emulsions stabilized by polyelectrolyte-grafted nanoparticles." *Langmuir*, 21, 9873-9878.

Saleh, N., Sirk, K., Liu, Y., Phenrat, T., Dufour, B., Matyjaszewski, K., Tilton, R., D., and Lowry, G., V. (2007). "Surface modifications enhance nanoiron transport and NAPL targeting in saturated porous media." *Environ. Eng. Sci.*, 24(1), 45-57.

Sarathy, V., Tratnyek, P. G., Nurmi, J. T., Baer, D. R., Amonette, J. E., Chun, C. L., Penn, R. L., and Reardon, E. J. (2008). "Aging of Iron Nanoparticles in Aqueous Soluton: Effects on Structure and Reactivity." *J. Phys. Chem. C*, 112, 2286-2293.

Schrick, B., Hydutsky, B. W., Blough, J. L., and Mallouk, T. E. (2004). "Delivery vehicles for zerovalent metal nanoparticles in soil and groundwater." *Chem. Mat.*, 16, 2187-2193.

Shi, Z. Q., Nurmi, J. T., and Tratnyek, P. G. (2011). "Effects of Nano Zero-Valent Iron on Oxidation-Reduction Potential." *Environmental Science & Technology*, 45(4), 1586-1592.

Song, L. F., Johnson, P. R., and Elimelech, M. (1994). "Kinetics of colloid deposition onto hetergeneously charged surfaces in porous media." *Environmental Science & Technology*, 28(6), 1164-1171.

Stroo, H., Unger, M., Ward, C. H., Kavanaugh, M., Vogel, C., Leeson, A., Marquesee, J., and Smith, B. (2003). "Remediating chlorinated solvent source zones." *Environ. Sci. Technol.*, 37, 193a-232a.

Tombacz, E., Filipcsei, G., Szekeres, M., and Gingl, Z. (1999). "Particle aggregation in complex aquatic systems." *Colloids and Surfaces a-Physicochemical and Engineering Aspects*, 151(1-2), 233-244.

Tombacz, E., Libor, Z., Illes, E., Majzik, A., and Klumpp, E. (2004). "The role of reactive surface sites and complexation by humic acids in the interaction of clay mineral and iron oxide particles." *Organic Geochemistry*, 35(3), 257-267.

Tombacz, E., and Szekeres, M. (2006). "Surface charge heterogeneity of kaolinite in aqueous suspension in comparison with montmorillonite." *Applied Clay Science*, 34(1-4), 105-124.

Torkzaban, S., Bradford, S. A., and Walker, S. L. (2007). "Resolving the coupled effects of hydrodynamics and DLVO forces on colloid attachment in porous media." *Langmuir*, 23, 9652-9660.

Tratnyek, P. G., and Johnson, R. L. (2006). "Nanotechnologies for environmental cleanup." *Nano Today*, 1(2), 44-48.

Tufenkji, N., and Elimelech, M. (2004). "Correlation equation for predicting single-collector efficiency in physicochemical filtration in saturated porous media." *Environ. Sci. Technol.*, 38, 529-536.

Varadhi, S., Gill, H., Apoldo, L., Liao, K., Blackman, R., and Wittman, W. (Year). "In-Situ Remediation of Chlorinated Solvent-Contaminated Groundwater in Weathered/Fractured Shale/Siltstone Bedrock Using Nanoiron." *the Gas Technology Institute (GTI) Natural Gas Technologies Conference*, Orlando, FL

Wu, Y., Versteeg, R., Slater, L., and LaBrecque, D. (2009). "Calcite precipitation dominates the electrical signatures of zero valent iron columns under simulated field conditions." *J. Contam. Hydrol.*, 106(3-4), 131-143.

Zhang, W. (2003). "Nanoscale iron particles for environmental remediation: An overview." *J. Nanopart. Res.*, 5, 323-332.

Zheng, C., and Wang, P. P. (1999). "MT3DMS: A modular three-dimensional multispecies transport model for simulation of advection, dispersion, and chemical reactions of contaminants in groundwater systems; documentation and user's guide,." U.S. Army Corps of Engineers, Washington, DC, U.S.A.

Zhulina, E. B., Borisov, O. V., and Birshtein, T. M. (2000). "Static forces in confined polyelectrolyte layers." *Macromolecules*, 33, 3488-3491.